

U-Pb geochronology of volcano-sedimentary
moraine sediments of the Bunger Hills:
Implications for Mesoproterozoic evolution of
East Antarctica

Thesis submitted in accordance with the requirements of the
University of Adelaide for an Honours Degree in Geology

Patrick Kolesik

November 2016



U-PB GEOCHRONOLOGY OF VOLCANO-SEDIMENTARY MORaine SEDIMENTS OF THE BUNGER HILLS: IMPLICATIONS FOR MESOPROTEROZOIC EVOLUTION OF EAST ANTARCTICA

RUNNING TITLE: VOLCANO-SEDIMENTARY MORaine SEDIMENTS OF THE BUNGER HILLS

ABSTRACT

The Bunger Hills and adjacent areas of Wilkes Land and Queen Mary Land occupy the very western periphery of the Musgrave–Albany–Fraser Orogen, and represent one of the few exposures within east Antarctica with direct correlations to Australian constituent terrains of this continental-scale system.

U–Pb analyses of detrital zircons from volcano–sedimentary moraine sediments of the Bunger Hills yield concordant $^{206}\text{Pb}/^{238}\text{U}$ ages ranging from ca. 1364 Ma to ca. 1040 Ma ($n = 842$), with a main late Mesoproterozoic magmatic zircon population clustered at ca. 1179–1161 Ma. Strong parallels with the time profile of in-situ rocks from the Stage 2 Albany–Fraser Orogen (AFO), the Bunger Hills and Windmill Islands, suggest these were the likely provenances for the associated moraine detritus.

The Bunger Hills lie downstream from outcrops of the geographically inaccessible Sandow Group, which comprises clastic and mafic volcanoclastic rocks. It is interpreted that the sedimentary moraine materials of the Bunger Hills were derived from the glacial erosion of the Sandow Group supracrustal successions.

The lithological character, sedimentary fill pattern and advanced diagenesis suggest that the Sandow Group formed within an active intra-continental rift-basin and represents the upper-crustal expression of extensional tectonism. Reconnaissance U–Pb geochronology of authigenic titanite suggests basin development occurred close to or within the time frame of the high-grade metamorphism recorded in the Bunger Hills. Therefore basin development was probably directly associated with the second major thermo-tectonic phase of the AFO (Stage 2; ca. 1215–1140 Ma). Due to the essentially non-metamorphosed volcano–sedimentary nature of the detritus in the sedimentary rocks, it seems likely that the evolving Mesoproterozoic orogenic system was not deeply exhumed during basin development.

KEYWORDS

U–Pb geochronology, detrital zircon, authigenic titanite, moraine, Mesoproterozoic, east Antarctica, Bunger Hills, Wilkes Land, Sandow Group

TABLE OF CONTENTS

Abstract.....	i
Keywords.....	i
List of Figures and Tables	5
Introduction	7
Geological setting.....	9
The Bunker Hills	10
The Sandow Group (Mt. Sandow & Mt. Amundsen).....	10
Wilkes Land – metamorphism & deformation.....	14
Glacial moraine sediments of the Bunker Hills.....	15
Methodology.....	16
Sample selection & description	16
Sample preparation & imaging.....	17
Zircon U–Pb geochronology	17
Authigenic titanite U–Pb geochronology	19
Kolmogorov–Smirnoff (K–S) test	19
Diagenetic mineral chemistry via electron microprobe.....	20
Results	20
Sample descriptions & petrography	20
Zircon U–Pb geochronology	25
Authigenic titanite U–Pb geochronology	36
Kolmogorov–Smirnoff (K–S) test	37
Diagenetic mineral chemistry	38
Discussion.....	41
Zircon U–Pb geochronology	41
Sedimentary moraine units of the Bunker Hills	41
The Sandow Group.....	42
Comparison of the moraine samples to the Sandow Group	42
Depositional setting	43
Authigenic mineral assemblages	43
Authigenic titanite U–Pb geochronology	44
Regional correlations	45
An intra-continental rift-style basin.....	48
A model for basin development.....	48
Conclusions	52

Acknowledgements	53
References	54
APPENDIX A: Extended methodology	57
APPENDIX B: Terra–Wasserberg concordia & probability density plots	67
APPENDIX C: LA-ICP-MS zircon U–Pb geochronology data.....	69
APPENDIX D: Microprobe mineral chemistry data.....	140

LIST OF FIGURES

Fig. 1: Paleogeography and tectonic elements of Australo–Antarctica. (a) Relative positions of Australia and Antarctica reflect previous connectivity during Gondwanan reconstructions. The boxed region, encompassing the Albany–Fraser Orogen, Bunger Hills and Windmill Islands, is expanded in (b). Geological boundaries–structures are adapted from White et al., (2013), Boger (2011) and Kirkland et al., (2013b). (b) Relative terranes which correlate between Australia and east Antarctica are displayed. Fig. modified from Tucker et al., (2016). Abbreviations: MAFO: Musgrave–Albany–Fraser Orogeny; NAC: North Australian Craton; WAC: West Australian Craton; AUS: Australia; ANT: Antarctica.	7
Fig. 2: Geological and physiological map of the Bunger Hills and adjacent areas of Wilkes Land and Queen Mary Land, east Antarctica, modified after Sheraton et al., (1994). Field photographs and approximate sample locations of collected moraine sediments are displayed on the map inset (top left). Sample coordinates are listed in Table 1.	13
Fig. 3: Photomicrographs of representative samples for each rock type. (A) SAN-2, arkosic sandstone; (B) SAN-12, coarse conglomerate; (C) SAN-14, quartzitic greywacke; (D) SAN-19, mafic greywacke. Imagery captured in plane-polarised light (PPL)....	23
Fig. 4: Hand sample photographs of representative moraine sedimentary rocks from the Bunger Hills, east Antarctica. Moraine samples are organised to reconstruct analogous successions of the Sandow Group in the inland of Wilkes Land and Queen-Mary Land (Ravich et al., 1968). The sedimentary moraine units share strong lithological and mineralogical similarities with the outcropping Sandow Group successions.	25
Fig. 5: Cathodoluminescence imagery of representative zircon grains from moraine sedimentary rocks from the Bunger Hills. The scale bar demonstrates size of zircon grains and fragments. The location of U–Pb spot analyses and corresponding $^{206}\text{Pb}/^{238}\text{U}$ ages are shown. For full isotopic dataset refer to Appendix C.28	
Fig. 6(a-b): Stacked Terra–Wasserburg Concordia diagrams for LA–ICP–MS zircon U–Pb geochronology. $^{206}\text{Pb}/^{238}\text{U}$ weighted average ages are quoted for each sample, which are presented in accordance to inferred stratigraphic position (see Fig. 3). Analyses that are $100 \pm 5\%$ discordant are shown as black ellipses, analyses that are $>5\%$ discordant are excluded from age estimations and appear as grey ellipses. Analyses which deviate significantly from prevalent age populations are not displayed, and are reported above corresponding Concordia; arrows represent direction of deviance. Weighted average age estimates do not represent a truly unimodal population as they reflect a provenance system; MSWD not an applicable measure of precision vs scatter.	33
Fig. 7: LA–ICP–MS zircon U–Pb geochronology. Individual probability density plots and cumulative frequency histograms of $^{206}\text{Pb}/^{238}\text{U}$ ages for all zircon analyses at $100 \pm 5\%$ discordance. Weighted average $^{206}\text{Pb}/^{238}\text{U}$ ages quoted for each sample. Number of analyses given by n=x.	35
Fig. 8: Authigenic titanite in sample SAN-17, a heavy-mineral bearing arkosic sandstone. (a) Photomicrograph showing diagenetic titanate (light–dark brown mineral) occurring as overgrowths on ilmenite (black mineral) within heavy-mineral bands; (b) Image emphasises diagenetic domains and spatial proximity between ilmenite and titanite mineral members; (c) BSE image displaying micro-scale compositional irregularities across titanite aggregates (grey). Captured with a Phillips XL30.	36
Fig. 9: Terra–Wasserburg Concordia diagram for SHRIMP titanite U–Pb reconnaissance geochronology (sample SAN-17). All analyses are shown. Data point error ellipses are to 2σ	37
Fig. 10: Photomicrographs of petrological relationships of representative diagenetic mineral domains within selected basaltic–volcanic moraine samples. (a–b) SAN-10, greywacke-style conglomerate; (c–d) SAN-14, quartzitic greywacke; (e–f) SAN-18, greywacke-style conglomerate; (g–h) SAN-19, mafic greywacke. Boxed areas are magnified in adjacent images. Abbreviations: chl, chlorite; qtz, quartz; alb, albite; ksp, orthoclase feldspar; ser, sericite; tit, titanite; zn, zircon. Imagery captured in PPL.....	40
Fig. 11: Zircon U–Pb geochronology regional correlations histograms. Composite probability density plots and cumulative frequency histograms of $^{206}\text{Pb}/^{238}\text{U}$ analyses at $100 \pm 5\%$ discordance are shown. (a) The Bunger Hills, sedimentary moraine sediments (this study); (b) The Bunger Hills, granulite and felsic plutonic rocks (Tucker et al., 2016); (c) Albany–Fraser Orogen, granulite and felsic plutonic rocks (Spaggiari et al., 2015; Kirkland et al., 2011); (d) Mt. Strathcona, Queen–Mary Land, granulite rocks (Halpin, unpublished data); (e) Windmill Islands, in-situ granulite and felsic plutonic rocks and moraine sediments (Zhang et al., 2012). Sample SAN-9 excluded from composite probability density plot (a)—statistically determined to derive from a different age distribution (K–S test; Table 2).	47
Fig. 12: A hypothesised tectonic scenario where intra-continental rift-basins evolve from basal mafic–volcanics to coarse, locally-derived clastic fill, within the confines of an extensional, high-temperature	

orogen (Stage 2 AFO). The hypothesised system shows local erosion and deposition of a magmatic-rich carapace, derived from the melting of the ductile lower crust (Stage 2 granitoids) prior to the exhumation and availability of granulite-facies metamorphic basement rocks. Basaltic feeder dykes derive from the melting of the upper-mantle during lithospheric stretching and are commonly expressed as extrusive lava flows that accumulate within crustal depressions. The high-heat flow system is responsible for the advanced diagenesis experienced by syn-rift sediments. Modified from Harris et al., 2002.....	49
Fig. 13: Spatial distribution of granitic magmatism and clastic sedimentation during the Cretaceous and Jurassic, Southeastern China block (SECB). Modified from Wang & Shu, (2012).....	50

LIST OF TABLES

Table 1: Summary of moraine sedimentary rock samples taken from the Bunger Hills, east Antarctica. Zone 47D.....	24
Table 2(a-b): K-S probability difference matrix comparing detrital age distributions of representative sedimentary moraines. Output tables (a–b) report P-Values and D-Values for the K-S test using uncertainties in the cumulative density function (CDF). A P-Value which exceeds 0.05 for a sample pair, indicates at a 95% confidence level, that the two age populations are statistically indifferent and satisfy the null hypothesis. Accepted values appear bold and highlighted in red. D-values indicate the maximum vertical deviation between two cumulative deviation plots. D has a maximum possible value of 1 and a minimum possible value of 0. K-S test Excel macro modified from Press et al., (1986) by Guynn & Gehrels (2010).....	38
Table 3: Mineral chemistry values measured for representative diagenetic minerals in basaltic–volcanic samples (SAN-10, 14, 18, 19). Weight percent for each measured elemental oxide is reported. Diagnostic elements for each mineral are highlighted. Number of analyses given by n=x.....	39

INTRODUCTION

The East Antarctic Craton (EAC; Fig. 1) is considered one of the most extensive high-grade metamorphic terrains on Earth (Stüwe & Wilson, 1990) and is a key constituent in Rodinian supercontinent reconstructions (White et al., 2013). Occupying the very western periphery of the Musgrave–Albany–Fraser Orogen (MAFO; Fig. 1), the Bunker Hills and adjacent areas of Wilkes Land and Queen–Mary Land represent one of the few exposures within east Antarctica with direct correlations to Australian constituent terrains of this continental-scale system (Tucker et al., 2016).

Being a landscape marked by extensive ice-covers and accordingly poor outcrop (~2% of bedrock exposed; Zhang et al., 2012), the geological and tectonothermal history of the EAC remains poorly understood. It is largely established by isolated outcrops of the

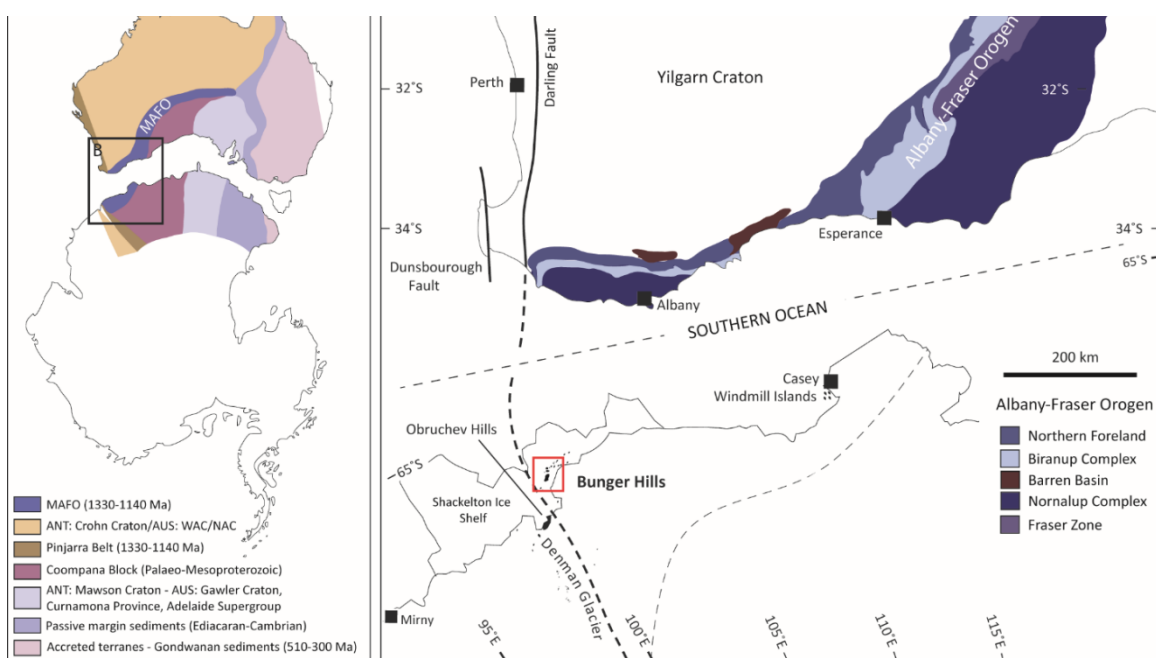


Fig. 1: Paleogeography and tectonic elements of Australo–Antarctica. (a) Relative positions of Australia and Antarctica reflect previous connectivity during Gondwanan reconstructions. The boxed region, encompassing the Albany–Fraser Orogen, Bunker Hills and Windmill Islands, is expanded in (b). Geological boundaries–structures are adapted from White et al. (2013), Boger (2011) and Kirkland et al., (2013b). (b) Relative terranes which correlate between Australia and East Antarctica are displayed. Figure modified from Tucker et al. (2016). Abbreviations: MAFO: Musgrave–Albany–Fraser Orogeny; NAC: North Australian Craton; WAC: West Australian Craton; AUS: Australia; ANT: Antarctica.

Bunger Hills, Highjump Archipelago, Obruchev Hills and Windmill Islands (Fig. 1) and satellite geophysical data (Aitken et al., 2014; Boger, 2011; Fitzsimons, 2000; 2003).

Several approaches are capable of examining the ice-covered interior. These include over-ice potential-field geophysics (e.g. Shepherd et al., 2006; Studinger et al., 2004) and subglacial drilling (e.g. Powell & Vogel, 2009; Van De Flierdt et al., 2008), however, they are logistically difficult and economically unviable (e.g. Aitken et al., 2014; Zhang et al., 2012). Utilising rocks within glacial moraine sediments presents an invaluable alternative in sampling the subglacial bedrock geology of the continental interior. By understanding the physiology and material distribution of glacial systems, provenance areas for associated moraine detritus can be estimated (e.g. Zhang et al., 2012).

Glacial moraine sediments were collected in the Bunger Hills by the Department of Earth Sciences at the University of Adelaide during the summer of 2014–2015. These sedimentary erratics occur in direct contact with the high-grade metamorphic and igneous rocks that dominate the in-situ bedrock of the Bunger Hills. However, examination of these sediments, as presented in this study, reveal an absence of high-grade metamorphic clasts and, conversely, a dominance of material from an inferred, largely volcano–sedimentary origin.

The sedimentary rocks sampled by the moraine are analogous to the successions exposed at Mt. Sandow and Mt. Amundsen (Ravich et al., 1968), located approximately 110 km south from the Bunger Hills, further inland of Queen-Mary Land and Wilkes Land, respectively. Up until now, no geological nor geochronological research has been undertaken on the moraine sedimentary rocks of the Bunger Hills, and their relationship with regional tectonic history is unknown.

The Bunker Hills and surrounding areas of Wilkes Land (Fig. 2) record a major thermo-tectonic event during the Mesoproterozoic (ca. 1190 ± 15 Ma), associated with granulite-facies metamorphism ($750\text{--}800^\circ\text{C}$, 5–6 kb), voluminous magmatism and the intrusion of multiple dyke generations (Sheraton et al., 1995; Stüwe & Powell, 1989). This metamorphic event is considered to have been associated with crustal extension (Sheraton et al., 1993) and upper-crustal reworking of dominantly igneous–volcanic sources (Tucker et al., 2016).

This study presents new U–Pb geochronology on detrital zircon and authigenic titanite from the sedimentary rock samples obtained from moraines in the Bunker Hills. It aims to distinguish a possible source terrain for the moraine detritus and to evaluate the timing of deposition and diagenesis of the inferred Sandow Group supracrustal successions.

Constraints on the subglacial geology of inland areas of Wilkes Land and Queen-Mary Land are presented (Fig. 1). Existing data from the MAFO is integrated to provide a synopsis on the association between the proposed subglacial sedimentary province and the crustal evolution of this region of Wilkes Land and Queen-Mary Land, with emphasis on late Mesoproterozoic tectonothermal events.

GEOLOGICAL SETTING

The Bunker Hills, Highjump Archipelago, Obruchev Hills and adjacent areas of Wilkes Land (Fig. 2) are located along the ice-bound coast of east Antarctica, separated from the Southern ocean by the Shackleton Ice-Shelf (Sheraton et al., 1995). These isolated outcrops represent contiguous components of the continental-scale Musgrave–Albany–

Fraser Orogen (MAFO; Fig. 1; Tucker et al., 2016) and form a well-exposed area (~1500 km²) of the Pre-Cambrian EAC (Sheraton et al., 1993).

The Bunger Hills

The Bunger Hills are low-lying rocky outcrops (~400 km²) characterised by deep lakes and glacially excavated valleys, commonly mantled by moraine deposits and locally derived rock debris (Sheraton et al., 1995). The moraine cover is considered to have been supplied locally, from the Bunger Hills themselves, and inland areas of Wilkes Land and Queen-Mary Land; transported by eastward and north-eastward trending glacial systems that were active through the Holocene (Sheraton et al., 1995; White et al., 2013).

The Bunger Hills consist of variable metamorphic rocks to granulite-facies, plutonic igneous rocks and mafic dykes which can be classified into five major lithological divisions (Tucker et al., 2016; Sheraton et al., 1992; 1995; 1993). The southeastern Bunger Hills consists of granulite-facies, mafic-felsic orthogneiss of tonalitic-doleritic composition (Association 1; Tucker et al., 2016; Sheraton et al. 1993). The orthogneiss composition is largely tonalitic-granitic to the northeast, commonly interlayered with subordinate metasedimentary rocks (Association 2; e.g. Tucker et al., 2016; Sheraton et al., 1992; 1993). Zircon U-Pb geochronology on granodioritic orthogneiss (southeastern Bunger Hills) and tonalitic orthogneiss (Thomas Island) dates the emplacement ages of the igneous protoliths at ca. 1700–1500 Ma (Sheraton et al., 1992; 1995; 1993).

The central Bunger Hills are dominated by a sequence of orthopyroxene-bearing tonalitic orthogneiss and garnet-cordierite ± sillimanite gneiss, finely interlayered with subordinate metapsammite, garnet ± biotite granitic gneiss, mafic gneiss and scarce calc-

silicate (Association 3; e.g. Tucker et al., 2016; Sheraton et al., 1992; 1995; 1993). The northern Bunger Hills are characterised by migmatitic garnet–cordierite ± sillimanite ± orthopyroxene ± spinel-bearing metapelitic, interlayered with subordinate metapsammite and quartzite (Association 4; e.g. Tucker et al., 2016).

Numerous pyroxene-bearing charnockites and plutonic bodies ranging from granite to gabbro intrude this predominantly granulite–facies terrain (Association 5; e.g. Stüwe & Wilson, 1990; Tucker et al., 2016). Zircon U–Pb geochronology dates the Algae Lake Pluton and Paz Cove Batholith at 1171 ± 3 Ma and 1170 ± 4 Ma, respectively (Sheraton et al., 1992). Multiple late-stage dolerite–basalt dyke generations of several chemically distinct suites also intrude the terrain, dated at ca. ≥ 1140 Ma and ca. 500 Ma (Sheraton et al., 1990; 1993).

The Sandow Group (Mt. Sandow and Mt. Amundsen)

Approximately 110 km south from the Bunger Hills, on the eastern bank of the Denman Glacier system, lie two isolated nunataks—Mt. Sandow and Mt. Amundsen (Fig. 2). These low-lying mountains, rising approximately 150m and 50m above the ice surface, respectively, expose rhythmically interlayered units of irregularly-metamorphosed terrigenous and basaltic lithologies (Ravich et al., 1968; Sheraton et al., 1995).

These low-grade supracrustal successions can be subdivided petrographically into five major lithological units. The following summary of the Sandow Group is compiled from previously published work by Ravich et al. (1968), who present the only detailed passages on the exposed stratigraphy.

The lowermost units consist of metamorphosed basaltic rocks, transformed to dark-green chlorite–epidote schists with disseminated pyrite and chalcopyrite (Association 1). The altered basaltic units are laminated, heteroblastic and relatively homogenous in composition. They consist of fine-grained chlorite aggregates (30–50 % abundance), epidote–saussurite aggregates (20–30 %), actinolitic–uralitic amphibole (3–10 %), ore minerals (i.e. haematite, leucoxene and titanomagnetite, 10–15 %), calcite (1–6 %), quartz (1–5 %) and relicts of albatised plagioclase (up to 10 %). The metabasaltic units were derived from an enriched mantle source, similar to that of the Bunger Hills dolerites; their magmatic origin is indisputable (Sheraton et al., 1995). It is unclear, however, whether the basalt originated as sheets or formed from layered intrusions.

Heavily indurated quartz conglomerates overlie the green–schists, characterised by cataclastic pebbles of grey to light-purple quartz, banded quartzite and sub-angular fragments of altered basalts (Association 2).

Terrigenous lithologies of the Sandow Group largely consist of inequigranular, variegated quartz–feldspathic sandstones (Association 3). The low-grade metamorphism experienced by these successions is expressed by intense recrystallisation of the cement and partial recrystallisation of the clasts themselves. The cement is dominated by fine-grained aggregates of quartz, sericite, saussurite and chlorite, with considerable dissemination of limonitised ore minerals, and less frequently titanite, tourmaline and zircon. Moderately-indurated ferruginous siltstones and argillites (Association 4) are commonly interlayered with various quartzitic sandstones, detailed above. These partially recrystallised rocks are cherry-brown in colour and occur as unsorted ellipsoidal pebbles with silty–pelitic textures.

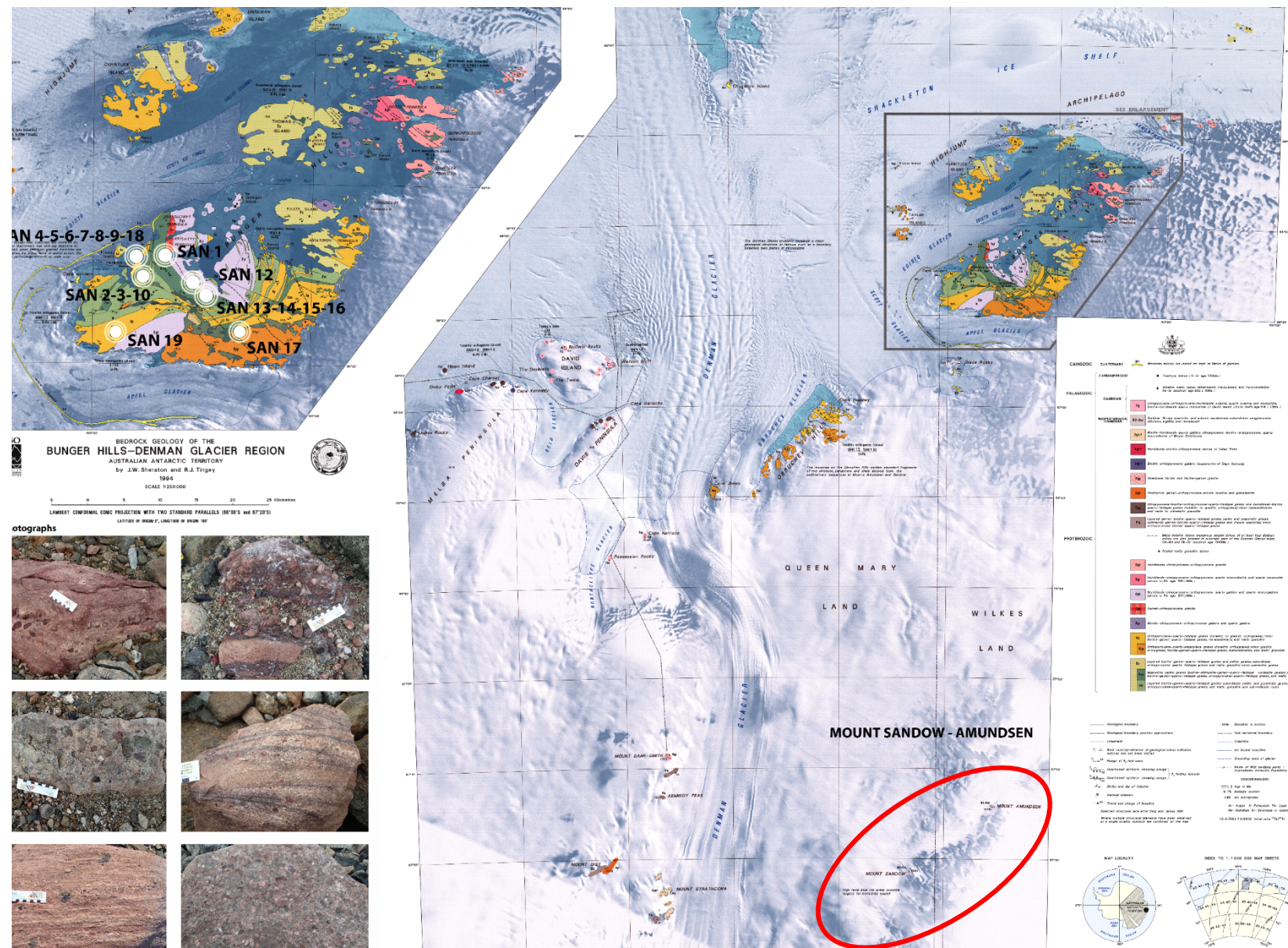


Fig. 2: Geological and physiographical map of the Bunker Hills and adjacent areas of Wilkes Land and Queen Mary Land, East Antarctica, modified after Sheraton et al., (1994). Field photographs and approximate sample locations of collected moraine sediments are displayed on the map inset (top left). Sample coordinates are listed in Table 1.

Sericite schists occur as thin sinuous bands (0.2–0.3 m) in the uppermost beds of the Sandow Group (Association 5). These are schistose rocks, pink to grey-yellow in colour and consist almost entirely of sericite flake aggregates.

The lithology of the terrigenous units indicates that deposition was facilitated by intermittent stream flow and eolian transport, under conditions of coastal-continental facies. The alternating degree of sorting and evidence of subtle pinching-out conglomerate lenses, suggests that deposition–erosion of these sediments was cyclical. The composition of clastic material in both conglomerates and sandstones indicates the source rocks for these terrigenous units were predominantly of igneous origin (granitised schists and granites).

Wilkes Land – Metamorphism & Deformation

The region of Wilkes Land is marked with at least three major stages of deformation, associated with Proterozoic tectonothermal activity (e.g. Sheraton et al., 1993; 1995; Ding & James, 1991; Stüwe & Wilson, 1990). The earliest recognisable deformational event recorded by the Bunger Hills (D_1) is considered to be contemporaneous with the onset of peak high-temperature granulite-facies metamorphism (~750–800 °C, 5–6 kbar) at ca. 1190 ± 15 Ma, provided by metamorphic zircon from tonalitic orthogneiss on Thomas Island (Sheraton et al., 1993; Stüwe & Powell, 1989). Boudinage of mafic-ultramafic dykes and numerous micro–macro structures in the region suggest this major tectonothermal event involved crustal extension (e.g. Stüwe & Wilson, 1990).

The terrain experienced two further episodes of ductile deformation (D_2 – D_3), associated with a phase of compression (D_2) and a regional doming event (D_3). The major

shortening event (D_2) was accompanied by the emplacement of multiple compositionally-diverse suites of plutonic bodies within 40 Ma of peak metamorphism, marked by the final intrusions of quartz monzodioritic–granitic rocks of the Booth Peninsula batholith at ca. 1150 Ma (e.g. Sheraton et al., 1992).

The timing of metamorphism recognised by the Bunger Hills is contemporaneous with the timing of metamorphism recorded in the Windmill Islands (ca. 1210–1180 Ma; Zhang et al., 2012; Post, 2000), the Albany–Fraser Orogeny (Stage 2; ca. 1215–1140 Ma; Clark et al., 2000; Kirkland et al., 2011) in southwestern Australia, and the Musgrave Orogeny (ca. 1225–1135 Ma; Tucker et al., 2015; Smithies et al., 2011; Walsh et al., 2015) in central Australia. Significant parallels between the age and isotope signature of igneous–metamorphic rocks from these regions suggest these were contiguous constituents of a single orogenic system at the time and the Paleo–Mesoproterozoic tectonic evolution of these regions is analogous (Clark et al., 2000; Kirkland et al., 2011; Fitzsimons 2003; 2000).

Unlike the Bunger Hills, the Windmill Islands also preserve an earlier phase of metamorphism and deformation at ca. 1340–1310 Ma, contemporaneous with Stage 1 of the AFO (ca. 1345–1260 Ma; Clark et al., 2000; Kirkland et al., 2011).

Glacial Moraine Sediments of the Bunger Hills

The moraine sedimentary rocks of the Bunger Hills comprise an assortment of conglomerates, quartzitic–feldspathic sandstones, cherry-brown siltstones and intensely-altered metabasalts. Examination of the sedimentary samples, presented in this study, reveal an absence of high-grade metamorphic clasts and dominance of material from an

inferred, largely volcano–sedimentary origin. The sedimentary rocks contained within moraines share markedly distinct similarities with the supracrustal successions of the Sandow Group, exposed at Mt. Sandow and Mt. Amundsen (Ravich et al., 1968). Given that the Bunker Hills lie downstream of the outcropping Sandow Group, it is likely that the sedimentary moraine materials were derived from, and as such, represent these largely inaccessible successions (White et al., 2015).

The non-metamorphosed and essentially undeformed nature of the Sandow Group contrasts with the highly-metamorphosed and igneous rocks exposed in Queen-Mary land. This implies that the Sandow Group forms a cover sequence on the metamorphic and igneous basement. The provenance of the Sandow Group is unknown and potentially contains information about bedrock systems within the interior of Antarctica.

METHODOLOGY

Sample Selection & Description

The following section summarises the analytical methods applied in this study. For further detail, refer to Appendix A. Twenty volcano–sedimentary moraine samples were collected from across the Bunker Hills. Nine representative samples were selected for zircon U–Pb geochronology. Field work and sample acquisition was undertaken through the summer of 2014–2015, by M. Hand and N. Tucker (University of Adelaide), C. Clark (Curtin University) and K. Wallace (Australian Antarctic Division).

Sample Preparation & Imaging

Zircons were separated from crushed samples via hand panning and conventional magnetic and heavy liquid (LST) techniques at the University of Adelaide. Approximately 200 zircon grains per sample were hand-picked under a binocular microscope, mounted in epoxy resin and ground and polished to expose the grain cores. Exposed grains were imaged in cathodoluminescence (CL) and back-scatter-electron (BSE) using a FEI Quanta600 MLA scanning electron microscope (SEM) housed at Adelaide Microscopy, The University of Adelaide.

Zircon U–Pb Geochronology

Laser–Ablation Inductively–Coupled–Plasma Mass–Spectrometry (LA–ICP–MS) zircon U–Pb analyses were performed on a New Wave Nd–YAG laser coupled with an Agilent 7500cs/7500s ICP–MS at Adelaide Microscopy, The University of Adelaide. Operating conditions and procedures for the LA–ICP–MS follow those of Payne et al., (2008). Analyses were performed at an output wavelength of 213 nm under an Ar–He ablation atmosphere.

Analysis locations were selected on the basis of CL imagery and transmitted photomicrograph imagery. A single analysis involved 30 seconds of background signal acquisition, including 10 seconds for laser beam stabilisation with the shutter closed, followed by 30 seconds of ablation. Each analysis was followed by a washout delay of 30 seconds. Ablation was carried out with a repetition rate of 5 Hz, spot size of 30 μm and fluence of $\sim 7 \text{ J cm}^{-2}$. Isotope masses ^{238}U , ^{207}Pb , ^{206}Pb and ^{204}Pb were measured for dwell times of 15 ms, 30 ms, 15 ms and 10 ms, respectively.

Data were processed using Iolite (v. 2.5; Paton et al., 2011). Instrumental mass bias and depth-dependant elemental and isotopic fractionation were corrected for using GJ-1 as the external zircon reference standard (TIMS normalisation data: $^{207}\text{Pb}/^{206}\text{Pb} = 607.7 \text{ Ma}$, $^{206}\text{Pb}/^{238}\text{U} = 600.7 \text{ Ma}$ and $^{207}\text{Pb}/^{235}\text{U} = 602.0 \text{ Ma}$; Jackson et al., 2004). Data accuracy was monitored by repeat analysis of secondary standard Plešovice and sample bracketing every 10–20 unknown analyses, of the Plešovice reference zircon standard ($337.13 \pm 0.37 \text{ Ma}$; Sláma et al., 2008). Throughout this study, GJ-1 analyses yielded weighted mean ages of $^{207}\text{Pb}/^{206}\text{Pb} = 592.2 \pm 3.0 \text{ Ma}$, $^{206}\text{Pb}/^{238}\text{U} = 600.7 \pm 0.98 \text{ Ma}$, $^{207}\text{Pb}/^{235}\text{U} = 602.8 \pm 0.89 \text{ Ma}$ ($n = 665$). GJ-1 standard analyses at $100 \pm 5\%$ discordance yielded weighted mean ages of $^{207}\text{Pb}/^{206}\text{Pb} = 600.6 \pm 3.4 \text{ Ma}$, $^{206}\text{Pb}/^{238}\text{U} = 600.0 \pm 1.2 \text{ Ma}$, $^{207}\text{Pb}/^{235}\text{U} = 602.8 \pm 1.2 \text{ Ma}$ ($n = 357$).

As a secondary standard, Plešovice analyses yielded weighted mean ages of $^{207}\text{Pb}/^{206}\text{Pb} = 364 \pm 15 \text{ Ma}$, $^{206}\text{Pb}/^{238}\text{U} = 337.1 \pm 1.2 \text{ Ma}$, $^{207}\text{Pb}/^{235}\text{U} = 342.2 \pm 2.0 \text{ Ma}$ ($n = 241$).

Plešovice standard analyses at $100 \pm 5\%$ discordance yielded weighted mean ages of $^{207}\text{Pb}/^{206}\text{Pb} = 336.8 \pm 6.2 \text{ Ma}$, $^{206}\text{Pb}/^{238}\text{U} = 335.6 \pm 1.9 \text{ Ma}$, $^{207}\text{Pb}/^{235}\text{U} = 338.3 \pm 2.2 \text{ Ma}$ ($n = 76$). All weighted mean ages attained from Plešovice and GJ-1 are within uncertainty with the reference values of these standards.

Weighted average age plots, probability density plots and Terra–Wasserburg (TW) Concordia diagrams for each sample were produced using the Microsoft Excel plug-in ISOPLOT (Ludwig, 2012), with the exclusion of statistical outliers.

A case could be made that the MSWD value for both Plešovice and unknown zircon analyses may be forced toward 1 through integration of additional uncertainty, for a

particular analytical session. This method forces a statistical correction which may not be justified due to differences in matrix characteristics (influencing ablation behaviour) of Plešovice and unknown detrital zircon grains. Weighted average age estimates for unknown detrital analyses do not represent truly unimodal populations as they reflect a provenance system; MSWD is not an applicable measure of precision vs scatter. For sake of simplicity and data integrity, all results are reported as is.

Authigenic Titanite U–Pb Geochronology

Titanite occurs as overgrowths on ilmenite within heavy mineral bands (Fig. 8) of an arkosic sandstone (SAN-17), and were separated using conventional crushing and heavy mineral separation techniques. Titanite aggregates were further separated on the basis of magnetic susceptibility, carried out with a Frantz Isodynamic Separator at the University of Adelaide, and imaged in BSE using a Phillips XL30 SEM. Uranium and lead contents were quantified using an ASI M50 laser, coupled with a 7700 ICP–MS at Adelaide Microscopy, in order to determine the feasibility of U–Pb geochronology.

U–Pb age analysis was undertaken by R. Taylor from the Department of Applied Geology at Curtin University using a SHRIMP II, following the method outlined by Rasmussen et al. (2013).

Kolmogorov–Smirnoff (K–S) Test

In order to compare several detrital age populations and determine whether a statistically significant difference exists between distributions, a Kolmogorov–Smirnoff (K–S) test was instigated. The K–S test was run through an Excel macro modified from Press et al. (1986) by Guynn and Gehrels (2010).

The statistical test compares the maximum probability difference between two Cumulative Distribution Functions (CDF) and tests the null hypothesis that two distributions are the same, or have derived from a single parent population (Guynn & Gehrels, 2010).

$^{206}\text{Pb}/^{238}\text{U}$ age data at $100 \pm 5\%$ discordancy (1σ uncertainty) was used as input. ‘CDF with error’ was selected as an analysis option—a class of the K–S test which incorporates uncertainty in construction of the Cumulative Distribution Function (CDF). ‘K–S distance matrix’ was selected as a form of output. This reports the maximum probability difference between the CDFs of all age series and generates a matrix of ‘P-Values’ and ‘D-Values’, essential in the K–S test (Table 2).

Diagenetic Mineral Chemistry via Electron Microprobe

Quantitative analysis of diagenetic mineral chemistry was performed using a CAMECA SXFive microprobe at Adelaide Microscopy, The University of Adelaide. A beam current of 20 nA and accelerating voltage of 15 kV and a focused beam were used for all point analyses. Routine analyses were made for SiO_2 , ZrO_2 , TiO_2 , ZnO , Al_2O_3 , V_2O_3 , Cr_2O_3 , FeO , MnO , MgO , CaO , BaO , Na_2O , K_2O , P_2O_5 , Cl and F on Wavelength Dispersive Spectrometers (WDS).

RESULTS

Sample Descriptions & Petrography

SAN-2: A pinkish, arkosic sandstone encompassing clasts (~5%) which range between 0.2–0.8 cm in size (Fig. 3a & 4a). The clasts are well-rounded to sub-rounded and

comprise of orthoclase feldspar, ferruginous siltstone and dark-grey argillite. The sandstone is indurated, medium-grained and dominated by moderately-sorted quartz and orthoclase feldspar grains. Accessory minerals include muscovite, epidote, zircon and iron-oxides. The diagenetic mineralogy consists of fine-grained aggregates of chlorite, sericite and minor titanite.

SAN-9: A dark red-brown, non-metamorphosed felsic-volcanic clast approximately 20 cm in diameter (Fig. 4i). The rhyolitic clast displays an aphanitic texture and encompasses infrequent fragments (~5%) of orthoclase feldspar, with subordinate volcanic quartz and sanidine. Accessory minerals include hornblende, biotite and zircon.

SAN-10: A grey-green, greywacke-style conglomerate supported by angular to sub-angular clasts between 0.3–2.3 cm in size (~60–70%; Fig. 4f). The clasts are partially-recrystallised, poorly sorted and comprise of highly-altered orthoclase feldspar, quartz and aphanitic volcanic fragments. Accessory minerals include titanite, hornblende, epidote and zircon. Clasts and lithic fragments are set in a clay-sized greenish matrix. The diagenetic mineralogy consists of fine-grained aggregates of chlorite, sericite and titanite.

SAN-12: A coarse conglomerate with clasts (~40–60%) ranging between 0.4–3.0 cm in size (Fig. 3b & 4c). The clasts are poorly sorted, well-rounded to sub-rounded and comprise largely of orthoclase feldspar and subordinate ferruginous siltstone, quartz, dark-grey argillite and aphanitic volcanic fragments. The clasts are set in a coarse grained, quartzitic-feldspathic matrix; both constituents exhibit partial-recrystallisation. Accessory phases include muscovite, biotite and rutile. Diagenetic mineralogy consists of chlorite, sericite and minor titanite and iron-oxides.

SAN-13: A medium–coarse grained, greenish arkosic sandstone with infrequent clasts (~10–15%) ranging between 0.5–4.0 cm in size (Fig. 4d). Clasts are poorly sorted, sub-rounded to sub-angular and largely comprise of orthoclase feldspar and subordinate ferruginous siltstone and argillite, as well as greenish-grey volcanic fragments. The sandstone is moderately indurated. Accessory minerals include hornblende, biotite, muscovite and zircon. Diagenetic mineralogy consists of chlorite, sericite and minor titanite and iron-oxides.

SAN-14: A quartzitic greywacke with highly angular, moderately sorted clasts (20–30%) ranging between 0.1–0.4 cm in size (Fig. 3c & 4e). Clasts largely comprise of quartz, orthoclase feldspar and dark mafic material which are set in a fine grained, heavily altered green-grey matrix. Diagenetic mineralogy includes chlorite, sericite, titanite and albitised plagioclase. Accessory phases include hornblende, biotite, muscovite, iron-oxides and zircon.

SAN-17: A heavy-mineral bearing arkosic sandstone with sporadic clasts (~5%) ranging between 0.2–0.8 cm (Fig. 4b). The clasts are largely sub-rounded and consist of orthoclase feldspar, ferruginous siltstone, argillite and rare volcanic material. The coarse-grained sandstone is marked by heavy-mineral bands, dominated by opaque iron-oxide species (i.e. magnetite, haematite) with an abundance of diagenetic titanite. Diagenetic mineralogy consists of chlorite, sericite and titanite.

SAN-18: A dark grey-green, greywacke-style conglomerate with angular to sub-angular clasts between 0.3–2.3 cm in size (~40%; Fig. 4f). The clasts are partially recrystallised, poorly sorted and comprise of orthoclase feldspar, quartz and aphanitic volcanic

fragments. Accessory minerals include titanite, hornblende, epidote and zircon. Clasts are partially recrystallised and are set in a clay-sized greenish matrix. Diagenetic mineralogy consists of fine-grained aggregates of chlorite, sericite and albatised plagioclase.

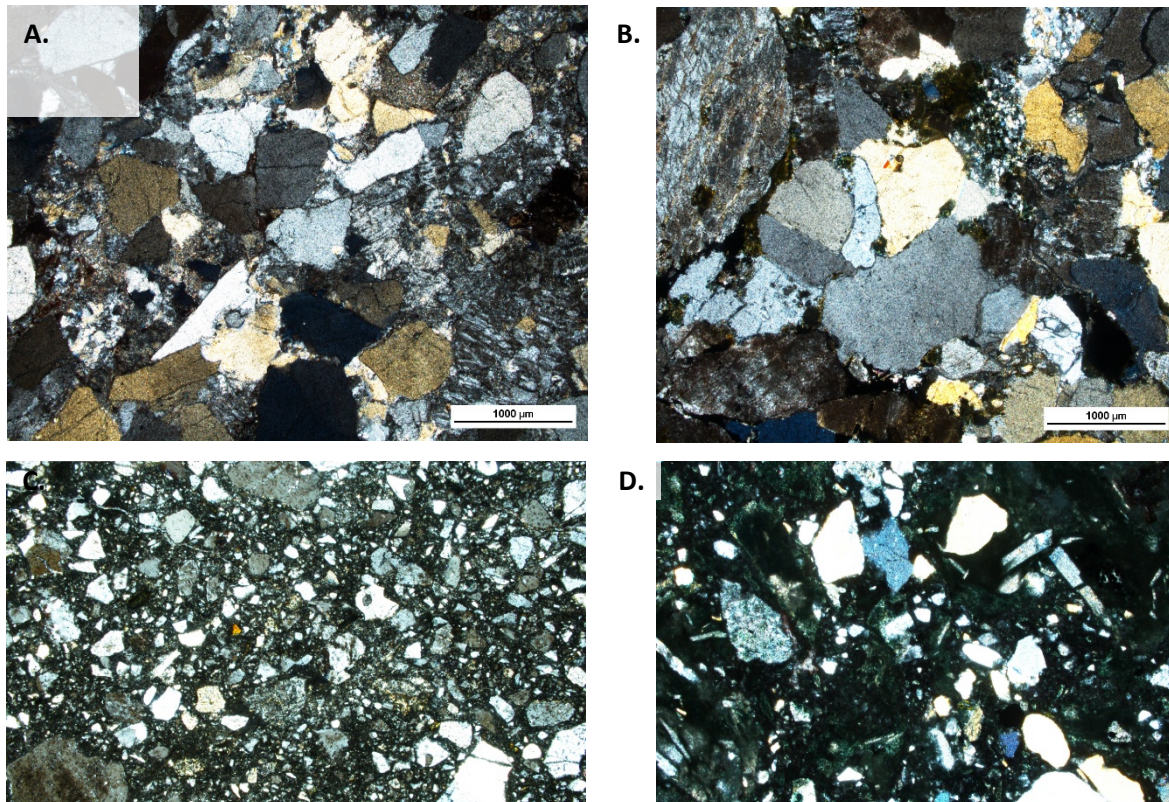


Fig. 3: Photomicrographs of representative samples for each rock type. (A) SAN-2, arkosic sandstone; (B) SAN-12, coarse conglomerate; (C) SAN-14, quartzitic greywacke; (D) SAN-19, mafic greywacke. Imagery captured in plane-polarised light (PPL)

SAN-19: A highly indurated mafic greywacke dominated by a highly chloritised clay-sized matrix (Fig. 3d & 4h). This unit encompasses angular volcanic quartz fragments (~20–30%) between 0.1–0.2 cm in size, disseminated pyrite and altered gas vesicles. Diagenetic mineralogy consists of albatised plagioclase crystals, chlorite, sericite, titanite

and a high abundance of iron-oxide minerals. Accessory minerals include hornblende, epidote and zircon.

SAN-19: A highly indurated mafic greywacke dominated by a chloritised clay-sized matrix (Fig. 3d & 4h). This unit encompasses angular volcanic quartz fragments (~20–30%) between 0.1–0.2 cm in size, disseminated pyrite and altered gas vesicles.

Diagenetic mineralogy consists of albatised plagioclase crystals, chlorite, sericite, titanite and a high abundance of iron-oxide minerals. Accessory minerals include hornblende, epidote and zircon.

Table 1: Summary of moraine sedimentary rock samples taken from the Bunger Hills, east Antarctica. Zone 47D.

Sample ID	Rock Type	Easting	Northing
SAN-2	Pink arkosic sandstone	2651338	0572277
SAN-9	Felsic volcanic clast	2651314	0572037
SAN-10	Greywacke-style conglomerate	2651214	0572661
SAN-12	Siltstone-argillite bearing conglomerate	2649773	0578173
SAN-13	Coarse greenish arkosic sandstone	2648402	0578422
SAN-14	Quartzitic greywacke	2648403	0578422
SAN-17	Heavy-mineral bearing sandstone	2644745	0582587
SAN-18	Greywacke-style conglomerate	2651314	0572037
SAN-19	Mafic greywacke	2644972	0569920

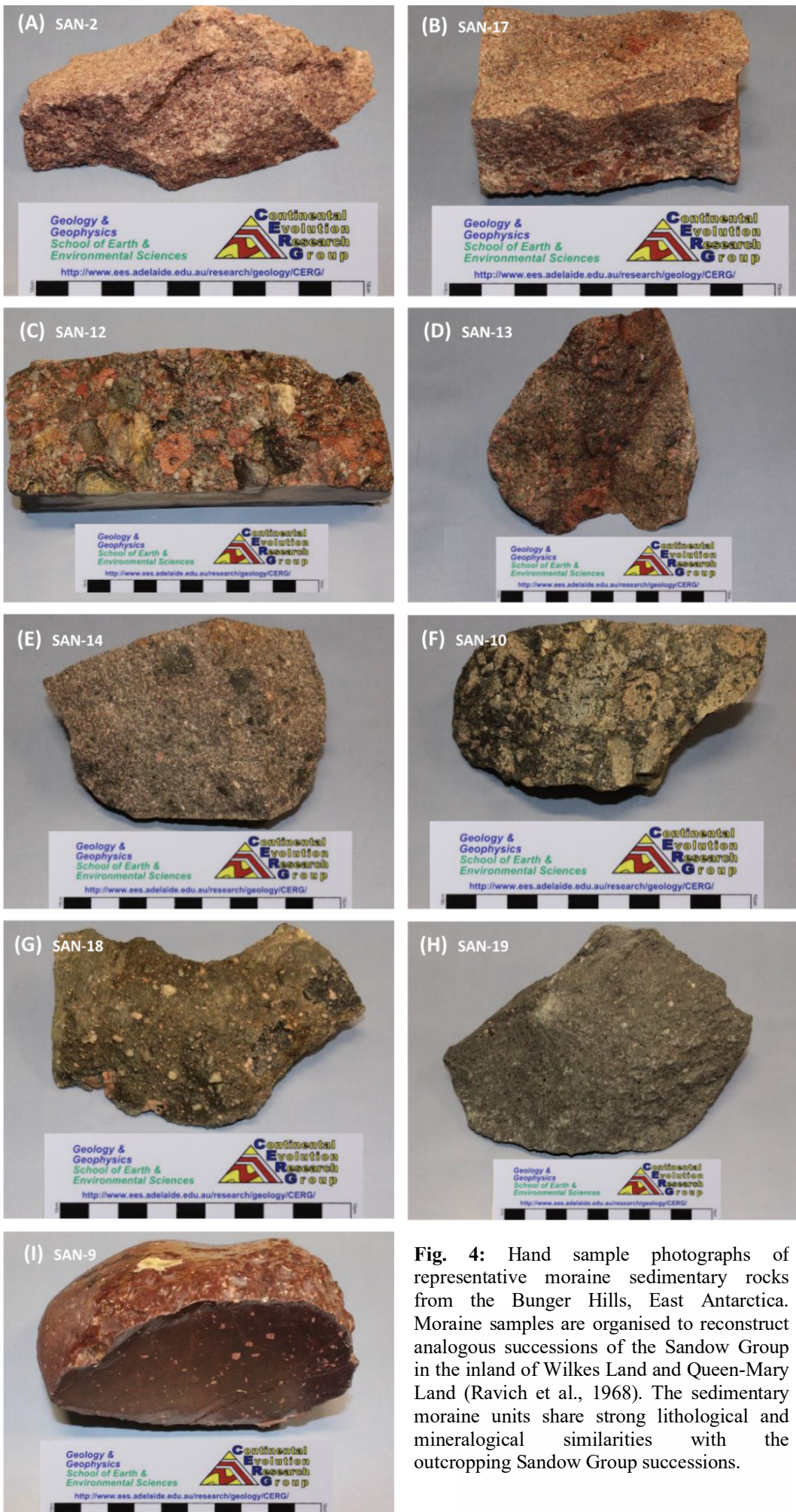


Fig. 4: Hand sample photographs of representative moraine sedimentary rocks from the Bunker Hills, East Antarctica. Moraine samples are organised to reconstruct analogous successions of the Sandow Group in the inland of Wilkes Land and Queen-Mary Land (Ravich et al., 1968). The sedimentary moraine units share strong lithological and mineralogical similarities with the outcropping Sandow Group successions.

Zircon U–Pb Geochronology

Zircon grain characterisation followed the classification scheme of Corfu (2003). CL imagery of representative zircon grains from all samples are presented in Fig. 5. Results from each sample are discussed below in order of their inferred stratigraphic position, as illustrated in Fig. 4.

Zircon U–Pb geochronology was undertaken on nine samples, representative of the moraine sedimentary lithologies collected from the Bunger Hills. Results of LA–ICP–MS detrital zircon U–Pb geochronology of all moraine samples are presented in Appendix C and illustrated on stacked TW Concordia diagrams in Fig. 6(a & b). Composite probability density plots and cumulative frequency histograms of $^{206}\text{Pb}/^{238}\text{U}$ ages for each sample are presented in Fig. 7. For independent probability density plots and histograms, and TW Concordia plots, refer to Appendix B.

Analyses that were $>5\%$ discordant and/or exhibited elevated concentrations of ^{204}Pb (non-radiogenic lead) were discarded from weighted mean calculations and appear as grey ellipses on the TW Concordia. Weighted average age calculations were performed using the $^{206}\text{Pb}/^{238}\text{U}$ age as the majority of concordant analyses yielded ages that were <1500 Ma (Roberts & Spencer, 2015).

SAN-2: pink arkosic sandstone

Zircon grains from this sample are typically red–brown to colourless and 70–500 μm in size. Grains are elongate–tabular with width to length aspect ratios of 1:2 to 1:4, and crystal faces are commonly euhedral–subhedral. CL imagery reveals weakly luminescent to bright, simple–complex oscillatory zoned rims marked by variable degrees of localised resorption. A minor zircon population preserves moderately-luminescent xenocryst cores

mantled by thin, dark overgrowths. Several grains are characterised as homogenous. Two-hundred analyses were collected; of which 89 were used to deduce detrital ages. Concordant data reveals a significant spread of ages between ca. 1361 and ca. 1087 Ma, with a principal unimodal population clustered at ca. 1160.9 ± 7.0 Ma ($n = 82/89$, MSWD = 14; weighted average $^{206}\text{Pb}/^{238}\text{U}$ age; Fig. 7a). Two analyses sit discordantly at ca. 1721 Ma and ca. 1720 Ma, these Paleoproterozoic ages are excluded from weighted average calculations.

SAN-17: heavy-mineral banded sandstone

Zircons from this sample exhibit both simple–complex oscillatory growth-zoning, a large population preserves dark to moderately luminescent xenocryst cores bordered by thin overgrowths. Grains are commonly euhedral, light-brown to colourless and 150–550 μm in size. Numerous intact grains display minor internal fracturing and the effects of-localised resorption of outer rims. Zircons are elongate–stubby with aspect ratios of 1:1 to 1:4. One-hundred and forty-five analyses were collected; of which 108 were <5% discordant. The data reveal a single unimodal population defined by a reasonably coherent, linear spread of ages between ca. 1362 Ma and ca. 1047 Ma, yielding a weighted average $^{206}\text{Pb}/^{238}\text{U}$ age of ca. 1171.3 ± 6.4 Ma ($n = 102/108$, MSWD = 16; Fig. 7b). A single analysis sits discordantly at ca. 1770 Ma.



Fig. 5: Cathodoluminescence imagery of representative zircon grains from moraine sedimentary rocks from the Bunker Hills. The scale bar demonstrates size of zircon grains and fragments. The location of U-Pb spot analyses and corresponding $^{206}\text{Pb}/^{238}\text{U}$ ages are shown. For full isotopic dataset refer to Appendix C.

SAN-12: siltstone–argillite bearing conglomerate

Zircons from this sample are typically elongate–tabular with subhedral crystal faces.

Grains are light-brown to colourless, range from 100–400 μm in size with aspect ratios of 1:2 to 1:3. CL imagery reveals moderately luminescent to bright, oscillatory-zoned cores and thin, dark overgrowth textures. Several grains are marked with apatite mineral inclusions, bright altered fracture seams and varying effects of metamictization. A minor proportion of zircons display well-defined sector zoning and extensive rim and core resorption and recrystallization. Two-hundred and two analyses were collected, of which 128 were used to deduce detrital ages. Concordant data reveal a substantial, but relatively coherent spread of ages between ca. 1355 Ma to ca. 1072 Ma, yielding a weighted mean $^{238}\text{U}/^{206}\text{Pb}$ age of ca. 1163.3 ± 5.3 Ma ($n = 119/128$, MSWD = 10.9; Fig. 7c).

SAN-13: coarse greenish arkosic sandstone

Zircons isolated from this sample display simple–complex oscillatory growth-zoning, are light-brown to colourless and 70–425 μm in size. Grains are highly elongate with aspect ratios of 1:2 to 1:5, with euhedral crystal faces. Numerous zircons display strongly luminescent, oscillatory-zoned xenocryst cores bordered by thin, dark overgrowths. Fewer grains are characterised as being homogenously unzoned and weakly luminescent, others exhibit variable localised resorption and re-crystallisation textures of outer rims. One-hundred analyses were collected, of which 73 were <5% discordant. A prevalent unimodal population spans between ca. 1223 Ma and ca. 1077 Ma ($n = 67$). A subordinate population of a several analyses appears to span discretely between ca. 1310 Ma and ca. 1267 Ma ($n = 6$). Concordant data yield a mean average $^{206}\text{Pb}/^{238}\text{U}$ age of ca. 1169.9 ± 5.7 Ma ($n = 65/73$, MSWD = 5.2; Fig. 7d).

SAN-14: quartzitic greywacke

Zircons from this sample are typically fragmented, light-brown to colourless, 100–450 μm in size and display simple–complex oscillatory growth-zoning. Grains are tabular–stubby with aspect ratios of 1:1 to 1.3, and crystal faces are subhedral–subrounded. A large proportion of grains preserve weakly-luminescent to bright, oscillatory zoned xenocryst cores mantled by thin, dark overgrowths. Some grains have experienced localised resorption, recrystallisation and metamictization of outer rims, while others are marked by mineral inclusions. One-hundred analyses were collected, of which 84 were used to deduce detrital ages. Concordant data reveal a relatively disseminated linear spread of ages ranging between ca. 1312 Ma and ca. 1073 Ma, yielding a weighted mean $^{206}\text{Pb}/^{238}\text{U}$ age of ca. 1162.7 ± 6.2 Ma ($n = 74/84$, MSWD = 9.1; Fig. 7e).

SAN-10: greywacke-style conglomerate

Zircons from this sample are typically colourless, exhibit highly-luminescent oscillatory growth-zoning and range between 100–450 μm in size. Grains are elongate–tabular and display euhedral–subhedral crystal faces, with aspect ratios of 1:2 to 1:5. Weakly luminescent, homogenously-zoned xenocryst cores are commonly preserved, mantled by thick oscillatory zoned domains and thin, dark overgrowths. Minor grain populations display complex oscillatory zonation, often disrupted by local recrystallization and metamictisation of outer rims. One-hundred and ninety-two analyses were collected, of which 122 were used to deduce detrital ages. Concordant data reveal a highly coherent unimodal population spanning between ca. 1223 Ma and ca. 1077 Ma, yielding a weighted mean $^{206}\text{Pb}/^{238}\text{U}$ age of ca. 1166.4 ± 3.6 Ma ($n = 116/122$, MSWD = 5.6; Fig. 7f).

SAN-18: greywacke-style conglomerate

Zircons from this sample are largely fragmented, light-brown to colourless, subhedral–anhedral and 100–400 μm in size. Grains are tabular–stubby with aspect ratios of 1:2 to 1:3. Majority of grains are characterised as homogenously unzoned and weakly luminescent or displaying complex oscillatory zonation. Commonly, highly resorbed, unzoned xenocryst cores are mantled by bright, fine-oscillatory growth bands. Two-hundred analyses were collected, of which 137 were <5% discordant. Concordant data reveal a largely coherent unimodal population clustering between ca. 1235 Ma and ca. 1131 Ma, yielding a weighted mean $^{206}\text{Pb}/^{238}\text{U}$ age of ca. 1179.1 ± 3.1 Ma ($n = 128/137$, MSWD = 8.2; Fig. 7g). Two analyses sit concordantly at ca. 1306 Ma and ca. 1271 Ma, detached from the main age population.

SAN-19: mafic greywacke

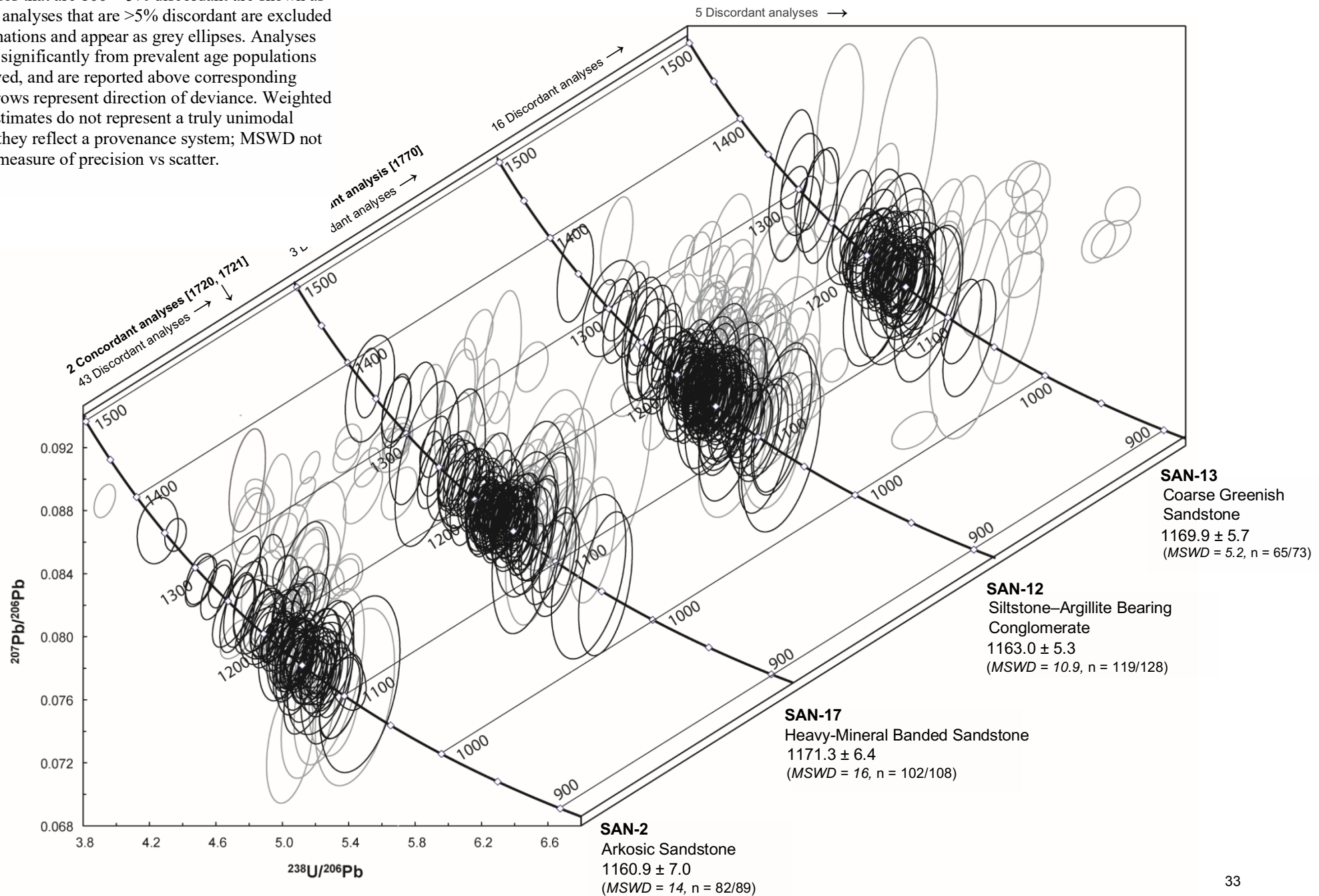
Zircons from this sample are commonly fragmented, brown–colourless, 100–400 μm in size and display both simple–complex oscillatory growth-zoning. Grains are generally tabular–stubby with aspect ratios of 1:1 to 1.3, and crystal faces are subhedral–subrounded. A large proportion of grains preserve weakly luminescent to bright, oscillatory zoned xenocryst cores mantled by thin, dark overgrowths. Some zircons have experienced localised resorption, recrystallisation and metamictization of outer rims, while others are marked by bright altered fracture seams. One-hundred analyses were collected, of which 73 analyses were used to deduce detrital populations. Concordant data reveal a relatively coherent, linear spread of ages spanning between ca. 1247 Ma and ca. 1090 Ma, yielding a weighted mean $^{206}\text{Pb}/^{238}\text{U}$ age of 1171.8 ± 5.5 Ma ($n = 68/73$, MSWD = 11.9; Fig. 7h). A single, isolated analysis sits concordantly at ca. 1312 Ma.

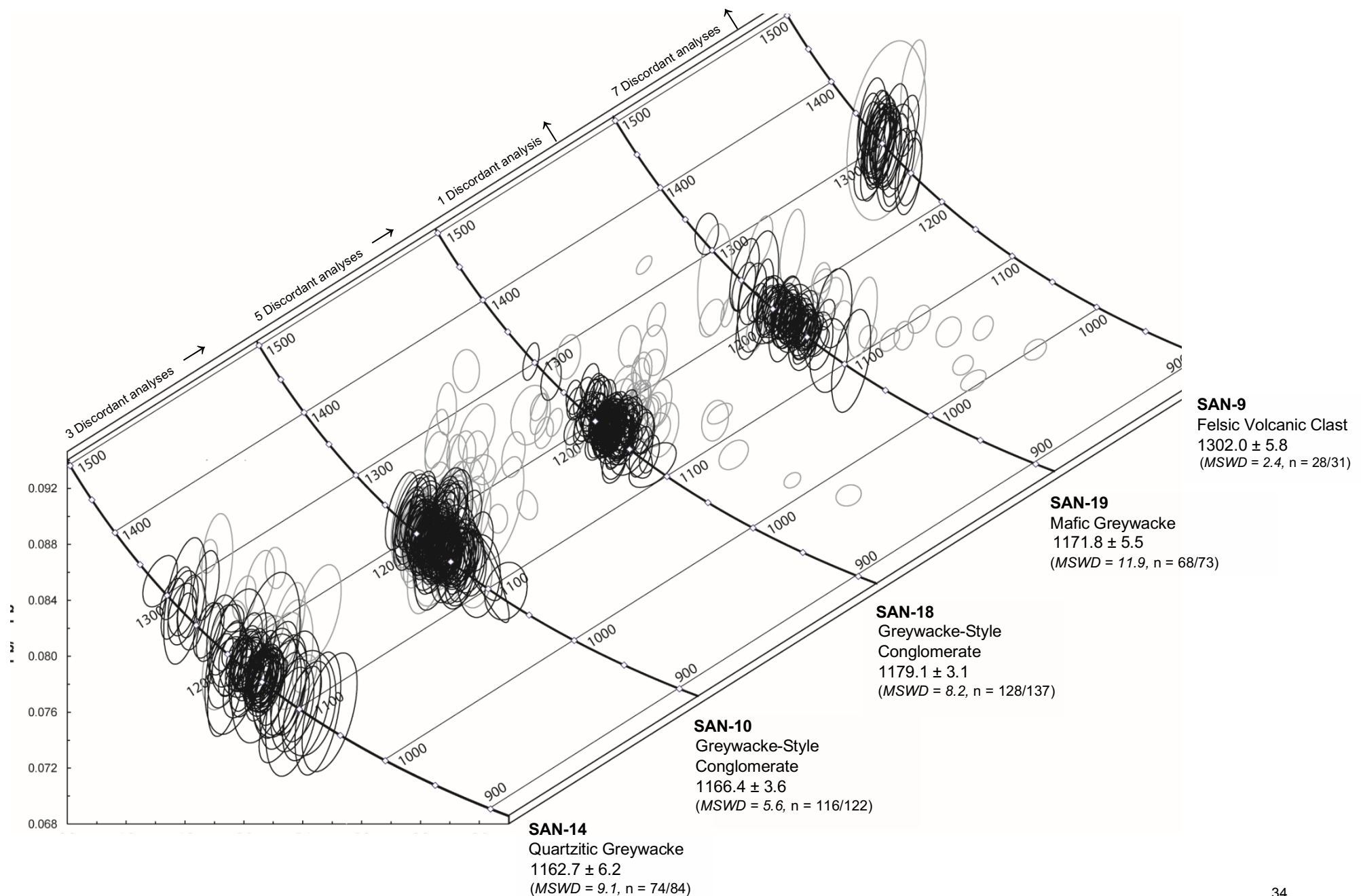
SAN-9: felsic volcanic clast

Zircons from this sample share distinctly similar morphologies. Grains are colourless, 70–250 μm in size and are largely undisturbed by post-crystallisation overprinting. A large proportion of zircons display a uniform, weakly luminescent central zone mantled by well-developed, finer oscillatory-zoned bands. Grains are typically elongate-tabular with euhedral–subhedral crystal faces. Zircons are moderately fragmented, with several grains marked by bright altered fracture seams, disrupting original zoning. Thirty-five analyses were collected to deduce detrital population ages, of these 31 analyses were used to deduce the crystallisation age. Concordant data reveal a moderately coherent, unimodal magmatic population spanning between ca. 1325 Ma and ca. 1251 Ma, yielding a weighted mean $^{206}\text{Pb}/^{238}\text{U}$ age of ca. 1302.0 ± 5.8 Ma ($n = 28/35$, MSWD = 2.4; Fig. 7i).

Fig. 6(a-b): Stacked Terra–Wasserburg Concordia diagrams for LA–ICP–MS zircon U–Pb geochronology. $^{206}\text{Pb}/^{238}\text{U}$ weighted average ages are quoted for each sample, which are presented in accordance to inferred stratigraphic position (see Fig. 3). Analyses that are $100 \pm 5\%$ discordant are shown as black ellipses, analyses that are $>5\%$ discordant are excluded from age estimations and appear as grey ellipses. Analyses which deviate significantly from prevalent age populations are not displayed, and are reported above corresponding Concordia; arrows represent direction of deviance. Weighted average age estimates do not represent a truly unimodal population as they reflect a provenance system; MSWD not an applicable measure of precision vs scatter.

Patrick Kolesik
Volcano-Sedimentary Moraines of the Bunker Hills





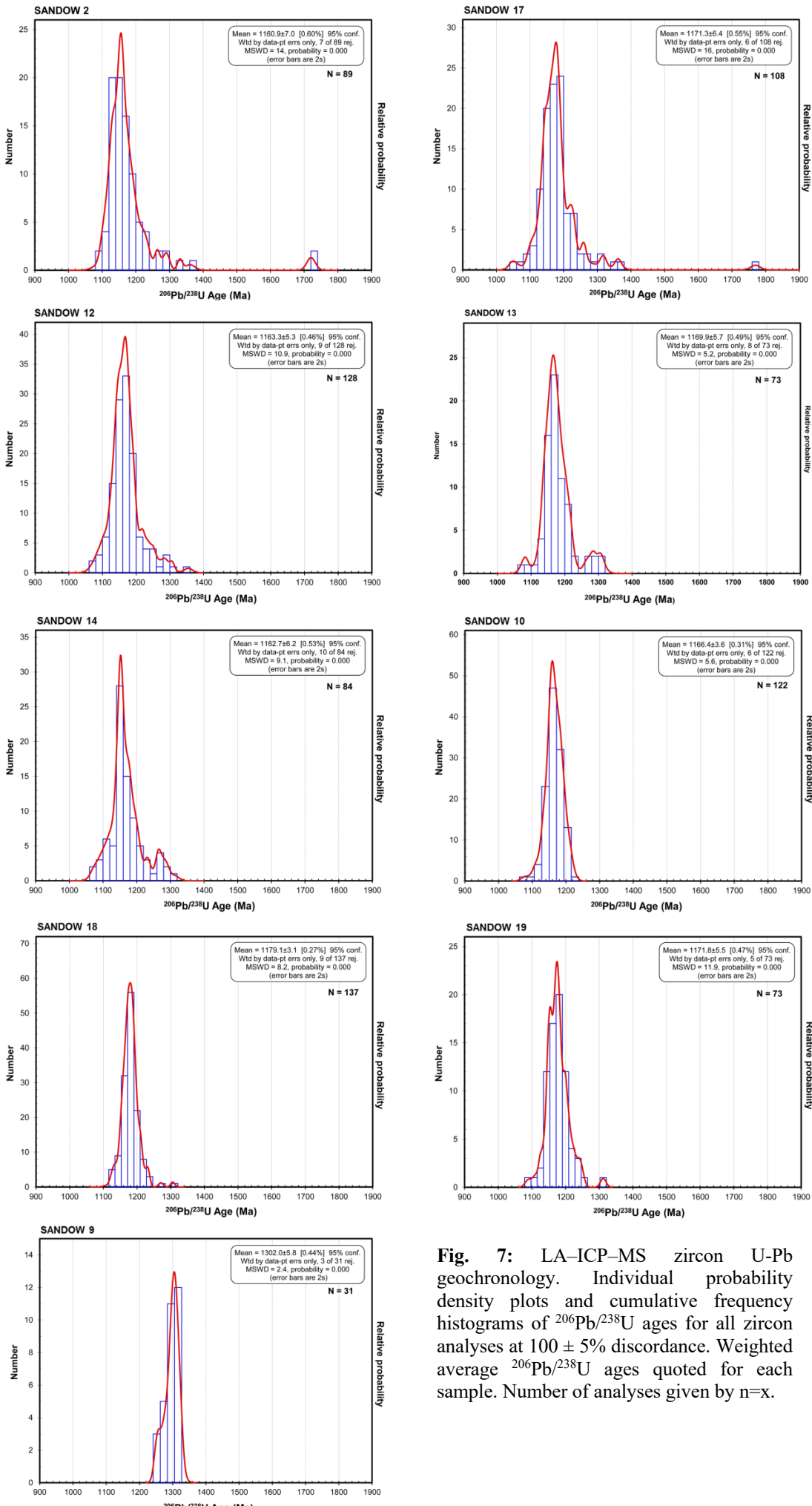


Fig. 7: LA–ICP–MS zircon U–Pb geochronology. Individual probability density plots and cumulative frequency histograms of $^{206}\text{Pb}/^{238}\text{U}$ ages for all zircon analyses at $100 \pm 5\%$ discordance. Weighted average $^{206}\text{Pb}/^{238}\text{U}$ ages quoted for each sample. Number of analyses given by n=x.

Authigenic Titanite U-Pb Geochronology

Fig. 9 shows the results of preliminary U–Pb age dating of authigenic titanite in sample SAN-17. Titanite occurs as overgrowths on ilmenite within heavy mineral bands (Fig. 8).

The analysed titanite grains contained large quantities of common Pb (up to 65 %). The data define a rough array that has a lower intercept of ca. 1070 Ma with a significant error. It is also evident that there may have been some modern Pb loss, as indicated by the patterns of horizontal analyses. For full isotopic dataset, refer to Appendix C.

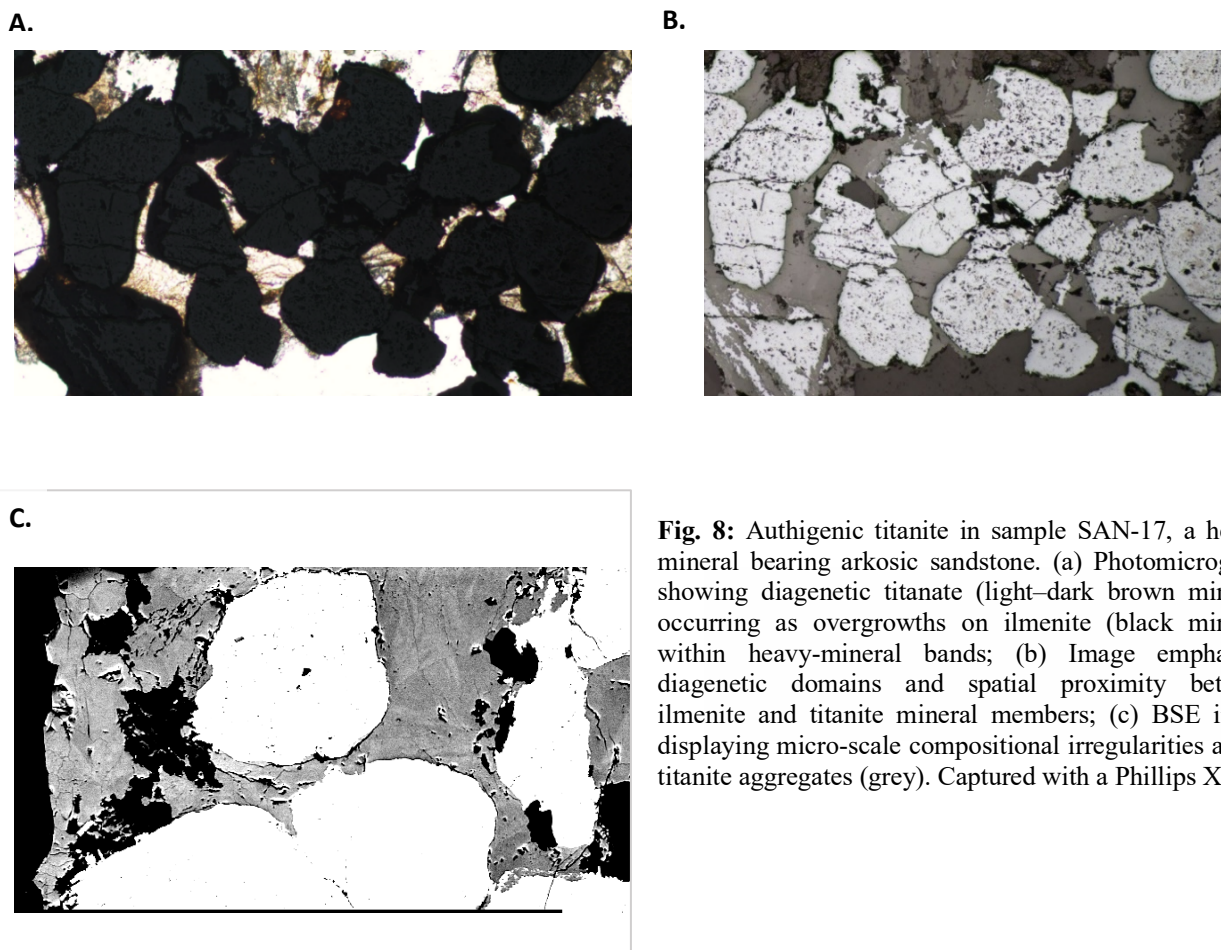


Fig. 8: Authigenic titanite in sample SAN-17, a heavy-mineral bearing arkosic sandstone. (a) Photomicrograph showing diagenetic titanate (light–dark brown mineral) occurring as overgrowths on ilmenite (black mineral) within heavy-mineral bands; (b) Image emphasises diagenetic domains and spatial proximity between ilmenite and titanite mineral members; (c) BSE image displaying micro-scale compositional irregularities across titanite aggregates (grey). Captured with a Phillips XL30.

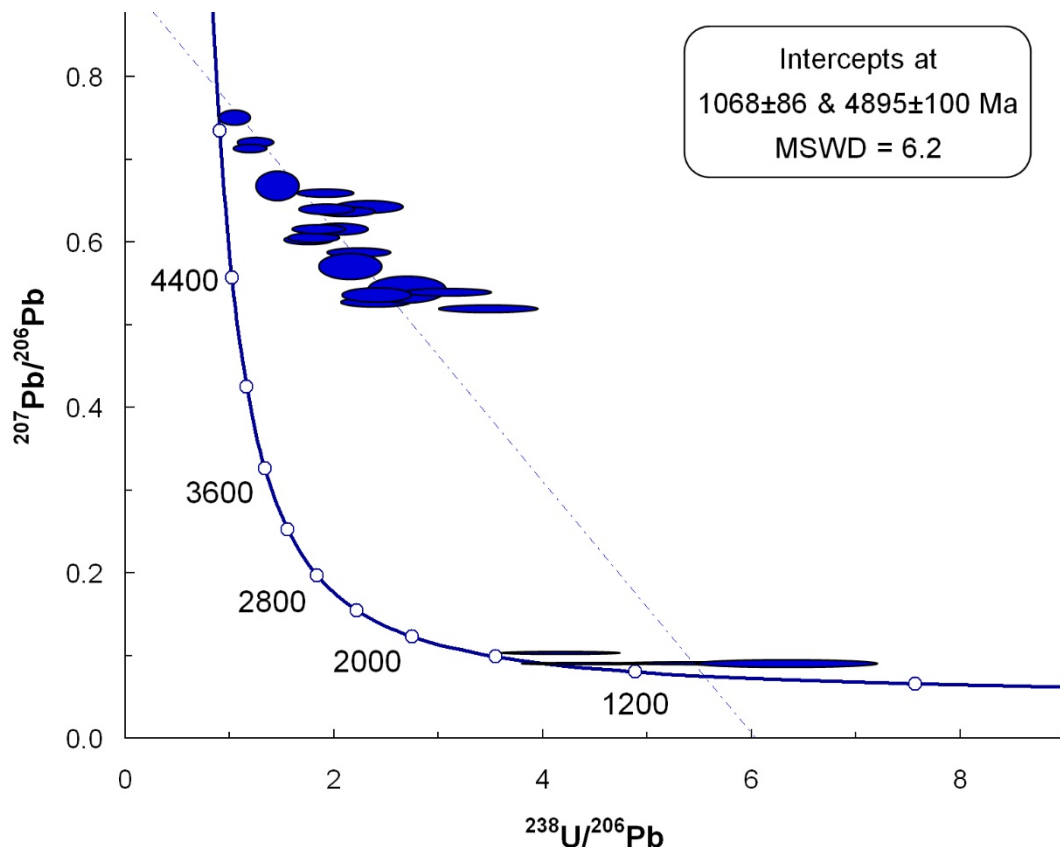


Fig. 9: Terra–Wasserburg Concordia diagram for SHRIMP titanite U–Pb reconnaissance geochronology (sample SAN-17). All analyses are shown. Data point error ellipses are to 2σ .

Kolmogorov–Smirnoff (K–S) Test

The Kolmogorov–Smirnoff (K–S) output matrix is reported in Table 2. The K–S test indicates that, at a 95% confidence level, all purely detrital age distributions are statistically indifferent and derive from a single parent population. The age distribution defining sample SAN-9, a single felsic–volcanic clast, was determined to be statistically incomparable, and failed the null hypothesis against all other sample distribution (Table 2a).

Table 2(a-b): K–S probability difference matrix comparing detrital age distributions of representative sedimentary moraines. Output tables (a–b) report P-Values and D-Values for the K–S test using uncertainties in the cumulative density function (CDF). A P-Value which exceeds 0.05 for a sample pair, indicates at a 95% confidence level, that the two age populations are statistically indifferent and satisfy the null hypothesis. Accepted values appear bold and highlighted in red. D-values indicate the maximum vertical deviation between two cumulative deviation plots. D has a maximum possible value of 1 and a minimum possible value of 0. K–S test Excel macro modified from Press et al., (1986) by Guynn & Gehrels (2010).

(a) K–S P-values using error in the CDF									
	SAN-10	SAN-12	SAN-13	SAN-14	SAN-17	SAN-18	SAN-19	SAN-2	SAN-9
SAN-10		0.910	0.509	0.906	0.515	0.052	0.835	0.820	0.000
SAN-12	0.910		0.997	1.000	0.980	0.025	0.566	1.000	0.000
SAN-13	0.509	0.997		0.993	1.000	0.297	0.966	0.975	0.000
SAN-14	0.906	1.000	0.993		0.956	0.038	0.544	1.000	0.000
SAN-17	0.515	0.980	1.000	0.956		0.323	0.996	0.891	0.000
SAN-18	0.052	0.025	0.297	0.038	0.323		0.941	0.024	0.000
SAN-19	0.835	0.566	0.966	0.544	0.996	0.941		0.465	0.000
SAN-2	0.820	1.000	0.975	1.000	0.891	0.024	0.465		0.000
SAN-9	0.000	0.000	0.000	0.000	0.000	0.000	0.000	0.000	

(b) D-values using error in the CDF									
	SAN-10	SAN-12	SAN-13	SAN-14	SAN-17	SAN-18	SAN-19	SAN-2	SAN-9
SAN-10		0.071	0.122	0.080	0.108	0.168	0.091	0.088	0.865
SAN-12	0.071		0.059	0.014	0.062	0.183	0.115	0.029	0.794
SAN-13	0.122	0.059		0.069	0.022	0.141	0.082	0.076	0.754
SAN-14	0.080	0.014	0.069		0.075	0.195	0.128	0.029	0.784
SAN-17	0.108	0.062	0.022	0.075		0.123	0.062	0.083	0.765
SAN-18	0.168	0.183	0.141	0.195	0.123		0.076	0.203	0.856
SAN-19	0.091	0.115	0.082	0.128	0.062	0.076		0.134	0.827
SAN-2	0.088	0.029	0.076	0.029	0.083	0.203	0.134		0.778
SAN-9	0.865	0.794	0.754	0.784	0.765	0.856	0.827	0.778	

Diagenetic Mineral Chemistry

Moraine samples of basaltic–volcanic character (SAN-10, 14, 18, 19) were selected for mineral chemistry analysis as the effects of diagenesis are more pronounced in these units. Elemental compositions for analysed diagenetic silicate minerals are presented in Table 3. For the full microprobe dataset, refer to Appendix C.

The authigenic mineral assemblages across all basaltic samples are dominated by fine-grained aggregates of chlorite–albite–sericite–quartz with minor titanite and iron-oxide minerals (i.e. magnetite, haematite). Apatite exists as an accessory phase.

Intergranular voids and intensely altered domains are occupied by excessive growth of chlorite with minor sericite and quartz. Sericite and quartz alteration products are commonly observed in close proximity to large, altered grains of orthoclase feldspar (Fig. 10b). Albite is typically observed as a replacement of plagioclase (pseudomorphed relicts; Fig. 10b), while titanite exists in close proximity to iron-oxide aggregates (Fig. 10d).

Table 3: Mineral chemistry values measured for representative diagenetic minerals in basaltic–volcanic samples (SAN-10, 14, 18, 19). Weight percent for each measured elemental oxide is reported. Diagnostic elements for each mineral are highlighted. Number of analyses given by n=x.

Element Oxide	Chlorite (n=33)	Orthoclase (n=14)	Sericite (n=9)	Albite (n=17)	Titanite (n=22)	Oxide (n=12)	Apatite (n=9)
CaO	0.53	0.01	0.22	0.27	24.34	0.15	53.26
MgO	11.85	0.00	2.15	0.07	0.27	0.09	0.14
TiO₂	0.64	0.01	0.20	0.03	31.93	1.28	0.08
SiO₂	26.26	63.82	49.32	66.24	29.16	0.36	0.77
Al₂O₃	18.20	18.11	29.11	20.57	4.76	0.65	0.37
FeO	27.56	0.12	4.34	0.46	3.03	100.04	0.39
MnO	0.63	0.00	0.02	0.01	0.06	0.04	0.06
Cr₂O₃	0.01	0.00	0.01	0.00	0.01	0.23	0.02
Cl	0.03	0.04	0.08	0.03	0.07	0.01	0.02
F	0.08	0.00	0.02	0.00	1.01	0.34	3.39
K₂O	0.29	15.96	6.06	0.19	0.08	0.05	0.02
P₂O₅	0.01	0.00	0.00	0.01	0.13	0.01	41.00
Na₂O	0.06	0.29	0.12	11.71	0.13	0.05	0.06
SrO	0.00	0.02	0.00	0.01	0.00	0.02	0.00
BaO	0.02	0.31	0.13	0.02	0.26	0.02	0.00
V₂O₃	0.02	0.00	0.05	0.00	0.23	0.20	0.01
ZrO₂	0.01	0.01	0.01	0.00	0.04	0.03	0.14
NiO	0.00	0.00	0.00	0.00	0.01	0.01	0.01
O	-0.04	-0.01	-0.03	-0.01	-0.44	-0.15	-1.43
TOTAL	86.20	98.71	91.83	99.64	95.10	103.46	98.34

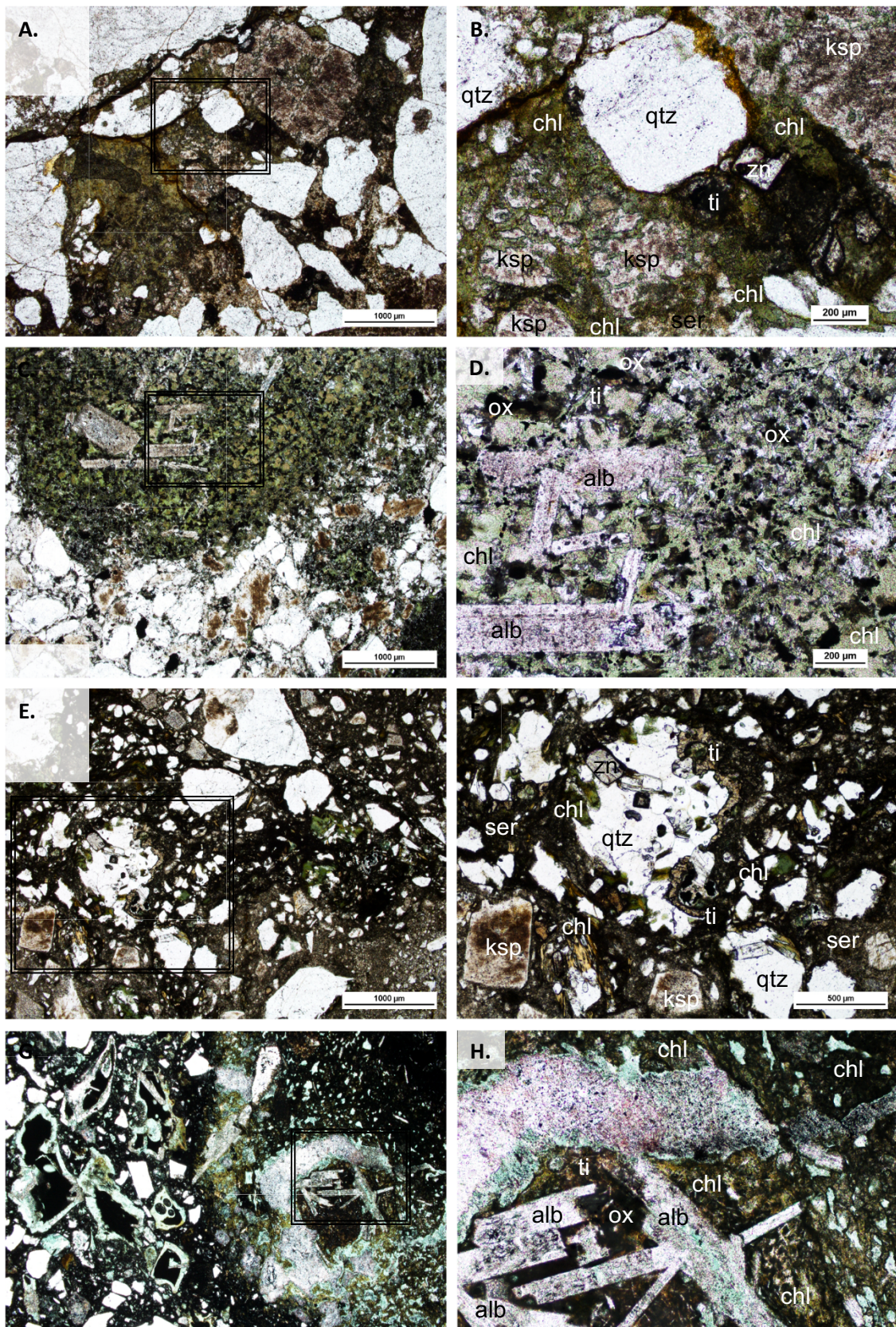


Fig. 10: Photomicrographs of petrological relationships of representative diagenetic mineral domains within selected basaltic–volcanic moraine samples. (a–b) SAN-10, greywacke-style conglomerate; (c–d) SAN-14, quartzitic greywacke; (e–f) SAN-18, greywacke-style conglomerate; (g–h) SAN-19, mafic greywacke. Boxed areas are magnified in adjacent images. Abbreviations: chl, chlorite; qtz, quartz; alb, albite; ksp, orthoclase feldspar; ser, sericite; tit, titanite; zn, zircon. Imagery captured in PPL.

DISCUSSION

Zircon U–Pb geochronology

U–Pb analyses of detrital zircons from volcano–sedimentary rocks of the Bunker Hills moraine yield concordant $^{206}\text{Pb}/^{238}\text{U}$ ages ranging from ca. 1364 Ma to ca. 1040 Ma ($n = 842$; Fig. 11a). The prevalent late Mesoproterozoic magmatic zircon population clusters discretely between ca. 1179 Ma and ca. 1161 Ma, provided by weighted average $^{206}\text{Pb}/^{238}\text{U}$ ages for all samples, excluding SAN-9. Sample SAN-9, a single non-metamorphosed felsic–volcanic clast, yields a well-defined crystallisation age of ca. 1302 ± 5.8 Ma, marking the position of a subordinate age population clustering between ca. 1261–1315 Ma. This secondary population, well-distinguished in SAN-9, is poorly represented in the remaining moraine zircon detritus, largely masked by a coherent linear spread of ages between the two principal age peaks (Fig. 11a).

In addition to the main ca. 1364–1040 Ma dataset acquired from all samples, three older analyses were obtained. These analyses lie concordantly at ca. 1721, ca. 1720 (SAN-2) and ca. 1785 Ma (SAN-17) and are inferred to represent inherited magmatic domains or minor components of older Paleoproterozoic zircons. The validity of these Paleoproterozoic ages is indisputable, however, due to poor representation it is impossible to attach any concrete significance or propose an entirely independent age component as a source region for the sedimentary detritus.

Sedimentary moraine units of the Bunker Hills

The moraine sedimentary rocks used in this study comprise an assortment of conglomerate, greywacke, quartzitic–feldspathic sandstone and intensely-altered

metabasalt. The majority of these units are highly indurated and encompass partially-recrystallised clasts of granitic material, rhyolite, argillite and cherry-brown siltstone.

The absence of high-grade metamorphic clasts and, conversely, a dominance of material of an igneous–volcanic and sedimentary nature, indicate the source region was non-metamorphosed and characterised by magmatic–volcanic rocks of felsic–mafic affinity. The pronounced angularity of the coarse igneous–volcanic clasts in particular, suggests derivation of material from a reasonably proximal system.

The Sandow Group

The non-metamorphosed and essentially undeformed nature of the Sandow Group, described by Ravich et al. (1968), contrasts with the highly metamorphosed and igneous bedrocks exposed in Queen–Mary Land. This suggests that the Sandow Group forms a cover sequence over the metamorphic and igneous basement.

The Sandow Group supracrustal successions consist of rhythmically-interlayered units of terrigenous and basaltic lithologies (Ravich et al., 1968; Sheraton et al., 1995). The sequence transitions from basal mafic-basaltic rocks (altered to dark-green chlorite – epidote schists) unconformably overlain by coarse conglomerates (various igneous–sedimentary clasts), towards finely interlayered quartzitic–feldspathic sandstones, argillites and ferruginous siltstones (Ravich et al., 1968).

Comparison of the moraine samples to the Sandow Group

The sedimentary rocks of the Bunger Hills moraine share marked lithological and mineralogical similarities, and are fundamentally identical to those of the Sandow Group. The Bunger Hills lie ~110 km downstream from outcrops of the Sandow Group and it is

interpreted that the sedimentary moraine materials of the Bunger Hills were derived from the glacial erosion of the Sandow Group successions, and as such, represent the essentially inaccessible and undocumented sedimentary province.

Depositional setting

The sedimentary fill pattern of the Sandow Group, which trends from basal, mafic-volcanoclastic and dominantly conglomeratic rocks to a largely siliceous sedimentary suite, is analogous to that of an intra-continental rift-basin sequence (Van Schmus & Hinze, 1985; Aharipour et al., 2009). The lowermost units (SAN-19) are suggested to have accumulated as basaltic lavas (Ravich et al., 1968) within crustal depressions during the early phase of rift-basin development, typically associated with the emplacement of basaltic dykes and voluminous bimodal igneous activity (e.g. Van Schmus, 1975; Aharipour et al., 2009).

Conversely, overlying terrigenous successions show close associations with developed rift-tectonism, and from the work of Van Schmus and Hinze (1985) are interpreted to have formed largely after cessation of igneous activity (post-volcanic). In particular, the massive quartzitic-feldspathic sandstone units (SAN-2, 17) which overly the primary, clastic rift-basin fill sediments (Van Schmus & Hinze, 1985), are interpreted to mark the transition into fluvial sedimentation under coastal–continental facies (Ravich et al., 1968), more characteristic of a well-developed rift system (Van Schmus & Hinze, 1985).

Authigenic mineral assemblages

The authigenic mineralogy of the moraine sedimentary rocks indicates that the Sandow Group sequence formed within a high-thermal, strain-free environment. Authigenic

assemblages in basaltic–volcanic samples include the extensive growth of chlorite–sericite–albite–quartz with minor amphibole, titanite and iron-oxides. In more felsic lithologies, diagenetic domains are dominated by quartz–chlorite–sericite with minor titanite and iron-oxide. These assemblages, particularly the widespread abundance of titanite across all samples, require reasonably high formation temperatures and are typically associated with burial metamorphism as opposed to diagenesis, reported by a number of workers (e.g. Kisch, 1979; Morad, 1988; Milliken, 2007).

Authigenic titanite U–Pb geochronology

U–Pb age data from authigenic titanite (SAN-17; Fig. 9) shows considerable scatter and is hampered by large amounts of common lead. The data define a common lead dominated array that has a lower intercept at around ca. 1070 Ma. Given the amount of common lead, and the scatter in the discordant array, means that any interpretation of the data is speculative. Nonetheless, the data make a case that authigenic titanite may have grown at around ca. 1070 Ma. The large MSWD reflects the scatter in the data, which is in part defined by horizontal data groups that suggest modern lead loss. If modern lead loss had occurred, the effect would be to draw the array regression to a slightly younger lower intercept. Based on the ages of detrital zircons, the maximum depositional age for SAN-17 is ca. 1362 Ma, providing a maximum age for authigenic mineral growth. Given the probability of some modern lead loss, authigenic titanite is likely to have grown sometime between ca. 1362 Ma and ca. 1070 Ma. If it is assumed that the authigenic mineral growth provides a minimum age for deposition, the data allow that basin development occurred close to or even within the time frame of the high-grade

metamorphism recorded in the Bunger Hills (e.g. Sheraton et al., 1993; 1995; Ding & James, 1991; Stüwe & Wilson, 1990).

Regional correlations

U–Pb analyses of detrital zircons from moraine sedimentary rocks of the Bunger Hills yield a spread of individual ages range from ca. 1364 Ma to ca. 1040 Ma, consistent with the timing of the two major phases of tectonothermal activity recorded by the AFO in southwestern Australia (Stage 1, ca. 1345–1260 Ma and Stage 2, ca. 1215–1140 Ma; Clark et al., 2000; Kirkland et al., 2011; Fig. 11c). It is apparent however, based on the principal late Mesoproterozoic age peak at ca. 1179–1161 Ma, that Stage 2 of the AFO has a pronounced imprint in the zircon detritus. A subordinate age population clusters between ca. 1315 Ma and ca. 1261 Ma and is consistent with the timing of Stage 1 AFO.

A Kolmogorov–Smirnoff (K–S) test had deduced that all purely detrital age distributions (excluding sample SAN-9) are statistically indifferent and reflect derivation from a single parent population (Table 2). This suggests, in conjunction with the pronounced angularity of the igneous–volcanic clasts in conglomeritic moraine samples, that the Mesoproterozoic-aged detritus is sourced locally from associated terrains of the secondary tectonothermal phase of the AFO.

Considering the majority of detrital zircons analysed are magmatic in origin, the principal late Mesoproterozoic zircon population is interpreted to reflect ages of igneous activity of the source regions, which coincides with the abundance of igneous–volcanic clasts, particularly of granitic composition, encompassed by the moraine sedimentary rocks. The emplacement of the Recherche Supersuite (ca. 1330–1280 Ma) and the Esperance Supersuite (ca. 1198–1135 Ma) mark the major pulses of magmatism associated with

Stage 1 and 2 of the AFO, respectively (e.g. Clark et al., 2000; Kirkland et al., 2011).

Sample SAN-9, a single non-metamorphosed rhyolite clast, yields a well-defined crystallisation age of ca. 1302.0 ± 5.8 Ma, with individual ages ranging between ca. 1251–1325 Ma, consistent with the emplacement of the Recherche Supersuite during Stage 1 AFO.

Combined zircon U–Pb data from the Bunger Hills bedrocks (Tucker et al., 2016; Tucker & Hand, 2016) reveal a younger Mesoproterozoic component comparable with the main age population recognised in the moraine detritus (Fig. 11b). The Bunger Hills record crystallisation of magmatic intrusives at ca. 1260 Ma and between ca. 1200 Ma (Tucker et al., 2016) to ca. 1150 Ma (Sheraton et al., 1995; 1995), with the latter coeval with the waning stages of granulite–facies metamorphism experienced by the region (Stüwe & Wilson, 1990; Sheraton et al., 1993; Tucker & Hand, 2016).

Detrital zircon U–Pb analyses from sand-sized moraine sediments from the Windmill Islands yields concordant $^{207}\text{Pb}/^{206}\text{Pb}$ ages ranging from ca. 1368 Ma to ca. 1107 Ma, with principal magmatic zircon populations at ca. 1107 Ma, 1150–1160 Ma, ca. 1196 Ma, 1231–1255 Ma, ca. 1317 Ma and ca. 1368 Ma, respectively (Fig. 11e; Zhang et al., 2012).

The moraine cover of the Windmill Islands is dominated by Mesoproterozoic high-grade metamorphic and igneous rocks comparable to those exposed in the bedrocks of Windmill Islands and the Bunger Hills, while a smaller proportion of the erratics reflect a basaltic–volcanic source, unrecognised in local in-situ outcrops (Zhang et al., 2012; Post, 2000; Rhodes, 2015). It is conceivable that a volcano–sedimentary province with a presumably comparable tectonic history to the Sandow Group occurs beneath the ice-concealed areas southeast of the Windmill Islands, Wilkes Land.

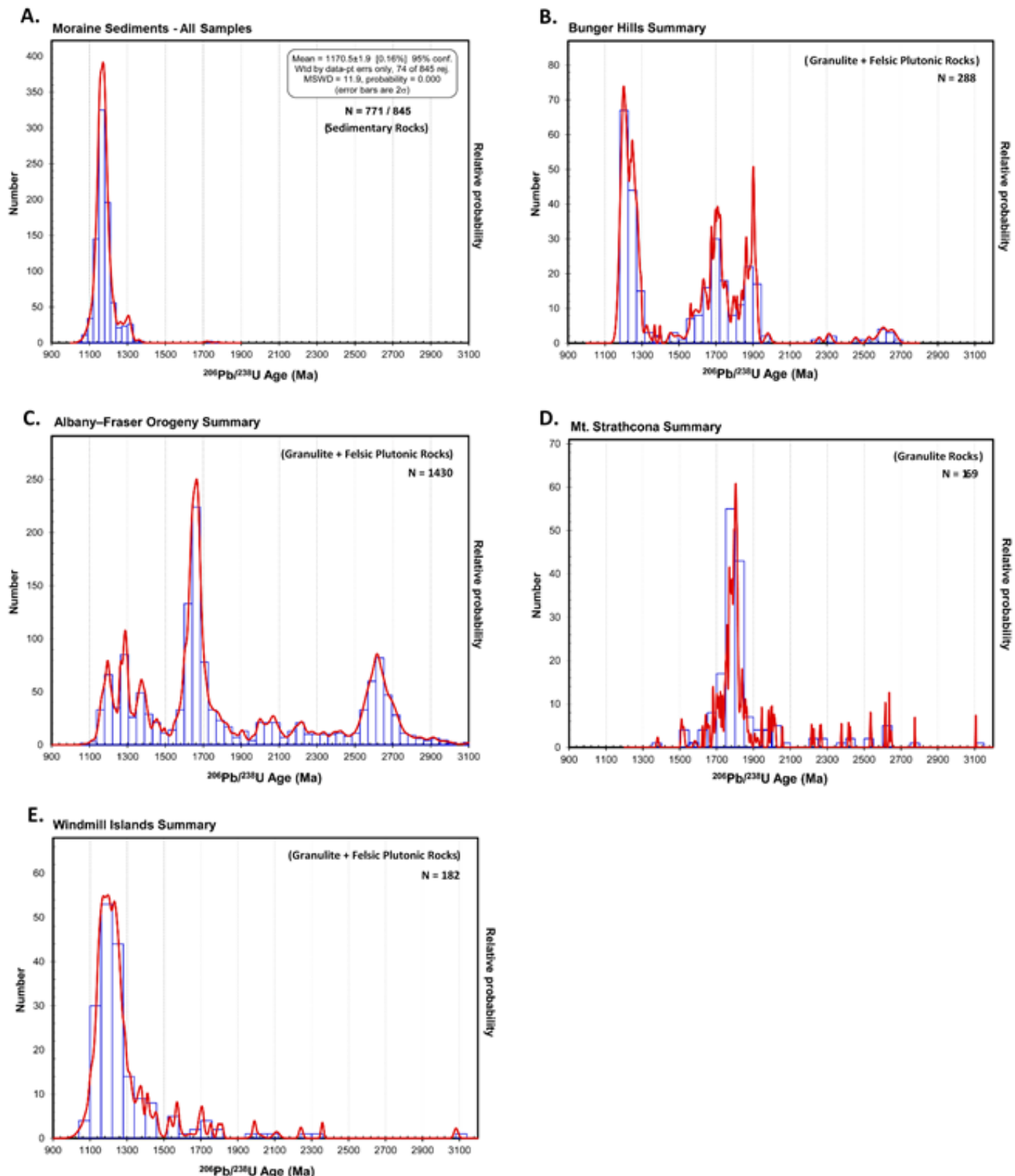


Fig. 11: Zircon U–Pb geochronology regional correlations histograms. Composite probability density plots and cumulative frequency histograms of $^{206}\text{Pb}/^{238}\text{U}$ analyses at $100 \pm 5\%$ discordance are shown. (a) The Bunger Hills, sedimentary moraine sediments (this study); (b) The Bunger Hills, granulite and felsic plutonic rocks (Tucker et al., 2016); (c) Albany–Fraser Orogen, granulite and felsic plutonic rocks (Spaggiari et al., 2015; Kirkland et al., 2011); (d) Mt. Strathcona, Queen–Mary Land, granulite rocks (Halpin, *unpublished data*); (e) Windmill Islands, in-situ granulite and felsic plutonic rocks and moraine sediments (Zhang et al., 2012). Sample SAN-9 excluded from composite probability density plot (a)—statistically determined to derive from a different age distribution (K–S test; Table 2).

An intra-continental rift-style basin

The lithological character, sedimentary fill pattern and essentially undeformed nature of the Sandow Group sequence (Ravich et al., 1968), suggests these supracrustal successions formed within an active intra-continental rift basin, compatible with the advanced diagenesis observed. The main late Mesoproterozoic magmatic zircon population in the sedimentary detritus is contemporaneous with the timing of the major phase of extension and associated voluminous magmatism during Stage 2 of the AFO (e.g. Clark et al., 2000; Kirkland et al., 2011), recognised in the Bunger Hills and adjacent areas of Wilkes Land and Queen-Mary Land (Stüwe & Wilson, 1990; Sheraton et al., 1993). In light of the reconnaissance U–Pb dating of authigenic titanite, it is permissible that basin development and the local erosion–sedimentation of a magmatic-rich carapace occurred syn-tectonically, and preceded the exhumation and availability of deeply-exposed crustal rocks. The proximity in space and time between intra-continental rifting and the developing Mesoproterozoic orogenic system (Stage 2 AFO) suggests that this tectonism is genetically related, as similarly proposed for the North American mid-continental rift system (Van Schmus & Hinze, 1985) and illustrated in the hypothesised tectonic scenario in Fig. 12 (discussed further).

A model for basin development

Several other well-recognised terrains (e.g. Southeast China block, Basin & Range Province – North America; Wang & Shu, 2012; Miller et al., 2001) are characterised by mid–lower crustal, high-temperature metamorphism, voluminous magmatism and volcano–sedimentary basin-fill systems associated with active extensional tectonism.

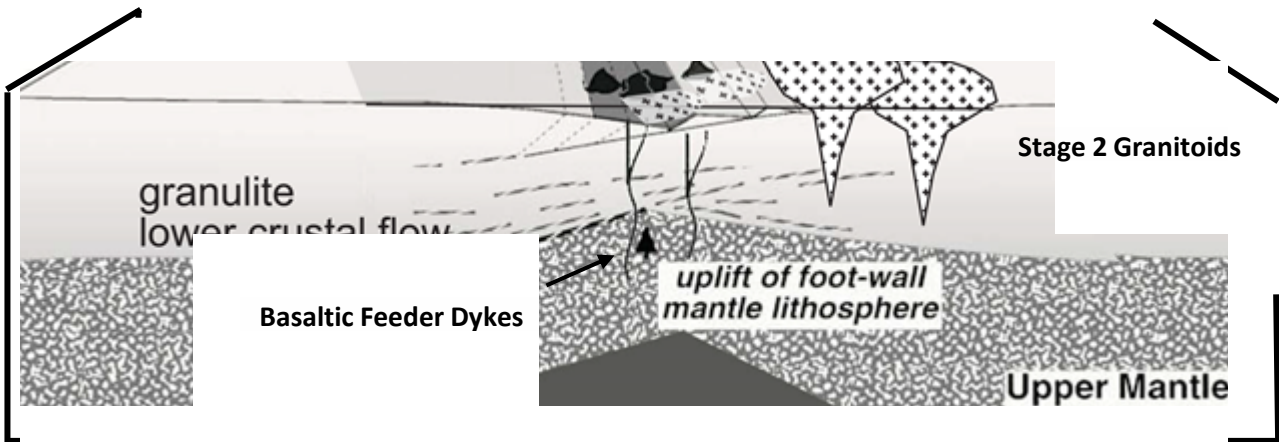


Fig. 12: A hypothesised tectonic scenario where intra-continental rift-basins evolve from basal mafic–volcanics to coarse, locally-derived clastic fill, within the confines of an extensional, high-temperature orogen (Stage 2 AFO). The hypothesised system shows local erosion and deposition of a magmatic-rich carapace, derived from the melting of the ductile lower crust (Stage 2 granitoids) prior to the exhumation and availability of granulite-facies metamorphic basement rocks. Basaltic feeder dykes derive from the melting of the upper-mantle during lithospheric stretching and are commonly expressed as extrusive lava flows that accumulate within crustal depressions. The high-heat flow system is responsible for the advanced diagenesis experienced by syn-rift sediments. Modified from Harris et al. 2002.

Occupying the Pacific coastal region of China, the Southeast China block (SECB) is characterised by a *basin-and-range-style* geomorphic–tectonic architecture (Wang & Shu, 2012) which developed as a result of extensional rifting within a back-arc setting during the Late Mesozoic, associated with the subduction of the paleo-Pacific Plate (e.g. Li, 2000; Zhou & Li, 2000; Zhou et al., 2006; Shu et al., 2009).

The tectonic evolution of this *basin-and-range-style* province, described by a series of asymmetric block-faulted fragments of continental crust (i.e. mountain ranges) that are separated by broad basins (Dickinson, 2002; American Geophysics Union, 1989), can serve as a tectonic analogue for the development of the Sandow Group sedimentary system.

Post-orogenic and intra-continental extensional basins formed during the Late Triassic–Early Jurassic, and developed syn-tectonically with a series of separate and parallel

mountain ranges (Miller et al., 2001), dome-type metamorphic core complexes and associated voluminous bimodal magmatism and volcanism (Wang & Shu, 2012; Dickinson, 2002).

The post-orogenic rift basins of interest formed through the Late Triassic–Early Jurassic (Wang & Shu, 2012) and received locally-derived terrestrial clastic, and coeval basaltic–rhyolitic fill, analogous to that of the Sandow Group sequence. The marked spatial proximity between Jurassic–Cretaceous magmatism and clastic sedimentation (SECB; Fig. 13) strongly suggests that the dominantly magmatic upper-crustal terrain was a primary source region for the syn-rift basin detritus, consistent with the lithological character of the marginally younger clastic sediments (Wang & Shu, 2012).

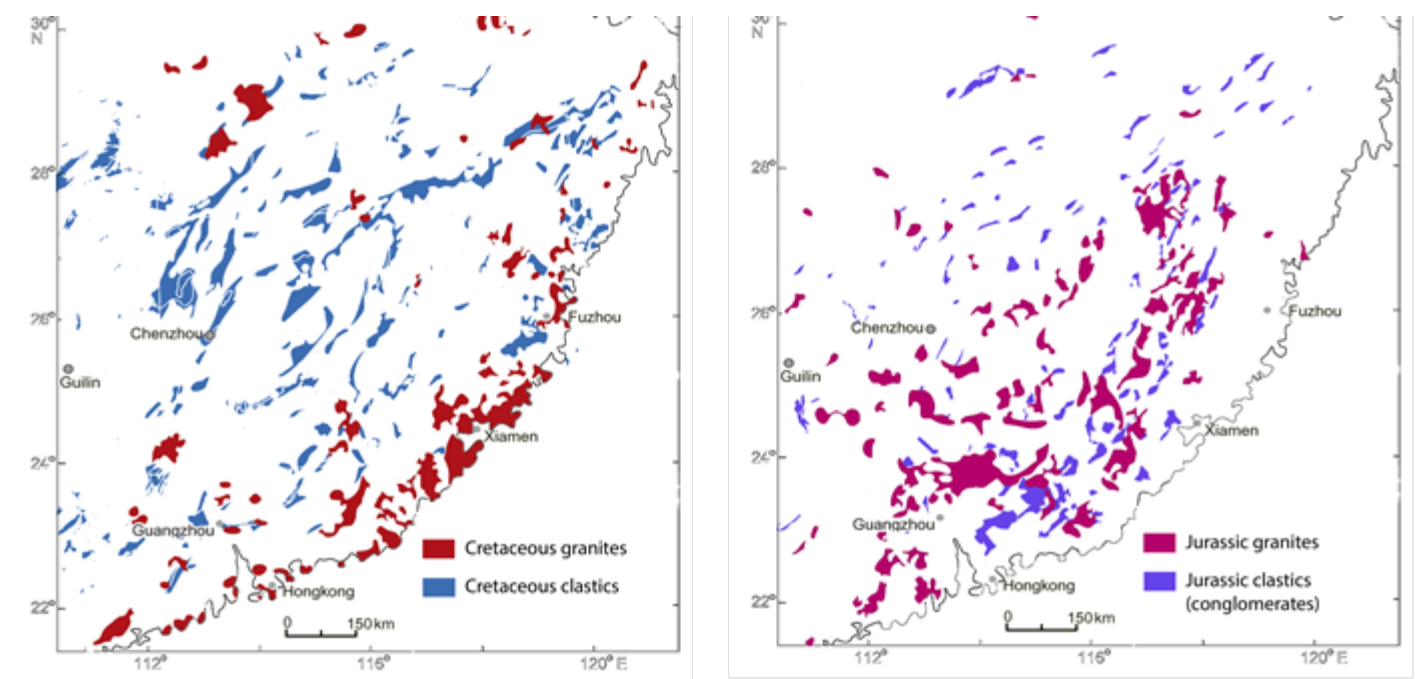


Fig. 13: Spatial distribution of granitic magmatism and clastic sedimentation during the Cretaceous and Jurassic, Southeastern China block (SECB). Modified from Wang & Shu, (2012).

A similar tectonic scenario can be envisaged for the development of the Sandow Group sedimentary system, hypothesised in Fig. 12, where basins that evolved from basal mafic-volcanics to coarse, locally-derived clastic fill could accumulate within the confines of a high-temperature orogen in an extensional setting.

If the hypothesised tectonic scenario is applicable, then it suggests that the development of the intra-continental rift basin occurred syn-tectonically, and is directly related to the geodynamic environment of granulite-facies metamorphic processes during the late Mesoproterozoic. It supports the notion that the second major tectonothermal phase of the AFO (Stage 2; ca. 1215–1140 Ma) was associated with extensional tectonism, voluminous magmatism–volcanism and high-thermal gradients, proposed by several previous works (e.g. Stüwe & Wilson, 1990; Sheraton et al., 1993). It is conceivable that this thermo-tectonic phase involved the evolution of basin-and-range-style architecture, which lead to the development of several rift-style volcano–sedimentary provinces with a similar tectonic history to the Sandow Group, concealed under thick ice-covers.

This study contributes to the geology and greater understanding of the East Antarctic Craton by elucidating the relationship of the geographically inaccessible Sandow Group supracrustal successions with the Mesoproterozoic evolution of east Antarctica.

CONCLUSIONS

- This study presents the first comprehensive zircon U–Pb geochronology of volcano–sedimentary rocks found in the moraine of the Bunger Hills, east Antarctica.
- U–Pb analyses of detrital zircons yield concordant $^{206}\text{Pb}/^{238}\text{U}$ ages ranging from ca. 1364 Ma to ca. 1040 Ma ($n = 842$), with a main late Mesoproterozoic magmatic zircon population clustered at ca. 1179–1161 Ma.
- Strong parallels with the time profile of in-situ rocks from the Stage 2 AFO, the Bunger Hills and Windmill Islands, suggest magmatic rocks associated with the high-grade metamorphism were the likely provenances for the associated moraine detritus.
- The sedimentary rock moraine clasts of the Bunger Hills are interpreted to have been glacially sourced from the Sandow Group, which outcrops on geographically inaccessible nunataks approximately 110 km inland from the Bunger Hills.
- The lithological character, sedimentary fill pattern and advanced diagenesis suggest that the Sandow Group formed within an active intra-continental rift-basin and represents the upper-crustal expression of extensional tectonism.
- Reconnaissance U–Pb geochronology of authigenic titanite suggests basin development occurred close to or within the time frame of the high-grade metamorphism recorded in the Bunger Hills, and is directly associated with the second major thermo–tectonic phase of the AFO.
- Due to the essentially non-metamorphosed volcano–sedimentary nature of the detritus in the sedimentary rocks, it seems likely that the evolving Mesoproterozoic orogenic system was not deeply exhumed during basin development.

ACKNOWLEDGMENTS

This thesis was conducted thanks to the financial support of the University of Adelaide. I sincerely thank M. Hand for excellent primary supervision, J. Payne (University of South Australia) for secondary supervision, and K. Howard and J. Farkas for ongoing guidance and support throughout the year.

I would like to sincerely express my gratitude to N. Tucker, for her invaluable support, advice and feedback on an earlier version of the manuscript. B. Wade, A. McFadden and staff of Adelaide Microscopy are thanked for training and support with analytical instrumentation.

I would like to acknowledge J. Halpin, the University of Tasmania, for her contribution of regional data, and R. Taylor, Curtin University, for conducting SHRIMP analysis on titanite samples.

REFERENCES

- AHARPOUR, R., MOUSSAVI, M., MOSADDEGH, R., & MISTIAEN, H. (2010). Facies features and paleoenvironmental reconstruction of the Early to Middle Devonian syn-rift volcano-sedimentary succession (Padeha Formation) in the Eastern-Alborz Mountains, NE Iran. *Facies*, 56(2), 279-294.
- AITKEN, A., YOUNG, D., FERRACCIOLI, F., BETTS, P., GREENBAUM, J., RICHTER, T., SIEGERT, M. (2014). The subglacial geology of Wilkes Land, East Antarctica. *Geophysical Research Letters*, 41(7), 2390-2400.
- BLACK, L. P., SHERATON, J.W., TINGEY, R., & MCCULLOCH, M. (1992). New U-Pb zircon ages from the Denman Glacier area, East Antarctica, and their significance for Gondwana reconstruction. *Antarctic Science*, 4(4), 447-460.
- BLACK, L. P., HARRIS, LYAL B., & DELOR, C.P. (1992). Reworking of Archaean and Early Proterozoic components during a progressive, Middle Proterozoic tectonothermal event in the Albany Mobile Belt, Western Australia. *Precambrian Research*, 59(1), 95-123.
- BOGER, S. D. (2011), Antarctica - Before and after Gondwana, *Gondwana Res.*, 19(2), 335–371.
- CANTARELLI, V., ALDEGA, L., CORRADO, S., INVERNIZZI, S., CASAS-SAINZ, A. (2013). Thermal history of the Aragón-Béarn basin (Late Paleozoic, western Pyrenees, Spain); insights into basin tectonic evolution. *Italian Journal of Geosciences*, 132(3), 443-462.
- CLARK, C., HENSEN, & KINNY. (2000). Geochronological constraints for a two-stage history of the Albany-Fraser Orogen, Western Australia. *Precambrian Research*, 102(3), 155-183.
- CORFU, F. (2003). Atlas of Zircon Textures. *Reviews in Mineralogy and Geochemistry*, 53 (1), 469-500.
- DICKINSON, W. (2002). The Basin and Range Province as a Composite Extensional Domain. *International Geology Review*, 44(1), 1-38.Li, 2000.
- DING, P., & JAMES P. (1991). Structural evolution of the Bunger Hills area of East Antarctica. *Geological Evolution of Antarctica*. Cambridge University Press, Cambridge, 13-18. *Extensional Tectonics in the Basin and Range Province between the Southern Sierra Nevada and the Colorado Plateau: The Basin and Range Province of Southern Nevada and Southeastern California June 30-July 7, 1989*. (1989). American Geophysical Union.
- FITZSIMONS, I. (2003). Proterozoic basement provinces of southern and southwestern Australia, and their correlation with Antarctica. *Geological Society, London, Special Publications*, 206(1), 93-130.
- FITZSIMONS, I. (2000). A review of tectonic events in the East Antarctic Shield and their implications for Gondwana and earlier supercontinents. *Journal of African Earth Sciences*, 31(1), 3-23.
- GOODGE, J. W., & FANNING, C. M. (2010). Composition and age of the East Antarctic Shield in eastern Wilkes Land determined by proxy from Oligocene-Pleistocene glaciomarine sediment and Beacon Supergroup sandstones, Antarctica. *The Geological Society of America Bulletin*, 122(7 8), 113.
- GOODGE, J. W., FANNING, C. M., BRECKE, D. M., LICHT, K. J., PALMER, E. F. (2010). Continuation of the Laurentian Grenville Province across the Ross Sea Margin of East Antarctica. *The Journal of Geology*, 118, 601–619.
- HALPIN, J. A., Mt. Strathcona U-Pb geochronology summary, *unpublished data*
- JACKSON, S.E., PEARSON, N.J., GRIFFIN, W.L., BELOUSOVA, E.A. (2004). The application of laser ablation-inductively coupled plasma mass spectrometry to in-situ U-Pb zircon geochronology. *Chemical Geology*, 211, 47-69.
- KIRKLAND, C.L., SPAGGIARI, C., PAWLEY, M.J., WINGATE, M., SMITHIES, R., HOWARD, H.M., POUJOL, M. (2011). On the edge: U-Pb, Lu-Hf, and Sm-Nd data suggests reworking of the Yilgarn craton margin during formation of the Albany-Fraser Orogen. *Precambrian Research*, 187(3), 223-247.
- KISCH, H. (1979). Chapter 5 Mineralogy and Petrology of Burial Diagenesis (Burial Metamorphism) and Incipient Metamorphism in Clastic Rocks11Manuscript completed in February, 1977. *Developments in Sedimentology*, 25, 289-493.
- LIU, XIAOCHUN, HU, JIANMIN, ZHAO, YUE, LOU, YUXING, WEI, CHUNJING, LIU, XIAOHAN. (2009). Late Neoproterozoic/Cambrian high-pressure mafic granulites from the Grove Mountains, East Antarctica: P-T-t path, collisional orogeny and implications for assembly of East Gondwana. *Precambrian Research*, 174(1), 181-199.
- LIU, XIAOCHUN, ZHAO, YUE, SONG, BIAO, LIU, JIAN, & CUI, JIANJUN. (2009). SHRIMP U-Pb zircon geochronology of high-grade rocks and charnockites from the eastern Amery Ice Shelf and southwestern Prydz Bay, East Antarctica: Constraints on Late Mesoproterozoic to Cambrian tectonothermal events related to supercontinent assembly. *Gondwana Research*, 16(2), 342-361.
- LUDWIG, K. R. (2012). User's manual for ISOPLOT 3.75, a geochronological toolkit for Microsoft Excel. *Berkley Geochronological Centre Special Publications* 5.

- MIKHALSKY, E.V., SHERATON, J.W., & HAHNE, K. (2006). Charnockite composition in relation to the tectonic evolution of East Antarctica. *Gondwana Research*, 9(4), 379-397.
- MILLER, J. (2001). Geological Society of London, & Tectonic Studies Group, UK. *Continental reactivation and reworking / edited by J.A. Miller [et al.]*. (Geological Society special publication, no. 184). Bath: Published by the Geological Society from the Geological Society Publishing House.
- MILLIKEN, K. (2007). Chapter 8 Provenance and Diagenesis of Heavy Minerals, Cenozoic Units of the Northwestern Gulf of Mexico Sedimentary Basin. *Developments in Sedimentology*, 58, 247-261.
- MORAD, S. (1988). Diagenesis of titaniferous minerals in Jurassic sandstones from the Norwegian Sea. *Sedimentary Geology*, 57(1), 17-40.
- PATON, C., HELLSTROM, J., PAUL, B., WOODHEAD, J., & HERGT, J. (2011). Iolite: Freeware for the visualisation and processing of mass spectrometric data. *Journal of Analytical Atomic Spectrometry*, 26(12), 2508-2518.
- PAYNE, J. L., HAND, M., BAROVICH, K., & WADE, B. (2008). Temporal constraints on the timing of high-grade metamorphism in the northern Gawler Craton: Implications for assembly of the Australian Proterozoic. *Australian Journal of Earth Sciences*, 55(5), 623-640.
- PEUCAT, J. J., CAPDEVILA, R., FANNING, C. M., MENOT, R. P., PECORA, L., TESTUT, L., (2002). 1.60 Ga felsic volcanic blocks in the moraines of the Terre Adelie craton, Antarctica: Comparisons with the Gawler Range volcanics, South Australia. *Australian Journal of Earth Sciences*, 49, 831-845.
- POST, N. J. (2000) Unravelling Gondwana fragments: An integrated structural, isotopic and petrographic investigation of the Windmill Islands, Antarctica. A thesis submitted for the degree of Doctor of Philosophy, University of New South Wales.
- POWELL, R. D., VOGEL, S.W., GRIFFITH, I., ANDERSON, K., SCHIRAGA, S. A. LAWSON, T. (2009) Subglacial Environment Exploration- Concept and Technological Challenges for the Development and Operation of a Sub Ice ROV'er and Advanced Sub-Ice Instrumentation for Short and Long-Term Observations. The IEEE/OES AUV 2008 Conference on Polar AUVs, October 13-14, 2008, Woods Hole, Ma, USA
- PRESS, W. (1986). *Numerical recipes: The art of scientific computing / William H. Press ... [et al.]*. Cambridge [England]; New York: Cambridge University Press.
- RASMUSSEN, FLETCHER, & MUHLING. (2013). Dating deposition and low-grade metamorphism by in situ U[²³⁸Pb]Pb geochronology of titanite in the Paleoproterozoic Timeball Hill Formation, southern Africa. *Chemical Geology*, 351, 29-39.
- RAVICH, M. G., KLIMOV, L. V & SOLOV'EV, D. S. (1968). The Pre-Cambrian of East Antarctica. Jerusalem. Israel Program for Scientific Translation Ltd. (Translation of Ravich *et al.*, 1965).
- REID, A., PAYNE, J. L., & WADE, B. (2006). A new geochronological capability for South Australia; U-Pb zircon dating via LA-ICPMS. *MESA Journal*, 42, 27-31.
- ROBERTS N. M. & SPENCER C. J. (2015). The zircon archive of continent formation through time. *Geological Society, London, Special Publications* 389, 197-225.
- SANDIFORD, M., & POWELL, R. (1986). Deep crustal metamorphism during continental extension: Modern and ancient examples. *Earth and Planetary Science Letters*, 79(1), 151-158.
- SHEPHERD, BAMBER, & FERRACCIOLI. (2006). Subglacial geology in Coats Land, East Antarctica, revealed by airborne magnetics and radar sounding. *Earth and Planetary Science Letters*, 244(1), 323-335
- SHERATON, J. W. (1995). Geology of the Bunger Hills-Denman glacier region, East Antarctica, Bulletin (*Australian Geological Survey Organisation*); 244). Canberra: Australian Govt. Pub. Service.
- SHERATON, J. W., TINGEY, R., BLACK, L. P., & OLIVER, R. (1993). Geology of the Bunger Hills area, Antarctica: Implications for Gondwana correlations. *Antarctic Science*, 5(1), 85-102.
- SHERATON, J. W., BLACK, L. P., & TINDLE, A. G. (1992). Petrogenesis of plutonic rocks in a Proterozoic granulite-facies terrain - the Bunger Hills, East Antarctica. *Chemical Geology*, 97(3), 163-198.
- SHERATON, J. W., BLACK, L. P., MCCULLOCH, M. T., & OLIVER, R. L. (1990). Age and origin of a compositionally varied mafic dyke swarm in the Bunger Hills, East Antarctica. *Chemical Geology*, 85(3), 215-246.
- SHERATON, J. W., & BLACK, L. P. (1983). Geochemistry of Precambrian gneisses: Relevance for the evolution of the East Antarctic Shield. *LITHOS*, 16(4), 273-296.
- SLAMA, J., KOSLER, J., CONDON D. J., CROWLEY, J. L., GERDES, A., HANCHAR, J. M., HORSTWOOD, M. S. A., MORRIS, G. A., NASDALA, L., NORBERG, N., SCHALTEGGER, U., SCHOENE, N., TUBRETT, M. N., & WHITEHOUSE M. J. (2008). Plešovice zircon - a new natural reference material for U-Pb and Hf isotopic microanalysis. *Chemical Geology*, 249, 1-35.
- SMITHIES, R. H., HOWARD, H. M., EVINS, P. M., KIRKLAND, C. L., KELSEY, D. E., HAND, M., WINGATE, M. T. D., COLLINS, A. S., BELOUSOVA, E. (2011). High-temperature granite magmatism, crust-mantle

- interaction and the mesoproterozoic intracontinental evolution of the Musgrave Province, central Australia. *Journal of Petrology* 52, 931–958.
- SPAGGIARI, C., KIRKLAND, C. L., SMITHIES, R., WINGATE, M., & BELOUSOVA, E. (2015). Transformation of an Archean craton margin during Proterozoic basin formation and magmatism: The Albany–Fraser Orogen, Western Australia. *Precambrian Research*, 266, 440.
- STUDINGER, BELL, BUCK, KARNER, & BLANKENSHIP. (2004). Sub-ice geology inland of the Transantarctic Mountains in light of new aerogeophysical data. *Earth and Planetary Science Letters*, 220(3), 391–408.
- STÜWE, K., & WILSON, C. J. L. (1990). Interaction between deformation and charnockite emplacement in the Bunger Hills, East Antarctica. *Journal of Structural Geology*, 12(5), 767–783.
- STÜWE, K., & POWELL, R. (1989). Metamorphic evolution of the Bunger Hills, East Antarctica: Evidence for substantial post-metamorphic peak compression with minimal cooling in a Proterozoic orogenic event. *Journal of Metamorphic Geology*, 7(4), 449–464.
- TUCKER, N. M., PAYNE, J. L., CLARK, C., HAND, M., TAYLOR, R. J., KYLANDER-CLARK, A. R. C. (2016) Proterozoic reworking of Archean (Yilgarn) basement in the Bunger Hills, east Antarctica (*Unpublished manuscript*)
- TUCKER, N. M., & HAND, M. (2016). New constraints on metamorphism in the Highjump Archipelago, East Antarctica. *Antarctic Science*, 1–17.
- TUCKER, N. M., HAND, M., KELSEY, D., & DUTCH. (2015). A duality of timescales: Short-lived ultrahigh temperature metamorphism preserving a long-lived monazite growth history in the Grenvillian Musgrave–Albany–Fraser Orogen. *Precambrian Research*, 264, 204–234.
- VAN DE FLIERDT, T., HEMMING, S., GOLDSTEIN, S., GEHRELS, G., COX, S. (2008). Evidence against a young volcanic origin of the Gamburtsev Subglacial Mountains, Antarctica. *Geophysical Research Letters*, 35(21)
- VAN SCHMUS, W., HINZE, W. (1985). The Midcontinent Rift System. *Annual Review of Earth and Planetary Sciences*, 13(1), 345–383.
- VAN SCHMUS, W. R. (1975). On the age of the Sudbury dike swarm. *Can. J. Earth Sci.* 86:907–14
- VEEVERS, J. J., SAEED, A., O'BRIEN, P. E. (2008). Provenance of the Gamburtsev Subglacial Mountains from U–Pb and Hf analysis of detrital zircons in Cretaceous to Quaternary sediments in Prydz Bay and beneath the Amery Ice Shelf. *Sedimentary Geology* 211, 12–32.
- VEEVERS, J. J., SAEED, A. (2008). Gamburtsev Subglacial Mountains provenance of Permian–Triassic sandstones in the Prince Charles Mountains and offshore Prydz Bay: integrated U–Pb and TDM ages and host-rock affinity from detrital zircons. *Gondwana Research* 14, 316–342.
- WANG & SHU, (2012). Late Mesozoic basin and range tectonics and related magmatism in Southeast China. *Geoscience Frontiers*, 3(2), 109–124.
- WHITE L. T., GIBSON G. M. & LISTER G. S. (2013). A reassessment of paleogeographic reconstructions of eastern 1048 Gondwana: Bringing geology back into the equation. *Gondwana Research* 24, 984–998.
- WONG, B. L., MORRISSEY, L. J., HAND, M., FIELDS, C. E., KELSEY, D. E. (2015). Grenvillian-aged reworking of late Paleoproterozoic crust of the southern North Australian Craton, central Australia: Implications for the assembly of Mesoproterozoic Australia. *Precambrian Research*, 270, 100–123.
- ZHANG, S.H., ZHAO, Y., LIU, X.C., LIU, Y.S., HOU, K.J., LI, C.F., YE, H. (2012). U–Pb geochronology and geochemistry of the bedrocks and moraine sediments from the Windmill Islands: Implications for Proterozoic evolution of East Antarctica. *Precambrian Research*, 206–207, 52–71.
- ZHAO, Y., ZHANG, S.H., LIU, X.C., HU, J.M., LIU, J., PAN, Y.B., AN, M.J., XU, G. (2007). Sub-glacial Geology of Antarctica: A preliminary investigation and results in the Grove Mountains and the Vestfold Hills, East Antarctica and its tectonic implication. In: Cooper, A.K., Raymond, C.R. (Eds.), *Antarctica: A Keystone in a Changing World*-Online Proceedings of the 10th ISAES X. U.S. Geological Survey and the National Academies, USGS Open-File Report 2007-1047, Extended Abstract 196, 4p.
- ZHOU, Y., JINCHENG, JIANG, SHAOYONG, WANG, XIAOLEI, MENGQUN. (2006). Study on lithogeochemistry of Middle Jurassic basalts from southern China represented by the Fankeng basalts from Yongding of Fujian Province - Study on lithogeochemistry of Middle Jurassic basalts from southern China represented by the Fankeng basalts from Yongding of Fujian Province. (10), 1020–1031.
- ZHOU, Y. & LIU, X. C. (2000). Origin of Late Mesozoic igneous rocks in Southeastern China: Implications for lithosphere subduction and underplating of mafic magmas. *Tectonophysics*, 326(3), 269–287.

APPENDIX A: EXTENDED METHODOLOGY

Sample acquisition/preparation

Twenty representative moraine sedimentary samples were collected from the Bunger Hills, East Antarctica, nine of which were selected for zircon U-Pb geochronology. Field work and sample acquisition was undertaken through 2014-2015, by M. Hand and PHD student N. Tucker of the University of Adelaide, C. Clark (Curtin University) and K. Wallace (field training officer). All samples were provided for this project in large hand sized form, to be processed for further analysis.

Petrography

Twenty thin sections were provided for this study, developed previously from acquired samples. An Olympus BX51 cross polarising optical microscope was used for investigation of sample mineralogy and acquisition of reflected photomicrograph imagery.

Petrographic analysis of a heavy mineral-banded sandstone, sample SAN-17, revealed a mineral with distinctly similar optical properties to titanite, recognised in close association with heavy mineral domains (presumably ilmenite/magnetite). The mineral was observed systematically separated (simple corona reaction texture) from heavy mineral domains, forming finer aggregates rather than euhedral grains, suggesting an authigenic nature. The domains of interest were marked on the slide and the sample was selected for imaging and further analysis (reflected photomicrograph and Back-Scatter-Electron (BSE) imagery, SHRIMP U-Pb geochronology), detailed in later sections.

Sample preparation

In order yield suitable zircon and titanite (titanite) grain sizes for analysis, the large samples required crushing before mineral separation was undertaken. These two methods were conducted in the basement lapidary of the Mawson Building, at the University of Adelaide. Samples were sawed, crushed and processed using conventional machinery and equipment, and separated both magnetic and heavy liquid (LST) techniques.

Preliminary laboratory training was conducted by Dr Katherine Howard (Teaching Support Officer – The University of Adelaide) with procedures and safety requirements clearly demonstrated and outlined as followed. Correct cleaning procedures were also outlined for each of the laboratories through training. Thorough cleaning of laboratories and equipment was essential before and after each sample was processed, in order to minimise bias and eliminate contamination. Appropriate safety apparel, including ear muffs, safety glasses and a lab coat was equipped prior to sample processing.

Sawing/crushing/sieving

Sawing, crushing and sieving of samples was carried out in the basement lapidary of the Mawson Building, following all required safety procedures. The laboratories were methodically cleaned prior to, and after each sample was processed as demonstrated through previous training. Samples were initially sawed to suitable sizes for Jaw Crusher processing, and the crushed material was then transferred between the Pulverisette Disc Mill and Sieve Shaker by large sheets of butcher's paper. The Jaw Crusher, Disc Mill, Sieves and Sieve Shaker equipment were cleaned thoroughly before and after the processing of each sample, using a high-pressure air gun and ethanol/cloth wipes.

The active components of the Jaw Crusher were initially set to a suitable width apart using the lever, to ensure effective functionality of the instrument. The underlying tray was lined with two sheets of butcher's paper to guarantee all processed material was collected. The Jaw Crusher was then correctly assembled and secured before samples were fed through and processed.

The two opposing discs of the Disc Mill were initially set to a width related to the size of the crushed material, to minimise strain on the instrument and allow a greater zircon yield. The disks were set to approximately 9 mm apart following crushing and graduated incrementally towards approximately 0.8 mm, at the final stages of processing. Once the instrument was secured, the crushed sample was progressively fed through from the butcher's paper and collected in the tray beneath. The milled sample was then transferred to the Sieve which was placed in the Sieve Shaker.

The Sieve was assembled on a sheet of butcher's paper, with new sieve mesh for each sample to avoid contamination. The Sieve was assembled in the following order: lower dish, fine (79 μm) sieve mesh, upper dish, another lower dish, coarse (425 μm) sieve mesh, upper dish, sieve lid. Milled material was transferred to the upper dish of the Sieve and secured in the Sieve Shaker by clamps on either side. The Sieve shaker was then run for approximately 5 minutes, until the milled sample was effectively separated between the sieve mesh. Disk Mill and Sieve processes were repeated, for every incremental reduction in Disk Mill separation width. Once the samples were milled down to a final ~0.9 mm and final stages of sieving were complete, the various grain sizes within the Sieve were collected into separate sealable sample bags and labelled accordingly. Sample material within the 79 – 425 μm range were used in mineral separation.

Mineral separation

Mineral Separation was carried out in the Mineral Separation laboratory located in the basement of the Mawson Building. The laboratory was methodically cleaned prior to, and after each sample was processed, as demonstrated through previous training. Zircon separation required three main steps: panning, magnetic and heavy liquid techniques. Panning was carried out on each sample (79 – 425 μm) using two panning bowels. The sample was

initially washed with water to remove all dust material and panned down to approximately 5% of the original quantity. The light minerals were separated through panning and captured into a large bowl, ensuring all material was retained. The panned light materials were then filtered (filter paper, funnel, beaker), dried in the oven (at <60°C), collected into separate sealable sample bags and labelled accordingly, for potential future use. The heavy mineral portion was filtered and dried on a hot plate (at <60°C) before application of magnetic techniques. Magnetic minerals were removed from the heavy mineral portion using two neodymium magnets wrapped in a number of kimwipes, and collected into a labelled vial.

Heavy liquid (lithium heteropolytungstates in water [LST], density 2.95 g/mL⁻¹ at 25 °C) was then used on the non-magnetic heavy mineral portion to further separate out the zircon population from minerals such as quartz/feldspars. This method was carried out in 15 ml sealable test tubes with the heavy portion thoroughly mixed with ~7-8 ml of LST. Materials with densities greater than 2.95 g/cm³ sank to the bottom of the test tube. The bottom tip of the test tube was then placed into contact with dry ice (carried out under the fume cupboard) and frozen, to allow the light mineral portion (densities <2.95 g/cm³) to be removed and filtered out effectively. Frozen zircon fractions were defrosted, filtered and rinsed multiple times with water to remove any residual LST. Filtered LST (concentrated and diluted) was retained and collected in appropriate containers. The rinsed zircon fractions were then dried on the hotplate (material on filter paper) and collected into small vials. All separated material was retained and labelled accordingly.

Picking and mounting mineral grains

Zircon grains were picked and mounted onto a teflon plate using two Olympus SZ61 optical microscopes at the University of Adelaide, Mawson Building. All picking/mounting equipment was thoroughly cleaned using ethanol and kimwipes between each sample, with a following visual check under the microscope. The bottom teflon plate for zircon mounting was prepared in the following way: bottom teflon plate, double sided sticky tape, single sided sticky tape (sticky side up). Protruding edges of the sticky tape were cut off and any bubbles were removed, to ensure relief differences did not develop in the epoxy resin. The non-magnetic heavy mineral zircon fraction was spread across a glass petri dish and zircons were picked using a standard needle pick (using natural skin oil as adhesive) under the microscope. The zircons were mounted on the teflon plate in a linear, orderly fashion, maintaining a ~4 mm distance away from the plate perimeter. Zircons were mounted as accurately as possible, to ensure fractures did not develop during grain re-positioning. Approximately 150 – 350 zircon grains were picked and mounted for each sample. It was critical to minimise selection bias, by picking all variable forms of zircon grains/fragments without conscious selection criteria. Once picking was complete, the residual sample material was returned to a vial.

Epoxy resin

Mounted zircons were entrained in epoxy resin; this was performed in the basement lapidary of the Mawson Building. All safety apparel was equipped (lab coat, safety glasses, gloves) and safety procedures were closely followed. The resin was prepared by combining EpoxiCure™ Epoxy Resin and EpoxiCure™ Epoxy Hardener (5:1 ratio, respectively) in a small plastic cup. Scales were used to ensure the mixture was prepared accurately. Using a wooden popstick, the mixture was mixed for ~10 minutes until completely transparent and homogenous. Mixing was done extremely slowly in a constant clockwise fashion, to ensure bubbles did not develop within the resin.

The mount mould was lined with a thin coat of Vaseline, prior to the application of the Epoxy resin to allow easy removal of the mount once the resin had set. The resin mixture was carefully poured into the mould, initially avoiding zircon grains, to ensure bubbles did not develop in these areas. A sample label (extremely small) was placed in the centre of the resin mould, as a form of permanent identification. The resin was then left to set over 24 hours before the mould was disassembled; separation of mould components was achieved with a thin blade. This procedure was repeated for each individual zircon mount.

Grinding

Epoxy mounts were ground to expose cores and reveal internal surfaces within zircon grains. This was conducted in the basement lapidary of the Mawson Building. The mounts were ground by running the zircon surface against the Zinc Lapping Disc in a figure-eight motion (minimal pressure applied). With the application of water to each, the Waterproof Silicon Carbide Paper FEPA P# 1000 was used for grinding initially, followed by FEPA P# 2000. Mounts were intermittently checked (reflected to transmitted light) under an optical microscope (Olympus BX51) to verify the degree of grinding and to ensure grains were not ground past the desired level. Once all the grains were ground to resin level and zircon cores were sufficiently exposed, the mounts were ready for polishing.

Polishing

Exposed zircon mounts were polished using the Struers™ DP-U4 Cloth Lap, located in the basement lapidary of the Mawson Building. Initially a 3µm Struers MD Dac™ polishing cloth was used to polish the mounts, followed by a 1µm Struers MD Nap™ polishing cloth (attached to magnetic plate of the cloth lap). 3µm and 1µm Diamond Suspension Polishing Lubricant was applied to the corresponding cloths prior to polishing. The Cloth Lap was configured to 100 RPM and the mounts were secured in the rotating arm (ensures even degrees of polishing), which was positioned ~4mm above the polishing cloth. The cloth lap (and rotating arm) was run for 10 minutes on each cloth size, with water applied to the surface throughout polishing. Mounts were intermittently

checked under an optical microscope (Olympus BX51) after each cloth size, to monitor the degree of polishing/removal of scratches.

Once polishing was complete, the mounts were submerged (zircon surface down) into a sonic bath which was run for approximately 5 minutes. This was performed after the use of each cloth size and had ensured residual diamond paste was removed from zircon surfaces (problems arise through imaging).

Zircon U-Pb geochronology

QUANTA 600 MLA SEM

Preliminary training for both the QUANTA 600 MLA scanning electron microscope (SEM) and New Wave Laser-Ablation-Inductive-Coupled-Plasma-as-Spectrometer (LA-ICP-MS) was conducted by A. McFadden (Microscopist – Adelaide Microscopy) with operating procedures clearly demonstrated and outlined as followed. Polished and carbon coated zircon mounts were imaged using the QUANTA 600 MLA (SEM) in both Back-Scatter-Electron (BSE) and Cathodoluminescence (CL). Carbon coating was essential for imaging, as to prevent negative charge build up at the mount surface (results in poor imagery). To further prevent charge build up, carbon tape was applied from the mount's edge to the SEM sample holder, care was taken to not cover zircons. Initially BSE imagery was taken of the mount (under lower magnification), to be stitched up at a later time. The composite BSE map proved a fundamental tool for spatial coordination across the zircon mount during laser ablation. CL imagery was taken at higher magnification (500x) revealing compositional variations/zonation and distinct growth domains in exposed internal zircon surfaces. Sites for LA-ICP-MS analyses were selected for on the basis of this CL and transmitted photomicrograph imagery. Ablation site selection was based on a number of characteristics relating to zircon nature, detailed in Corfu (2003). Areas marked with alteration, metamictization, fracturing and inclusions were strictly avoided as may account for and contribute to non-radiogenic lead contamination. A significant proportion of grains were excluded due to metamictization, metamorphic rims and complex recrystallization.

NEW WAVE LA-ICP-MS

LA-ICP-MS U-Pb zircon analyses were performed on the New Wave Nd-YAG laser operating at an output wavelength of 213nm under an Ar-He ablation atmosphere, coupled with an Agilent 7500cs/7500s ICP-MS at Adelaide Microscopy. The system was used to determine elemental concentrations and isotope ratios for elemental species ^{206}Pb , ^{207}Pb , ^{208}Pb , ^{238}U , while ^{235}U was calculated directly from ^{238}U (using a $^{238}\text{U}/^{235}\text{U}$ ratio of 137.88). Non-radiogenic ('common') ^{204}Pb was also monitored through analyses. Operating procedures and conditions for the laser ablation and ICP-MS system are detailed in, and follow those of Payne et al. (2008).

A single analysis involved 30 seconds of background signal acquisition, including 10 seconds for laser beam stabilisation (laser operational whilst shutter closed), followed by 30 seconds of ablation. Following each ablation, a washout delay of 30 seconds was configured. Ablation was carried out with a spot size of 30 μm , repetition rate of 5 Hz, fluence of 7 J μm^{-2} and energies of 65%. ^{238}U , ^{207}Pb , ^{206}Pb and ^{204}Pb isotopes were measured, for dwell times 15ms, 30ms, 15ms and 10ms, respectively.

The ablation process was run as a sequence of primary standards (GJ-1), secondary standards (PLES) and unknowns, repeated for each laser run until \sim 100 unknowns were analysed. The sequence order in which ablation sites were set was recorded to ease the process of data reduction. The basal sequence outline was as follows:

- **5X primary zircon standard (GJ-1)** [First sequence in laser run is set with **8X GJ-1**]
- **3X secondary zircon standard (PLES)**
- **3X primary zircon standard (GJ-1)**
- **1X secondary zircon standard (PLES)**
- **20X Bunger Hills sample (Unknowns)** [First sequence in laser run is set with **10X Unknowns**]

GJ-1 primary zircon standard was used to monitor data quality during analyses and yield weighted mean $^{206}\text{Pb}/^{238}\text{U}$ age of XXX.X \pm XX Ma (n= XXX), consistent with recommended values for this reference standard and analytical method.

To monitor data accuracy, repeat analysis of the Plesovich (PLES) secondary reference standard was undertaken by standard bracketing of every 10-20 unknown analyses. A linear-fit algorithm was applied to account for mass spectrometer drift. Repeat analysis of Plesovich during the analytical session yielded a $^{206}\text{Pb}/^{238}\text{U}$ weighted mean age of XXX.X \pm XX (n= XXX), also consistent with recommended values for this reference standard and analytical method (Sláma et al. 2008).

Titanite U-Pb geochronology

XL30 SEM

Preliminary training for the ‘Phillips XL30 SEM’ was conducted by B. Wade (Trained Expert – Adelaide Microscopy) with operating procedures clearly demonstrated and outlined as followed. The thin section was initially polished and carbon coated, before spot analysis (Back-Scatter-Electron – EDAX Genesis) was undertaken to verify the presence of authigenic titanite (rather than siderite – optically similar mineral). Spot analysis is useful in establishing elemental concentrations/ratios, and the output revealed the dominant elemental species in the mineral to be Ca, Ti, Si, O (titanite – CaTiSiO_5). Spot analysis also revealed compositional variability across the titanite grains, attributed to U, Fe and Al elemental proportions.

Once authigenic titanite was confirmed, the reaction domains were imaged in Back-Scatter-Electron (BSE) to capture and account for the compositional variability and the spatial distribution relative to surrounding mineralogy.

ASI M50 LA-ICP-MS

The ASI M50 laser system, coupled with a 7700 ICP-MS at Adelaide Microscopy was used to determine total Uranium content of the authigenic titanate (sample SAN-17) and its different compositional domains; sufficient U content is required for reliable SHRIMP U-Pb geochronology.

A single analysis involved 30 seconds of background signal acquisition, including 20 seconds for laser beam stabilisation (laser operational whilst shutter closed), followed by 30 seconds of ablation. Following each ablation, a washout delay of 20 seconds was configured. Ablation was carried out with a spot size of 20 μm , repetition rate of 5 Hz, fluence of 4 J μm^{-2} and energies of 50%. Desired elemental species, U, Ca, Ti, Pb, Fe, Al, Si, were selected for measurement for dwell times 0.10, 0.05, 0.05, 0.05, 0.05, 0.03, 0.03, respectively. The sequence order for ablation sites was recorded to ease the process of data reduction. The basal sequence outline was as follows:

- **3X Primary Concentration Standard (NIST610 ~500ppm)**
- **3X Secondary Concentration Standard (NIST612 ~50ppm)**
- **20X Titanite sites, SAN17 (Unknowns)**

Total Uranium counts (^{238}U and ^{235}U) were measured using the natural ^{238}U ratio of 133.88 (**AUTHOR???**). EDS spectra collected using the Phillips XL30 SEM, revealed an insignificant Ca variability across titanite compositional domains and hence Ca content (CPS) was used to correctly quantify total Uranium concentrations. ^{238}U content quantified using the molecular Ca weight percentage of 21.2 rather than the natural titanate stoichiometric ratio.

Frantz isodynamic magnetic barrier laboratory separator

Initially, highly magnetic minerals were removed from the SAN-17 heavy mineral portion ($>2.7 \text{ g/cm}^3$) using two neodymium magnets wrapped in a number of kimwipes, and collected into a labelled vial. The Frantz Magnetic Separator was then used to accurately separate titanite (titanite) from the remaining heavy mineral portion. Preliminary training with the instrument was conducted by K. Howard (Teaching Support Officer – The University of Adelaide) with procedures and safety requirements clearly demonstrated and outlined as followed.

The Frantz was configured with a tilt angle of 15° and a track angle of 20° and cleaned methodically prior to use, to prevent contamination. Based on the general magnetic susceptibility range of 0.7 → 1.7 amps for titanite, the Frantz was initially operated at 0.7 amps and 1.7 amps. The 0.7 – 1.7 amp portion was further run at 1.0 amps and 1.3 amps to

ensure effective magnetic separation of the mineral and potentially variable magnetic domains. Separates were examined under an optical microscope to ensure effective separation.

Sensitive high mass resolution ion microprobe (SHRIMP)

U-Pb geochronology on authigenic titanite was undertaken using the SHRIMP at Curtin University, Perth. Titanite was separated from crushed moraine sample ‘SAN 17’ using conventional magnetic and heavy liquid (LST) techniques at the University of Adelaide; analytical methods/techniques are identical to those utilised for zircon separation, detailed in earlier sections of Appendix A.

Data reduction & representation/modelling

DATA REDUCTION

Using *Iolite* 2.5, instrumental mass bias and depth-dependant elemental and isotopic fractionation were corrected for using GJ-1 as an external zircon reference standard (TIMS normalisation data: $^{207}\text{Pb}/^{206}\text{Pb} = 607.7$ Ma, $^{206}\text{Pb}/^{238}\text{U} = 600.7$ Ma and $^{207}\text{Pb}/^{235}\text{U} = 602.0$ Ma; Jackson et al., 2004). Data accuracy was monitored using Plesovich (PLES) as a secondary zircon standard of known age (337.13 ± 0.37 Ma; Sláma et al. 2008). U-Pb isotopic ratios and age estimates were determined using the same software.

Channels for ‘baseline’, ‘output’ and ‘standard’ signals were formed from each sample data set and fit with ‘linear interpolation’, ‘no fit’ and ‘linear fit’ integrations, respectively. ‘Visual Age (DRS)’ was selected as the data reduction scheme with ‘Z GJ-1’ as the primary reference standard. An isotopic count threshold of 10 was applied. Composite signals for all channels were trimmed at their ends (~2 seconds) and GJ-1 analyses which strayed significantly from the applied linear regression were discarded. Non-radiogenic lead (^{204}Pb) was not corrected for in age calculations due to unresolvable interference of ^{204}Hg on ^{204}Pb ; however, analyses were rejected if elevated ^{204}Pb signal was observed.

MODELLING AND DATA REPRESENTATION

U-Pb data subjected to data reduction, was transposed to a new *Excel* workbook where the rho and discordancy was calculated. Age estimations were calculated with uncertainties of 2σ (2 standard error) and a $100 \pm 5\%$ discordancy threshold was used in data interpretation. Individual Terra-Wasserburg concordia diagrams ($^{207}\text{Pb}/^{206}\text{Pb}$ vs. $^{206}\text{Pb}/^{238}\text{U}$), probability density plots ($^{206}\text{Pb}/^{207}\text{Pb}$) and weighted mean averages ($^{206}\text{Pb}/^{238}\text{U}$) were generated using *Isoplot* 3.75 in accordance to Isoplot Manual 4.1 (Ludwig, 2012).

Stacked Terra-Wasserburg concordia diagrams were generated for comparative purposes. Scales were fixed for each sample (900 – 1500 Ma) to allow effective comparison and discordant analyses were included, appearing in grey. Composite probability density plots from moraine sediments and surrounding regions were generated to help illustrate any parallels and identify possible provenance systems.

KOLMOGOROV-SMIRNOFF (K-S) TEST

In order to compare several detrital age populations and determine if a statistically significant difference exists between distributions, a Kolmogorov-Smirnoff (K-S) test was instigated. The K-S test was run through an Excel macro adapted from Press et al. (1986) by Guynn and Gehrels (2010).

The test specifically compares the maximum probability difference between two Cumulative Distribution Functions (CDF) and tests the null hypothesis that two distributions are the same, or have come from a single parent population. If the observed difference (D_{obs}) exceeds a pre-defined critical value (D_{crit}), the null hypothesis is rejected. D_{crit} is pre-defined and dependant on the number of samples in the distribution and the desired confidence level. To ensure statistical significance, it is recommended for number of samples for each distribution to exceed 20.

Initially all $^{206}\text{Pb}/^{238}\text{U}$ age data series refined to an uncertainty of 1σ (1 standard error) at 100 \pm 5% discordancy, entered into a data worksheet and categorized appropriately. The series were entered into the Excel macro unsorted and any data breaks were removed; these are considered as series terminations.

As an analysis option ‘CDF with error’ was selected; this K-S test includes uncertainty in the construction of the Cumulative Distribution Function (CDF). The CDF is similar to the Probability Density Function (PDF) however it sums the probabilities with increasing age. As a form of output ‘K-S distance matrix’ was selected; this reports the maximum probability difference between the CDF’s of all age series and generates a matrix of ‘P-Values’ and ‘D-Values’, used in the K-S test. Additional analysis/output options available were left unselected, as were not a requirement in running the statistical test. Once the macro was run, results were output in a new spreadsheet. The output table contains the ‘P-Values’ and ‘D-Values’ for each sample pair. The ‘P-Value’ indicates the probability that two samples were drawn from a single population. A ‘P-Value’ which exceeds 0.05, indicates at a 95% confidence level, that the two populations are statistically indifferent.

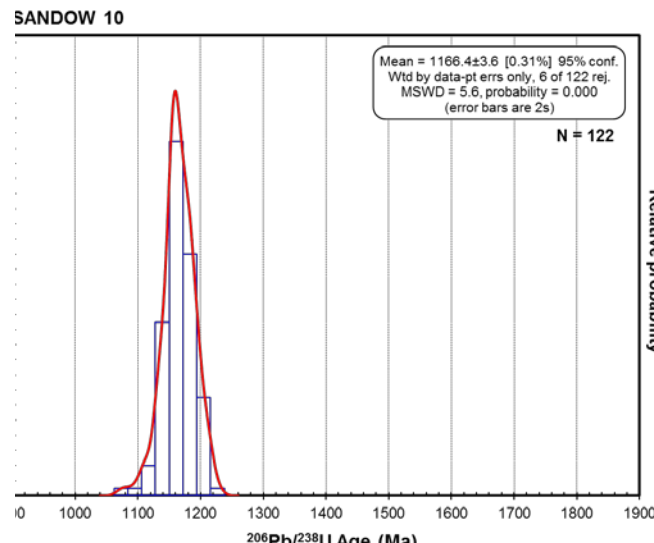
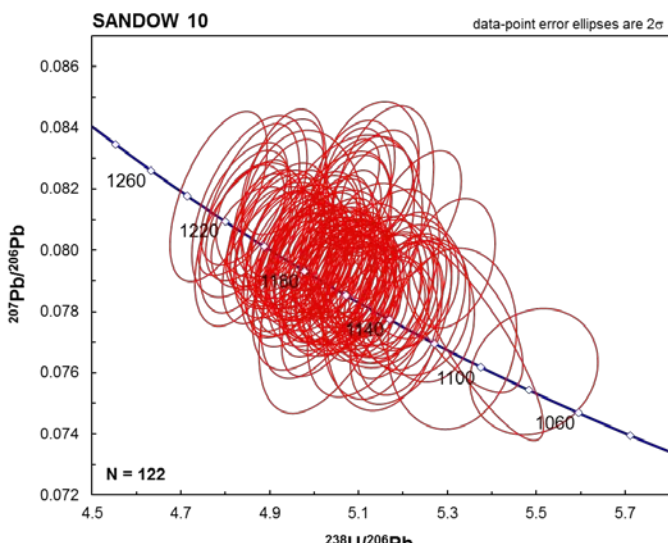
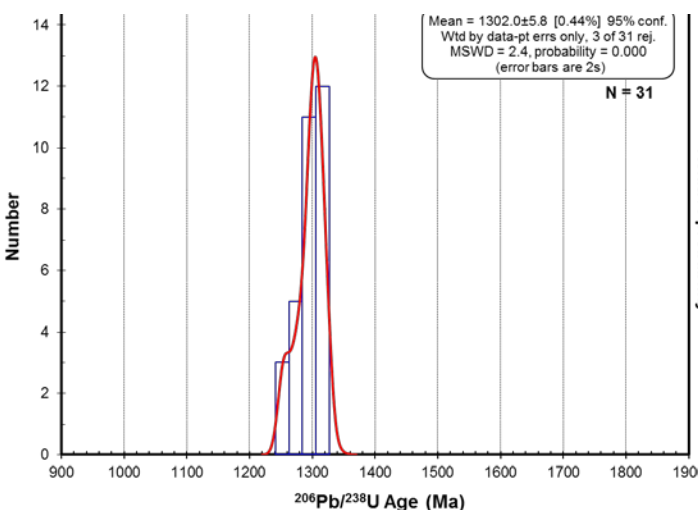
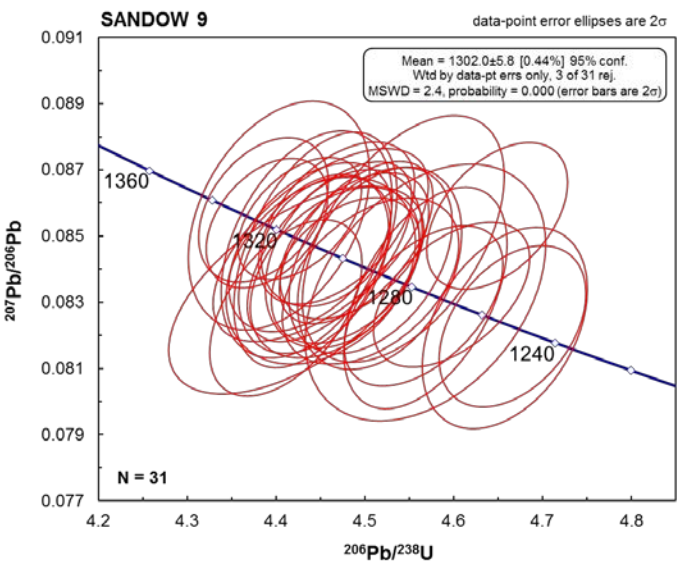
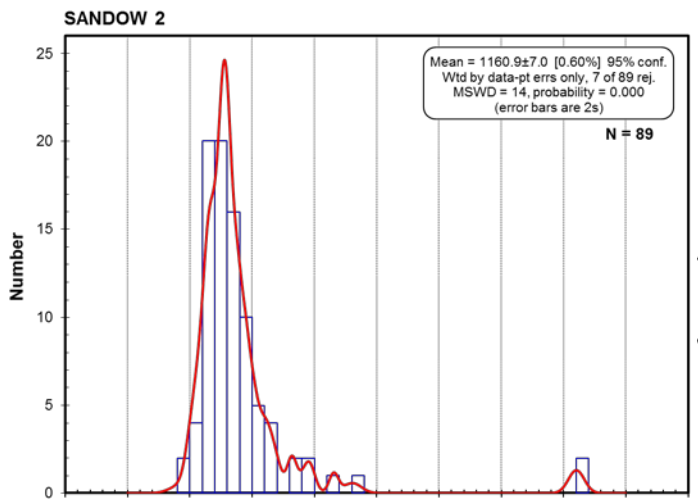
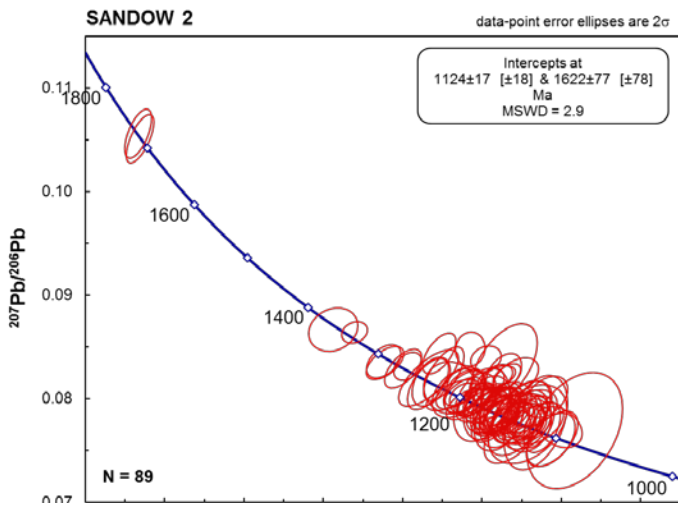
Diagenetic Mineral Chemistry via Electron Microprobe

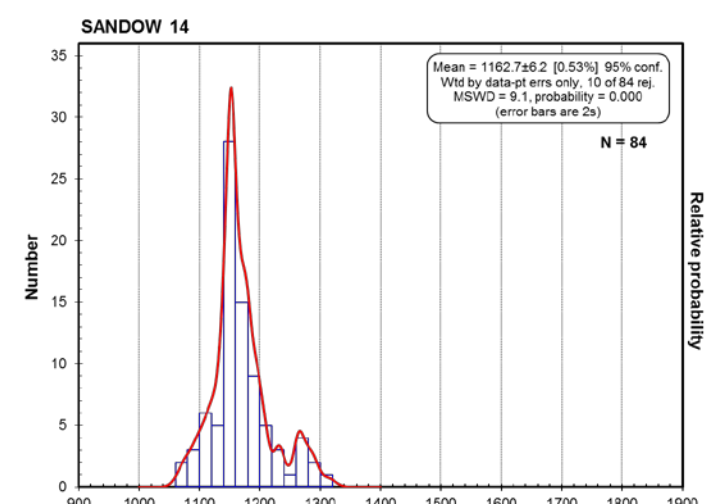
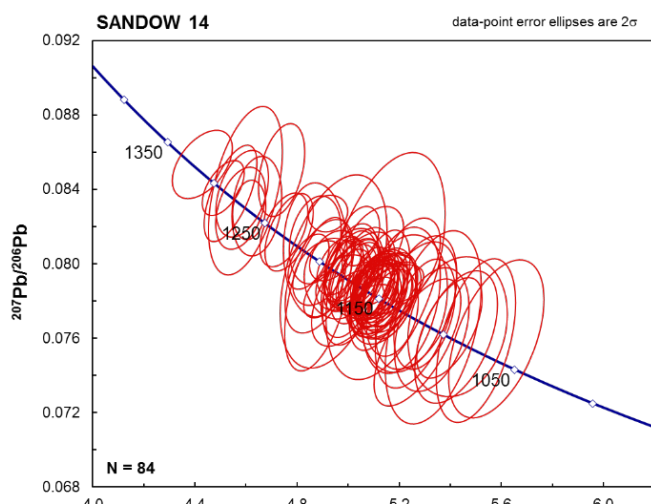
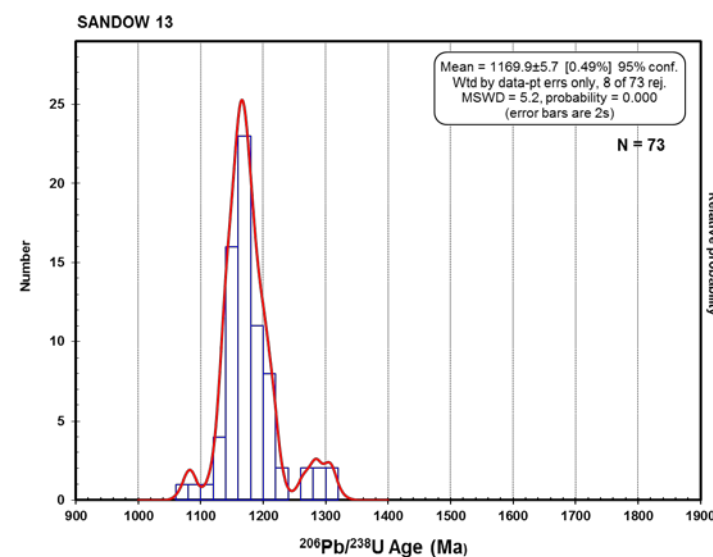
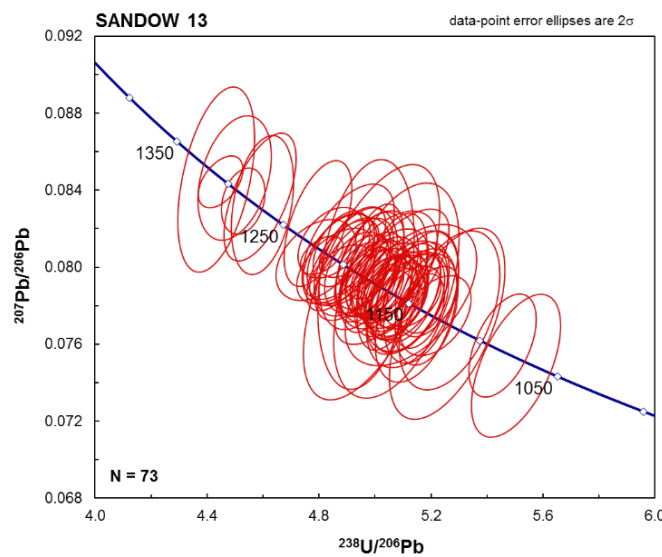
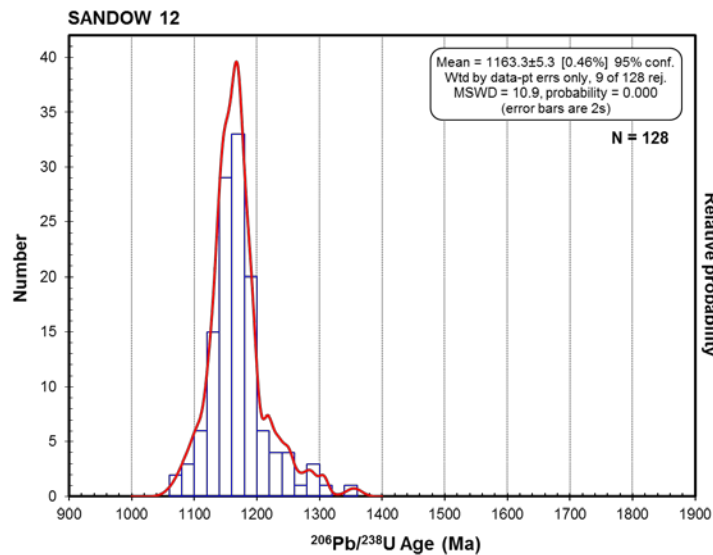
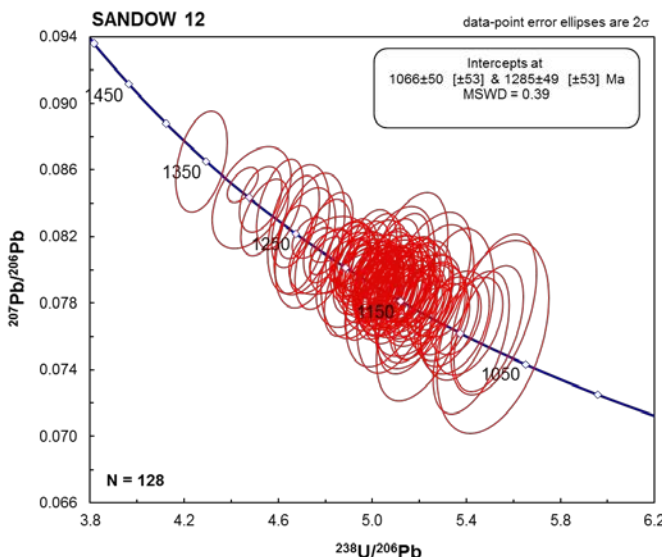
Quantitative analysis of diagenetic mineral chemistry was performed using a CAMECA SX 5 microprobe at Adelaide Microscopy, the University of Adelaide. Operating procedures follow those of Adelaide Microscopy. Calibration was done on natural and synthetic mineral standards following the standard protocols at Adelaide Microscopy.

A beam current of 20 nA and accelerating voltage of 15 kV and a focused beam were used for all point analyses. Routine analyses were made for SiO₂, ZrO₂, TiO₂, ZnO, Al₂O₃, V₂O₃, Cr₂O₃, FeO, MnO, MgO, CaO, BaO, Na₂O, K₂O, P₂O₅, Cl and F on Wavelength Dispersive Spectrometers (WDS).

1. To place a sample into the microprobe: Sample exchange-Transfer sample into microprobe. Follow the prompts. Next, turn the extraction handle on the airlock to the extract symbol.
2. Open the airlock (push airlock handle in and swing up). Note that handle locks and rotates slightly. Push extraction handle in all the way, then pull out to remove sample block. Close the airlock (rotate handle and swing down). Note that handle locks and moves out slightly.
4. After a minute or so, the airlock is vented. Open the airlock door by depressing the latch button and remove the sample cassette by pushing the sample block onto the extraction handle until it clicks and releases the sample block.
5. Change the samples as needed on the sample preparation pad.
6. Place the sample on the sample preparation pad and change samples and standard mounts as necessary. Be sure to document sample placement and identification by filling out the sample mount map in one of the 3 ring binders. Be sure to orient the sample block correctly. The small hole goes to the front of the sample mount. See the sample location chart for the correct orientation.
7. Place the prepared sample block back in the airlock: When ready, open the airlock door (depress the spring latch) and turn the extraction handle to the insert symbol. Then slide the sample block onto the extraction handle rails until it clicks.
8. Close the airlock door. During this time, the system may request that the gun valve be turned to position 2. If this is requested, turn the gun valve to position 2 and wait for the Vacuum ready message, if not, then the arlk command can be given immediately. When ready, pump out the airlock: Now open the airlock (push airlock handle in and swing up). Note that handle locks and rotates slightly. Push extraction handle in all the way, then pull the empty extraction handle back out all the way. Close the airlock (rotate handle and swing down). Note that handle locks and moves out slightly. Wait until the system is ready as seen on the screen.
11. Imaging is done via the SEM tab with a frame time of 15.32. Tick the box and press save and display. Once this is done, un-tick the box and return to 0.32 for the frame time. 12. To store points, ensure that the reflected image is focused. Move the white cross to desired position. On the left hand screen where the software is displayed, click ‘digitize’. Type in the name of the file. Finally, click add new unknown. Adding a single point is done by clicking ‘single point’
13. Once all points have been selected, select all. Click sample set up, then yes. Finally, to start the acquisition, press the button ‘run samples’ .

APPENDIX B: TW CONCORDIA & PROBABILITY DENSITY PLOTS





APPENDIX C: LA-ICP-MS ZIRCON U-PB GEOCHRONOLOGY

UNKNOWN ANALYSES

Analysis #	$^{207}\text{Pb}/^{206}\text{Pb}$	$\pm 2\sigma$	$^{207}\text{Pb}/^{235}\text{U}$	$\pm 2\sigma$	$^{206}\text{Pb}/^{238}\text{U}$	$\pm 2\sigma$	$^{207}\text{Pb}/^{206}\text{Pb}$ age	$\pm 2\sigma$	$^{206}\text{Pb}/^{238}\text{U}$ age	$\pm 2\sigma$	$^{207}\text{Pb}/^{235}\text{U}$ age	$\pm 2\sigma$	Concordancy		
SAN-2		<i>(Concordant Analyses)</i>													
SAN2L_010	0.1044	0.0019	4.4240	0.0630	0.3053	0.0053	1698	33	1721	25	1718	12	101		
SAN2L_010	0.1036	0.0019	4.4580	0.0690	0.3062	0.0052	1681	35	1720	26	1723	13	102		
SAN2L_053	0.0857	0.0017	2.8120	0.0790	0.2353	0.0056	1340	38	1361	29	1360	21	102		
SAN2B_018	0.0843	0.0008	2.7340	0.0380	0.2295	0.0028	1301	19	1331	15	1336	11	102		
SAN2L_012	0.0829	0.0013	2.5510	0.0390	0.2217	0.0038	1268	30	1291	20	1289	11	102		
SAN2L_012	0.0825	0.0013	2.5590	0.0420	0.2220	0.0035	1261	29	1291	18	1288	12	102		
SAN2L_014	0.0807	0.0015	2.4840	0.0390	0.2173	0.0036	1222	35	1268	19	1267	11	104		
SAN2B_045	0.0824	0.0011	2.4780	0.0360	0.2162	0.0027	1252	26	1263	14	1264	11	101		
SAN2L_014	0.0811	0.0022	2.3900	0.0490	0.2114	0.0055	1207	55	1238	28	1237	15	103		
SAN2L_047	0.0807	0.0020	2.3740	0.0480	0.2115	0.0038	1210	48	1236	20	1234	15	102		
SAN2L_047	0.0803	0.0019	2.3730	0.0520	0.2108	0.0035	1200	46	1232	19	1233	16	103		
SAN2L_041	0.0839	0.0016	2.4310	0.0380	0.2090	0.0030	1285	36	1223	16	1253	11	95		
SAN2L_059	0.0811	0.0021	2.3630	0.0460	0.2080	0.0036	1218	51	1218	19	1231	14	100		
SAN2L_041	0.0827	0.0021	2.3100	0.0790	0.2067	0.0046	1252	50	1210	24	1210	25	97		
SAN2L_023	0.0813	0.0016	2.2950	0.0380	0.2056	0.0033	1222	39	1208	17	1210	12	99		
SAN2L_034	0.0791	0.0012	2.2820	0.0410	0.2060	0.0047	1174	31	1207	25	1206	13	103		
SAN2L_060	0.0815	0.0020	2.2760	0.0580	0.2048	0.0046	1226	47	1205	23	1206	19	98		
SAN2B_076	0.0806	0.0017	2.2680	0.0460	0.2037	0.0035	1212	40	1198	19	1201	14	99		
SAN2L_026	0.0796	0.0011	2.2690	0.0280	0.2039	0.0031	1184	27	1198	17	1202	9	101		
SAN2B_074	0.0792	0.0012	2.2290	0.0320	0.2035	0.0032	1181	32	1195	17	1190	10	101		
SAN2L_023	0.0809	0.0017	2.2620	0.0450	0.2035	0.0035	1216	40	1193	19	1197	15	98		
SAN2B_074	0.0780	0.0012	2.2430	0.0410	0.2033	0.0028	1146	31	1192	15	1192	13	104		
SAN2L_040	0.0821	0.0013	2.3660	0.0460	0.2024	0.0025	1241	32	1188	13	1229	14	96		
SAN2B_083	0.0796	0.0013	2.2000	0.0380	0.2011	0.0034	1189	33	1183	18	1179	12	99		
SAN2L_058	0.0804	0.0012	2.2150	0.0290	0.2013	0.0029	1208	28	1182	16	1185	9	98		
SAN2L_058	0.0781	0.0013	2.2190	0.0300	0.2013	0.0030	1151	33	1182	16	1186	10	69	103	

Analysis #	$^{207}\text{Pb}/^{206}\text{Pb}$	$\pm 2\sigma$	$^{207}\text{Pb}/^{235}\text{U}$	$\pm 2\sigma$	$^{206}\text{Pb}/^{238}\text{U}$	$\pm 2\sigma$	$^{207}\text{Pb}/^{206}\text{Pb}$ age	$\pm 2\sigma$	$^{206}\text{Pb}/^{238}\text{U}$ age	$\pm 2\sigma$	$^{207}\text{Pb}/^{235}\text{U}$ age	$\pm 2\sigma$	Concordancy
SAN2B_076	0.0799	0.0010	2.2100	0.0260	0.1951	0.0022	1193	25	1148	12	1183	8	96
SAN2B_030	0.0790	0.0015	2.1100	0.0520	0.1949	0.0034	1167	38	1147	18	1149	17	98
SAN2B_080	0.0799	0.0013	2.1070	0.0600	0.1940	0.0028	1197	32	1143	15	1147	22	95
SAN2B_064	0.0770	0.0015	2.0770	0.0350	0.1935	0.0028	1123	38	1141	15	1139	12	102
SAN2B_024	0.0788	0.0015	2.1880	0.0430	0.1934	0.0035	1166	38	1139	19	1175	14	98
SAN2B_026	0.0777	0.0016	2.0680	0.0500	0.1933	0.0037	1146	42	1139	20	1140	17	99
SAN2B_042	0.0776	0.0020	2.0850	0.0540	0.1935	0.0035	1125	51	1139	19	1140	18	101
SAN2L_037	0.0778	0.0029	2.0610	0.0620	0.1934	0.0049	1149	77	1138	27	1135	21	99
SAN2B_064	0.0761	0.0014	2.0750	0.0390	0.1930	0.0026	1105	37	1138	14	1135	14	103
SAN2B_014	0.0796	0.0025	2.0860	0.0580	0.1923	0.0046	1171	60	1136	24	1140	19	97
SAN2L_037	0.0794	0.0030	2.0770	0.0670	0.1928	0.0048	1191	76	1135	26	1139	23	95
SAN2B_013	0.0756	0.0018	2.0710	0.0480	0.1919	0.0027	1081	50	1134	15	1138	16	105
SAN2B_065	0.0785	0.0015	2.0640	0.0540	0.1916	0.0032	1153	39	1131	18	1133	19	98
SAN2L_019	0.0774	0.0031	2.0440	0.0810	0.1912	0.0059	1114	82	1131	31	1130	26	102
SAN2B_041	0.0770	0.0015	2.0770	0.0430	0.1917	0.0034	1111	39	1130	19	1133	16	102
SAN2B_082	0.0778	0.0013	2.0570	0.0360	0.1915	0.0028	1141	33	1129	15	1134	12	99
SAN2L_011	0.0773	0.0021	2.0500	0.0550	0.1914	0.0037	1129	55	1128	20	1126	18	100
SAN2B_033	0.0768	0.0014	2.0520	0.0420	0.1913	0.0026	1106	37	1128	14	1128	15	102
SAN2B_027	0.0773	0.0015	2.0420	0.0410	0.1912	0.0036	1129	40	1127	20	1127	14	100
SAN2L_011	0.0777	0.0021	2.0400	0.0580	0.1911	0.0035	1132	54	1126	19	1128	21	99
SAN2L_027	0.0752	0.0036	2.0320	0.0890	0.1897	0.0047	1078	96	1124	26	1121	29	104
SAN2B_083	0.0786	0.0014	2.0730	0.0440	0.1900	0.0034	1162	35	1122	18	1134	16	97
SAN2B_035	0.0790	0.0021	2.0360	0.0510	0.1899	0.0029	1171	53	1121	16	1124	17	96
SAN2B_082	0.0753	0.0016	2.0260	0.0440	0.1893	0.0038	1078	43	1120	20	1124	15	104
SAN2B_032	0.0774	0.0020	2.0090	0.0470	0.1886	0.0027	1124	52	1113	15	1115	16	99
SAN2B_078	0.0789	0.0016	2.0760	0.0430	0.1878	0.0031	1162	40	1108	17	1139	14	95
SAN2L_046	0.0766	0.0022	1.9610	0.0480	0.1868	0.0037	1106	58	1105	20	1101	16	100
SAN2L_046	0.0760	0.0021	1.9610	0.0490	0.1870	0.0035	1093	55	1104	19	1102	18	101
SAN2B_072	0.0766	0.0016	1.9770	0.0620	0.1856	0.0033	1111	44	1099	18	1103	22	99
SAN2L_004	0.0756	0.0045	1.9400	0.1100	0.1829	0.0066	1080	130	1087	35	1091	39	101

Analysis #	$^{207}\text{Pb}/^{206}\text{Pb}$	$\pm 2\sigma$	$^{207}\text{Pb}/^{235}\text{U}$	$\pm 2\sigma$	$^{206}\text{Pb}/^{238}\text{U}$	$\pm 2\sigma$	$^{207}\text{Pb}/^{206}\text{Pb}$ age	$\pm 2\sigma$	$^{206}\text{Pb}/^{238}\text{U}$ age	$\pm 2\sigma$	$^{207}\text{Pb}/^{235}\text{U}$ age	$\pm 2\sigma$	Concordancy
SAN2B_025	0.0758	0.0019	2.0960	0.0450	0.1937	0.0034	1081	49	1141	18	1146	15	106
SAN2L_050	0.0723	0.0034	2.0120	0.0870	0.1938	0.0051	1000	100	1140	28	1107	30	114
SAN2L_036	0.0878	0.0008	2.4190	0.0200	0.1935	0.0018	1380	17	1140	10	1248	6	83
SAN2L_020	0.0827	0.0013	2.2730	0.0350	0.1934	0.0027	1258	31	1139	14	1203	11	91
SAN2B_020	0.0807	0.0013	2.1970	0.0400	0.1930	0.0026	1220	30	1137	14	1179	13	93
SAN2L_020	0.0832	0.0013	2.2390	0.0360	0.1928	0.0029	1269	30	1136	15	1192	12	90
SAN2B_040	0.0814	0.0019	2.0580	0.0720	0.1923	0.0037	1230	44	1133	20	1131	25	92
SAN2L_008	0.0870	0.0019	2.2530	0.0650	0.1921	0.0044	1367	44	1132	24	1193	22	83
SAN2L_018	0.0894	0.0033	2.2700	0.0770	0.1917	0.0050	1396	71	1130	27	1199	24	81
SAN2L_027	0.0747	0.0044	2.0200	0.1000	0.1893	0.0062	1050	120	1119	34	1116	34	107
SAN2B_011	0.0808	0.0009	2.1670	0.0330	0.1884	0.0019	1215	21	1112	10	1166	11	92
SAN2B_048	0.0749	0.0041	1.9780	0.0840	0.1882	0.0044	1020	110	1110	24	1109	29	109
SAN2L_018	0.0905	0.0024	2.3580	0.0540	0.1877	0.0030	1425	49	1108	16	1227	16	78
SAN2L_042	0.0838	0.0010	2.1470	0.0290	0.1860	0.0024	1283	22	1099	13	1165	9	86
SAN2L_035	0.0904	0.0009	2.3420	0.0280	0.1857	0.0022	1432	19	1098	12	1225	8	77
SAN2L_035	0.0895	0.0009	2.3570	0.0310	0.1852	0.0022	1413	20	1095	12	1225	10	77
SAN2L_042	0.0829	0.0010	2.1440	0.0330	0.1851	0.0023	1264	23	1094	12	1161	11	87
SAN2L_004	0.0745	0.0045	1.9300	0.1100	0.1839	0.0066	1030	130	1087	36	1088	40	106
SAN2B_071	0.0924	0.0013	2.3390	0.0360	0.1818	0.0040	1473	26	1079	21	1223	11	73
SAN2B_019	0.0841	0.0014	2.2350	0.0330	0.1823	0.0032	1286	33	1079	17	1192	10	84
SAN2B_023	0.0872	0.0010	2.2680	0.0260	0.1814	0.0021	1366	22	1074	12	1203	8	79
SAN2B_038	0.0891	0.0011	2.2420	0.0430	0.1772	0.0031	1408	24	1051	17	1189	14	75
SAN2B_071	0.0920	0.0013	2.2970	0.0430	0.1766	0.0037	1464	26	1047	21	1208	14	72
SAN2L_024	0.0916	0.0008	2.2350	0.0210	0.1758	0.0021	1456	18	1044	12	1192	7	72
SAN2B_066	0.0923	0.0011	2.2400	0.0330	0.1756	0.0023	1472	23	1043	13	1193	11	71
SAN2L_024	0.0908	0.0009	2.2350	0.0250	0.1756	0.0020	1448	19	1042	11	1191	8	72
SAN2B_068	0.0786	0.0012	2.1520	0.0340	0.1753	0.0027	1157	32	1042	15	1164	11	90
SAN2B_066	0.0910	0.0011	2.2460	0.0330	0.1754	0.0022	1444	23	1041	12	1196	10	72
SAN2L_016	0.0947	0.0017	2.2830	0.0460	0.1738	0.0025	1521	33	1033	14	1206	14	68
SAN2L_029	0.1013	0.0012	2.4470	0.0290	0.1737	0.0028	1649	22	1032	16	1257	9	63
SAN2L_016	0.0947	0.0018	2.3150	0.0510	0.1733	0.0026	1521	34	1030	14	1214	16	68
SAN2L_029	0.1004	0.0011	2.4490	0.0350	0.1726	0.0026	1630	22	1026	14	1255	10	63
SAN2L_007	0.0972	0.0011	2.3120	0.0270	0.1723	0.0026	1568	22	1024	14	1215	8	73

Analysis #	$^{207}\text{Pb}/^{206}\text{Pb}$	$\pm 2\sigma$	$^{207}\text{Pb}/^{235}\text{U}$	$\pm 2\sigma$	$^{206}\text{Pb}/^{238}\text{U}$	$\pm 2\sigma$	$^{207}\text{Pb}/^{206}\text{Pb}$ age	$\pm 2\sigma$	$^{206}\text{Pb}/^{238}\text{U}$ age	$\pm 2\sigma$	$^{207}\text{Pb}/^{235}\text{U}$ age	$\pm 2\sigma$	Concordancy
SAN2L_007	0.0967	0.0011	2.3320	0.0270	0.1715	0.0024	1558	22	1022	13	1221	8	66
SAN2L_028	0.6500	0.4900	9.5000	6.0000	0.1800	0.1400	4400	1300	1020	750	2050	650	23
SAN2L_001	0.0935	0.0041	2.2290	0.0840	0.1716	0.0039	1460	85	1020	22	1181	26	70
SAN2L_001	0.0950	0.0039	2.2250	0.0790	0.1707	0.0038	1486	80	1015	21	1182	25	68
SAN2B_022	0.0904	0.0012	2.1920	0.0300	0.1698	0.0021	1432	26	1012	12	1176	10	71
SAN2B_075	0.1044	0.0009	2.4340	0.0290	0.1690	0.0022	1703	16	1007	12	1252	9	59
SAN2B_008	0.0893	0.0009	2.1470	0.0240	0.1678	0.0018	1407	20	1000	10	1164	8	71
SAN2B_070	0.1085	0.0017	2.4990	0.0240	0.1671	0.0027	1778	27	996	15	1272	7	56
SAN2B_075	0.1028	0.0009	2.4440	0.0290	0.1671	0.0020	1673	17	996	11	1255	9	60
SAN2B_073	0.0998	0.0010	2.2860	0.0230	0.1672	0.0020	1616	18	996	11	1209	7	62
SAN2L_033	0.1050	0.0010	2.4000	0.0330	0.1668	0.0022	1711	18	994	12	1243	10	58
SAN2L_033	0.1042	0.0010	2.3960	0.0380	0.1659	0.0021	1697	18	989	11	1239	12	58
SAN2B_037	0.0942	0.0009	2.2160	0.0290	0.1658	0.0018	1508	18	989	10	1182	10	66
SAN2L_030	0.0898	0.0024	2.1050	0.0570	0.1659	0.0055	1415	51	989	30	1153	17	70
SAN2B_070	0.1074	0.0016	2.5160	0.0250	0.1653	0.0024	1757	27	986	13	1277	7	56
SAN2B_073	0.0986	0.0009	2.2940	0.0280	0.1651	0.0017	1593	18	985	10	1208	10	62
SAN2L_015	0.1018	0.0012	2.3370	0.0270	0.1619	0.0025	1657	22	967	14	1223	8	58
SAN2L_015	0.1030	0.0013	2.3090	0.0290	0.1610	0.0026	1681	23	962	14	1215	9	57
SAN2L_049	0.0983	0.0012	2.2080	0.0250	0.1588	0.0020	1589	24	950	11	1184	8	60
SAN2L_025	0.1010	0.0009	2.2290	0.0190	0.1586	0.0018	1640	17	949	10	1190	6	58
SAN2L_025	0.1004	0.0010	2.2310	0.0220	0.1583	0.0018	1629	18	947	10	1192	7	58
SAN2B_028	0.1018	0.0012	2.2610	0.0250	0.1580	0.0020	1651	22	945	11	1199	8	57
SAN2L_049	0.0999	0.0011	2.1600	0.0260	0.1571	0.0020	1621	21	941	11	1167	8	58
SAN2L_013	0.1031	0.0008	2.2260	0.0160	0.1547	0.0014	1680	14	927	8	1189	5	55
SAN2L_013	0.1022	0.0008	2.2450	0.0150	0.1536	0.0016	1663	14	922	9	1196	5	55
SAN2B_031	0.1141	0.0018	2.4310	0.0430	0.1531	0.0030	1863	29	918	17	1251	13	49
SAN2L_030	0.0887	0.0022	2.1120	0.0570	0.1518	0.0049	1400	50	911	28	1156	17	65
SAN2B_067	0.1021	0.0018	2.1280	0.0510	0.1506	0.0025	1656	33	904	14	1159	16	55
SAN2B_081	0.1031	0.0009	2.1350	0.0290	0.1503	0.0020	1686	16	902	11	1159	10	53
SAN2L_002	0.1070	0.0007	2.2400	0.0270	0.1499	0.0015	1749	13	901	9	1190	9	52
SAN2L_002	0.1074	0.0007	2.2420	0.0240	0.1496	0.0018	1753	12	899	10	1193	8	51
SAN2B_067	0.1007	0.0019	2.1440	0.0510	0.1496	0.0021	1631	34	898	12	1161	16	55
SAN2B_081	0.1014	0.0009	2.1520	0.0260	0.1488	0.0017	1652	16	894	10	1167	8	74

Analysis #	$^{207}\text{Pb}/^{206}\text{Pb}$	$\pm 2\sigma$	$^{207}\text{Pb}/^{235}\text{U}$	$\pm 2\sigma$	$^{206}\text{Pb}/^{238}\text{U}$	$\pm 2\sigma$	$^{207}\text{Pb}/^{206}\text{Pb}$ age	$\pm 2\sigma$	$^{206}\text{Pb}/^{238}\text{U}$ age	$\pm 2\sigma$	$^{207}\text{Pb}/^{235}\text{U}$ age	$\pm 2\sigma$	Concordancy
SAN2B_044	0.0987	0.0009	2.0830	0.0280	0.1488	0.0016	1598	18	894	9	1138	10	56
SAN2L_055	0.1050	0.0012	2.1660	0.0300	0.1482	0.0021	1710	20	891	12	1168	10	52
SAN2L_032	0.1010	0.0012	2.0710	0.0240	0.1483	0.0019	1638	22	891	11	1138	8	54
SAN2L_032	0.1001	0.0012	2.0770	0.0260	0.1476	0.0018	1619	22	887	10	1138	9	55
SAN2L_054	0.1039	0.0011	2.1100	0.0240	0.1472	0.0021	1693	19	885	12	1152	8	52
SAN2L_055	0.1038	0.0011	2.1390	0.0370	0.1473	0.0018	1688	20	885	10	1156	13	52
SAN2L_054	0.1028	0.0011	2.1180	0.0240	0.1457	0.0019	1671	20	877	11	1154	8	52
SAN2L_057	0.1012	0.0011	2.0300	0.0230	0.1454	0.0016	1641	20	875	9	1125	8	53
SAN2B_077	0.1061	0.0009	2.1080	0.0340	0.1452	0.0019	1735	16	873	11	1151	11	50
SAN2L_057	0.1001	0.0011	2.0500	0.0230	0.1441	0.0018	1623	21	868	10	1131	8	53
SAN2B_077	0.1042	0.0009	2.1140	0.0310	0.1437	0.0016	1701	16	866	9	1152	10	51
SAN2L_017	0.1130	0.0016	2.2760	0.0380	0.1428	0.0019	1839	27	860	11	1202	12	47
SAN2L_017	0.1138	0.0016	2.2650	0.0370	0.1427	0.0020	1852	27	859	11	1200	12	46
SAN2B_079	0.0944	0.0011	1.7820	0.0230	0.1374	0.0015	1515	21	830	9	1038	8	55
SAN2B_063	0.0991	0.0015	1.8640	0.0470	0.1361	0.0019	1605	28	823	11	1066	17	51
SAN2B_079	0.0929	0.0011	1.7900	0.0230	0.1359	0.0015	1484	21	821	8	1041	8	55
SAN2B_063	0.0959	0.0014	1.8050	0.0500	0.1339	0.0017	1542	28	810	10	1042	18	53
SAN2B_069	0.1042	0.0013	1.9370	0.0210	0.1335	0.0016	1696	23	808	9	1094	7	48
SAN2B_069	0.1026	0.0013	1.9660	0.0200	0.1328	0.0014	1666	23	804	8	1104	7	48
SAN2B_046	0.0904	0.0009	1.6820	0.0230	0.1315	0.0014	1435	19	797	8	1000	9	56
SAN2L_044	0.0940	0.0009	1.7160	0.0150	0.1316	0.0014	1506	18	797	8	1014	6	53
SAN2L_044	0.0930	0.0009	1.7230	0.0160	0.1309	0.0014	1486	18	793	8	1017	6	53
SAN2L_056	0.0934	0.0009	1.6810	0.0220	0.1309	0.0016	1494	19	793	9	1000	8	53
SAN2L_056	0.0922	0.0010	1.6920	0.0220	0.1304	0.0015	1469	21	790	9	1005	8	54
SAN2L_038	0.0950	0.0009	1.7130	0.0180	0.1301	0.0015	1528	18	789	9	1013	7	52
SAN2L_038	0.0940	0.0009	1.7230	0.0210	0.1294	0.0014	1510	18	785	8	1016	8	52
SAN2B_084	0.0890	0.0008	1.5160	0.0140	0.1234	0.0013	1405	18	750	7	937	6	53
SAN2B_084	0.0877	0.0009	1.5180	0.0170	0.1219	0.0012	1373	18	742	7	935	8	54

(Concordant Analyses)

SAN9_01	0.0866	0.0018	2.6970	0.0540	0.2280	0.0031	1340	40	1325	16	1326	15	99
SAN9_02	0.0855	0.0016	2.6820	0.0480	0.2278	0.0029	1321	35	1322	15	1324	13	100

Analysis #	$^{207}\text{Pb}/^{206}\text{Pb}$	$\pm 2\sigma$	$^{207}\text{Pb}/^{235}\text{U}$	$\pm 2\sigma$	$^{206}\text{Pb}/^{238}\text{U}$	$\pm 2\sigma$	$^{207}\text{Pb}/^{206}\text{Pb}$ age	$\pm 2\sigma$	$^{206}\text{Pb}/^{238}\text{U}$ age	$\pm 2\sigma$	$^{207}\text{Pb}/^{235}\text{U}$ age	$\pm 2\sigma$	Concordancy
SAN9_30	0.0849	0.0028	2.6810	0.0840	0.2271	0.0043	1330	61	1319	23	1322	23	99
SAN9_07	0.0845	0.0026	2.5990	0.0690	0.2261	0.0060	1290	59	1318	33	1315	17	102
SAN9_22	0.0837	0.0022	2.5890	0.0590	0.2267	0.0036	1276	51	1316	19	1300	18	103
SAN9_03	0.0852	0.0015	2.6640	0.0430	0.2259	0.0029	1324	36	1312	15	1316	12	99
SAN9_21	0.0843	0.0029	2.6240	0.0790	0.2250	0.0038	1296	68	1311	20	1312	22	101
SAN9_05	0.0837	0.0022	2.6120	0.0650	0.2251	0.0035	1300	49	1310	18	1313	18	101
SAN9_33	0.0835	0.0031	2.6350	0.0800	0.2255	0.0040	1285	73	1310	21	1310	22	102
SAN9_24	0.0852	0.0021	2.6300	0.0590	0.2253	0.0038	1322	46	1309	20	1308	16	99
SAN9_09	0.0854	0.0024	2.6250	0.0600	0.2247	0.0050	1316	56	1306	26	1310	17	99
SAN9_08	0.0836	0.0023	2.6010	0.0740	0.2247	0.0044	1288	54	1306	23	1306	20	101
SAN9_35	0.0845	0.0016	2.6250	0.0520	0.2244	0.0030	1306	36	1305	16	1307	14	100
SAN9_06	0.0837	0.0022	2.6130	0.0550	0.2242	0.0038	1282	51	1305	20	1302	15	102
SAN9_27	0.0853	0.0020	2.6350	0.0550	0.2238	0.0036	1322	46	1303	19	1308	15	99
SAN9_11	0.0836	0.0021	2.5900	0.0620	0.2239	0.0039	1284	51	1302	21	1299	18	101
SAN9_26	0.0842	0.0022	2.5970	0.0670	0.2234	0.0036	1284	51	1301	19	1301	18	101
SAN9_28	0.0844	0.0018	2.6020	0.0510	0.2228	0.0034	1312	42	1300	18	1301	14	99
SAN9_23	0.0840	0.0018	2.5850	0.0530	0.2233	0.0034	1286	42	1299	18	1294	15	101
SAN9_34	0.0847	0.0020	2.6040	0.0510	0.2227	0.0035	1298	45	1295	18	1300	14	100
SAN9_12	0.0842	0.0023	2.5780	0.0660	0.2219	0.0037	1299	51	1293	19	1289	19	100
SAN9_31	0.0853	0.0053	2.6100	0.1700	0.2220	0.0110	1350	120	1292	58	1295	48	96
SAN9_10	0.0857	0.0021	2.5590	0.0590	0.2219	0.0040	1322	51	1291	21	1287	16	98
SAN9_29	0.0841	0.0025	2.5650	0.0730	0.2214	0.0037	1308	59	1291	20	1287	21	99
SAN9_16	0.0859	0.0033	2.5770	0.0800	0.2201	0.0045	1334	74	1284	24	1291	23	96
SAN9_04	0.0841	0.0032	2.5140	0.0920	0.2189	0.0053	1307	70	1280	27	1276	27	98
SAN9_19	0.0838	0.0020	2.5030	0.0520	0.2190	0.0035	1276	47	1276	19	1271	15	100
SAN9_17	0.0842	0.0028	2.5090	0.0720	0.2189	0.0036	1271	65	1276	19	1273	21	100
SAN9_18	0.0838	0.0018	2.4960	0.0480	0.2175	0.0034	1300	43	1268	18	1270	14	98
SAN9_20	0.0851	0.0018	2.5390	0.0490	0.2151	0.0030	1316	42	1257	16	1280	14	96
SAN9_13	0.0826	0.0025	2.4340	0.0690	0.2147	0.0035	1259	60	1253	18	1257	21	100
SAN9_25	0.0826	0.0020	2.4310	0.0550	0.2143	0.0031	1256	46	1251	17	1252	17	100

Analysis #	$^{207}\text{Pb}/^{206}\text{Pb}$	$\pm 2\sigma$	$^{207}\text{Pb}/^{235}\text{U}$	$\pm 2\sigma$	$^{206}\text{Pb}/^{238}\text{U}$	$\pm 2\sigma$	$^{207}\text{Pb}/^{206}\text{Pb}$ age	$\pm 2\sigma$	$^{206}\text{Pb}/^{238}\text{U}$ age	$\pm 2\sigma$	$^{207}\text{Pb}/^{235}\text{U}$ age	$\pm 2\sigma$	Concordancy	
SAN-9	(Discordant Analyses)													
SAN9_14	0.1107	0.0046	3.3000	0.1400	0.2176	0.0030	1767	74	1269	16	1468	32	72	
SAN9_15	0.0885	0.0023	2.6160	0.0590	0.2132	0.0032	1387	51	1245	17	1303	16	90	
SAN9_32	0.1210	0.0051	3.4600	0.1600	0.2097	0.0028	1982	71	1227	15	1512	37	62	
SAN-10	(Concordant Analyses)													
SAN10L_001	0.0791	0.0022	2.3560	0.0540	0.2090	0.0039	1168	56	1223	21	1228	16	105	
SAN10L_019	0.0806	0.0024	2.3130	0.0600	0.2060	0.0045	1205	62	1213	25	1213	19	101	
SAN10B_099	0.0797	0.0016	2.3210	0.0410	0.2065	0.0034	1179	39	1213	18	1217	13	103	
SAN10L_031	0.0781	0.0026	2.2900	0.0580	0.2066	0.0038	1184	60	1210	20	1208	18	102	
SAN10B_085	0.0785	0.0015	2.3020	0.0400	0.2064	0.0031	1168	37	1210	17	1211	12	104	
SAN10L_051	0.0789	0.0015	2.3080	0.0340	0.2065	0.0036	1160	37	1210	19	1213	11	104	
SAN10B_097	0.0802	0.0025	2.3020	0.0600	0.2060	0.0039	1197	60	1207	21	1212	19	101	
SAN10L_049	0.0779	0.0013	2.2800	0.0410	0.2056	0.0033	1150	34	1207	17	1208	12	105	
SAN10L_014	0.0794	0.0015	2.2880	0.0520	0.2049	0.0035	1176	38	1200	19	1204	16	102	
SAN10L_059	0.0775	0.0015	2.2760	0.0390	0.2045	0.0029	1143	37	1199	16	1204	12	105	
SAN10B_087	0.0787	0.0014	2.2700	0.0480	0.2039	0.0029	1152	37	1196	15	1199	15	104	
SAN10B_074	0.0782	0.0015	2.2670	0.0370	0.2040	0.0034	1145	39	1196	18	1201	12	104	
SAN10B_052	0.0781	0.0017	2.2580	0.0480	0.2035	0.0035	1158	44	1194	19	1198	15	103	
SAN10L_046	0.0783	0.0025	2.2630	0.0550	0.2036	0.0040	1145	66	1194	21	1198	17	104	
SAN10B_056	0.0776	0.0020	2.2480	0.0530	0.2030	0.0036	1154	52	1193	19	1196	17	103	
SAN10L_010	0.0785	0.0016	2.2470	0.0500	0.2035	0.0035	1152	40	1193	19	1195	16	104	
SAN10L_038	0.0785	0.0013	2.2480	0.0410	0.2031	0.0034	1154	33	1191	18	1193	13	103	
SAN10B_055	0.0774	0.0016	2.2460	0.0450	0.2031	0.0034	1137	41	1191	18	1194	14	105	
SAN10B_098	0.0801	0.0022	2.2890	0.0580	0.2028	0.0032	1212	53	1190	17	1211	19	98	
SAN10B_091	0.0800	0.0015	2.3050	0.0400	0.2029	0.0031	1193	37	1190	16	1213	13	100	
SAN10B_103	0.0782	0.0015	2.2370	0.0440	0.2026	0.0030	1150	39	1190	16	1193	14	103	
SAN10B_047	0.0780	0.0020	2.2180	0.0510	0.2020	0.0038	1144	50	1189	21	1185	16	104	
SAN10L_034	0.0775	0.0014	2.2360	0.0420	0.2022	0.0033	1138	34	1188	17	1192	13	104	
SAN10B_106	0.0781	0.0021	2.2310	0.0530	0.2023	0.0034	1137	55	1187	18	1190	17	104	
SAN10L_075	0.0778	0.0017	2.2330	0.0510	0.2019	0.0032	1134	45	1185	17	1189	16	104	
SAN10L_047	0.0776	0.0012	2.2170	0.0330	0.2017	0.0027	1130	32	1184	15	1186	11	105	

Analysis #	$^{207}\text{Pb}/^{206}\text{Pb}$	$\pm 2\sigma$	$^{207}\text{Pb}/^{235}\text{U}$	$\pm 2\sigma$	$^{206}\text{Pb}/^{238}\text{U}$	$\pm 2\sigma$	$^{207}\text{Pb}/^{206}\text{Pb}$ age	$\pm 2\sigma$	$^{206}\text{Pb}/^{238}\text{U}$ age	$\pm 2\sigma$	$^{207}\text{Pb}/^{235}\text{U}$ age	$\pm 2\sigma$	Concordancy
SAN10L_073	0.0779	0.0016	2.2150	0.0420	0.2016	0.0031	1150	42	1183	17	1186	14	103
SAN10L_018	0.0784	0.0026	2.2350	0.0870	0.2010	0.0046	1141	65	1183	24	1179	29	104
SAN10B_101	0.0776	0.0014	2.2160	0.0390	0.2012	0.0022	1139	37	1182	12	1184	12	104
SAN10B_092	0.0777	0.0014	2.2030	0.0460	0.2010	0.0033	1138	37	1182	17	1185	14	104
SAN10B_038	0.0775	0.0013	2.2010	0.0390	0.2012	0.0026	1141	34	1181	14	1178	13	104
SAN10L_054	0.0775	0.0015	2.2190	0.0420	0.2012	0.0034	1140	40	1181	18	1185	13	104
SAN10L_053	0.0780	0.0021	2.2130	0.0490	0.2011	0.0041	1136	53	1181	22	1184	15	104
SAN10B_015	0.0777	0.0012	2.2130	0.0360	0.2007	0.0024	1140	31	1179	13	1180	13	103
SAN10B_076	0.0781	0.0015	2.2050	0.0410	0.2007	0.0029	1144	39	1178	16	1182	13	103
SAN10L_048	0.0769	0.0021	2.2100	0.0520	0.2006	0.0039	1143	54	1178	21	1182	17	103
SAN10B_100	0.0782	0.0016	2.2010	0.0450	0.2007	0.0031	1140	41	1178	17	1183	14	103
SAN10B_104	0.0774	0.0020	2.1950	0.0450	0.2006	0.0040	1135	52	1178	21	1178	14	104
SAN10L_003	0.0772	0.0014	2.2060	0.0420	0.2007	0.0030	1130	37	1178	16	1182	13	104
SAN10L_045	0.0773	0.0011	2.2080	0.0330	0.2000	0.0027	1128	27	1178	15	1182	10	104
SAN10L_058	0.0772	0.0026	2.1750	0.0630	0.1995	0.0043	1128	67	1178	24	1183	20	104
SAN10B_037	0.0779	0.0012	2.1860	0.0330	0.1995	0.0027	1148	32	1176	15	1177	11	102
SAN10L_025	0.0773	0.0010	2.1770	0.0320	0.1999	0.0025	1132	27	1176	14	1176	10	104
SAN10L_042	0.0771	0.0014	2.1930	0.0390	0.2002	0.0031	1121	35	1176	17	1178	12	105
SAN10B_040	0.0783	0.0010	2.2020	0.0380	0.1997	0.0021	1159	25	1173	11	1177	13	101
SAN10L_002	0.0783	0.0021	2.1870	0.0570	0.1996	0.0038	1137	54	1173	20	1174	18	103
SAN10L_057	0.0792	0.0029	2.1890	0.0670	0.1993	0.0051	1150	72	1171	28	1174	21	102
SAN10L_021	0.0769	0.0019	2.1630	0.0440	0.1988	0.0035	1122	49	1170	19	1171	14	104
SAN10B_059	0.0767	0.0011	2.1810	0.0280	0.1991	0.0021	1116	28	1170	11	1175	9	105
SAN10B_061	0.0771	0.0013	2.1790	0.0410	0.1991	0.0025	1115	35	1170	14	1173	13	105
SAN10B_069	0.0788	0.0018	2.1730	0.0520	0.1990	0.0037	1158	46	1169	20	1171	17	101
SAN10B_070	0.0771	0.0021	2.1880	0.0510	0.1989	0.0034	1125	57	1169	18	1175	16	104
SAN10L_069	0.0773	0.0027	2.1830	0.0820	0.1971	0.0054	1162	71	1168	29	1171	26	101
SAN10B_012	0.0778	0.0014	2.1820	0.0440	0.1985	0.0023	1139	33	1168	12	1172	14	103
SAN10L_013	0.0774	0.0014	2.1750	0.0480	0.1983	0.0032	1130	35	1167	17	1169	16	103
SAN10L_033	0.0770	0.0018	2.1690	0.0420	0.1984	0.0030	1116	48	1167	16	1169	13	105
SAN10L_066	0.0776	0.0020	2.1670	0.0500	0.1984	0.0036	1132	52	1166	19	1170	16	103
SAN10L_055	0.0775	0.0012	2.1730	0.0360	0.1984	0.0029	1124	30	1166	15	1170	12	104
SAN10B_084	0.0779	0.0023	2.1470	0.0460	0.1982	0.0038	1133	59	1165	21	1162	15	78 103

Analysis #	$^{207}\text{Pb}/^{206}\text{Pb}$	$\pm 2\sigma$	$^{207}\text{Pb}/^{235}\text{U}$	$\pm 2\sigma$	$^{206}\text{Pb}/^{238}\text{U}$	$\pm 2\sigma$	$^{207}\text{Pb}/^{206}\text{Pb}$ age	$\pm 2\sigma$	$^{206}\text{Pb}/^{238}\text{U}$ age	$\pm 2\sigma$	$^{207}\text{Pb}/^{235}\text{U}$ age	$\pm 2\sigma$	Concordancy
SAN10L_082	0.0771	0.0020	2.1710	0.0630	0.1982	0.0043	1115	53	1165	23	1169	20	104
SAN10B_033	0.0769	0.0014	2.1480	0.0390	0.1978	0.0031	1112	37	1165	17	1168	13	105
SAN10B_009	0.0789	0.0012	2.1600	0.0560	0.1979	0.0026	1164	31	1164	14	1165	19	100
SAN10B_045	0.0785	0.0019	2.1550	0.0550	0.1977	0.0032	1144	49	1164	18	1164	19	102
SAN10B_039	0.0775	0.0013	2.1650	0.0440	0.1977	0.0025	1132	33	1164	13	1166	14	103
SAN10B_043	0.0774	0.0013	2.1590	0.0440	0.1977	0.0022	1126	33	1164	12	1164	15	103
SAN10L_008	0.0772	0.0036	2.1620	0.0830	0.1980	0.0056	1112	93	1163	30	1166	26	105
SAN10B_093	0.0783	0.0018	2.1980	0.0480	0.1972	0.0032	1146	47	1162	17	1180	15	101
SAN10B_065	0.0779	0.0013	2.1500	0.0420	0.1976	0.0026	1136	34	1162	14	1165	14	102
SAN10L_027	0.0782	0.0015	2.1430	0.0510	0.1973	0.0032	1147	38	1161	17	1157	17	101
SAN10L_044	0.0772	0.0016	2.1930	0.0390	0.1974	0.0027	1131	42	1161	15	1179	12	103
SAN10L_017	0.0762	0.0017	2.1440	0.0490	0.1976	0.0040	1106	45	1161	22	1159	16	105
SAN10B_014	0.0792	0.0014	2.2270	0.0330	0.1973	0.0025	1167	34	1160	13	1188	10	99
SAN10L_020	0.0786	0.0011	2.1580	0.0440	0.1973	0.0030	1159	27	1160	16	1164	15	100
SAN10L_022	0.0773	0.0012	2.1450	0.0350	0.1970	0.0028	1120	31	1160	15	1162	12	104
SAN10L_015	0.0763	0.0016	2.1490	0.0490	0.1974	0.0035	1111	42	1160	19	1157	18	104
SAN10L_023	0.0769	0.0014	2.1530	0.0420	0.1970	0.0027	1116	34	1159	15	1163	13	104
SAN10B_096	0.0799	0.0016	2.2290	0.0440	0.1966	0.0030	1188	40	1158	16	1187	14	97
SAN10B_108	0.0767	0.0016	2.1430	0.0440	0.1969	0.0034	1110	41	1158	19	1164	15	104
SAN10B_072	0.0768	0.0017	2.1380	0.0430	0.1970	0.0032	1105	46	1158	17	1160	14	105
SAN10B_026	0.0764	0.0017	2.1380	0.0420	0.1969	0.0028	1103	43	1158	15	1162	14	105
SAN10B_020	0.0768	0.0012	2.1320	0.0430	0.1967	0.0024	1109	32	1157	13	1157	15	104
SAN10B_073	0.0781	0.0017	2.1410	0.0620	0.1966	0.0030	1143	45	1156	16	1160	21	101
SAN10B_068	0.0773	0.0014	2.1240	0.0370	0.1965	0.0023	1140	37	1156	12	1156	12	101
SAN10B_011	0.0764	0.0013	2.1290	0.0450	0.1960	0.0025	1115	37	1156	13	1160	14	104
SAN10B_041	0.0796	0.0015	2.2210	0.0450	0.1962	0.0024	1177	37	1155	13	1186	14	98
SAN10B_053	0.0777	0.0016	2.1460	0.0570	0.1963	0.0028	1126	43	1155	15	1159	19	103
SAN10L_004	0.0767	0.0017	2.1220	0.0440	0.1960	0.0026	1112	43	1155	14	1155	14	104
SAN10B_050	0.0779	0.0017	2.1320	0.0540	0.1961	0.0032	1135	45	1154	17	1156	18	102
SAN10B_042	0.0773	0.0015	2.1200	0.0490	0.1961	0.0028	1119	39	1154	15	1155	17	103
SAN10L_067	0.0765	0.0011	2.1220	0.0450	0.1959	0.0028	1107	29	1154	15	1152	15	104
SAN10B_057	0.0775	0.0012	2.1220	0.0390	0.1955	0.0025	1130	30	1153	14	1156	13	102
SAN10L_063	0.0767	0.0010	2.1290	0.0390	0.1956	0.0026	1108	26	1151	14	1155	13	79 104

Analysis #	$^{207}\text{Pb}/^{206}\text{Pb}$	$\pm 2\sigma$	$^{207}\text{Pb}/^{235}\text{U}$	$\pm 2\sigma$	$^{206}\text{Pb}/^{238}\text{U}$	$\pm 2\sigma$	$^{207}\text{Pb}/^{206}\text{Pb}$ age	$\pm 2\sigma$	$^{206}\text{Pb}/^{238}\text{U}$ age	$\pm 2\sigma$	$^{207}\text{Pb}/^{235}\text{U}$ age	$\pm 2\sigma$	Concordancy
SAN10L_032	0.0784	0.0016	2.1980	0.0440	0.1947	0.0031	1146	39	1150	17	1177	14	100
SAN10L_012	0.0797	0.0019	2.2190	0.0550	0.1952	0.0035	1194	47	1149	19	1189	17	96
SAN10B_058	0.0778	0.0014	2.1120	0.0460	0.1949	0.0025	1138	37	1149	13	1147	17	101
SAN10B_083	0.0776	0.0016	2.1030	0.0440	0.1942	0.0029	1140	42	1148	15	1147	15	101
SAN10L_007	0.0770	0.0020	2.1220	0.0630	0.1948	0.0033	1111	51	1148	18	1145	22	103
SAN10B_048	0.0769	0.0024	2.0960	0.0670	0.1946	0.0037	1126	66	1146	20	1150	22	102
SAN10L_050	0.0773	0.0021	2.1300	0.0690	0.1942	0.0037	1124	55	1146	20	1147	26	102
SAN10B_025	0.0770	0.0016	2.0980	0.0580	0.1947	0.0038	1121	41	1146	21	1145	19	102
SAN10L_076	0.0766	0.0027	2.1110	0.0640	0.1948	0.0046	1111	68	1146	25	1150	21	103
SAN10B_067	0.0795	0.0012	2.1970	0.0360	0.1945	0.0025	1186	31	1145	14	1181	12	97
SAN10B_066	0.0784	0.0014	2.0890	0.0420	0.1942	0.0031	1155	36	1145	17	1148	15	99
SAN10L_030	0.0792	0.0025	2.1830	0.0660	0.1941	0.0036	1169	62	1143	19	1169	22	98
SAN10B_031	0.0761	0.0017	2.0930	0.0470	0.1935	0.0031	1091	43	1142	16	1143	16	105
SAN10B_062	0.0765	0.0025	2.0820	0.0730	0.1939	0.0040	1102	67	1141	21	1134	25	104
SAN10L_079	0.0763	0.0014	2.0830	0.0440	0.1925	0.0029	1106	35	1139	15	1139	15	103
SAN10L_064	0.0762	0.0016	2.0920	0.0480	0.1933	0.0032	1103	44	1139	17	1144	16	103
SAN10B_023	0.0775	0.0015	2.0710	0.0490	0.1927	0.0027	1144	39	1136	15	1137	17	99
SAN10B_075	0.0768	0.0024	2.0750	0.0620	0.1923	0.0033	1126	61	1136	18	1138	21	101
SAN10B_034	0.0769	0.0019	2.0770	0.0430	0.1927	0.0033	1108	50	1135	18	1139	14	102
SAN10L_068	0.0770	0.0021	2.0770	0.0730	0.1918	0.0041	1116	57	1133	22	1136	24	102
SAN10B_082	0.0775	0.0022	2.0550	0.0520	0.1919	0.0039	1131	59	1131	21	1135	18	100
SAN10L_061	0.0765	0.0014	2.0750	0.0400	0.1916	0.0027	1101	36	1131	15	1135	14	103
SAN10L_065	0.0784	0.0017	2.1390	0.0400	0.1913	0.0031	1154	41	1129	16	1161	13	98
SAN10B_017	0.0777	0.0015	2.0840	0.0480	0.1914	0.0030	1138	39	1129	16	1130	22	99
SAN10B_080	0.0782	0.0019	2.0490	0.0620	0.1905	0.0033	1156	48	1123	18	1128	22	97
SAN10B_081	0.0782	0.0017	2.0660	0.0460	0.1883	0.0028	1160	45	1112	15	1136	15	96
SAN10B_018	0.0766	0.0024	2.0020	0.0730	0.1883	0.0042	1113	63	1112	23	1113	26	100
SAN10B_024	0.0785	0.0021	2.0150	0.0880	0.1876	0.0040	1153	54	1108	22	1104	38	96
SAN10B_019	0.0783	0.0027	1.9800	0.1100	0.1864	0.0043	1158	67	1101	24	1100	38	95
SAN10B_008	0.0768	0.0017	1.9080	0.0540	0.1820	0.0039	1126	40	1077	21	1081	20	96

Analysis #	$^{207}\text{Pb}/^{206}\text{Pb}$	$\pm 2\sigma$	$^{207}\text{Pb}/^{235}\text{U}$	$\pm 2\sigma$	$^{206}\text{Pb}/^{238}\text{U}$	$\pm 2\sigma$	$^{207}\text{Pb}/^{206}\text{Pb}$ age	$\pm 2\sigma$	$^{206}\text{Pb}/^{238}\text{U}$ age	$\pm 2\sigma$	$^{207}\text{Pb}/^{235}\text{U}$ age	$\pm 2\sigma$	Concordancy
SAN10B_107	0.0781	0.0020	2.3030	0.0500	0.2063	0.0040	1151	52	1211	22	1212	15	105
SAN10B_002	0.0779	0.0009	2.2920	0.0360	0.2064	0.0021	1142	24	1209	11	1208	11	106
SAN10L_006	0.0774	0.0028	2.3070	0.0780	0.2063	0.0046	1122	75	1209	25	1211	24	108
SAN10L_009	0.0776	0.0023	2.2860	0.0500	0.2060	0.0039	1121	58	1207	21	1206	16	108
SAN10L_083	0.1160	0.0051	3.2900	0.1500	0.2061	0.0036	1851	80	1207	19	1470	37	65
SAN10L_029	0.0778	0.0018	2.2770	0.0500	0.2051	0.0032	1138	45	1205	16	1208	14	106
SAN10B_051	0.0773	0.0018	2.2790	0.0470	0.2050	0.0029	1135	43	1204	16	1206	15	106
SAN10L_026	0.0781	0.0016	2.2660	0.0460	0.2048	0.0028	1143	39	1201	15	1203	14	105
SAN10L_041	0.0778	0.0017	2.2770	0.0450	0.2043	0.0034	1139	44	1200	18	1203	14	105
SAN10L_070	0.0765	0.0018	2.2660	0.0530	0.2039	0.0036	1105	46	1199	20	1200	17	109
SAN10B_090	0.0782	0.0026	2.2550	0.0840	0.2039	0.0044	1136	66	1196	24	1194	26	105
SAN10L_081	0.0770	0.0024	2.2390	0.0530	0.2037	0.0044	1134	59	1194	24	1190	17	105
SAN10L_037	0.0778	0.0020	2.2440	0.0450	0.2036	0.0033	1126	51	1194	18	1195	14	106
SAN10B_044	0.0771	0.0020	2.2460	0.0450	0.2032	0.0033	1116	53	1192	18	1196	14	107
SAN10B_003	0.0766	0.0011	2.2320	0.0420	0.2033	0.0027	1109	29	1192	15	1191	13	107
SAN10B_054	0.0771	0.0015	2.2370	0.0390	0.2027	0.0031	1120	39	1191	16	1193	13	106
SAN10B_001	0.0773	0.0014	2.2300	0.0430	0.2021	0.0027	1119	35	1188	15	1187	14	106
SAN10L_074	0.0771	0.0017	2.2230	0.0450	0.2012	0.0037	1116	44	1185	20	1185	14	106
SAN10B_077	0.0773	0.0024	2.2250	0.0680	0.2008	0.0035	1126	59	1183	18	1187	21	105
SAN10B_030	0.0762	0.0030	2.2230	0.0620	0.2016	0.0054	1090	76	1183	29	1186	20	109
SAN10B_004	0.0770	0.0013	2.2180	0.0460	0.2011	0.0024	1117	33	1182	13	1180	16	106
SAN10B_071	0.0769	0.0010	2.1900	0.0320	0.2008	0.0023	1120	26	1181	12	1178	10	105
SAN10B_007	0.0763	0.0018	2.1960	0.0420	0.2010	0.0035	1109	46	1180	19	1182	14	106
SAN10L_043	0.0759	0.0019	2.1990	0.0570	0.2007	0.0038	1111	52	1179	20	1183	18	106
SAN10L_039	0.0986	0.0020	2.8060	0.0490	0.2003	0.0028	1584	38	1179	15	1351	15	74
SAN10B_010	0.0771	0.0015	2.2010	0.0390	0.2001	0.0031	1114	39	1178	17	1181	12	106
SAN10L_052	0.0769	0.0036	2.1760	0.0810	0.2007	0.0052	1113	94	1178	28	1174	25	106
SAN10B_016	0.0762	0.0022	2.2080	0.0580	0.2004	0.0036	1111	58	1177	20	1182	18	106
SAN10B_088	0.0906	0.0018	2.6190	0.0740	0.2001	0.0030	1440	37	1177	16	1296	22	82
SAN10B_005	0.0760	0.0014	2.1830	0.0470	0.2003	0.0027	1098	37	1176	15	1171	15	107
SAN10B_022	0.0759	0.0016	2.1870	0.0370	0.2001	0.0027	1095	40	1176	15	1175	12	107
SAN10L_005	0.0766	0.0018	2.1770	0.0480	0.2000	0.0031	1111	46	1175	17	1175	16	106
SAN10B_013	0.0769	0.0013	2.1770	0.0350	0.1991	0.0022	1113	34	1173	12	1172	11	⁸¹ 105

Analysis #	$^{207}\text{Pb}/^{206}\text{Pb}$	$\pm 2\sigma$	$^{207}\text{Pb}/^{235}\text{U}$	$\pm 2\sigma$	$^{206}\text{Pb}/^{238}\text{U}$	$\pm 2\sigma$	$^{207}\text{Pb}/^{206}\text{Pb}$ age	$\pm 2\sigma$	$^{206}\text{Pb}/^{238}\text{U}$ age	$\pm 2\sigma$	$^{207}\text{Pb}/^{235}\text{U}$ age	$\pm 2\sigma$	Concordancy	
SAN10B_036	0.0836	0.0013	2.1330	0.0350	0.1803	0.0021	1282	29	1068	12	1153	13	83	
SAN10B_105	0.0801	0.0008	2.0090	0.0320	0.1773	0.0018	1200	21	1052	10	1113	13	88	
SAN10L_011	0.0866	0.0017	2.1580	0.0520	0.1766	0.0034	1344	38	1049	19	1162	17	78	
SAN10L_040	0.0770	0.0010	1.6180	0.0300	0.1475	0.0022	1117	26	886	12	972	13	79	
SAN-12	(Concordant Analyses)													
SAN12_60	0.1487	0.0017	8.6300	0.1200	0.4192	0.0060	2332	20	2255	27	2300	13	97	
SAN12_151	0.0873	0.0025	2.7910	0.0790	0.2340	0.0049	1364	54	1355	25	1353	22	99	
SAN12_44	0.0845	0.0009	2.6380	0.0280	0.2248	0.0027	1303	19	1307	14	1310	8	100	
SAN12_40	0.0843	0.0025	2.5920	0.0830	0.2229	0.0068	1310	62	1296	36	1300	24	99	
SAN12_100	0.0840	0.0016	2.5670	0.0500	0.2210	0.0036	1296	39	1287	19	1290	14	99	
SAN12_133	0.0840	0.0019	2.5250	0.0520	0.2202	0.0040	1280	45	1282	21	1286	15	100	
SAN12_154	0.0837	0.0022	2.5130	0.0580	0.2171	0.0038	1267	53	1266	20	1273	17	100	
SAN12_191	0.0844	0.0023	2.4460	0.0590	0.2140	0.0038	1302	53	1252	21	1256	18	96	
SAN12_112	0.0819	0.0013	2.4290	0.0400	0.2141	0.0027	1237	32	1250	14	1251	12	101	
SAN12_06	0.0834	0.0032	2.4260	0.0890	0.2134	0.0049	1254	74	1248	26	1252	27	100	
SAN12_140	0.0808	0.0026	2.3910	0.0720	0.2122	0.0048	1191	62	1240	26	1238	22	104	
SAN12_134	0.0817	0.0033	2.3810	0.0880	0.2112	0.0054	1187	79	1236	29	1233	26	104	
SAN12_04	0.0822	0.0010	2.3870	0.0320	0.2113	0.0027	1248	24	1235	14	1240	10	99	
SAN12_131	0.0800	0.0016	2.3360	0.0450	0.2103	0.0038	1197	39	1230	20	1223	13	103	
SAN12_136	0.0812	0.0027	2.3290	0.0690	0.2087	0.0043	1214	68	1221	23	1222	21	101	
SAN12_127	0.0816	0.0022	2.3480	0.0540	0.2078	0.0037	1229	52	1219	20	1224	16	99	
SAN12_132	0.0795	0.0009	2.3210	0.0250	0.2082	0.0025	1182	23	1219	14	1218	8	103	
SAN12_193	0.0807	0.0008	2.3300	0.0290	0.2075	0.0029	1211	20	1216	15	1221	9	100	
SAN12_41	0.0802	0.0019	2.3170	0.0680	0.2078	0.0059	1211	52	1216	31	1218	20	100	
SAN12_03	0.0810	0.0016	2.3000	0.0480	0.2071	0.0033	1212	40	1213	18	1212	15	100	
SAN12_10	0.0798	0.0015	2.2840	0.0430	0.2043	0.0032	1188	39	1200	17	1205	13	101	
SAN12_176	0.0804	0.0022	2.2330	0.0660	0.2045	0.0044	1201	53	1199	24	1194	20	100	
SAN12_172	0.0809	0.0013	2.2670	0.0380	0.2038	0.0030	1225	33	1197	16	1200	12	98	
SAN12_155	0.0810	0.0029	2.2280	0.0870	0.2036	0.0044	1206	75	1194	24	1196	27	99	
SAN12_113	0.0800	0.0012	2.2550	0.0340	0.2033	0.0026	1193	31	1194	14	1200	10	100	
SAN12_01	0.0795	0.0014	2.2480	0.0380	0.2035	0.0027	1184	34	1193	14	1196	12	101	
SAN12_11	0.0796	0.0019	2.2530	0.0530	0.2033	0.0033	1190	46	1192	18	1197	17	⁸³ 100	

Analysis #	$^{207}\text{Pb}/^{206}\text{Pb}$	$\pm 2\sigma$	$^{207}\text{Pb}/^{235}\text{U}$	$\pm 2\sigma$	$^{206}\text{Pb}/^{238}\text{U}$	$\pm 2\sigma$	$^{207}\text{Pb}/^{206}\text{Pb}$ age	$\pm 2\sigma$	$^{206}\text{Pb}/^{238}\text{U}$ age	$\pm 2\sigma$	$^{207}\text{Pb}/^{235}\text{U}$ age	$\pm 2\sigma$	Concordancy
SAN12_116	0.0793	0.0016	2.2520	0.0530	0.2026	0.0029	1173	38	1191	15	1194	16	102
SAN12_66	0.0797	0.0021	2.2490	0.0600	0.2027	0.0032	1188	51	1189	17	1194	19	100
SAN12_143	0.0791	0.0028	2.2200	0.0640	0.2026	0.0047	1161	70	1189	25	1190	19	102
SAN12_51	0.0783	0.0016	2.2100	0.0470	0.2021	0.0038	1149	41	1188	20	1186	15	103
SAN12_199	0.0803	0.0014	2.2270	0.0390	0.2016	0.0036	1206	34	1187	19	1189	12	98
SAN12_198	0.0799	0.0014	2.2220	0.0420	0.2020	0.0030	1196	35	1187	17	1191	13	99
SAN12_161	0.0795	0.0016	2.2370	0.0490	0.2019	0.0037	1178	40	1187	20	1190	15	101
SAN12_26	0.0802	0.0012	2.2310	0.0320	0.2018	0.0028	1204	28	1184	15	1192	10	98
SAN12_13	0.0801	0.0011	2.2230	0.0330	0.2015	0.0027	1192	29	1183	14	1186	10	99
SAN12_09	0.0800	0.0015	2.2200	0.0400	0.2012	0.0029	1193	37	1181	16	1185	13	99
SAN12_62	0.0794	0.0019	2.2170	0.0560	0.2012	0.0038	1178	47	1181	20	1185	18	100
SAN12_58	0.0795	0.0017	2.2140	0.0550	0.2007	0.0039	1175	43	1181	20	1186	18	101
SAN12_200	0.0803	0.0014	2.1890	0.0430	0.2010	0.0033	1197	36	1180	18	1177	14	99
SAN12_71	0.0791	0.0016	2.1910	0.0610	0.2010	0.0043	1166	41	1180	23	1180	19	101
SAN12_182	0.0805	0.0023	2.2150	0.0570	0.1994	0.0035	1202	54	1179	20	1182	18	98
SAN12_91	0.0773	0.0021	2.1660	0.0460	0.2004	0.0035	1122	52	1177	19	1172	15	105
SAN12_93	0.0817	0.0020	2.2380	0.0560	0.1999	0.0033	1237	46	1176	18	1191	17	95
SAN12_150	0.0786	0.0020	2.1890	0.0480	0.2002	0.0039	1165	51	1176	21	1180	16	101
SAN12_173	0.0813	0.0015	2.1930	0.0390	0.1995	0.0033	1217	37	1174	18	1178	12	96
SAN12_52	0.0792	0.0018	2.1800	0.0480	0.1999	0.0028	1169	45	1174	15	1170	16	100
SAN12_35	0.0796	0.0018	2.1920	0.0430	0.1990	0.0031	1189	42	1172	16	1175	14	99
SAN12_152	0.0789	0.0009	2.1820	0.0280	0.1994	0.0025	1173	24	1172	14	1175	9	100
SAN12_86	0.0787	0.0018	2.1780	0.0560	0.1988	0.0033	1165	43	1172	18	1172	18	101
SAN12_192	0.0787	0.0012	2.1730	0.0320	0.1992	0.0028	1162	31	1172	15	1172	10	101
SAN12_185	0.0787	0.0012	2.1870	0.0320	0.1993	0.0030	1165	30	1171	16	1175	10	101
SAN12_126	0.0791	0.0027	2.1890	0.0730	0.1993	0.0047	1160	66	1171	25	1175	23	101
SAN12_165	0.0796	0.0018	2.1760	0.0490	0.1991	0.0030	1196	44	1170	16	1171	16	98
SAN12_56	0.0785	0.0015	2.1840	0.0340	0.1991	0.0032	1158	38	1170	17	1175	11	101
SAN12_81	0.0779	0.0015	2.1640	0.0440	0.1991	0.0035	1153	38	1170	19	1170	14	101
SAN12_162	0.0800	0.0017	2.1710	0.0440	0.1987	0.0031	1187	42	1169	16	1173	15	98
SAN12_74	0.0782	0.0010	2.1510	0.0260	0.1990	0.0026	1160	26	1169	14	1166	9	101
SAN12_189	0.0784	0.0014	2.1550	0.0340	0.1990	0.0030	1155	36	1169	16	1166	11	101
SAN12_31	0.0781	0.0016	2.1540	0.0410	0.1989	0.0030	1144	40	1169	16	1165	13	⁸⁴ 102

Analysis #	$^{207}\text{Pb}/^{206}\text{Pb}$	$\pm 2\sigma$	$^{207}\text{Pb}/^{235}\text{U}$	$\pm 2\sigma$	$^{206}\text{Pb}/^{238}\text{U}$	$\pm 2\sigma$	$^{207}\text{Pb}/^{206}\text{Pb}$ age	$\pm 2\sigma$	$^{206}\text{Pb}/^{238}\text{U}$ age	$\pm 2\sigma$	$^{207}\text{Pb}/^{235}\text{U}$ age	$\pm 2\sigma$	Concordancy
SAN12_05	0.0792	0.0016	2.1700	0.0430	0.1988	0.0034	1164	41	1168	18	1172	14	100
SAN12_48	0.0788	0.0008	2.1590	0.0290	0.1985	0.0023	1165	19	1167	12	1170	9	100
SAN12_18	0.0793	0.0014	2.1510	0.0360	0.1983	0.0030	1176	35	1165	16	1165	11	99
SAN12_78	0.0798	0.0022	2.1760	0.0550	0.1982	0.0041	1173	55	1165	22	1170	17	99
SAN12_196	0.0798	0.0021	2.1560	0.0540	0.1980	0.0040	1201	52	1164	21	1168	17	97
SAN12_08	0.0798	0.0019	2.1600	0.0400	0.1979	0.0037	1179	47	1163	20	1168	13	99
SAN12_195	0.0802	0.0046	2.1460	0.0950	0.1970	0.0060	1160	110	1163	32	1164	31	100
SAN12_183	0.0784	0.0016	2.1670	0.0440	0.1979	0.0034	1153	40	1163	18	1167	14	101
SAN12_153	0.0787	0.0021	2.1540	0.0540	0.1972	0.0044	1149	53	1163	23	1166	18	101
SAN12_125	0.0787	0.0027	2.1600	0.0640	0.1979	0.0040	1140	70	1163	22	1168	21	102
SAN12_137	0.0780	0.0016	2.1480	0.0380	0.1968	0.0032	1146	40	1162	16	1163	12	101
SAN12_160	0.0775	0.0021	2.1380	0.0570	0.1970	0.0044	1127	52	1162	24	1161	19	103
SAN12_163	0.0792	0.0016	2.1560	0.0490	0.1974	0.0029	1192	39	1161	15	1166	16	97
SAN12_15	0.0791	0.0013	2.1410	0.0340	0.1975	0.0024	1171	31	1161	13	1163	11	99
SAN12_84	0.0791	0.0016	2.1290	0.0380	0.1970	0.0031	1167	40	1159	17	1161	13	99
SAN12_194	0.0776	0.0018	2.1260	0.0490	0.1969	0.0031	1142	46	1159	17	1155	16	101
SAN12_19	0.0794	0.0019	2.1380	0.0530	0.1967	0.0033	1187	48	1157	18	1161	17	97
SAN12_186	0.0798	0.0027	2.1370	0.0680	0.1966	0.0041	1187	65	1156	22	1161	22	97
SAN12_43	0.0787	0.0016	2.1400	0.0420	0.1963	0.0032	1176	38	1156	17	1162	14	98
SAN12_168	0.0790	0.0017	2.1480	0.0430	0.1965	0.0026	1163	39	1156	14	1162	14	99
SAN12_28	0.0790	0.0020	2.1230	0.0520	0.1963	0.0047	1161	49	1155	25	1155	17	99
SAN12_63	0.0794	0.0019	2.1810	0.0500	0.1960	0.0031	1184	47	1154	17	1175	16	97
SAN12_22	0.0783	0.0011	2.1320	0.0340	0.1961	0.0026	1155	29	1154	14	1158	11	100
SAN12_73	0.0784	0.0023	2.1420	0.0630	0.1961	0.0046	1143	57	1153	25	1158	20	101
SAN12_61	0.0799	0.0045	2.1300	0.1000	0.1950	0.0060	1190	110	1152	33	1152	33	97
SAN12_39	0.0782	0.0013	2.1180	0.0380	0.1957	0.0026	1148	33	1152	14	1155	12	100
SAN12_142	0.0793	0.0022	2.1280	0.0490	0.1948	0.0041	1166	56	1150	22	1156	16	99
SAN12_34	0.0794	0.0018	2.1290	0.0540	0.1947	0.0036	1185	42	1149	20	1157	17	97
SAN12_128	0.0789	0.0017	2.1180	0.0450	0.1944	0.0031	1158	42	1149	16	1152	15	99
SAN12_167	0.0778	0.0014	2.1150	0.0370	0.1952	0.0029	1135	35	1149	16	1154	12	101
SAN12_47	0.0787	0.0021	2.1100	0.0490	0.1949	0.0041	1165	51	1147	22	1151	16	98
SAN12_69	0.0778	0.0019	2.1240	0.0520	0.1945	0.0031	1153	48	1147	16	1154	17	99
SAN12_20	0.0809	0.0018	2.1760	0.0470	0.1944	0.0030	1206	44	1146	16	1170	15	85 95

Analysis #	$^{207}\text{Pb}/^{206}\text{Pb}$	$\pm 2\sigma$	$^{207}\text{Pb}/^{235}\text{U}$	$\pm 2\sigma$	$^{206}\text{Pb}/^{238}\text{U}$	$\pm 2\sigma$	$^{207}\text{Pb}/^{206}\text{Pb}$ age	$\pm 2\sigma$	$^{206}\text{Pb}/^{238}\text{U}$ age	$\pm 2\sigma$	$^{207}\text{Pb}/^{235}\text{U}$ age	$\pm 2\sigma$	Concordancy
SAN12_90	0.0786	0.0013	2.1040	0.0370	0.1944	0.0026	1167	35	1145	14	1150	12	98
SAN12_30	0.0790	0.0020	2.1180	0.0470	0.1946	0.0040	1160	51	1145	22	1153	15	99
SAN12_77	0.0784	0.0010	2.1030	0.0290	0.1941	0.0022	1151	26	1145	12	1149	10	99
SAN12_85	0.0769	0.0026	2.0820	0.0730	0.1945	0.0040	1131	69	1145	21	1146	23	101
SAN12_104	0.0775	0.0022	2.0990	0.0560	0.1933	0.0035	1127	56	1144	19	1148	18	102
SAN12_177	0.0790	0.0015	2.0890	0.0390	0.1941	0.0030	1168	37	1143	16	1147	13	98
SAN12_80	0.0788	0.0019	2.0820	0.0480	0.1936	0.0033	1169	50	1142	18	1142	15	98
SAN12_75	0.0799	0.0012	2.1450	0.0320	0.1932	0.0027	1189	29	1141	15	1163	10	96
SAN12_27	0.0778	0.0019	2.0890	0.0470	0.1937	0.0035	1137	47	1141	19	1146	15	100
SAN12_59	0.0781	0.0021	2.1100	0.0510	0.1931	0.0034	1151	52	1140	19	1149	16	99
SAN12_122	0.0783	0.0012	2.0870	0.0460	0.1932	0.0037	1164	32	1139	20	1143	15	98
SAN12_32	0.0785	0.0033	2.0690	0.0740	0.1930	0.0048	1159	83	1139	25	1141	23	98
SAN12_45	0.0774	0.0025	2.0680	0.0630	0.1926	0.0055	1113	66	1139	29	1142	22	102
SAN12_118	0.0780	0.0020	2.0490	0.0470	0.1929	0.0028	1137	50	1137	15	1136	15	100
SAN12_166	0.0777	0.0025	2.0880	0.0660	0.1929	0.0044	1146	64	1136	24	1142	22	99
SAN12_117	0.0780	0.0014	2.0800	0.0340	0.1927	0.0026	1145	35	1135	14	1142	11	99
SAN12_33	0.0775	0.0023	2.0570	0.0560	0.1927	0.0035	1130	59	1135	19	1132	19	100
SAN12_164	0.0779	0.0038	2.0820	0.0850	0.1917	0.0061	1141	96	1134	32	1137	28	99
SAN12_29	0.0781	0.0015	2.0700	0.0410	0.1915	0.0027	1159	39	1133	15	1137	14	98
SAN12_82	0.0773	0.0018	2.0600	0.0410	0.1914	0.0035	1135	45	1131	19	1134	14	100
SAN12_121	0.0787	0.0022	2.0560	0.0490	0.1906	0.0029	1144	56	1129	16	1133	16	99
SAN12_12	0.0788	0.0044	2.0430	0.0960	0.1914	0.0062	1110	110	1127	33	1131	32	102
SAN12_130	0.0777	0.0012	2.0350	0.0310	0.1904	0.0026	1139	30	1123	14	1126	10	99
SAN12_149	0.0777	0.0018	2.0460	0.0600	0.1898	0.0040	1135	44	1123	21	1131	19	99
SAN12_83	0.0774	0.0012	2.0440	0.0330	0.1904	0.0024	1135	31	1123	13	1128	11	99
SAN12_55	0.0780	0.0023	2.0320	0.0630	0.1897	0.0036	1141	61	1119	20	1120	21	98
SAN12_123	0.0764	0.0019	2.0010	0.0490	0.1888	0.0034	1112	51	1114	18	1114	17	100
SAN12_159	0.0770	0.0022	1.9920	0.0540	0.1879	0.0037	1119	56	1109	20	1110	19	99
SAN12_102	0.0773	0.0037	2.0050	0.0950	0.1866	0.0045	1145	94	1108	24	1109	33	97
SAN12_109	0.0760	0.0025	1.9800	0.0640	0.1869	0.0042	1115	65	1104	23	1104	22	99
SAN12_138	0.0781	0.0018	1.9850	0.0470	0.1868	0.0031	1151	46	1103	17	1111	16	96
SAN12_16	0.0769	0.0024	1.9520	0.0560	0.1848	0.0040	1100	62	1094	22	1099	19	99
SAN12_135	0.0752	0.0035	1.9240	0.0760	0.1845	0.0045	1046	96	1091	24	1094	27	⁸⁶ 104

Analysis #	$^{207}\text{Pb}/^{206}\text{Pb}$	$\pm 2\sigma$	$^{207}\text{Pb}/^{235}\text{U}$	$\pm 2\sigma$	$^{206}\text{Pb}/^{238}\text{U}$	$\pm 2\sigma$	$^{207}\text{Pb}/^{206}\text{Pb}$ age	$\pm 2\sigma$	$^{206}\text{Pb}/^{238}\text{U}$ age	$\pm 2\sigma$	$^{207}\text{Pb}/^{235}\text{U}$ age	$\pm 2\sigma$	Concordancy
SAN12_146	0.0767	0.0031	1.9190	0.0670	0.1820	0.0040	1089	83	1085	22	1090	24	100
SAN12_101	0.0753	0.0047	1.9000	0.1100	0.1814	0.0064	1070	140	1079	36	1075	40	101
SAN12_95	0.0784	0.0040	1.9330	0.0850	0.1813	0.0049	1070	110	1072	27	1080	30	100
SAN-12 <i>(Discordant Analyses)</i>													
SAN12_65	0.3250	0.0150	11.3900	0.3900	0.2580	0.0100	3570	68	1481	52	2550	33	41
SAN12_70	0.1018	0.0009	3.1740	0.0380	0.2247	0.0028	1654	16	1306	15	1450	9	79
SAN12_197	0.0896	0.0023	2.7020	0.0640	0.2211	0.0039	1399	51	1288	21	1329	18	92
SAN12_02	0.0864	0.0010	2.5540	0.0300	0.2150	0.0025	1341	21	1255	13	1288	9	94
SAN12_171	0.1064	0.0019	3.0520	0.0580	0.2097	0.0030	1728	32	1228	16	1420	14	71
SAN12_92	0.0767	0.0015	2.2280	0.0380	0.2093	0.0035	1116	39	1226	18	1188	12	110
SAN12_96	0.1003	0.0015	2.9100	0.0400	0.2082	0.0024	1625	28	1220	13	1383	10	75
SAN12_25	0.0848	0.0013	2.4120	0.0360	0.2059	0.0028	1303	29	1206	15	1245	11	93
SAN12_184	0.1080	0.0034	3.1000	0.1100	0.2045	0.0033	1746	57	1200	17	1427	28	69
SAN12_36	0.0886	0.0011	2.4590	0.0280	0.2035	0.0026	1390	23	1193	14	1260	8	86
SAN12_23	0.0835	0.0025	2.3400	0.0670	0.2034	0.0037	1269	61	1193	20	1217	21	94
SAN12_37	0.0936	0.0017	2.6080	0.0590	0.2029	0.0035	1496	34	1190	19	1306	16	80
SAN12_188	0.1363	0.0032	3.7610	0.0800	0.2012	0.0031	2167	40	1181	17	1581	17	54
SAN12_129	0.0864	0.0018	2.3910	0.0510	0.1994	0.0027	1350	40	1172	14	1242	15	87
SAN12_175	0.0837	0.0011	2.2960	0.0350	0.1993	0.0029	1283	26	1171	16	1211	11	91
SAN12_89	0.0877	0.0014	2.4010	0.0390	0.1976	0.0029	1371	30	1162	16	1241	12	85
SAN12_38	0.0842	0.0017	2.2820	0.0450	0.1977	0.0033	1305	40	1162	18	1211	14	89
SAN12_111	0.0818	0.0025	2.2200	0.0620	0.1977	0.0039	1231	58	1162	21	1188	20	94
SAN12_54	0.0849	0.0011	2.2970	0.0340	0.1968	0.0031	1309	25	1159	16	1211	10	89
SAN12_98	0.0817	0.0020	2.2400	0.0500	0.1969	0.0029	1236	47	1158	16	1193	16	94
SAN12_174	0.0844	0.0012	2.2990	0.0370	0.1962	0.0027	1296	27	1154	15	1211	11	89
SAN12_64	0.0836	0.0014	2.2770	0.0370	0.1958	0.0029	1291	32	1152	15	1203	11	89
SAN12_106	0.0928	0.0024	2.5180	0.0750	0.1954	0.0025	1475	46	1151	14	1275	21	78
SAN12_46	0.0945	0.0020	2.5510	0.0520	0.1953	0.0032	1522	40	1149	17	1285	15	75
SAN12_99	0.1017	0.0030	2.7540	0.0950	0.1939	0.0026	1650	57	1145	14	1335	26	69
SAN12_79	0.0869	0.0011	2.3260	0.0340	0.1940	0.0022	1357	25	1145	12	1221	10	84

Analysis #	$^{207}\text{Pb}/^{206}\text{Pb}$	$\pm 2\sigma$	$^{207}\text{Pb}/^{235}\text{U}$	$\pm 2\sigma$	$^{206}\text{Pb}/^{238}\text{U}$	$\pm 2\sigma$	$^{207}\text{Pb}/^{206}\text{Pb}$ age	$\pm 2\sigma$	$^{206}\text{Pb}/^{238}\text{U}$ age	$\pm 2\sigma$	$^{207}\text{Pb}/^{235}\text{U}$ age	$\pm 2\sigma$	Concordancy
SAN12_120	0.0840	0.0010	2.2550	0.0320	0.1941	0.0021	1288	24	1144	11	1199	10	89
SAN12_21	0.0823	0.0014	2.1790	0.0370	0.1931	0.0026	1253	34	1138	14	1175	12	91
SAN12_07	0.0808	0.0026	2.1980	0.0600	0.1934	0.0041	1212	65	1138	22	1178	19	94
SAN12_187	0.0869	0.0039	2.3070	0.0910	0.1927	0.0048	1342	88	1134	26	1224	27	85
SAN12_53	0.0829	0.0010	2.2160	0.0290	0.1917	0.0023	1269	24	1130	12	1186	9	89
SAN12_115	0.0800	0.0010	2.1270	0.0300	0.1916	0.0027	1196	26	1130	15	1157	10	94
SAN12_107	0.0863	0.0018	2.2790	0.0460	0.1911	0.0034	1341	40	1129	19	1207	14	84
SAN12_145	0.0809	0.0015	2.1620	0.0410	0.1916	0.0030	1208	38	1129	16	1170	13	93
SAN12_141	0.0825	0.0015	2.1610	0.0390	0.1913	0.0027	1252	35	1128	15	1170	12	90
SAN12_105	0.0820	0.0015	2.1680	0.0470	0.1907	0.0031	1236	36	1125	17	1170	15	91
SAN12_14	0.0757	0.0041	2.0040	0.0960	0.1909	0.0066	1060	110	1124	36	1121	32	106
SAN12_57	0.0859	0.0012	2.2440	0.0320	0.1903	0.0027	1330	26	1124	14	1194	10	85
SAN12_108	0.0848	0.0009	2.2190	0.0250	0.1903	0.0019	1307	21	1124	10	1187	8	86
SAN12_169	0.0809	0.0017	2.1400	0.0440	0.1904	0.0030	1210	42	1123	17	1160	14	93
SAN12_178	0.0844	0.0019	2.2330	0.0490	0.1895	0.0033	1309	43	1118	18	1190	15	85
SAN12_42	0.0816	0.0026	2.1020	0.0580	0.1888	0.0041	1221	61	1114	22	1149	18	91
SAN12_68	0.0799	0.0019	2.0770	0.0420	0.1884	0.0034	1204	47	1112	18	1140	14	92
SAN12_103	0.0798	0.0017	2.0880	0.0400	0.1884	0.0029	1175	43	1112	16	1146	13	95
SAN12_88	0.0800	0.0013	2.0750	0.0340	0.1878	0.0026	1192	32	1109	14	1139	11	93
SAN12_76	0.0810	0.0026	2.1090	0.0580	0.1865	0.0043	1211	63	1101	23	1152	18	91
SAN12_157	0.0833	0.0020	2.1330	0.0500	0.1860	0.0032	1274	48	1099	18	1158	17	86
SAN12_148	0.0825	0.0013	2.1280	0.0320	0.1855	0.0025	1247	32	1096	14	1156	11	88
SAN12_158	0.0804	0.0032	2.0750	0.0780	0.1851	0.0041	1217	79	1094	22	1133	26	90
SAN12_147	0.0822	0.0034	2.0380	0.0770	0.1847	0.0046	1232	79	1092	25	1127	27	89
SAN12_190	0.0921	0.0020	2.4010	0.0560	0.1839	0.0030	1472	42	1090	16	1240	17	74
SAN12_114	0.0851	0.0042	2.1560	0.0890	0.1839	0.0051	1305	97	1086	28	1166	29	83
SAN12_179	0.0835	0.0012	2.1000	0.0350	0.1832	0.0031	1284	28	1086	16	1147	11	85
SAN12_17	0.0750	0.0034	1.9150	0.0850	0.1831	0.0049	1009	96	1084	26	1086	30	107
SAN12_124	0.1652	0.0066	4.2100	0.1400	0.1832	0.0052	2473	69	1083	28	1686	27	44
SAN12_24	0.0799	0.0019	2.0340	0.0490	0.1819	0.0032	1194	46	1080	17	1125	16	90
SAN12_94	0.0757	0.0071	1.8500	0.1500	0.1813	0.0068	960	190	1075	36	1078	54	112
SAN12_87	0.0809	0.0050	2.0100	0.1100	0.1816	0.0065	1150	130	1073	36	1109	35	93
SAN12_180	0.1034	0.0031	2.5950	0.0670	0.1804	0.0042	1685	55	1072	23	1298	19	88

Analysis #	$^{207}\text{Pb}/^{206}\text{Pb}$	$\pm 2\sigma$	$^{207}\text{Pb}/^{235}\text{U}$	$\pm 2\sigma$	$^{206}\text{Pb}/^{238}\text{U}$	$\pm 2\sigma$	$^{207}\text{Pb}/^{206}\text{Pb}$ age	$\pm 2\sigma$	$^{206}\text{Pb}/^{238}\text{U}$ age	$\pm 2\sigma$	$^{207}\text{Pb}/^{235}\text{U}$ age	$\pm 2\sigma$	Concordancy	
SAN12_110	0.0853	0.0043	2.1030	0.0900	0.1804	0.0051	1301	96	1070	27	1153	29	82	
SAN12_119	0.0782	0.0030	1.9480	0.0650	0.1794	0.0040	1129	78	1064	22	1098	23	94	
SAN12_67	0.0786	0.0031	1.9400	0.0660	0.1783	0.0038	1125	78	1059	21	1096	23	94	
SAN12_97	0.0830	0.0009	2.0460	0.0250	0.1782	0.0018	1269	21	1057	10	1132	8	83	
SAN12_170	0.0782	0.0008	1.9420	0.0220	0.1777	0.0023	1151	21	1054	12	1095	7	92	
SAN12_181	0.0776	0.0009	1.9010	0.0270	0.1758	0.0021	1139	24	1044	11	1080	10	92	
SAN12_72	0.0888	0.0010	2.1270	0.0340	0.1719	0.0025	1396	21	1023	14	1156	11	73	
SAN12_49	0.0802	0.0009	1.9070	0.0250	0.1713	0.0019	1205	21	1019	10	1082	9	85	
SAN12_50	0.0766	0.0010	1.6720	0.0260	0.1583	0.0028	1110	25	947	16	997	10	85	
SAN12_156	0.0748	0.0009	1.3120	0.0180	0.1275	0.0018	1060	24	774	10	851	8	73	
SAN-13	(Concordant Analyses)													
SAN13_72	0.0839	0.0039	2.6300	0.1100	0.2256	0.0057	1265	95	1310	30	1307	31	104	
SAN13_03	0.0845	0.0011	2.6170	0.0370	0.2248	0.0033	1303	25	1307	18	1304	10	100	
SAN13_20	0.0833	0.0026	2.5940	0.0830	0.2223	0.0053	1277	62	1297	28	1294	24	102	
SAN13_62	0.0832	0.0014	2.5400	0.0480	0.2208	0.0031	1272	32	1285	16	1283	14	101	
SAN13_76	0.0833	0.0027	2.5130	0.0660	0.2179	0.0050	1297	67	1270	27	1272	19	98	
SAN13_96	0.0846	0.0030	2.4960	0.0860	0.2175	0.0043	1273	69	1267	23	1272	25	100	
SAN13_70	0.0832	0.0027	2.3650	0.0650	0.2085	0.0043	1250	65	1223	22	1229	20	98	
SAN13_05	0.0795	0.0017	2.3140	0.0590	0.2088	0.0051	1193	42	1222	27	1221	18	102	
SAN13_89	0.0804	0.0008	2.3110	0.0280	0.2079	0.0027	1209	20	1217	14	1215	9	101	
SAN13_59	0.0813	0.0015	2.3140	0.0490	0.2065	0.0041	1233	34	1210	22	1214	15	98	
SAN13_22	0.0802	0.0016	2.2720	0.0490	0.2058	0.0048	1198	40	1205	26	1202	15	101	
SAN13_56	0.0801	0.0018	2.2800	0.0500	0.2053	0.0044	1197	43	1205	24	1209	15	101	
SAN13_37	0.0803	0.0013	2.2470	0.0440	0.2048	0.0040	1200	33	1202	21	1198	13	100	
SAN13_77	0.0808	0.0016	2.2870	0.0440	0.2049	0.0035	1218	37	1201	19	1206	14	99	
SAN13_12	0.0797	0.0012	2.2750	0.0360	0.2038	0.0036	1187	29	1201	20	1204	11	101	
SAN13_41	0.0799	0.0019	2.2720	0.0560	0.2048	0.0043	1196	49	1200	23	1200	18	100	
SAN13_13	0.0790	0.0025	2.2820	0.0650	0.2039	0.0056	1163	61	1199	30	1204	20	103	
SAN13_08	0.0809	0.0022	2.2640	0.0460	0.2042	0.0048	1210	53	1197	26	1200	14	99	
SAN13_42	0.0805	0.0021	2.2430	0.0580	0.2033	0.0046	1196	54	1195	25	1194	18	100	
SAN13_49	0.0798	0.0026	2.2310	0.0730	0.2024	0.0047	1166	67	1192	26	1188	23	102	

Analysis #	$^{207}\text{Pb}/^{206}\text{Pb}$	$\pm 2\sigma$	$^{207}\text{Pb}/^{235}\text{U}$	$\pm 2\sigma$	$^{206}\text{Pb}/^{238}\text{U}$	$\pm 2\sigma$	$^{207}\text{Pb}/^{206}\text{Pb}$ age	$\pm 2\sigma$	$^{206}\text{Pb}/^{238}\text{U}$ age	$\pm 2\sigma$	$^{207}\text{Pb}/^{235}\text{U}$ age	$\pm 2\sigma$	Concordancy
SAN13_85	0.0792	0.0013	2.1220	0.0380	0.1964	0.0028	1170	31	1155	15	1158	12	99
SAN13_80	0.0787	0.0021	2.1190	0.0520	0.1954	0.0036	1152	53	1152	20	1154	17	100
SAN13_47	0.0786	0.0019	2.1210	0.0490	0.1959	0.0041	1148	46	1152	22	1157	16	100
SAN13_21	0.0803	0.0024	2.1170	0.0630	0.1956	0.0046	1190	60	1150	25	1153	21	97
SAN13_65	0.0789	0.0024	2.1120	0.0570	0.1954	0.0046	1171	60	1150	25	1153	18	98
SAN13_90	0.0783	0.0029	2.1040	0.0730	0.1948	0.0051	1151	74	1149	28	1151	23	100
SAN13_18	0.0782	0.0021	2.1030	0.0510	0.1953	0.0040	1150	54	1149	21	1152	17	100
SAN13_95	0.0787	0.0030	2.1120	0.0800	0.1950	0.0073	1155	75	1148	39	1151	26	99
SAN13_84	0.0789	0.0013	2.1080	0.0380	0.1948	0.0032	1172	32	1146	17	1150	12	98
SAN13_100	0.0781	0.0017	2.0990	0.0490	0.1935	0.0029	1151	40	1144	15	1149	16	99
SAN13_48	0.0793	0.0029	2.0760	0.0700	0.1943	0.0045	1165	70	1143	24	1145	23	98
SAN13_74	0.0787	0.0016	2.0770	0.0400	0.1938	0.0027	1151	42	1141	15	1144	12	99
SAN13_43	0.0783	0.0028	2.0940	0.0690	0.1936	0.0041	1154	73	1140	22	1143	23	99
SAN13_69	0.0795	0.0024	2.0690	0.0600	0.1929	0.0034	1163	59	1136	18	1139	20	98
SAN13_99	0.0784	0.0015	2.0760	0.0360	0.1925	0.0031	1156	37	1134	17	1138	12	98
SAN13_01	0.0776	0.0017	2.0480	0.0460	0.1917	0.0038	1130	45	1132	20	1129	15	100
SAN13_36	0.0784	0.0034	2.0360	0.0810	0.1899	0.0053	1161	88	1124	28	1122	28	97
SAN13_40	0.0760	0.0040	2.0210	0.0880	0.1902	0.0061	1080	110	1119	33	1117	30	104
SAN13_94	0.0764	0.0022	1.9190	0.0480	0.1833	0.0033	1110	56	1084	18	1087	17	98
SAN13_60	0.0744	0.0031	1.8760	0.0630	0.1817	0.0043	1051	83	1077	24	1074	23	102

SAN-13 (Discordant Analyses)

SAN13_93	0.0811	0.0007	2.5230	0.0280	0.2267	0.0031	1219	18	1316	16	1278	8	108
SAN13_87	0.0888	0.0036	2.6000	0.1000	0.2116	0.0051	1372	76	1236	27	1299	29	90
SAN13_19	0.0897	0.0048	2.7500	0.2700	0.2100	0.0046	1308	51	1227	24	1265	30	94
SAN13_78	0.0843	0.0025	2.3410	0.0550	0.2017	0.0040	1306	57	1186	22	1222	17	91
SAN13_64	0.0830	0.0013	2.2970	0.0400	0.1999	0.0028	1274	31	1174	15	1210	12	92
SAN13_32	0.0851	0.0054	2.3500	0.1300	0.1952	0.0058	1340	120	1149	31	1222	41	86
SAN13_38	0.0814	0.0014	2.1860	0.0470	0.1934	0.0035	1226	36	1142	19	1175	15	93
SAN13_79	0.0983	0.0044	2.6000	0.1000	0.1907	0.0043	1559	84	1123	23	1297	29	72
SAN13_33	0.0812	0.0022	2.1250	0.0470	0.1874	0.0038	1217	52	1106	21	1155	15	91
SAN13_88	0.0800	0.0020	2.0600	0.0530	0.1871	0.0034	1196	48	1105	18	1139	18	92

Analysis #	$^{207}\text{Pb}/^{206}\text{Pb}$	$\pm 2\sigma$	$^{207}\text{Pb}/^{235}\text{U}$	$\pm 2\sigma$	$^{206}\text{Pb}/^{238}\text{U}$	$\pm 2\sigma$	$^{207}\text{Pb}/^{206}\text{Pb}$ age	$\pm 2\sigma$	$^{206}\text{Pb}/^{238}\text{U}$ age	$\pm 2\sigma$	$^{207}\text{Pb}/^{235}\text{U}$ age	$\pm 2\sigma$	Concordancy
SAN13_68	0.0807	0.0020	2.0720	0.0500	0.1867	0.0032	1191	49	1103	17	1138	16	93
SAN13_73	0.0966	0.0072	2.3400	0.1600	0.1842	0.0079	1450	140	1084	43	1215	51	75
SAN13_26	0.0801	0.0030	2.0540	0.0710	0.1829	0.0037	1197	74	1082	20	1133	24	90
SAN13_58	0.0744	0.0056	1.8900	0.1300	0.1817	0.0065	1010	160	1078	35	1075	46	107
SAN13_55	0.0807	0.0041	1.9540	0.0860	0.1773	0.0053	1160	100	1050	29	1092	29	91
SAN13_66	0.0791	0.0049	1.8580	0.0990	0.1740	0.0047	1110	130	1032	26	1072	36	93
SAN13_91	0.0797	0.0012	1.8680	0.0320	0.1717	0.0030	1185	30	1022	16	1071	12	86
SAN13_67	0.0858	0.0010	2.0100	0.0270	0.1716	0.0025	1330	21	1020	14	1122	9	77
SAN13_04	0.0820	0.0012	1.9530	0.0300	0.1711	0.0024	1242	27	1018	13	1097	10	82
SAN13_07	0.0841	0.0013	1.9800	0.0360	0.1702	0.0027	1296	31	1014	15	1111	12	78
SAN13_81	0.0811	0.0011	1.9120	0.0280	0.1700	0.0021	1226	27	1013	11	1085	10	83
SAN13_97	0.0813	0.0011	1.7780	0.0260	0.1592	0.0021	1225	25	952	12	1037	10	78
SAN13_44	0.0805	0.0010	1.7600	0.0250	0.1573	0.0024	1213	24	941	13	1030	9	78
SAN13_71	0.0975	0.0011	2.0840	0.0230	0.1558	0.0017	1584	22	934	10	1144	7	59
SAN13_75	0.0822	0.0010	1.7860	0.0270	0.1556	0.0021	1251	23	932	12	1040	10	75
SAN13_82	0.0769	0.0008	1.5550	0.0200	0.1481	0.0020	1118	22	890	11	953	8	80
SAN13_34	0.0768	0.0009	1.5410	0.0200	0.1446	0.0025	1114	25	870	14	946	8	78

SAN-14	(Concordant Analyses)												
SAN14_95	0.0853	0.0015	2.6570	0.0540	0.2258	0.0049	1325	32	1312	26	1315	15	99
SAN14_59	0.0836	0.0012	2.5700	0.0360	0.2217	0.0033	1280	27	1290	17	1292	10	101
SAN14_61	0.0831	0.0021	2.5450	0.0500	0.2203	0.0041	1270	48	1283	22	1285	15	101
SAN14_83	0.0829	0.0018	2.4990	0.0550	0.2184	0.0038	1267	44	1272	20	1274	16	100
SAN14_27	0.0836	0.0019	2.5190	0.0580	0.2181	0.0040	1278	46	1271	21	1275	17	99
SAN14_67	0.0844	0.0042	2.5170	0.0990	0.2175	0.0056	1262	99	1267	30	1270	28	100
SAN14_46	0.0826	0.0013	2.4780	0.0450	0.2168	0.0025	1257	31	1264	13	1265	13	101
SAN14_100	0.0836	0.0022	2.4680	0.0700	0.2154	0.0037	1280	50	1257	20	1261	21	98
SAN14_73	0.0834	0.0020	2.4740	0.0570	0.2110	0.0033	1289	49	1233	18	1265	17	96
SAN14_99	0.0807	0.0016	2.3760	0.0440	0.2106	0.0034	1225	37	1232	18	1235	13	101
SAN14_24	0.0815	0.0017	2.3620	0.0440	0.2097	0.0034	1227	41	1230	18	1231	13	100
SAN14_51	0.0794	0.0012	2.2800	0.0330	0.2064	0.0028	1189	29	1209	15	1205	10	102
SAN14_57	0.0800	0.0019	2.3010	0.0590	0.2053	0.0035	1204	50	1204	19	1210	18	100

Analysis #	$^{207}\text{Pb}/^{206}\text{Pb}$	$\pm 2\sigma$	$^{207}\text{Pb}/^{235}\text{U}$	$\pm 2\sigma$	$^{206}\text{Pb}/^{238}\text{U}$	$\pm 2\sigma$	$^{207}\text{Pb}/^{206}\text{Pb}$ age	$\pm 2\sigma$	$^{206}\text{Pb}/^{238}\text{U}$ age	$\pm 2\sigma$	$^{207}\text{Pb}/^{235}\text{U}$ age	$\pm 2\sigma$	Concordancy
SAN14_33	0.0797	0.0029	2.2860	0.0960	0.2053	0.0043	1192	67	1203	23	1204	29	101
SAN14_92	0.0784	0.0014	2.2440	0.0440	0.2047	0.0035	1158	37	1200	19	1198	13	104
SAN14_93	0.0790	0.0034	2.2130	0.0820	0.2048	0.0045	1198	84	1200	24	1196	27	100
SAN14_91	0.0795	0.0025	2.2380	0.0630	0.2046	0.0046	1171	64	1199	25	1195	20	102
SAN14_47	0.0784	0.0010	2.2030	0.0290	0.2040	0.0026	1155	25	1196	14	1182	10	104
SAN14_94	0.0820	0.0008	2.3170	0.0350	0.2032	0.0026	1246	19	1192	14	1217	11	96
SAN14_36	0.0801	0.0011	2.2460	0.0350	0.2025	0.0030	1202	27	1190	16	1194	11	99
SAN14_34	0.0787	0.0042	2.2200	0.1100	0.2023	0.0070	1160	100	1187	37	1183	36	102
SAN14_81	0.0805	0.0018	2.2060	0.0680	0.2020	0.0041	1201	45	1186	22	1183	21	99
SAN14_06	0.0802	0.0013	2.2180	0.0360	0.2013	0.0030	1203	31	1182	16	1186	11	98
SAN14_74	0.0795	0.0013	2.2010	0.0390	0.2005	0.0025	1181	33	1180	14	1183	12	100
SAN14_63	0.0796	0.0014	2.2080	0.0340	0.2009	0.0024	1184	34	1180	13	1184	11	100
SAN14_32	0.0779	0.0012	2.1860	0.0420	0.2007	0.0036	1140	30	1179	20	1175	13	103
SAN14_03	0.0790	0.0015	2.1940	0.0430	0.2002	0.0029	1167	38	1178	16	1176	13	101
SAN14_37	0.0786	0.0018	2.1870	0.0570	0.1991	0.0038	1148	46	1175	21	1176	19	102
SAN14_35	0.0784	0.0013	2.1790	0.0360	0.1996	0.0027	1174	32	1174	15	1177	11	100
SAN14_12	0.0797	0.0013	2.1870	0.0380	0.1996	0.0033	1183	31	1173	18	1177	12	99
SAN14_28	0.0791	0.0025	2.1780	0.0630	0.1997	0.0037	1188	65	1173	20	1174	20	99
SAN14_58	0.0784	0.0025	2.1660	0.0640	0.1996	0.0036	1145	64	1172	19	1171	20	102
SAN14_62	0.0793	0.0016	2.1830	0.0390	0.1994	0.0036	1171	40	1172	19	1174	12	100
SAN14_30	0.0786	0.0008	2.1590	0.0280	0.1991	0.0027	1162	21	1171	15	1167	9	101
SAN14_42	0.0785	0.0025	2.1600	0.0580	0.1992	0.0053	1150	60	1170	29	1171	18	102
SAN14_87	0.0789	0.0016	2.1670	0.0430	0.1981	0.0028	1162	39	1166	15	1167	14	100
SAN14_52	0.0786	0.0016	2.1650	0.0410	0.1983	0.0029	1164	39	1166	16	1169	14	100
SAN14_20	0.0789	0.0021	2.1690	0.0500	0.1982	0.0037	1178	48	1165	20	1169	16	99
SAN14_70	0.0814	0.0013	2.2270	0.0370	0.1982	0.0025	1226	31	1165	14	1187	12	95
SAN14_68	0.0778	0.0013	2.1350	0.0390	0.1970	0.0029	1142	32	1160	15	1159	12	102
SAN14_16	0.0786	0.0013	2.1320	0.0340	0.1966	0.0030	1159	34	1156	16	1157	11	100
SAN14_66	0.0782	0.0015	2.1210	0.0420	0.1964	0.0033	1154	38	1155	18	1158	14	100
SAN14_90	0.0786	0.0014	2.1260	0.0360	0.1960	0.0029	1160	35	1155	16	1157	12	100
SAN14_64	0.0790	0.0015	2.1410	0.0400	0.1964	0.0026	1165	37	1155	14	1160	13	99
SAN14_15	0.0791	0.0009	2.1350	0.0300	0.1963	0.0024	1182	22	1155	13	1158	10	98
SAN14_05	0.0778	0.0011	2.0970	0.0380	0.1961	0.0032	1139	29	1154	17	1149	13	93

Analysis #	$^{207}\text{Pb}/^{206}\text{Pb}$	$\pm 2\sigma$	$^{207}\text{Pb}/^{235}\text{U}$	$\pm 2\sigma$	$^{206}\text{Pb}/^{238}\text{U}$	$\pm 2\sigma$	$^{207}\text{Pb}/^{206}\text{Pb}$ age	$\pm 2\sigma$	$^{206}\text{Pb}/^{238}\text{U}$ age	$\pm 2\sigma$	$^{207}\text{Pb}/^{235}\text{U}$ age	$\pm 2\sigma$	Concordancy
SAN14_07	0.0807	0.0017	2.1910	0.0470	0.1962	0.0038	1209	41	1154	20	1178	15	95
SAN14_04	0.0778	0.0011	2.1030	0.0320	0.1957	0.0027	1146	29	1153	14	1150	10	101
SAN14_45	0.0785	0.0015	2.1110	0.0470	0.1956	0.0030	1158	35	1153	16	1154	15	100
SAN14_55	0.0779	0.0012	2.1160	0.0290	0.1955	0.0021	1153	30	1152	11	1155	9	100
SAN14_39	0.0783	0.0011	2.1230	0.0320	0.1958	0.0027	1155	28	1152	15	1156	11	100
SAN14_14	0.0780	0.0011	2.1190	0.0370	0.1954	0.0031	1156	28	1152	17	1154	12	100
SAN14_98	0.0782	0.0016	2.1210	0.0420	0.1957	0.0027	1160	41	1152	14	1155	14	99
SAN14_49	0.0773	0.0026	2.1150	0.0610	0.1952	0.0037	1143	66	1151	20	1152	20	101
SAN14_02	0.0782	0.0016	2.1010	0.0410	0.1953	0.0035	1146	41	1151	19	1150	14	100
SAN14_43	0.0785	0.0015	2.1240	0.0410	0.1952	0.0034	1155	38	1150	18	1155	14	100
SAN14_48	0.0779	0.0018	2.1150	0.0480	0.1955	0.0033	1156	49	1150	18	1149	16	99
SAN14_77	0.0792	0.0016	2.1230	0.0390	0.1955	0.0027	1168	39	1150	15	1154	13	98
SAN14_38	0.0783	0.0013	2.1150	0.0400	0.1950	0.0029	1157	35	1149	16	1152	13	99
SAN14_13	0.0782	0.0015	2.1160	0.0450	0.1950	0.0033	1162	38	1149	18	1151	15	99
SAN14_01	0.0778	0.0017	2.1000	0.0510	0.1950	0.0039	1142	43	1148	21	1148	16	101
SAN14_10	0.0784	0.0020	2.0970	0.0550	0.1940	0.0034	1142	49	1146	18	1148	18	100
SAN14_11	0.0785	0.0020	2.0950	0.0530	0.1945	0.0040	1151	49	1145	21	1144	17	99
SAN14_29	0.0782	0.0019	2.0950	0.0480	0.1941	0.0037	1159	48	1145	20	1146	16	99
SAN14_22	0.0782	0.0014	2.0960	0.0400	0.1941	0.0030	1150	35	1143	16	1146	13	99
SAN14_23	0.0801	0.0050	2.1400	0.1200	0.1943	0.0072	1130	120	1142	39	1147	38	101
SAN14_25	0.0783	0.0017	2.0960	0.0470	0.1939	0.0035	1145	43	1142	19	1146	15	100
SAN14_08	0.0779	0.0011	2.0980	0.0370	0.1936	0.0040	1148	27	1140	21	1147	12	99
SAN14_44	0.0778	0.0014	2.0900	0.0380	0.1934	0.0035	1134	35	1139	19	1143	13	100
SAN14_80	0.0771	0.0019	2.0620	0.0520	0.1933	0.0031	1125	50	1138	17	1140	17	101
SAN14_31	0.0773	0.0030	2.0570	0.0860	0.1916	0.0051	1128	76	1134	27	1130	29	101
SAN14_21	0.0778	0.0032	2.0660	0.0830	0.1920	0.0046	1133	83	1131	25	1133	28	100
SAN14_26	0.0786	0.0018	2.1080	0.0460	0.1906	0.0034	1151	45	1125	18	1151	15	98
SAN14_71	0.0756	0.0030	1.9820	0.0550	0.1897	0.0050	1083	80	1119	27	1113	20	103
SAN14_82	0.0764	0.0033	2.0270	0.0760	0.1899	0.0047	1101	82	1119	25	1123	25	102
SAN14_09	0.0778	0.0028	2.0360	0.0680	0.1899	0.0047	1158	74	1119	26	1122	23	97
SAN14_69	0.0767	0.0024	2.0110	0.0590	0.1887	0.0035	1118	65	1117	20	1119	20	100
SAN14_85	0.0760	0.0027	1.9790	0.0680	0.1877	0.0042	1105	76	1109	23	1106	23	100
SAN14_76	0.0758	0.0042	1.9800	0.1000	0.1875	0.0054	1080	120	1107	29	1112	35	94

Analysis #	$^{207}\text{Pb}/^{206}\text{Pb}$	$\pm 2\sigma$	$^{207}\text{Pb}/^{235}\text{U}$	$\pm 2\sigma$	$^{206}\text{Pb}/^{238}\text{U}$	$\pm 2\sigma$	$^{207}\text{Pb}/^{206}\text{Pb}$ age	$\pm 2\sigma$	$^{206}\text{Pb}/^{238}\text{U}$ age	$\pm 2\sigma$	$^{207}\text{Pb}/^{235}\text{U}$ age	$\pm 2\sigma$	Concordancy	
SAN14_53	0.0763	0.0022	1.9560	0.0460	0.1853	0.0036	1104	56	1097	20	1100	16	99	
SAN14_96	0.0759	0.0029	1.9340	0.0650	0.1844	0.0045	1080	73	1096	25	1095	22	101	
SAN14_18	0.0748	0.0030	1.9460	0.0880	0.1842	0.0054	1062	83	1089	29	1093	30	103	
SAN14_86	0.0760	0.0036	1.9020	0.0800	0.1818	0.0042	1050	91	1076	23	1076	27	102	
SAN14_78	0.0766	0.0035	1.8770	0.0750	0.1792	0.0049	1115	91	1073	27	1074	27	96	
SAN-14	(Discordant Analyses)													
SAN14_60	0.1059	0.0029	3.1800	0.1000	0.2165	0.0050	1722	49	1263	26	1455	23	73	
SAN14_89	0.0864	0.0010	2.5250	0.0340	0.2102	0.0022	1341	22	1229	12	1281	10	92	
SAN14_97	0.0853	0.0027	2.4850	0.0810	0.2076	0.0037	1326	64	1217	20	1263	23	92	
SAN14_72	0.0777	0.0031	2.2660	0.0810	0.2053	0.0054	1131	75	1203	29	1202	25	106	
SAN14_41	0.0957	0.0031	2.7200	0.1100	0.2019	0.0036	1518	62	1184	19	1320	30	78	
SAN14_54	0.0842	0.0013	2.3200	0.0380	0.2000	0.0026	1301	31	1176	14	1218	12	90	
SAN14_75	0.0856	0.0019	2.3010	0.0490	0.1958	0.0031	1324	43	1152	17	1216	15	87	
SAN14_19	0.0814	0.0017	2.1510	0.0560	0.1930	0.0038	1222	44	1137	21	1166	18	93	
SAN14_65	0.0813	0.0008	2.1720	0.0260	0.1924	0.0021	1229	20	1135	11	1171	8	92	
SAN14_40	0.0966	0.0028	2.5350	0.0730	0.1921	0.0027	1536	50	1132	15	1278	19	74	
SAN14_79	0.0861	0.0012	2.2820	0.0410	0.1918	0.0021	1343	27	1131	11	1206	13	84	
SAN14_17	0.0818	0.0026	2.1360	0.0560	0.1888	0.0034	1226	61	1116	19	1158	19	91	
SAN14_88	0.0818	0.0009	2.1320	0.0320	0.1886	0.0025	1238	22	1115	14	1159	10	90	
SAN14_50	0.0800	0.0032	2.0750	0.0810	0.1879	0.0042	1195	82	1111	23	1135	26	93	
SAN14_56	0.0787	0.0011	2.0060	0.0300	0.1848	0.0023	1163	28	1093	12	1118	10	94	
SAN14_84	0.0824	0.0028	2.0800	0.0640	0.1816	0.0041	1222	67	1075	22	1139	21	88	
SAN-17	(Concordant Analyses)													
SAN17L_70	0.1079	0.0021	4.6840	0.0960	0.3163	0.0058	1771	35	1770	28	1765	17	100	
SAN17_22	0.0874	0.0018	2.8420	0.0610	0.2355	0.0035	1369	41	1362	18	1367	16	99	
SAN17L_120	0.0883	0.0028	2.8230	0.0940	0.2349	0.0067	1382	59	1359	35	1362	24	98	
SAN17L_67	0.0862	0.0017	2.6800	0.0540	0.2264	0.0037	1333	39	1319	19	1323	15	99	
SAN17L_81	0.0851	0.0019	2.6780	0.0550	0.2265	0.0037	1323	45	1316	20	1320	15	99	
SAN17L_133	0.0845	0.0037	2.5730	0.0970	0.2213	0.0058	1295	87	1287	31	1290	27	99	
SAN17_12	0.0827	0.0043	2.4700	0.1100	0.2174	0.0074	1240	110	1266	39	1269	29	102	

Analysis #	$^{207}\text{Pb}/^{206}\text{Pb}$	$\pm 2\sigma$	$^{207}\text{Pb}/^{235}\text{U}$	$\pm 2\sigma$	$^{206}\text{Pb}/^{238}\text{U}$	$\pm 2\sigma$	$^{207}\text{Pb}/^{206}\text{Pb}$ age	$\pm 2\sigma$	$^{206}\text{Pb}/^{238}\text{U}$ age	$\pm 2\sigma$	$^{207}\text{Pb}/^{235}\text{U}$ age	$\pm 2\sigma$	Concordancy
SAN17L_73	0.0831	0.0012	2.4730	0.0400	0.2161	0.0027	1276	28	1261	14	1264	12	99
SAN17L_71	0.0823	0.0018	2.4300	0.0470	0.2156	0.0036	1246	44	1258	19	1254	14	101
SAN17L_96	0.0840	0.0021	2.4580	0.0560	0.2151	0.0035	1286	49	1255	19	1259	17	98
SAN17_05	0.0805	0.0022	2.3820	0.0610	0.2119	0.0043	1208	54	1238	23	1237	18	102
SAN17_53	0.0819	0.0016	2.3690	0.0410	0.2105	0.0030	1244	38	1231	16	1233	12	99
SAN17_16	0.0807	0.0013	2.3500	0.0380	0.2104	0.0029	1210	32	1230	15	1227	12	102
SAN17L_91	0.0820	0.0016	2.3680	0.0480	0.2094	0.0027	1241	40	1228	14	1232	15	99
SAN17L_69	0.0809	0.0020	2.3640	0.0610	0.2091	0.0042	1210	51	1223	22	1227	19	101
SAN17L_75	0.0830	0.0037	2.3700	0.1000	0.2080	0.0051	1272	82	1222	26	1231	31	96
SAN17L_132	0.0787	0.0022	2.3330	0.0720	0.2086	0.0045	1171	55	1220	24	1218	22	104
SAN17_38	0.0806	0.0018	2.3050	0.0470	0.2077	0.0036	1201	43	1218	19	1218	15	101
SAN17L_97	0.0822	0.0019	2.3340	0.0530	0.2079	0.0039	1261	45	1217	21	1220	16	97
SAN17_09	0.0819	0.0015	2.3290	0.0400	0.2079	0.0031	1235	36	1217	17	1220	12	99
SAN17L_66	0.0800	0.0010	2.3010	0.0350	0.2078	0.0027	1194	24	1216	14	1212	11	102
SAN17L_138	0.0807	0.0025	2.2820	0.0620	0.2062	0.0038	1205	61	1208	20	1209	20	100
SAN17L_134	0.0797	0.0018	2.2930	0.0610	0.2050	0.0044	1186	44	1204	24	1207	19	102
SAN17_59	0.0821	0.0018	2.2920	0.0460	0.2048	0.0032	1252	44	1201	17	1209	14	96
SAN17L_86	0.0797	0.0018	2.2690	0.0450	0.2045	0.0029	1188	44	1199	16	1203	14	101
SAN17_51	0.0805	0.0020	2.2680	0.0570	0.2044	0.0037	1206	48	1198	20	1200	18	99
SAN17_52	0.0800	0.0010	2.2640	0.0310	0.2043	0.0024	1195	25	1198	13	1201	10	100
SAN17L_87	0.0795	0.0011	2.2360	0.0300	0.2037	0.0025	1183	29	1196	13	1192	10	101
SAN17_06	0.0797	0.0016	2.2430	0.0380	0.2033	0.0030	1185	38	1192	16	1193	12	101
SAN17L_119	0.0805	0.0011	2.2450	0.0360	0.2029	0.0026	1209	27	1190	14	1195	11	98
SAN17_60	0.0802	0.0011	2.2420	0.0290	0.2027	0.0028	1211	24	1189	15	1194	9	98
SAN17_63	0.0798	0.0012	2.2240	0.0340	0.2023	0.0026	1190	30	1188	14	1189	11	100
SAN17L_84	0.0804	0.0025	2.2150	0.0670	0.2020	0.0036	1185	64	1187	19	1189	21	100
SAN17_58	0.0791	0.0014	2.2050	0.0390	0.2023	0.0030	1169	35	1187	16	1184	12	102
SAN17_61	0.0794	0.0011	2.2200	0.0310	0.2021	0.0028	1179	26	1186	15	1188	10	101
SAN17_39	0.0790	0.0008	2.2010	0.0290	0.2019	0.0026	1172	20	1185	14	1182	9	101
SAN17_34	0.0798	0.0024	2.2130	0.0710	0.2011	0.0037	1215	57	1184	20	1187	23	97
SAN17_02	0.0792	0.0011	2.1940	0.0340	0.2017	0.0026	1173	26	1184	14	1180	11	101
SAN17L_68	0.0818	0.0032	2.2320	0.0750	0.2011	0.0046	1218	78	1182	24	1186	24	97
SAN17_35	0.0802	0.0012	2.2030	0.0340	0.2008	0.0028	1199	29	1182	16	1182	11	99

Analysis #	$^{207}\text{Pb}/^{206}\text{Pb}$	$\pm 2\sigma$	$^{207}\text{Pb}/^{235}\text{U}$	$\pm 2\sigma$	$^{206}\text{Pb}/^{238}\text{U}$	$\pm 2\sigma$	$^{207}\text{Pb}/^{206}\text{Pb}$ age	$\pm 2\sigma$	$^{206}\text{Pb}/^{238}\text{U}$ age	$\pm 2\sigma$	$^{207}\text{Pb}/^{235}\text{U}$ age	$\pm 2\sigma$	Concordancy
SAN17L_88	0.0800	0.0019	2.2100	0.0520	0.2015	0.0034	1188	47	1182	18	1184	16	99
SAN17_26	0.0797	0.0014	2.2130	0.0380	0.2013	0.0026	1185	35	1182	14	1185	12	100
SAN17_20	0.0803	0.0019	2.1950	0.0480	0.2006	0.0036	1192	47	1181	19	1182	15	99
SAN17_15	0.0793	0.0022	2.2070	0.0560	0.2012	0.0044	1188	52	1181	23	1184	19	99
SAN17_08	0.0793	0.0014	2.2070	0.0400	0.2010	0.0025	1175	36	1180	13	1182	12	100
SAN17_17	0.0793	0.0014	2.1910	0.0410	0.2010	0.0031	1171	36	1180	17	1176	13	101
SAN17_19	0.0785	0.0018	2.1860	0.0540	0.2009	0.0034	1165	45	1180	18	1178	17	101
SAN17_31	0.0784	0.0012	2.1950	0.0350	0.2009	0.0024	1157	30	1180	13	1177	11	102
SAN17L_113	0.0791	0.0012	2.2080	0.0380	0.2009	0.0027	1170	31	1179	14	1182	12	101
SAN17_32	0.0795	0.0013	2.1970	0.0360	0.2004	0.0028	1182	33	1177	15	1181	12	100
SAN17_01	0.0798	0.0010	2.1910	0.0320	0.2002	0.0027	1192	23	1176	15	1177	10	99
SAN17_65	0.0797	0.0011	2.1890	0.0330	0.2001	0.0025	1183	28	1176	13	1177	11	99
SAN17_37	0.0784	0.0008	2.1860	0.0320	0.2003	0.0027	1157	21	1176	14	1176	10	102
SAN17L_144	0.0789	0.0016	2.1790	0.0400	0.1998	0.0039	1158	40	1173	21	1176	13	101
SAN17_23	0.0794	0.0012	2.1840	0.0360	0.1995	0.0025	1186	30	1172	13	1176	12	99
SAN17_41	0.0793	0.0013	2.1910	0.0340	0.1995	0.0026	1182	32	1172	14	1177	11	99
SAN17_07	0.0791	0.0011	2.1820	0.0370	0.1993	0.0025	1177	28	1171	14	1174	12	99
SAN17_25	0.0787	0.0013	2.1830	0.0320	0.1990	0.0028	1159	32	1171	15	1175	10	101
SAN17_21	0.0792	0.0029	2.1830	0.0720	0.1987	0.0037	1169	74	1170	20	1173	23	100
SAN17_30	0.0799	0.0017	2.1660	0.0430	0.1989	0.0027	1184	44	1169	15	1170	14	99
SAN17L_116	0.0787	0.0012	2.1710	0.0390	0.1986	0.0029	1155	31	1167	16	1170	13	101
SAN17L_137	0.0787	0.0016	2.1440	0.0450	0.1987	0.0031	1143	41	1167	17	1164	15	102
SAN17L_80	0.0799	0.0023	2.1710	0.0570	0.1971	0.0035	1189	58	1166	19	1169	19	98
SAN17_33	0.0784	0.0009	2.1580	0.0260	0.1984	0.0022	1160	23	1166	12	1166	8	101
SAN17_49	0.0781	0.0015	2.1430	0.0410	0.1978	0.0033	1146	38	1165	18	1164	13	102
SAN17L_124	0.0793	0.0016	2.1600	0.0440	0.1980	0.0026	1175	40	1164	14	1167	14	99
SAN17_62	0.0791	0.0015	2.1630	0.0390	0.1976	0.0029	1185	38	1162	16	1168	12	98
SAN17_55	0.0790	0.0016	2.1480	0.0410	0.1975	0.0053	1180	41	1161	28	1164	13	98
SAN17_27	0.0788	0.0011	2.1440	0.0330	0.1971	0.0029	1167	28	1161	15	1161	11	99
SAN17_47	0.0786	0.0019	2.1510	0.0550	0.1974	0.0044	1166	50	1161	23	1163	18	100
SAN17_48	0.0791	0.0015	2.1430	0.0490	0.1973	0.0032	1175	37	1160	17	1160	16	99
SAN17_57	0.0794	0.0012	2.1520	0.0350	0.1971	0.0025	1181	30	1159	14	1163	11	98
SAN17L_141	0.0784	0.0015	2.1460	0.0430	0.1967	0.0035	1150	40	1157	19	1161	14	97

Analysis #	$^{207}\text{Pb}/^{206}\text{Pb}$	$\pm 2\sigma$	$^{207}\text{Pb}/^{235}\text{U}$	$\pm 2\sigma$	$^{206}\text{Pb}/^{238}\text{U}$	$\pm 2\sigma$	$^{207}\text{Pb}/^{206}\text{Pb}$ age	$\pm 2\sigma$	$^{206}\text{Pb}/^{238}\text{U}$ age	$\pm 2\sigma$	$^{207}\text{Pb}/^{235}\text{U}$ age	$\pm 2\sigma$	Concordancy
SAN17L_114	0.0791	0.0012	2.1330	0.0360	0.1966	0.0026	1175	30	1156	14	1157	12	98
SAN17_50	0.0792	0.0010	2.1310	0.0310	0.1959	0.0026	1170	26	1156	14	1157	10	99
SAN17_24	0.0786	0.0012	2.1090	0.0360	0.1965	0.0026	1163	32	1156	14	1152	11	99
SAN17L_118	0.0777	0.0015	2.1350	0.0430	0.1962	0.0031	1132	39	1156	17	1159	14	102
SAN17_28	0.0784	0.0020	2.1320	0.0350	0.1963	0.0044	1148	51	1155	24	1159	12	101
SAN17_43	0.0785	0.0013	2.1100	0.0360	0.1961	0.0027	1153	33	1154	14	1151	12	100
SAN17_04	0.0790	0.0024	2.1280	0.0610	0.1960	0.0038	1159	61	1153	20	1155	20	99
SAN17L_74	0.0792	0.0015	2.1340	0.0470	0.1957	0.0036	1183	39	1151	19	1158	15	97
SAN17_54	0.0780	0.0025	2.1150	0.0590	0.1950	0.0042	1155	65	1150	23	1151	19	100
SAN17_56	0.0784	0.0020	2.1130	0.0590	0.1951	0.0037	1148	51	1149	20	1151	19	100
SAN17L_93	0.0787	0.0013	2.1150	0.0330	0.1949	0.0022	1155	32	1148	12	1152	11	99
SAN17L_98	0.0799	0.0019	2.1070	0.0530	0.1946	0.0030	1204	46	1147	16	1151	17	95
SAN17L_94	0.0788	0.0015	2.1110	0.0410	0.1941	0.0025	1152	39	1146	14	1150	13	99
SAN17L_111	0.0783	0.0013	2.1050	0.0360	0.1945	0.0024	1153	34	1145	13	1150	12	99
SAN17L_90	0.0789	0.0008	2.1000	0.0250	0.1943	0.0016	1165	20	1144	9	1148	8	98
SAN17_42	0.0790	0.0021	2.0800	0.0560	0.1938	0.0028	1149	55	1142	15	1142	19	99
SAN17L_127	0.0776	0.0016	2.0750	0.0400	0.1937	0.0025	1137	40	1141	14	1137	13	100
SAN17L_101	0.0782	0.0014	2.0870	0.0380	0.1936	0.0029	1160	36	1140	16	1144	12	98
SAN17L_78	0.0794	0.0038	2.0850	0.0940	0.1925	0.0055	1162	95	1139	29	1137	31	98
SAN17L_125	0.0777	0.0023	2.0850	0.0620	0.1933	0.0028	1124	55	1138	15	1141	19	101
SAN17L_145	0.0797	0.0010	2.1420	0.0270	0.1927	0.0021	1184	24	1137	12	1163	9	96
SAN17L_121	0.0798	0.0012	2.1330	0.0350	0.1926	0.0026	1190	31	1136	14	1158	11	95
SAN17L_123	0.0783	0.0055	2.0700	0.1300	0.1916	0.0068	1090	160	1134	36	1134	45	104
SAN17L_136	0.0777	0.0022	2.0730	0.0540	0.1918	0.0034	1137	56	1132	18	1134	18	100
SAN17L_100	0.0776	0.0015	2.0550	0.0400	0.1915	0.0024	1133	37	1129	13	1131	13	100
SAN17L_85	0.0774	0.0024	2.0530	0.0610	0.1910	0.0038	1134	60	1128	21	1130	20	99
SAN17L_106	0.0773	0.0015	2.0200	0.0380	0.1908	0.0026	1125	37	1125	14	1128	12	100
SAN17L_142	0.0779	0.0030	2.0450	0.0650	0.1907	0.0042	1132	76	1124	23	1129	22	99
SAN17L_129	0.0792	0.0018	2.0690	0.0440	0.1889	0.0029	1170	46	1115	16	1138	15	95
SAN17L_130	0.0781	0.0019	1.9780	0.0450	0.1875	0.0031	1143	47	1109	17	1108	16	97
SAN17L_77	0.0795	0.0040	2.0260	0.0890	0.1877	0.0046	1134	98	1107	25	1111	30	98
SAN17_11	0.0764	0.0027	1.9490	0.0610	0.1860	0.0040	1116	70	1099	22	1100	21	98
SAN17L_72	0.0769	0.0026	1.9570	0.0600	0.1856	0.0031	1110	65	1098	17	1097	21	98

Analysis #	$^{207}\text{Pb}/^{206}\text{Pb}$	$\pm 2\sigma$	$^{207}\text{Pb}/^{235}\text{U}$	$\pm 2\sigma$	$^{206}\text{Pb}/^{238}\text{U}$	$\pm 2\sigma$	$^{207}\text{Pb}/^{206}\text{Pb}$ age	$\pm 2\sigma$	$^{206}\text{Pb}/^{238}\text{U}$ age	$\pm 2\sigma$	$^{207}\text{Pb}/^{235}\text{U}$ age	$\pm 2\sigma$	Concordancy
SAN17_18	0.0759	0.0043	1.8610	0.0970	0.1794	0.0059	1060	120	1063	32	1066	33	100
SAN17L_140	0.0762	0.0038	1.8170	0.0820	0.1762	0.0041	1040	100	1047	22	1046	29	101
SAN-17 (<i>Discordant Analyses</i>)													
SAN17_13	0.3230	0.0260	15.8000	1.9000	0.3130	0.0190	3360	150	1733	91	2610	140	52
SAN17L_107	0.0869	0.0014	2.5870	0.0470	0.2157	0.0028	1356	32	1258	15	1295	14	93
SAN17L_105	0.0864	0.0031	2.4830	0.0750	0.2097	0.0044	1365	68	1225	23	1267	22	90
SAN17L_104	0.0865	0.0030	2.4930	0.0800	0.2086	0.0040	1329	68	1222	21	1266	24	92
SAN17L_126	0.0844	0.0018	2.4340	0.0490	0.2084	0.0026	1297	41	1220	14	1249	15	94
SAN17L_99	0.0905	0.0013	2.5430	0.0380	0.2036	0.0029	1434	27	1195	16	1284	11	83
SAN17_29	0.0829	0.0010	2.2960	0.0350	0.2016	0.0021	1269	24	1184	11	1212	11	93
SAN17L_89	0.0862	0.0017	2.4150	0.0440	0.2015	0.0025	1348	37	1183	14	1245	13	88
SAN17L_95	0.0833	0.0015	2.2850	0.0400	0.2010	0.0028	1274	33	1180	15	1209	12	93
SAN17L_117	0.0837	0.0024	2.3230	0.0580	0.2005	0.0036	1271	56	1177	19	1215	18	93
SAN17_14	0.0908	0.0035	2.4320	0.0860	0.1978	0.0036	1408	68	1162	19	1244	24	83
SAN17_45	0.0802	0.0008	2.1450	0.0270	0.1940	0.0023	1204	20	1143	12	1163	9	95
SAN17_36	0.0824	0.0009	2.2030	0.0290	0.1936	0.0026	1250	22	1142	14	1182	9	91
SAN17L_122	0.0803	0.0011	2.1440	0.0310	0.1928	0.0028	1202	28	1136	15	1164	10	95
SAN17L_112	0.0817	0.0007	2.1570	0.0320	0.1920	0.0027	1238	17	1133	14	1168	10	92
SAN17L_135	0.0744	0.0033	2.0180	0.0900	0.1918	0.0042	1048	99	1130	23	1132	31	108
SAN17L_79	0.0892	0.0013	2.3330	0.0390	0.1911	0.0029	1405	28	1127	16	1224	12	80
SAN17_64	0.0823	0.0009	2.1750	0.0280	0.1905	0.0022	1252	22	1124	12	1172	9	90
SAN17_40	0.0810	0.0008	2.1100	0.0280	0.1901	0.0027	1219	19	1123	15	1152	9	92
SAN17_44	0.0804	0.0018	2.1060	0.0470	0.1897	0.0034	1197	43	1119	18	1149	15	93
SAN17L_103	0.0797	0.0014	2.1000	0.0380	0.1891	0.0028	1190	35	1117	15	1148	12	94
SAN17L_131	0.0817	0.0047	2.1000	0.1100	0.1872	0.0061	1190	110	1106	33	1138	35	93
SAN17L_83	0.0816	0.0033	2.0870	0.0810	0.1867	0.0047	1217	85	1102	25	1136	26	91
SAN17L_115	0.0812	0.0018	2.0720	0.0470	0.1863	0.0032	1204	44	1102	17	1141	15	92
SAN17L_109	0.0817	0.0029	2.1070	0.0650	0.1864	0.0037	1234	72	1101	20	1145	22	89
SAN17L_110	0.0818	0.0022	2.0810	0.0540	0.1861	0.0031	1227	51	1101	17	1143	18	90
SAN17L_139	0.0824	0.0010	2.0940	0.0300	0.1847	0.0027	1249	24	1092	15	1149	10	87
SAN17L_76	0.0798	0.0034	2.0400	0.0780	0.1841	0.0049	1206	87	1087	27	1126	26	90

Analysis #	$^{207}\text{Pb}/^{206}\text{Pb}$	$\pm 2\sigma$	$^{207}\text{Pb}/^{235}\text{U}$	$\pm 2\sigma$	$^{206}\text{Pb}/^{238}\text{U}$	$\pm 2\sigma$	$^{207}\text{Pb}/^{206}\text{Pb}$ age	$\pm 2\sigma$	$^{206}\text{Pb}/^{238}\text{U}$ age	$\pm 2\sigma$	$^{207}\text{Pb}/^{235}\text{U}$ age	$\pm 2\sigma$	Concordancy	
SAN17L_92	0.0798	0.0010	2.0230	0.0250	0.1838	0.0019	1188	25	1087	10	1122	8	91	
SAN17L_102	0.0822	0.0042	2.0480	0.0900	0.1837	0.0048	1230	100	1085	26	1134	30	88	
SAN17L_82	0.0906	0.0040	2.2450	0.0820	0.1821	0.0049	1422	85	1079	27	1192	26	76	
SAN17_10	0.0787	0.0028	1.9640	0.0670	0.1824	0.0039	1142	71	1079	21	1102	23	94	
SAN17L_143	0.0782	0.0034	1.9100	0.0720	0.1786	0.0036	1132	87	1058	20	1090	24	93	
SAN17L_128	0.0836	0.0056	2.0100	0.1300	0.1749	0.0058	1230	140	1036	32	1107	44	84	
SAN17_46	0.0859	0.0009	2.0560	0.0280	0.1724	0.0022	1330	20	1026	12	1134	9	77	
SAN17L_108	0.0877	0.0009	1.9210	0.0210	0.1575	0.0015	1377	20	942	9	1089	7	68	
SAN17_03	0.0921	0.0006	1.8030	0.0160	0.1411	0.0013	1469	13	851	7	1047	6	58	
SAN-18 <i>(Concordant Analyses)</i>														
SAN18_92	0.0849	0.0011	2.6150	0.0320	0.2247	0.0023	1310	25	1306	12	1305	9	100	
SAN18_131	0.0828	0.0012	2.4980	0.0390	0.2180	0.0027	1266	27	1271	14	1272	11	100	
SAN18_105	0.0795	0.0008	2.3140	0.0270	0.2112	0.0022	1183	21	1235	12	1217	8	104	
SAN18_52	0.0819	0.0010	2.3790	0.0330	0.2108	0.0020	1241	25	1233	10	1236	10	99	
SAN18_71	0.0808	0.0009	2.3600	0.0300	0.2103	0.0022	1217	22	1231	11	1230	9	101	
SAN18_76	0.0807	0.0006	2.3430	0.0220	0.2098	0.0020	1212	14	1227	11	1226	7	101	
SAN18_27	0.0803	0.0010	2.2880	0.0260	0.2083	0.0022	1205	24	1219	12	1210	8	101	
SAN18_74	0.0816	0.0012	2.3450	0.0340	0.2079	0.0025	1236	30	1217	13	1226	10	98	
SAN18_51	0.0802	0.0011	2.2890	0.0340	0.2074	0.0027	1195	27	1214	14	1209	11	102	
SAN18_33	0.0823	0.0011	2.3570	0.0310	0.2062	0.0022	1249	26	1212	12	1231	9	97	
SAN18_113	0.0804	0.0013	2.3000	0.0390	0.2068	0.0027	1213	32	1211	15	1211	12	100	
SAN18_101	0.0805	0.0009	2.3050	0.0300	0.2065	0.0020	1210	23	1211	11	1214	9	100	
SAN18_82	0.0798	0.0007	2.2720	0.0230	0.2064	0.0016	1189	17	1211	9	1203	7	102	
SAN18_132	0.0802	0.0008	2.2870	0.0260	0.2064	0.0020	1196	18	1209	10	1207	8	101	
SAN18_24	0.0803	0.0007	2.2840	0.0240	0.2062	0.0021	1203	18	1208	11	1207	8	100	
SAN18_38	0.0807	0.0013	2.2710	0.0340	0.2054	0.0022	1208	32	1204	12	1202	10	100	
SAN18_40	0.0823	0.0009	2.3230	0.0250	0.2053	0.0019	1257	20	1203	10	1220	8	96	
SAN18_189	0.0803	0.0009	2.2600	0.0530	0.2052	0.0034	1204	23	1203	18	1201	17	100	
SAN18_49	0.0815	0.0012	2.3080	0.0370	0.2049	0.0025	1230	30	1202	13	1215	12	98	
SAN18_151	0.0798	0.0014	2.2660	0.0380	0.2045	0.0029	1189	34	1201	15	1200	12	101	
SAN18_35	0.0827	0.0013	2.3140	0.0350	0.2047	0.0023	1253	30	1200	12	1216	11	96	

Analysis #	$^{207}\text{Pb}/^{206}\text{Pb}$	$\pm 2\sigma$	$^{207}\text{Pb}/^{235}\text{U}$	$\pm 2\sigma$	$^{206}\text{Pb}/^{238}\text{U}$	$\pm 2\sigma$	$^{207}\text{Pb}/^{206}\text{Pb}$ age	$\pm 2\sigma$	$^{206}\text{Pb}/^{238}\text{U}$ age	$\pm 2\sigma$	$^{207}\text{Pb}/^{235}\text{U}$ age	$\pm 2\sigma$	Concordancy
SAN18_29	0.0782	0.0009	2.2130	0.0290	0.2047	0.0023	1156	23	1200	12	1185	9	104
SAN18_185	0.0816	0.0009	2.2950	0.0860	0.2044	0.0024	1233	22	1198	13	1203	26	97
SAN18_65	0.0809	0.0010	2.2800	0.0380	0.2042	0.0024	1213	26	1198	13	1204	11	99
SAN18_181	0.0797	0.0008	2.2820	0.0840	0.2044	0.0026	1191	19	1198	14	1197	25	101
SAN18_18	0.0816	0.0011	2.3070	0.0360	0.2039	0.0026	1233	26	1196	14	1214	11	97
SAN18_44	0.0794	0.0009	2.2460	0.0270	0.2040	0.0021	1189	21	1196	11	1194	9	101
SAN18_172	0.0789	0.0011	2.2540	0.0760	0.2039	0.0024	1177	26	1196	13	1195	24	102
SAN18_30	0.0790	0.0013	2.2230	0.0340	0.2038	0.0024	1171	32	1196	13	1187	11	102
SAN18_96	0.0813	0.0010	2.2760	0.0270	0.2039	0.0018	1224	24	1196	10	1205	9	98
SAN18_31	0.0814	0.0009	2.3010	0.0310	0.2038	0.0021	1227	22	1195	11	1213	10	97
SAN18_13	0.0799	0.0007	2.2390	0.0230	0.2037	0.0021	1191	17	1195	11	1192	7	100
SAN18_36	0.0806	0.0009	2.2500	0.0240	0.2034	0.0022	1212	21	1193	12	1196	7	98
SAN18_97	0.0794	0.0010	2.2400	0.0290	0.2033	0.0022	1185	25	1193	12	1195	9	101
SAN18_28	0.0816	0.0012	2.2890	0.0380	0.2029	0.0023	1237	29	1192	12	1208	12	96
SAN18_80	0.0801	0.0010	2.2340	0.0310	0.2033	0.0024	1195	24	1192	13	1192	10	100
SAN18_53	0.0799	0.0009	2.2360	0.0290	0.2027	0.0021	1195	24	1191	11	1192	9	100
SAN18_115	0.0797	0.0012	2.2310	0.0340	0.2030	0.0027	1190	30	1191	14	1192	11	100
SAN18_152	0.0799	0.0007	2.2340	0.0330	0.2029	0.0029	1193	18	1190	15	1191	10	100
SAN18_119	0.0794	0.0011	2.2430	0.0400	0.2028	0.0024	1184	29	1190	13	1193	12	101
SAN18_39	0.0793	0.0010	2.2220	0.0290	0.2028	0.0023	1179	26	1190	12	1190	9	101
SAN18_23	0.0808	0.0013	2.2350	0.0340	0.2026	0.0022	1211	32	1189	12	1190	11	98
SAN18_54	0.0800	0.0008	2.2410	0.0220	0.2025	0.0019	1196	18	1188	10	1193	7	99
SAN18_25	0.0800	0.0011	2.2210	0.0340	0.2024	0.0023	1186	28	1188	12	1187	11	100
SAN18_37	0.0796	0.0010	2.2140	0.0310	0.2025	0.0026	1179	24	1188	14	1184	10	101
SAN18_14	0.0793	0.0008	2.2160	0.0200	0.2022	0.0021	1178	19	1188	11	1187	6	101
SAN18_90	0.0794	0.0012	2.2020	0.0340	0.2023	0.0024	1192	29	1187	13	1185	11	100
SAN18_116	0.0796	0.0012	2.2290	0.0350	0.2021	0.0024	1191	30	1186	13	1189	11	100
SAN18_78	0.0797	0.0010	2.2160	0.0310	0.2020	0.0024	1186	23	1186	13	1184	10	100
SAN18_154	0.0790	0.0009	2.2020	0.0250	0.2020	0.0023	1170	22	1186	12	1182	8	101
SAN18_193	0.0810	0.0007	2.2310	0.0830	0.2012	0.0022	1224	18	1185	12	1186	26	97
SAN18_114	0.0800	0.0009	2.2260	0.0240	0.2017	0.0020	1198	22	1185	11	1190	7	99
SAN18_67	0.0801	0.0010	2.2270	0.0290	0.2018	0.0026	1196	26	1185	14	1192	9	99
SAN18_45	0.0800	0.0010	2.2410	0.0300	0.2020	0.0023	1194	26	1185	12	1194	10^{101}	99

Analysis #	$^{207}\text{Pb}/^{206}\text{Pb}$	$\pm 2\sigma$	$^{207}\text{Pb}/^{235}\text{U}$	$\pm 2\sigma$	$^{206}\text{Pb}/^{238}\text{U}$	$\pm 2\sigma$	$^{207}\text{Pb}/^{206}\text{Pb}$ age	$\pm 2\sigma$	$^{206}\text{Pb}/^{238}\text{U}$ age	$\pm 2\sigma$	$^{207}\text{Pb}/^{235}\text{U}$ age	$\pm 2\sigma$	Concordancy
SAN18_01	0.0796	0.0011	2.2180	0.0310	0.2017	0.0023	1188	27	1185	13	1187	10	100
SAN18_95	0.0791	0.0012	2.2020	0.0320	0.2020	0.0024	1172	30	1185	13	1183	10	101
SAN18_155	0.0792	0.0012	2.2160	0.0300	0.2019	0.0027	1170	29	1185	15	1185	9	101
SAN18_11	0.0812	0.0010	2.2760	0.0300	0.2016	0.0022	1226	25	1184	12	1205	9	97
SAN18_183	0.0810	0.0007	2.2200	0.0740	0.2018	0.0025	1220	18	1184	13	1184	24	97
SAN18_26	0.0797	0.0011	2.2220	0.0350	0.2015	0.0025	1186	28	1184	14	1187	11	100
SAN18_177	0.0792	0.0009	2.2240	0.0780	0.2018	0.0026	1173	22	1184	14	1185	25	101
SAN18_47	0.0789	0.0010	2.2160	0.0270	0.2015	0.0023	1171	25	1184	12	1188	8	101
SAN18_178	0.0804	0.0008	2.2290	0.0830	0.2016	0.0026	1210	20	1183	14	1187	26	98
SAN18_107	0.0805	0.0010	2.2260	0.0300	0.2014	0.0019	1205	24	1183	10	1188	10	98
SAN18_98	0.0799	0.0008	2.2240	0.0230	0.2013	0.0017	1195	19	1183	9	1188	7	99
SAN18_173	0.0794	0.0010	2.2460	0.0850	0.2013	0.0027	1175	26	1183	14	1183	26	101
SAN18_153	0.0800	0.0012	2.2170	0.0320	0.2014	0.0026	1201	29	1182	14	1186	10	98
SAN18_50	0.0800	0.0012	2.2220	0.0380	0.2011	0.0022	1190	30	1182	12	1189	12	99
SAN18_182	0.0817	0.0014	2.2350	0.0850	0.2011	0.0028	1229	32	1181	15	1185	26	96
SAN18_34	0.0802	0.0012	2.2280	0.0350	0.2012	0.0026	1203	29	1181	14	1189	11	98
SAN18_140	0.0800	0.0010	2.2050	0.0320	0.2011	0.0025	1200	25	1181	13	1183	10	98
SAN18_136	0.0797	0.0015	2.2030	0.0460	0.2012	0.0036	1199	40	1181	20	1180	14	98
SAN18_102	0.0800	0.0008	2.2090	0.0290	0.2010	0.0023	1197	21	1181	12	1184	9	99
SAN18_08	0.0796	0.0010	2.1910	0.0290	0.2011	0.0023	1185	24	1181	12	1178	9	100
SAN18_194	0.0808	0.0012	2.2170	0.0850	0.2009	0.0025	1219	28	1180	14	1179	27	97
SAN18_02	0.0801	0.0010	2.2120	0.0280	0.2009	0.0023	1197	24	1180	13	1184	9	99
SAN18_123	0.0793	0.0015	2.2030	0.0450	0.2005	0.0032	1182	36	1180	17	1183	14	100
SAN18_16	0.0790	0.0013	2.1940	0.0350	0.2005	0.0022	1172	32	1180	12	1180	11	101
SAN18_186	0.0797	0.0008	2.2430	0.0840	0.2005	0.0024	1188	18	1179	13	1182	25	99
SAN18_112	0.0808	0.0018	2.1910	0.0540	0.2005	0.0034	1229	41	1178	18	1178	18	96
SAN18_87	0.0802	0.0007	2.2180	0.0260	0.2005	0.0021	1201	17	1178	11	1186	8	98
SAN18_79	0.0799	0.0012	2.2070	0.0320	0.2005	0.0023	1194	31	1178	12	1183	10	99
SAN18_120	0.0786	0.0015	2.2050	0.0450	0.2002	0.0032	1173	38	1178	18	1181	14	100
SAN18_85	0.0794	0.0012	2.1920	0.0350	0.2004	0.0023	1176	30	1177	12	1178	11	100
SAN18_195	0.0806	0.0011	2.2090	0.0830	0.2002	0.0023	1206	26	1176	13	1174	26	98
SAN18_89	0.0799	0.0010	2.2010	0.0310	0.2003	0.0022	1192	25	1176	12	1180	10	99
SAN18_70	0.0798	0.0012	2.1920	0.0270	0.2001	0.0022	1190	30	1176	12	1179	8 ¹⁰²	99

Analysis #	$^{207}\text{Pb}/^{206}\text{Pb}$	$\pm 2\sigma$	$^{207}\text{Pb}/^{235}\text{U}$	$\pm 2\sigma$	$^{206}\text{Pb}/^{238}\text{U}$	$\pm 2\sigma$	$^{207}\text{Pb}/^{206}\text{Pb}$ age	$\pm 2\sigma$	$^{206}\text{Pb}/^{238}\text{U}$ age	$\pm 2\sigma$	$^{207}\text{Pb}/^{235}\text{U}$ age	$\pm 2\sigma$	Concordancy
SAN18_86	0.0793	0.0011	2.2020	0.0300	0.2002	0.0021	1177	27	1176	12	1180	10	100
SAN18_157	0.0793	0.0012	2.1880	0.0330	0.2002	0.0032	1177	29	1176	17	1178	11	100
SAN18_84	0.0787	0.0019	2.2060	0.0460	0.2003	0.0029	1161	50	1176	15	1183	14	101
SAN18_191	0.0818	0.0010	2.2230	0.0820	0.1998	0.0025	1235	26	1175	14	1176	25	95
SAN18_20	0.0804	0.0011	2.2100	0.0310	0.1998	0.0020	1207	27	1175	11	1185	10	97
SAN18_197	0.0797	0.0010	2.1990	0.0820	0.1999	0.0027	1189	26	1175	14	1177	26	99
SAN18_22	0.0794	0.0016	2.2000	0.0390	0.2001	0.0032	1188	40	1175	17	1178	12	99
SAN18_41	0.0799	0.0017	2.2060	0.0430	0.2001	0.0027	1186	40	1175	14	1181	13	99
SAN18_81	0.0791	0.0011	2.1870	0.0320	0.2001	0.0022	1174	27	1175	12	1177	10	100
SAN18_171	0.0788	0.0011	2.1900	0.0720	0.2001	0.0028	1166	27	1175	15	1177	23	101
SAN18_110	0.0810	0.0007	2.2400	0.0240	0.1999	0.0020	1217	17	1174	11	1193	7	96
SAN18_104	0.0789	0.0008	2.1760	0.0260	0.1998	0.0019	1166	20	1174	10	1173	9	101
SAN18_118	0.0786	0.0014	2.2000	0.0400	0.1999	0.0026	1162	36	1174	14	1179	13	101
SAN18_164	0.0802	0.0010	2.2150	0.0330	0.1997	0.0029	1201	26	1173	16	1185	10	98
SAN18_122	0.0796	0.0012	2.1830	0.0320	0.1996	0.0024	1195	31	1173	13	1175	10	98
SAN18_124	0.0790	0.0010	2.1740	0.0270	0.1996	0.0022	1168	26	1173	12	1173	9	100
SAN18_103	0.0793	0.0008	2.1890	0.0280	0.1995	0.0018	1181	21	1172	10	1177	9	99
SAN18_17	0.0800	0.0010	2.1880	0.0300	0.1995	0.0024	1193	26	1172	13	1176	10	98
SAN18_100	0.0796	0.0010	2.1880	0.0280	0.1994	0.0021	1190	25	1172	11	1176	9	98
SAN18_198	0.0797	0.0012	2.1750	0.0810	0.1996	0.0027	1187	30	1172	15	1168	26	99
SAN18_69	0.0792	0.0010	2.1950	0.0300	0.1993	0.0026	1181	25	1171	14	1179	10	99
SAN18_99	0.0792	0.0012	2.1870	0.0320	0.1992	0.0021	1174	30	1171	11	1176	10	100
SAN18_60	0.0782	0.0012	2.1200	0.0330	0.1993	0.0027	1148	31	1171	14	1157	11	102
SAN18_143	0.0780	0.0019	2.1510	0.0540	0.1992	0.0032	1137	49	1171	17	1169	17	103
SAN18_190	0.0785	0.0016	2.1680	0.0590	0.1991	0.0034	1162	44	1170	18	1168	19	101
SAN18_108	0.0778	0.0013	2.1520	0.0350	0.1991	0.0023	1146	33	1170	13	1164	11	102
SAN18_176	0.0783	0.0013	2.1830	0.0810	0.1991	0.0027	1143	33	1170	14	1169	26	102
SAN18_03	0.0800	0.0012	2.1970	0.0300	0.1990	0.0025	1192	29	1169	14	1179	9	98
SAN18_88	0.0802	0.0011	2.2000	0.0350	0.1986	0.0022	1197	27	1168	12	1182	11	98
SAN18_58	0.0797	0.0010	2.1910	0.0280	0.1987	0.0020	1189	25	1168	11	1177	9	98
SAN18_175	0.0789	0.0012	2.1900	0.0780	0.1983	0.0030	1159	29	1168	16	1167	24	101
SAN18_15	0.0807	0.0012	2.2110	0.0330	0.1985	0.0023	1214	29	1167	12	1182	11	96
SAN18_75	0.0799	0.0007	2.1990	0.0230	0.1986	0.0020	1199	17	1167	11	1180	7 ¹⁰³	97

Analysis #	$^{207}\text{Pb}/^{206}\text{Pb}$	$\pm 2\sigma$	$^{207}\text{Pb}/^{235}\text{U}$	$\pm 2\sigma$	$^{206}\text{Pb}/^{238}\text{U}$	$\pm 2\sigma$	$^{207}\text{Pb}/^{206}\text{Pb}$ age	$\pm 2\sigma$	$^{206}\text{Pb}/^{238}\text{U}$ age	$\pm 2\sigma$	$^{207}\text{Pb}/^{235}\text{U}$ age	$\pm 2\sigma$	Concordancy
SAN18_117	0.0775	0.0013	2.1430	0.0290	0.1985	0.0026	1126	32	1167	14	1164	10	104
SAN18_180	0.0795	0.0013	2.1630	0.0760	0.1981	0.0028	1175	33	1166	15	1168	24	99
SAN18_133	0.0782	0.0012	2.1540	0.0380	0.1982	0.0026	1154	30	1166	14	1165	12	101
SAN18_187	0.0802	0.0012	2.1480	0.0730	0.1982	0.0030	1201	29	1165	16	1168	24	97
SAN18_192	0.0798	0.0014	2.1830	0.0830	0.1983	0.0027	1190	35	1165	15	1169	27	98
SAN18_127	0.0787	0.0011	2.1530	0.0310	0.1982	0.0024	1160	27	1165	13	1165	10	100
SAN18_196	0.0793	0.0011	2.1660	0.0790	0.1980	0.0026	1176	28	1164	14	1161	25	99
SAN18_148	0.0786	0.0008	2.1440	0.0290	0.1979	0.0025	1165	20	1164	14	1163	9	100
SAN18_12	0.0805	0.0015	2.1650	0.0450	0.1979	0.0027	1209	37	1163	14	1170	15	96
SAN18_144	0.0795	0.0014	2.1550	0.0440	0.1978	0.0030	1182	34	1163	16	1166	14	98
SAN18_48	0.0793	0.0012	2.1690	0.0350	0.1978	0.0024	1174	30	1163	13	1171	11	99
SAN18_125	0.0783	0.0012	2.1580	0.0340	0.1978	0.0019	1159	29	1163	10	1167	11	100
SAN18_134	0.0792	0.0015	2.1520	0.0370	0.1975	0.0022	1175	37	1162	12	1166	12	99
SAN18_66	0.0798	0.0006	2.1670	0.0200	0.1974	0.0019	1192	14	1162	10	1170	6	97
SAN18_161	0.0795	0.0009	2.1620	0.0300	0.1973	0.0027	1184	23	1161	15	1168	10	98
SAN18_145	0.0782	0.0013	2.1510	0.0420	0.1973	0.0033	1155	31	1161	18	1164	14	101
SAN18_55	0.0794	0.0011	2.1510	0.0290	0.1969	0.0022	1175	27	1160	12	1167	9	99
SAN18_158	0.0789	0.0018	2.1540	0.0550	0.1972	0.0036	1160	46	1160	19	1164	18	100
SAN18_04	0.0803	0.0010	2.1930	0.0270	0.1969	0.0021	1202	24	1158	11	1181	9	96
SAN18_21	0.0792	0.0007	2.1510	0.0200	0.1968	0.0019	1172	18	1158	10	1165	7	99
SAN18_135	0.0801	0.0011	2.1790	0.0310	0.1967	0.0021	1193	27	1157	11	1175	10	97
SAN18_106	0.0786	0.0010	2.1340	0.0390	0.1963	0.0035	1160	25	1157	19	1160	13	100
SAN18_169	0.0802	0.0013	2.1730	0.0400	0.1964	0.0031	1195	32	1156	17	1174	13	97
SAN18_128	0.0788	0.0007	2.1370	0.0220	0.1964	0.0021	1168	18	1156	11	1161	7	99
SAN18_163	0.0806	0.0011	2.1910	0.0270	0.1961	0.0023	1210	26	1155	12	1178	9	95
SAN18_184	0.0802	0.0014	2.1700	0.0860	0.1962	0.0027	1199	35	1154	14	1158	27	96
SAN18_162	0.0792	0.0010	2.1260	0.0290	0.1957	0.0022	1183	24	1153	12	1158	9	97
SAN18_61	0.0796	0.0010	2.1490	0.0300	0.1954	0.0023	1183	25	1152	13	1163	10	97
SAN18_57	0.0798	0.0010	2.1630	0.0300	0.1956	0.0020	1192	25	1151	11	1170	10	97
SAN18_174	0.0786	0.0009	2.1250	0.0710	0.1956	0.0028	1164	24	1151	15	1155	23	99
SAN18_109	0.0796	0.0010	2.1440	0.0280	0.1953	0.0019	1184	25	1150	10	1162	9	97
SAN18_83	0.0786	0.0015	2.1030	0.0460	0.1953	0.0041	1159	38	1149	22	1153	15	99
SAN18_19	0.0803	0.0012	2.1610	0.0330	0.1949	0.0024	1199	28	1148	13	1168	11^{104}	96

Analysis #	$^{207}\text{Pb}/^{206}\text{Pb}$	$\pm 2\sigma$	$^{207}\text{Pb}/^{235}\text{U}$	$\pm 2\sigma$	$^{206}\text{Pb}/^{238}\text{U}$	$\pm 2\sigma$	$^{207}\text{Pb}/^{206}\text{Pb}$ age	$\pm 2\sigma$	$^{206}\text{Pb}/^{238}\text{U}$ age	$\pm 2\sigma$	$^{207}\text{Pb}/^{235}\text{U}$ age	$\pm 2\sigma$	Concordancy	
SAN18_05	0.0799	0.0010	2.1560	0.0300	0.1948	0.0023	1193	26	1147	12	1165	10	96	
SAN18_188	0.0792	0.0014	2.1280	0.0720	0.1949	0.0031	1180	35	1147	17	1148	23	97	
SAN18_168	0.0796	0.0011	2.1350	0.0340	0.1937	0.0025	1184	27	1141	14	1160	11	96	
SAN18_199	0.0784	0.0012	2.0650	0.0520	0.1932	0.0030	1158	29	1138	16	1135	17	98	
SAN18_149	0.0789	0.0015	2.0680	0.0360	0.1924	0.0024	1169	40	1134	13	1139	12	97	
SAN18_56	0.0795	0.0013	2.1000	0.0390	0.1918	0.0023	1176	34	1132	13	1147	13	96	
SAN18_156	0.0791	0.0012	2.0980	0.0310	0.1919	0.0022	1172	30	1131	12	1151	10	97	
SAN18_62	0.0776	0.0011	2.0410	0.0280	0.1903	0.0020	1132	28	1123	11	1128	9	99	
SAN18_160	0.0765	0.0013	2.0120	0.0430	0.1895	0.0047	1106	34	1118	26	1119	14	101	
SAN-18		(Discordant Analyses)												
SAN18_111	0.0813	0.0008	2.4850	0.0270	0.2221	0.0023	1229	19	1294	12	1267	8	105	
SAN18_91	0.0805	0.0012	2.4690	0.0320	0.2220	0.0024	1210	28	1292	13	1262	9	107	
SAN18_32	0.0797	0.0009	2.4090	0.0310	0.2203	0.0025	1183	23	1283	13	1246	10	108	
SAN18_72	0.0798	0.0008	2.3940	0.0250	0.2169	0.0021	1192	20	1265	11	1240	8	106	
SAN18_73	0.0847	0.0013	2.4840	0.0450	0.2126	0.0031	1314	29	1242	17	1271	12	95	
SAN18_93	0.0792	0.0012	2.2900	0.0330	0.2102	0.0025	1167	29	1230	13	1207	10	105	
SAN18_179	0.0845	0.0010	2.2790	0.0650	0.2051	0.0026	1298	23	1204	14	1205	21	93	
SAN18_141	0.0951	0.0012	2.6480	0.0480	0.2030	0.0024	1527	24	1191	13	1314	14	78	
SAN18_94	0.0817	0.0006	2.2400	0.0250	0.1970	0.0022	1241	14	1160	12	1193	8	93	
SAN18_200	0.0824	0.0012	2.1290	0.0640	0.1970	0.0027	1255	28	1159	14	1155	21	92	
SAN18_68	0.0830	0.0012	2.2430	0.0340	0.1968	0.0027	1264	29	1157	14	1195	11	92	
SAN18_166	0.0847	0.0012	2.3010	0.0390	0.1952	0.0024	1309	29	1149	13	1213	12	88	
SAN18_121	0.0820	0.0010	2.2160	0.0290	0.1951	0.0022	1246	25	1148	12	1184	9	92	
SAN18_63	0.0820	0.0007	2.1970	0.0230	0.1943	0.0015	1245	17	1145	8	1179	7	92	
SAN18_07	0.0807	0.0010	2.1560	0.0260	0.1936	0.0021	1212	25	1142	11	1166	8	94	
SAN18_137	0.0805	0.0012	2.1700	0.0330	0.1929	0.0020	1199	29	1137	11	1171	10	95	
SAN18_126	0.0819	0.0009	2.1730	0.0240	0.1924	0.0020	1242	22	1134	11	1171	8	91	
SAN18_43	0.0832	0.0010	2.2120	0.0300	0.1923	0.0017	1266	24	1134	9	1183	10	90	
SAN18_09	0.0842	0.0011	2.2190	0.0330	0.1922	0.0021	1296	25	1133	11	1185	10	87	
SAN18_150	0.0810	0.0011	2.1590	0.0290	0.1922	0.0020	1222	27	1133	11	1166	9	93	
SAN18_06	0.0804	0.0015	2.1180	0.0390	0.1921	0.0026	1207	37	1132	14	1156	13	94	

Analysis #	$^{207}\text{Pb}/^{206}\text{Pb}$	$\pm 2\sigma$	$^{207}\text{Pb}/^{235}\text{U}$	$\pm 2\sigma$	$^{206}\text{Pb}/^{238}\text{U}$	$\pm 2\sigma$	$^{207}\text{Pb}/^{206}\text{Pb}$ age	$\pm 2\sigma$	$^{206}\text{Pb}/^{238}\text{U}$ age	$\pm 2\sigma$	$^{207}\text{Pb}/^{235}\text{U}$ age	$\pm 2\sigma$	Concordancy
SAN18_159	0.0812	0.0010	2.1300	0.0310	0.1916	0.0029	1225	24	1130	16	1159	10	92
SAN18_130	0.0912	0.0005	2.4120	0.0160	0.1916	0.0016	1450	11	1130	8	1246	5	78
SAN18_129	0.0800	0.0013	2.1110	0.0350	0.1904	0.0024	1200	31	1126	13	1154	11	94
SAN18_167	0.0852	0.0018	2.2150	0.0510	0.1894	0.0028	1312	41	1118	15	1185	16	85
SAN18_165	0.0838	0.0008	2.1990	0.0280	0.1891	0.0020	1287	18	1116	11	1181	9	87
SAN18_139	0.0814	0.0010	2.1080	0.0310	0.1888	0.0022	1229	24	1114	12	1150	10	91
SAN18_147	0.0794	0.0010	2.0680	0.0340	0.1886	0.0028	1180	24	1114	15	1138	12	94
SAN18_59	0.0866	0.0010	2.2730	0.0250	0.1886	0.0018	1348	21	1113	10	1203	8	83
SAN18_138	0.0819	0.0014	2.1080	0.0350	0.1878	0.0024	1242	32	1109	13	1151	11	89
SAN18_170	0.0801	0.0016	2.0480	0.0410	0.1868	0.0029	1199	39	1104	16	1131	13	92
SAN18_42	0.0874	0.0011	2.1250	0.0280	0.1761	0.0021	1366	25	1045	11	1156	9	77
SAN18_146	0.0808	0.0012	1.9390	0.0340	0.1754	0.0023	1208	30	1041	13	1099	11	86
SAN18_46	0.0810	0.0006	1.9400	0.0200	0.1744	0.0021	1223	15	1036	12	1095	7	85
SAN18_64	0.0777	0.0009	1.8390	0.0260	0.1716	0.0024	1137	22	1021	13	1061	10	90
SAN18_77	0.0959	0.0011	2.2150	0.0350	0.1679	0.0024	1545	23	1000	13	1185	11	65
SAN18_10	0.0758	0.0005	1.6810	0.0130	0.1606	0.0012	1090	12	961	6	1001	5	88
SAN18_142	0.0749	0.0006	1.5610	0.0190	0.1513	0.0016	1066	17	908	9	955	8	85

SAN-19	(Concordant Analyses)												
SAN19_29	0.0852	0.0012	2.6560	0.0490	0.2253	0.0033	1319	26	1312	17	1315	14	99
SAN19_62	0.0814	0.0014	2.4030	0.0380	0.2132	0.0030	1242	31	1247	16	1245	12	100
SAN19_43	0.0817	0.0021	2.4250	0.0550	0.2130	0.0037	1245	50	1244	20	1248	16	100
SAN19_78	0.0799	0.0020	2.3020	0.0550	0.2115	0.0033	1188	51	1238	17	1209	17	104
SAN19_05	0.0814	0.0018	2.3570	0.0500	0.2105	0.0034	1234	44	1231	18	1228	15	100
SAN19_04	0.0799	0.0011	2.3250	0.0300	0.2092	0.0023	1200	26	1224	12	1220	9	102
SAN19_75	0.0804	0.0035	2.3440	0.0900	0.2089	0.0050	1225	87	1221	27	1222	28	100
SAN19_72	0.0814	0.0019	2.3270	0.0480	0.2074	0.0025	1217	45	1217	13	1218	15	100
SAN19_81	0.0801	0.0013	2.3050	0.0390	0.2068	0.0031	1193	30	1211	17	1213	12	102
SAN19_10	0.0801	0.0014	2.2730	0.0380	0.2061	0.0025	1191	35	1208	13	1203	12	101
SAN19_06	0.0787	0.0015	2.2730	0.0420	0.2062	0.0027	1162	37	1208	15	1203	13	104
SAN19_63	0.0799	0.0012	2.2970	0.0330	0.2060	0.0026	1193	31	1207	14	1210	10	101
SAN19_07	0.0798	0.0015	2.2450	0.0430	0.2048	0.0029	1186	37	1200	16	1196	13	101

Analysis #	$^{207}\text{Pb}/^{206}\text{Pb}$	$\pm 2\sigma$	$^{207}\text{Pb}/^{235}\text{U}$	$\pm 2\sigma$	$^{206}\text{Pb}/^{238}\text{U}$	$\pm 2\sigma$	$^{207}\text{Pb}/^{206}\text{Pb}$ age	$\pm 2\sigma$	$^{206}\text{Pb}/^{238}\text{U}$ age	$\pm 2\sigma$	$^{207}\text{Pb}/^{235}\text{U}$ age	$\pm 2\sigma$	Concordancy
SAN19_82	0.0800	0.0015	2.2490	0.0480	0.2041	0.0039	1195	37	1199	21	1196	15	100
SAN19_09	0.0796	0.0015	2.2410	0.0460	0.2045	0.0049	1187	39	1199	26	1193	14	101
SAN19_58	0.0797	0.0011	2.2440	0.0300	0.2044	0.0019	1186	26	1199	10	1196	9	101
SAN19_76	0.0812	0.0012	2.2660	0.0320	0.2043	0.0025	1222	30	1198	13	1202	10	98
SAN19_91	0.0795	0.0012	2.2520	0.0310	0.2040	0.0025	1194	30	1197	13	1197	10	100
SAN19_67	0.0799	0.0011	2.2580	0.0300	0.2038	0.0025	1191	28	1197	14	1199	10	101
SAN19_45	0.0804	0.0015	2.2680	0.0560	0.2039	0.0030	1197	36	1196	16	1199	17	100
SAN19_69	0.0794	0.0009	2.2330	0.0280	0.2034	0.0022	1178	22	1194	12	1191	9	101
SAN19_64	0.0788	0.0011	2.2100	0.0310	0.2021	0.0020	1165	27	1186	11	1184	10	102
SAN19_88	0.0803	0.0011	2.2240	0.0330	0.2017	0.0022	1199	27	1184	12	1190	10	99
SAN19_51	0.0796	0.0014	2.2140	0.0400	0.2015	0.0026	1186	36	1183	14	1186	13	100
SAN19_41	0.0797	0.0013	2.2150	0.0360	0.2016	0.0025	1183	32	1183	13	1184	11	100
SAN19_77	0.0795	0.0012	2.2090	0.0320	0.2014	0.0025	1176	31	1183	13	1185	10	101
SAN19_94	0.0802	0.0009	2.2050	0.0330	0.2008	0.0025	1200	22	1181	13	1185	10	98
SAN19_42	0.0802	0.0025	2.2010	0.0600	0.2011	0.0037	1192	60	1181	20	1180	19	99
SAN19_87	0.0785	0.0010	2.2040	0.0300	0.2005	0.0028	1159	25	1181	15	1181	10	102
SAN19_60	0.0794	0.0019	2.2060	0.0530	0.2009	0.0027	1176	49	1180	14	1182	17	100
SAN19_93	0.0791	0.0018	2.2080	0.0470	0.2011	0.0032	1170	48	1180	17	1182	15	101
SAN19_71	0.0791	0.0011	2.1920	0.0280	0.2005	0.0021	1175	27	1178	11	1181	9	100
SAN19_49	0.0792	0.0021	2.2110	0.0550	0.2007	0.0033	1172	54	1178	18	1183	17	101
SAN19_57	0.0798	0.0011	2.2030	0.0290	0.2001	0.0022	1186	27	1177	12	1182	9	99
SAN19_55	0.0784	0.0010	2.1760	0.0300	0.2002	0.0023	1155	24	1177	12	1173	10	102
SAN19_23	0.0793	0.0011	2.1930	0.0270	0.1997	0.0021	1190	26	1174	11	1178	9	99
SAN19_79	0.0797	0.0010	2.1910	0.0310	0.1997	0.0024	1186	24	1174	13	1179	10	99
SAN19_83	0.0793	0.0012	2.1810	0.0370	0.1999	0.0027	1183	30	1174	14	1175	12	99
SAN19_53	0.0798	0.0011	2.2070	0.0340	0.1997	0.0022	1194	28	1173	12	1181	11	98
SAN19_22	0.0787	0.0010	2.1750	0.0290	0.1997	0.0021	1157	26	1173	11	1172	10	101
SAN19_89	0.0798	0.0011	2.1850	0.0300	0.1994	0.0027	1189	27	1172	15	1175	10	99
SAN19_73	0.0787	0.0007	2.1690	0.0230	0.1993	0.0021	1167	18	1171	12	1172	7	100
SAN19_84	0.0799	0.0012	2.1830	0.0330	0.1990	0.0029	1192	31	1169	16	1174	11	98
SAN19_59	0.0794	0.0013	2.1670	0.0330	0.1990	0.0021	1184	33	1169	11	1170	11	99
SAN19_50	0.0800	0.0020	2.1780	0.0600	0.1988	0.0043	1198	47	1168	23	1173	19	97
SAN19_27	0.0790	0.0010	2.1750	0.0290	0.1988	0.0023	1173	27	1168	12	1173	9 ¹⁰⁷	100

Analysis #	$^{207}\text{Pb}/^{206}\text{Pb}$	$\pm 2\sigma$	$^{207}\text{Pb}/^{235}\text{U}$	$\pm 2\sigma$	$^{206}\text{Pb}/^{238}\text{U}$	$\pm 2\sigma$	$^{207}\text{Pb}/^{206}\text{Pb}$ age	$\pm 2\sigma$	$^{206}\text{Pb}/^{238}\text{U}$ age	$\pm 2\sigma$	$^{207}\text{Pb}/^{235}\text{U}$ age	$\pm 2\sigma$	Concordancy	
SAN19_56	0.0790	0.0008	2.1680	0.0250	0.1985	0.0021	1175	20	1167	11	1170	8	99	
SAN19_12	0.0794	0.0014	2.1580	0.0350	0.1980	0.0025	1182	35	1164	14	1166	11	98	
SAN19_85	0.0792	0.0008	2.1590	0.0310	0.1979	0.0023	1176	22	1164	12	1168	10	99	
SAN19_48	0.0789	0.0011	2.1470	0.0280	0.1975	0.0022	1170	27	1162	12	1163	9	99	
SAN19_86	0.0790	0.0011	2.1400	0.0330	0.1971	0.0024	1172	28	1160	13	1161	11	99	
SAN19_14	0.0787	0.0018	2.1480	0.0540	0.1972	0.0030	1169	46	1160	16	1162	18	99	
SAN19_26	0.0786	0.0018	2.1330	0.0510	0.1966	0.0028	1144	48	1158	15	1156	17	101	
SAN19_32	0.0791	0.0009	2.1280	0.0210	0.1966	0.0019	1172	24	1157	10	1158	7	99	
SAN19_34	0.0783	0.0012	2.1360	0.0330	0.1964	0.0022	1156	31	1156	12	1159	11	100	
SAN19_80	0.0787	0.0018	2.1090	0.0500	0.1963	0.0032	1188	47	1155	17	1158	16	97	
SAN19_39	0.0790	0.0016	2.1240	0.0400	0.1962	0.0025	1162	42	1155	13	1157	13	99	
SAN19_37	0.0785	0.0010	2.1260	0.0260	0.1961	0.0021	1153	24	1154	11	1157	9	100	
SAN19_52	0.0788	0.0012	2.1320	0.0310	0.1957	0.0020	1162	31	1153	11	1157	10	99	
SAN19_99	0.0798	0.0010	2.1640	0.0300	0.1956	0.0025	1187	24	1151	13	1171	9	97	
SAN19_25	0.0783	0.0012	2.1180	0.0310	0.1954	0.0022	1162	30	1151	12	1155	10	99	
SAN19_11	0.0784	0.0013	2.1240	0.0350	0.1954	0.0021	1157	32	1150	11	1154	12	99	
SAN19_15	0.0784	0.0014	2.1040	0.0360	0.1949	0.0024	1167	39	1148	13	1149	12	98	
SAN19_95	0.0782	0.0009	2.1050	0.0270	0.1951	0.0027	1155	23	1148	15	1152	9	99	
SAN19_40	0.0777	0.0015	2.0980	0.0280	0.1950	0.0032	1138	37	1148	17	1148	9	101	
SAN19_33	0.0790	0.0009	2.1060	0.0230	0.1946	0.0018	1171	22	1146	10	1150	7	98	
SAN19_13	0.0790	0.0010	2.1030	0.0290	0.1944	0.0023	1173	25	1145	12	1149	10	98	
SAN19_16	0.0779	0.0012	2.0900	0.0380	0.1938	0.0030	1145	31	1141	16	1145	12	100	
SAN19_92	0.0780	0.0017	2.0640	0.0460	0.1923	0.0029	1144	42	1135	16	1136	15	99	
SAN19_36	0.0777	0.0009	2.0650	0.0250	0.1925	0.0023	1141	22	1135	12	1137	9	99	
SAN19_17	0.0795	0.0009	2.0940	0.0240	0.1905	0.0018	1184	23	1125	10	1146	8	95	
SAN19_19	0.0783	0.0022	2.0100	0.0620	0.1898	0.0038	1138	56	1123	21	1118	21	99	
SAN19_90	0.0798	0.0023	2.0830	0.0620	0.1884	0.0034	1161	58	1111	18	1139	21	96	
SAN19_18	0.0775	0.0032	1.9440	0.0680	0.1845	0.0037	1138	81	1090	20	1095	23	96	
SAN-19	(Discordant Analyses)													
SAN19_01	0.1052	0.0012	4.8550	0.0500	0.3341	0.0035	1713	20	1859	17	1794	9	109	
SAN19_02	0.0810	0.0032	2.5240	0.0990	0.2226	0.0047	1195	81	1294	25	1270	28	108	

Analysis #	$^{207}\text{Pb}/^{206}\text{Pb}$	$\pm 2\sigma$	$^{207}\text{Pb}/^{235}\text{U}$	$\pm 2\sigma$	$^{206}\text{Pb}/^{238}\text{U}$	$\pm 2\sigma$	$^{207}\text{Pb}/^{206}\text{Pb}$ age	$\pm 2\sigma$	$^{206}\text{Pb}/^{238}\text{U}$ age	$\pm 2\sigma$	$^{207}\text{Pb}/^{235}\text{U}$ age	$\pm 2\sigma$	Concordancy
SAN19_03	0.0799	0.0008	2.4050	0.0240	0.2184	0.0017	1201	20	1273	9	1243	7	106
SAN19_08	0.0785	0.0012	2.2720	0.0350	0.2097	0.0022	1160	31	1227	12	1203	11	106
SAN19_97	0.0862	0.0015	2.4370	0.0380	0.2080	0.0028	1340	32	1222	15	1255	11	91
SAN19_74	0.0850	0.0023	2.3200	0.0560	0.1992	0.0027	1324	52	1170	15	1220	17	88
SAN19_19B	0.0806	0.0010	2.1320	0.0320	0.1933	0.0019	1210	25	1139	10	1159	10	94
SAN19_66	0.0822	0.0012	2.1670	0.0330	0.1917	0.0020	1257	28	1130	11	1170	11	90
SAN19_30	0.0823	0.0007	2.1660	0.0230	0.1913	0.0019	1248	17	1129	10	1171	7	90
SAN19_96	0.0807	0.0011	2.1150	0.0300	0.1893	0.0024	1210	27	1117	13	1153	10	92
SAN19_70	0.0797	0.0009	2.0510	0.0270	0.1867	0.0020	1191	21	1103	11	1134	9	93
SAN19_47	0.0783	0.0023	1.9950	0.0510	0.1819	0.0027	1174	56	1078	15	1110	17	92
SAN19_54	0.0779	0.0007	1.9470	0.0210	0.1807	0.0016	1143	17	1071	9	1097	7	94
SAN19_28	0.0775	0.0007	1.8910	0.0180	0.1760	0.0017	1133	17	1045	9	1077	6	92
SAN19_65	0.0787	0.0008	1.8670	0.0240	0.1731	0.0016	1162	21	1029	9	1070	9	89
SAN19_44	0.0794	0.0008	1.8610	0.0210	0.1700	0.0018	1179	20	1012	10	1069	8	86
SAN19_31	0.1430	0.0150	3.6800	0.5500	0.1661	0.0059	1970	160	987	32	1392	99	50
SAN19_100	0.0783	0.0009	1.7790	0.0240	0.1644	0.0019	1157	22	981	11	1040	9	85
SAN19_35	0.0770	0.0006	1.6980	0.0170	0.1618	0.0015	1119	15	966	8	1008	7	86
SAN19_24	0.0748	0.0006	1.6550	0.0170	0.1600	0.0018	1061	17	957	10	991	7	90
SAN19_38	0.0787	0.0007	1.7190	0.0170	0.1583	0.0014	1161	18	948	8	1016	6	82
SAN19_68	0.0770	0.0006	1.5960	0.0160	0.1499	0.0014	1120	16	900	8	968	6	80
SAN19_61	0.0725	0.0005	1.4060	0.0130	0.1406	0.0013	999	15	848	7	891	5	85
SAN19_46	0.0755	0.0007	1.4250	0.0180	0.1372	0.0014	1079	18	829	8	900	7	77
SAN19_20	0.0711	0.0005	1.3430	0.0250	0.1360	0.0022	962	13	823	13	863	11	86
SAN19_21	0.0711	0.0004	1.3340	0.0230	0.1360	0.0021	961	13	822	12	860	10	86
SAN19_98	0.0765	0.0009	1.4070	0.0190	0.1340	0.0017	1103	22	811	10	891	8	73

STANDARD ANALYSES

Analysis #	$^{207}\text{Pb}/^{206}\text{Pb}$	$\pm 2\sigma$	$^{207}\text{Pb}/^{235}\text{U}$	$\pm 2\sigma$	$^{206}\text{Pb}/^{238}\text{U}$	$\pm 2\sigma$	$^{207}\text{Pb}/^{206}\text{Pb}$ age	$\pm 2\sigma$	$^{206}\text{Pb}/^{238}\text{U}$ age	$\pm 2\sigma$	$^{207}\text{Pb}/^{235}\text{U}$ age	$\pm 2\sigma$	Concordancy
SAN-2 (Concordant Standards)													
STDGJ16	0.0599	0.0018	0.8290	0.0210	0.0995	0.0017	597	63	613	10.0	614	12.0	103
STDGJ16	0.0604	0.0019	0.8430	0.0240	0.0988	0.0019	597	69	608	11.0	623	13.0	102
STDGJ31	0.0601	0.0018	0.8280	0.0200	0.0987	0.0017	599	65	608	9.8	611	11.0	101
STDGJ44	0.0602	0.0022	0.8260	0.0260	0.0985	0.0021	580	81	605	12.0	609	14.0	104
STDGJ27	0.0623	0.0028	0.8190	0.0260	0.0985	0.0025	628	89	605	15.0	609	15.0	96
STDGJ05	0.0612	0.0025	0.8210	0.0280	0.0984	0.0019	634	87	605	11.0	607	15.0	95
STDGJ17	0.0607	0.0021	0.8550	0.0270	0.0985	0.0017	636	70	605	10.0	632	15.0	95
STDGJ15	0.0595	0.0022	0.8210	0.0270	0.0983	0.0016	578	82	604	9.5	608	15.0	105
STDGJ28	0.0602	0.0021	0.8180	0.0260	0.0981	0.0019	595	76	604	11.0	608	15.0	102
STDGJ17	0.0616	0.0030	0.8210	0.0350	0.0978	0.0031	630	100	604	19.0	606	20.0	96
STDGJ32	0.0600	0.0018	0.8180	0.0250	0.0978	0.0019	602	65	602	11.0	607	14.0	100
STDGJ33	0.0601	0.0020	0.8090	0.0250	0.0979	0.0020	606	70	602	12.0	603	14.0	99
STDGJ05	0.0591	0.0018	0.8150	0.0220	0.0978	0.0016	575	67	602	9.2	605	12.0	105
STDGJ28	0.0597	0.0024	0.8050	0.0310	0.0978	0.0020	577	87	601	12.0	601	17.0	104
STDGJ18	0.0594	0.0021	0.8040	0.0260	0.0978	0.0019	581	74	601	11.0	601	15.0	103
STDGJ24	0.0602	0.0020	0.8060	0.0240	0.0977	0.0017	587	69	601	10.0	604	12.0	102
STDGJ44	0.0608	0.0025	0.8160	0.0260	0.0978	0.0022	609	86	601	13.0	605	15.0	99
STDGJ33	0.0606	0.0018	0.8120	0.0240	0.0978	0.0018	610	66	601	11.0	605	14.0	99
STDGJ64	0.0606	0.0018	0.8120	0.0210	0.0975	0.0017	614	62	601	10.0	603	12.0	98
STDGJ10	0.0599	0.0023	0.8200	0.0290	0.0977	0.0017	573	82	601	9.9	605	16.0	105
STDGJ09	0.0601	0.0017	0.8110	0.0230	0.0977	0.0015	578	63	601	8.6	604	13.0	104
STDGJ22	0.0599	0.0018	0.7890	0.0220	0.0976	0.0015	593	64	600	8.9	592	12.0	101
STDGJ41	0.0597	0.0017	0.8140	0.0240	0.0976	0.0014	592	62	600	8.5	603	13.0	101
STDGJ35	0.0592	0.0018	0.8090	0.0200	0.0975	0.0018	582	65	600	10.0	602	11.0	103
STDGJ20	0.0601	0.0025	0.8030	0.0340	0.0976	0.0029	586	92	600	17.0	601	19.0	102
STDGJ42	0.0600	0.0025	0.8030	0.0310	0.0975	0.0021	589	92	600	12.0	597	18.0	102
STDGJ43	0.0597	0.0017	0.8110	0.0250	0.0977	0.0018	591	66	600	11.0	604	15.0	102
STDGJ49	0.0596	0.0024	0.7970	0.0280	0.0976	0.0021	603	84	600	12.0	597	16.0	¹¹¹ 100

Analysis #	$^{207}\text{Pb}/^{206}\text{Pb}$	$\pm 2\sigma$	$^{207}\text{Pb}/^{235}\text{U}$	$\pm 2\sigma$	$^{206}\text{Pb}/^{238}\text{U}$	$\pm 2\sigma$	$^{207}\text{Pb}/^{206}\text{Pb}$ age	$\pm 2\sigma$	$^{206}\text{Pb}/^{238}\text{U}$ age	$\pm 2\sigma$	$^{207}\text{Pb}/^{235}\text{U}$ age	$\pm 2\sigma$	Concordancy
STDGJ43	0.0619	0.0031	0.8020	0.0330	0.0977	0.0024	617	99	600	14.0	599	18.0	97
STDGJ08	0.0601	0.0018	0.8060	0.0200	0.0975	0.0015	582	63	600	8.9	600	11.0	103
STDGJ26	0.0624	0.0023	0.7990	0.0290	0.0973	0.0017	626	77	600	9.9	602	14.0	96
STDGJ09	0.0605	0.0017	0.8060	0.0230	0.0974	0.0014	598	64	599	8.5	601	13.0	100
STDGJ41	0.0598	0.0018	0.8100	0.0250	0.0974	0.0016	597	69	599	9.3	603	13.0	100
STDGJ21	0.0609	0.0021	0.7970	0.0230	0.0972	0.0018	583	73	599	10.0	595	13.0	103
STDGJ37	0.0604	0.0022	0.7970	0.0270	0.0974	0.0022	592	79	599	13.0	596	15.0	101
STDGJ14	0.0604	0.0019	0.8090	0.0210	0.0975	0.0018	598	67	599	11.0	600	12.0	100
STDGJ35	0.0597	0.0019	0.8050	0.0200	0.0975	0.0019	613	67	599	11.0	600	11.0	98
STDGJ39	0.0601	0.0019	0.8020	0.0250	0.0974	0.0016	583	68	599	9.6	596	14.0	103
STDGJ26	0.0600	0.0021	0.8080	0.0230	0.0973	0.0016	575	77	598	9.6	603	13.0	104
STDGJ48	0.0594	0.0017	0.8080	0.0230	0.0973	0.0015	596	65	598	9.0	603	13.0	100
STDGJ49	0.0586	0.0021	0.7970	0.0260	0.0972	0.0017	573	75	598	10.0	594	15.0	104
STDGJ27	0.0581	0.0020	0.7910	0.0240	0.0973	0.0018	576	79	598	11.0	594	13.0	104
STDGJ20	0.0605	0.0022	0.7960	0.0230	0.0971	0.0019	582	75	598	11.0	596	13.0	103
STDGJ28	0.0616	0.0025	0.8040	0.0250	0.0973	0.0019	585	75	598	11.0	603	15.0	102
STDGJ36	0.0607	0.0020	0.8320	0.0230	0.0972	0.0015	628	71	598	8.8	613	12.0	95
STDGJ18	0.0602	0.0021	0.7960	0.0260	0.0968	0.0018	578	74	596	11.0	591	15.0	103
STDGJ47	0.0598	0.0022	0.8010	0.0260	0.0967	0.0017	582	80	596	10.0	596	14.0	102
STDGJ64	0.0612	0.0026	0.8050	0.0270	0.0969	0.0021	596	84	596	12.0	596	15.0	100
STDGJ48	0.0610	0.0021	0.7890	0.0310	0.0968	0.0017	599	71	595	9.8	592	16.0	99
STDGJ21	0.0606	0.0023	0.7940	0.0280	0.0967	0.0017	585	80	595	9.9	591	15.0	102
STDGJ10	0.0609	0.0020	0.8350	0.0250	0.0967	0.0015	614	69	595	8.6	618	13.0	97
STDGJ36	0.0600	0.0019	0.8360	0.0230	0.0966	0.0015	603	71	594	8.6	617	13.0	99
STDGJ32	0.0594	0.0017	0.8240	0.0230	0.0965	0.0017	580	61	594	10.0	609	13.0	102
STDGJ25	0.0608	0.0020	0.8420	0.0250	0.0966	0.0018	613	73	594	11.0	622	13.0	97
STDGJ67	0.0602	0.0017	0.7920	0.0210	0.0963	0.0014	590	64	592	8.3	592	12.0	100
STDGJ45	0.0615	0.0020	0.8380	0.0250	0.0962	0.0019	614	71	592	11.0	617	14.0	96
STDGJ66	0.0605	0.0022	0.7960	0.0260	0.0961	0.0015	572	71	592	9.0	594	14.0	103
STDGJ14	0.0597	0.0019	0.7990	0.0220	0.0962	0.0020	576	68	591	12.0	594	12.0	103
STDGJ34	0.0597	0.0020	0.8000	0.0230	0.0961	0.0019	580	72	591	11.0	594	13.0	102
STDGJ11	0.0624	0.0027	0.7860	0.0270	0.0959	0.0019	602	88	591	11.0	588	15.0	98
STDGJ42	0.0622	0.0024	0.7970	0.0250	0.0961	0.0017	606	77	591	10.0	594	14.0	¹¹² 98

Analysis #	$^{207}\text{Pb}/^{206}\text{Pb}$	$\pm 2\sigma$	$^{207}\text{Pb}/^{235}\text{U}$	$\pm 2\sigma$	$^{206}\text{Pb}/^{238}\text{U}$	$\pm 2\sigma$	$^{207}\text{Pb}/^{206}\text{Pb}$ age	$\pm 2\sigma$	$^{206}\text{Pb}/^{238}\text{U}$ age	$\pm 2\sigma$	$^{207}\text{Pb}/^{235}\text{U}$ age	$\pm 2\sigma$	Concordancy
STDGJ67	0.0605	0.0020	0.7880	0.0250	0.0959	0.0014	582	67	590	8.5	590	14.0	101
STDGJ11	0.0608	0.0022	0.7870	0.0240	0.0960	0.0017	586	79	590	10.0	589	14.0	101
STDGJ19	0.0599	0.0024	0.7970	0.0320	0.0929	0.0022	583	89	574	13.0	599	19.0	98
PLES06	0.0536	0.0013	0.3973	0.0081	0.0538	0.0008	343	53	338	4.6	340	5.9	98
PLES11	0.0533	0.0014	0.3987	0.0091	0.0537	0.0009	324	56	337	5.2	341	6.8	104
PLES10	0.0541	0.0017	0.3969	0.0094	0.0537	0.0009	343	67	337	5.3	341	6.7	98
PLES08	0.0534	0.0014	0.3975	0.0094	0.0537	0.0008	322	58	337	4.8	339	6.8	105
PLES08	0.0536	0.0014	0.3999	0.0097	0.0537	0.0008	339	58	337	5.0	341	7.1	99
PLES11	0.0539	0.0017	0.4046	0.0094	0.0537	0.0009	340	63	337	5.3	344	6.8	99
PLES12	0.0534	0.0018	0.3970	0.0110	0.0535	0.0010	329	73	336	6.3	339	7.5	102
PLES04	0.0536	0.0014	0.3910	0.0100	0.0535	0.0008	323	54	336	4.7	335	7.3	104
SAN-2		(Discordant Standards)											
STDGJ04	0.0597	0.0017	0.8680	0.0230	0.1048	0.0016	566	63	642	9.6	634	13.0	113
STDGJ05	0.0599	0.0020	0.8860	0.0270	0.1018	0.0020	591	70	625	12.0	642	15.0	106
STDGJ65	0.0579	0.0019	0.8010	0.0220	0.1004	0.0017	505	70	617	9.7	596	12.0	122
STDGJ23	0.0590	0.0018	0.8140	0.0230	0.0996	0.0018	544	68	613	10.0	601	13.0	113
STDGJ29	0.0584	0.0017	0.8310	0.0220	0.0995	0.0013	532	65	612	7.9	611	12.0	115
STDGJ06	0.0592	0.0019	0.8330	0.0240	0.0991	0.0014	557	67	611	7.8	613	13.0	110
STDGJ30	0.0596	0.0018	0.8320	0.0220	0.0990	0.0017	568	63	609	10.0	612	12.0	107
STDGJ04	0.0631	0.0032	0.8100	0.0420	0.0990	0.0023	680	110	608	13.0	606	22.0	89
STDGJ65	0.0579	0.0023	0.8300	0.0280	0.0988	0.0023	534	86	607	13.0	612	15.0	114
STDGJ23	0.0582	0.0019	0.8190	0.0260	0.0985	0.0017	524	74	606	10.0	604	14.0	116
STDGJ12	0.0590	0.0027	0.8110	0.0350	0.0985	0.0021	533	97	606	12.0	602	19.0	114
STDGJ17	0.0587	0.0021	0.8190	0.0260	0.0985	0.0019	542	73	606	11.0	608	15.0	112
STDGJ15	0.0615	0.0021	0.8260	0.0250	0.0985	0.0016	639	74	606	9.2	610	14.0	95
STDGJ38	0.0581	0.0019	0.8090	0.0230	0.0984	0.0017	513	72	605	10.0	601	13.0	118
STDGJ23	0.0594	0.0022	0.8220	0.0250	0.0985	0.0018	561	80	605	11.0	609	14.0	108
STDGJ37	0.0588	0.0018	0.8040	0.0240	0.0982	0.0018	539	69	604	11.0	599	13.0	112
STDGJ29	0.0584	0.0018	0.8200	0.0260	0.0982	0.0016	529	68	604	9.4	605	14.0	114
STDGJ09	0.0583	0.0017	0.8020	0.0220	0.0982	0.0015	528	60	604	9.1	600	12.0	114
STDGJ30	0.0593	0.0024	0.8070	0.0270	0.0980	0.0019	531	86	603	11.0	600	15.0	114

Analysis #	$^{207}\text{Pb}/^{206}\text{Pb}$	$\pm 2\sigma$	$^{207}\text{Pb}/^{235}\text{U}$	$\pm 2\sigma$	$^{206}\text{Pb}/^{238}\text{U}$	$\pm 2\sigma$	$^{207}\text{Pb}/^{206}\text{Pb}$ age	$\pm 2\sigma$	$^{206}\text{Pb}/^{238}\text{U}$ age	$\pm 2\sigma$	$^{207}\text{Pb}/^{235}\text{U}$ age	$\pm 2\sigma$	Concordancy
STDGJ18	0.0583	0.0019	0.8040	0.0260	0.0981	0.0020	537	70	603	12.0	599	15.0	112
STDGJ25	0.0588	0.0018	0.8170	0.0240	0.0979	0.0015	539	66	602	9.0	606	13.0	112
STDGJ46	0.0589	0.0022	0.8050	0.0290	0.0978	0.0019	525	81	601	11.0	598	16.0	114
STDGJ38	0.0586	0.0021	0.8010	0.0240	0.0978	0.0020	541	79	601	12.0	597	13.0	111
STDGJ08	0.0591	0.0017	0.8120	0.0200	0.0977	0.0015	565	63	601	8.8	604	11.0	106
STDGJ29	0.0594	0.0020	0.7980	0.0220	0.0977	0.0018	567	70	601	10.0	597	13.0	106
STDGJ30	0.0601	0.0021	0.8020	0.0250	0.0978	0.0018	570	78	601	10.0	597	14.0	105
STDGJ45	0.0624	0.0018	0.8350	0.0210	0.0973	0.0017	651	62	600	9.9	616	12.0	92
STDGJ16	0.0595	0.0019	0.8180	0.0230	0.0974	0.0018	545	69	600	11.0	604	13.0	110
STDGJ13	0.0601	0.0022	0.8010	0.0260	0.0974	0.0018	554	77	600	10.0	597	15.0	108
STDGJ39	0.0595	0.0019	0.8020	0.0250	0.0976	0.0017	555	68	600	10.0	597	14.0	108
STDGJ20	0.0594	0.0021	0.8040	0.0250	0.0975	0.0019	561	73	600	11.0	596	14.0	107
STDGJ34	0.0632	0.0030	0.7970	0.0280	0.0977	0.0022	650	91	600	13.0	599	16.0	92
STDGJ31	0.0627	0.0026	0.8140	0.0290	0.0976	0.0027	657	89	600	16.0	602	17.0	91
STDGJ46	0.0587	0.0018	0.8130	0.0230	0.0976	0.0016	537	64	600	9.3	602	13.0	112
STDGJ25	0.0612	0.0018	0.8400	0.0220	0.0975	0.0016	637	66	599	9.7	620	12.0	94
STDGJ22	0.0593	0.0017	0.8080	0.0220	0.0975	0.0015	564	63	599	8.7	601	13.0	106
STDGJ15	0.0608	0.0022	0.8040	0.0250	0.0974	0.0016	565	71	599	9.6	597	14.0	106
STDGJ22	0.0582	0.0024	0.8080	0.0320	0.0975	0.0018	498	91	599	11.0	598	18.0	120
STDGJ07	0.0586	0.0020	0.8000	0.0230	0.0974	0.0017	524	72	599	10.0	595	13.0	114
STDGJ66	0.0586	0.0019	0.8020	0.0230	0.0973	0.0018	547	69	599	11.0	596	13.0	110
STDGJ13	0.0598	0.0021	0.8040	0.0250	0.0974	0.0017	563	76	599	10.0	599	14.0	106
STDGJ24	0.0589	0.0019	0.7920	0.0230	0.0972	0.0016	543	67	599	9.5	594	13.0	110
STDGJ24	0.0592	0.0019	0.7960	0.0230	0.0972	0.0016	552	69	599	9.5	596	13.0	108
STDGJ21	0.0601	0.0020	0.8060	0.0220	0.0969	0.0017	561	70	597	9.8	600	12.0	106
STDGJ06	0.0580	0.0021	0.7910	0.0270	0.0971	0.0019	535	71	597	11.0	593	15.0	112
STDGJ27	0.0582	0.0020	0.7930	0.0220	0.0968	0.0016	540	72	595	9.7	595	12.0	110
STDGJ07	0.0584	0.0026	0.7990	0.0310	0.0968	0.0021	532	96	595	12.0	593	17.0	112
STDGJ07	0.0618	0.0026	0.8030	0.0340	0.0967	0.0021	644	91	595	12.0	598	18.0	92
STDGJ32	0.0582	0.0020	0.8020	0.0230	0.0966	0.0017	509	72	594	10.0	595	13.0	117
STDGJ31	0.0566	0.0020	0.7860	0.0250	0.0965	0.0017	457	74	593	10.0	591	14.0	130
STDGJ26	0.0578	0.0024	0.7970	0.0300	0.0964	0.0020	505	87	593	12.0	590	17.0	117
STDGJ12	0.0600	0.0024	0.8040	0.0300	0.0961	0.0018	562	88	593	10.0	596	17.0	¹¹⁴ 106

Analysis #	$^{207}\text{Pb}/^{206}\text{Pb}$	$\pm 2\sigma$	$^{207}\text{Pb}/^{235}\text{U}$	$\pm 2\sigma$	$^{206}\text{Pb}/^{238}\text{U}$	$\pm 2\sigma$	$^{207}\text{Pb}/^{206}\text{Pb}$ age	$\pm 2\sigma$	$^{206}\text{Pb}/^{238}\text{U}$ age	$\pm 2\sigma$	$^{207}\text{Pb}/^{235}\text{U}$ age	$\pm 2\sigma$	Concordancy
STDGJ11	0.0582	0.0021	0.7820	0.0240	0.0961	0.0016	501	77	591	9.4	590	13.0	118
STDGJ06	0.0575	0.0019	0.7790	0.0260	0.0960	0.0016	541	66	591	9.6	587	14.0	109
STDGJ19	0.0630	0.0026	0.7890	0.0320	0.0959	0.0020	650	85	590	12.0	593	17.0	91
STDGJ12	0.0593	0.0028	0.7930	0.0330	0.0957	0.0019	540	100	589	11.0	593	19.0	109
STDGJ08	0.0595	0.0022	0.7770	0.0250	0.0955	0.0016	531	77	588	9.5	583	14.0	111
STDGJ40	0.0622	0.0020	0.8260	0.0260	0.0955	0.0015	669	70	588	9.1	611	14.0	88
STDGJ19	0.0587	0.0026	0.7930	0.0330	0.0953	0.0017	543	97	588	9.7	591	19.0	108
STDGJ10	0.0584	0.0020	0.7740	0.0240	0.0952	0.0016	513	68	586	9.3	582	13.0	114
STDGJ40	0.0614	0.0020	0.8300	0.0260	0.0947	0.0015	642	71	583	9.0	613	14.0	91
STDGJ14	0.0597	0.0021	0.7700	0.0220	0.0944	0.0016	544	75	581	9.6	581	12.0	107
STDGJ13	0.0618	0.0030	0.8000	0.0350	0.0944	0.0025	640	100	581	15.0	598	20.0	91
PLES01	0.0536	0.0016	0.4050	0.0120	0.0568	0.0008	322	60	356	4.6	346	8.3	110
PLES01	0.0527	0.0013	0.4100	0.0092	0.0563	0.0008	313	55	353	4.6	348	6.6	113
PLES02	0.0527	0.0016	0.3990	0.0110	0.0557	0.0008	289	62	350	4.8	341	8.0	121
PLES02	0.0538	0.0016	0.4148	0.0091	0.0557	0.0007	317	55	349	4.4	352	6.6	110
PLES02	0.0525	0.0015	0.3980	0.0100	0.0553	0.0008	284	60	347	5.1	339	7.6	122
PLES08	0.0516	0.0014	0.4071	0.0097	0.0548	0.0009	265	58	344	5.3	347	6.9	130
PLES04	0.0521	0.0016	0.4030	0.0110	0.0542	0.0010	273	65	340	5.8	344	7.7	125
PLES06	0.0519	0.0016	0.4030	0.0120	0.0541	0.0008	282	67	340	5.2	344	8.6	120
PLES03	0.0517	0.0014	0.3890	0.0110	0.0541	0.0007	255	57	340	4.4	334	7.8	133
PLES12	0.0527	0.0017	0.3980	0.0100	0.0540	0.0010	304	70	339	6.1	340	7.3	112
PLES14	0.0527	0.0016	0.3970	0.0110	0.0540	0.0007	306	65	339	4.4	342	8.0	111
PLES05	0.0520	0.0013	0.4021	0.0092	0.0538	0.0007	275	56	338	4.5	342	6.7	123
PLES03	0.0522	0.0013	0.3837	0.0096	0.0538	0.0007	280	52	338	4.5	331	7.0	121
PLES01	0.0566	0.0034	0.3980	0.0190	0.0538	0.0013	520	130	338	7.9	339	13.0	65
PLES10	0.0527	0.0012	0.3989	0.0093	0.0538	0.0008	302	51	338	5.0	342	6.5	112
PLES13	0.0528	0.0013	0.4022	0.0093	0.0538	0.0007	302	54	338	4.1	343	6.8	112
PLES09	0.0513	0.0014	0.3900	0.0100	0.0538	0.0009	242	60	338	5.2	335	7.2	140
PLES09	0.0521	0.0014	0.3910	0.0095	0.0538	0.0008	286	59	338	5.0	334	6.9	118
PLES07	0.0528	0.0016	0.3940	0.0120	0.0538	0.0010	308	64	338	6.1	339	9.2	110
PLES06	0.0529	0.0013	0.4000	0.0084	0.0538	0.0008	314	55	337	5.0	341	6.1	107
PLES13	0.0549	0.0016	0.4004	0.0099	0.0537	0.0007	381	61	337	4.5	341	7.2	89
PLES14	0.0518	0.0018	0.3980	0.0130	0.0536	0.0009	266	74	337	5.5	342	9.4	¹¹⁵ 127

Analysis #	$^{207}\text{Pb}/^{206}\text{Pb}$	$\pm 2\sigma$	$^{207}\text{Pb}/^{235}\text{U}$	$\pm 2\sigma$	$^{206}\text{Pb}/^{238}\text{U}$	$\pm 2\sigma$	$^{207}\text{Pb}/^{206}\text{Pb}$ age	$\pm 2\sigma$	$^{206}\text{Pb}/^{238}\text{U}$ age	$\pm 2\sigma$	$^{207}\text{Pb}/^{235}\text{U}$ age	$\pm 2\sigma$	Concordancy	
PLES05	0.0519	0.0013	0.3936	0.0081	0.0537	0.0008	280	52	337	4.6	336	5.9	120	
PLES07	0.0522	0.0013	0.3870	0.0090	0.0537	0.0008	281	55	337	4.8	333	6.4	120	
PLES07	0.0524	0.0015	0.3880	0.0094	0.0537	0.0008	282	59	337	4.9	333	7.0	119	
PLES05	0.0523	0.0013	0.3913	0.0081	0.0536	0.0008	292	55	337	4.7	336	6.0	115	
PLES04	0.0527	0.0014	0.3920	0.0110	0.0536	0.0009	309	60	337	5.7	336	7.9	109	
PLES03	0.0522	0.0015	0.3960	0.0110	0.0532	0.0008	284	61	334	4.7	338	7.8	118	
SAN-9		(Concordant Standards)												
STDGJ06	0.0614	0.0020	0.8340	0.0230	0.0987	0.0016	636	70	608	9.4	614	13.0	96	
STDGJ05	0.0600	0.0018	0.8220	0.0210	0.0987	0.0014	579	65	607	8.1	609	11.0	105	
STDGJ12	0.0598	0.0015	0.8180	0.0210	0.0986	0.0010	589	55	606	6.2	606	12.0	103	
STDGJ29	0.0608	0.0018	0.8110	0.0230	0.0982	0.0017	628	64	604	10.0	603	13.0	96	
STDGJ08	0.0604	0.0015	0.8100	0.0200	0.0980	0.0011	595	52	603	6.5	600	11.0	101	
STDGJ07	0.0599	0.0014	0.8050	0.0170	0.0978	0.0012	605	51	602	7.1	599	9.9	99	
STDGJ10	0.0600	0.0020	0.8020	0.0310	0.0976	0.0026	607	77	600	15.0	599	18.0	99	
STDGJ15	0.0596	0.0015	0.7970	0.0180	0.0974	0.0012	586	54	599	7.3	596	10.0	102	
STDGJ32	0.0591	0.0020	0.7920	0.0210	0.0974	0.0020	598	77	599	12.0	592	12.0	100	
STDGJ21	0.0604	0.0012	0.8090	0.0160	0.0974	0.0015	618	43	599	8.6	600	9.1	97	
STDGJ26	0.0596	0.0019	0.8050	0.0220	0.0973	0.0020	599	64	598	12.0	600	13.0	100	
STDGJ17	0.0601	0.0017	0.8060	0.0190	0.0971	0.0017	624	58	598	10.0	601	10.0	96	
STDGJ11	0.0595	0.0013	0.7980	0.0180	0.0972	0.0013	580	47	598	7.6	595	10.0	103	
STDGJ25	0.0608	0.0014	0.8050	0.0190	0.0966	0.0013	625	50	595	7.7	598	11.0	95	
STDGJ20	0.0599	0.0020	0.8040	0.0270	0.0965	0.0022	597	69	594	13.0	598	15.0	99	
STDGJ16	0.0607	0.0015	0.7990	0.0180	0.0958	0.0016	619	54	591	9.4	595	10.0	95	
STDGJ23	0.0597	0.0016	0.7870	0.0210	0.0956	0.0015	599	60	588	8.8	590	12.0	98	
STDGJ19	0.0592	0.0014	0.7850	0.0180	0.0954	0.0013	570	52	588	7.8	589	10.0	103	
STDGJ22	0.0606	0.0016	0.7830	0.0180	0.0949	0.0013	607	57	584	7.9	585	11.0	96	
STDGJ24	0.0598	0.0015	0.7840	0.0180	0.0946	0.0014	588	54	583	8.4	587	10.0	99	
PLES05	0.0536	0.0013	0.4040	0.0110	0.0542	0.0013	345	55	340	8.0	345	7.8	99	
SAN-9		(Discordant Standards)												
STDGJ28	0.0584	0.0015	0.8140	0.0220	0.1008	0.0014	542	58	619	8.3	603	12.0	$^{116}\text{14}$	

Analysis #	$^{207}\text{Pb}/^{206}\text{Pb}$	$\pm 2\sigma$	$^{207}\text{Pb}/^{235}\text{U}$	$\pm 2\sigma$	$^{206}\text{Pb}/^{238}\text{U}$	$\pm 2\sigma$	$^{207}\text{Pb}/^{206}\text{Pb}$ age	$\pm 2\sigma$	$^{206}\text{Pb}/^{238}\text{U}$ age	$\pm 2\sigma$	$^{207}\text{Pb}/^{235}\text{U}$ age	$\pm 2\sigma$	Concordancy	
STDGJ30	0.0594	0.0014	0.8180	0.0190	0.1004	0.0013	576	53	617	7.8	606	11.0	107	
STDGJ13	0.0597	0.0019	0.8130	0.0250	0.0996	0.0020	581	70	612	12.0	609	15.0	105	
STDGJ27	0.0588	0.0022	0.8100	0.0290	0.0987	0.0023	553	81	607	14.0	603	17.0	110	
STDGJ09	0.0594	0.0014	0.8100	0.0170	0.0984	0.0013	575	53	605	7.8	601	9.3	105	
STDGJ31	0.0594	0.0017	0.8050	0.0210	0.0981	0.0015	568	64	603	8.5	599	11.0	106	
STDGJ14	0.0589	0.0015	0.7920	0.0190	0.0971	0.0013	548	55	597	7.5	593	11.0	109	
STDGJ18	0.0585	0.0018	0.7790	0.0230	0.0958	0.0019	545	63	590	11.0	586	13.0	108	
PLES06	0.0697	0.0015	0.5340	0.0120	0.0556	0.0007	921	44	349	4.0	435	7.9	38	
PLES01	0.0530	0.0029	0.4010	0.0200	0.0548	0.0016	310	120	344	9.5	342	15.0	111	
PLES02	0.0550	0.0027	0.4100	0.0180	0.0547	0.0015	390	110	343	9.4	348	13.0	88	
PLES07	0.0566	0.0013	0.4173	0.0092	0.0539	0.0009	480	50	338	5.3	355	6.6	70	
PLES09	0.0748	0.0020	0.5500	0.0160	0.0537	0.0008	1052	54	338	4.6	445	10.0	32	
PLES03	0.0529	0.0012	0.3879	0.0082	0.0536	0.0008	312	50	337	4.6	332	6.0	108	
PLES11	0.0542	0.0012	0.3958	0.0088	0.0531	0.0007	365	47	334	4.2	339	6.3	91	
PLES10	0.0555	0.0018	0.4070	0.0110	0.0530	0.0010	431	72	333	5.9	346	7.9	77	
SAN-10		(Concordant Standards)												
STDGJ16	0.0606	0.0017	0.8530	0.0210	0.1001	0.0017	602	59	615	9.8	625	12.0	102	
STDGJ22	0.0620	0.0024	0.8270	0.0230	0.0998	0.0020	627	78	613	12.0	609	13.0	98	
STDGJ37	0.0615	0.0021	0.8550	0.0230	0.0996	0.0019	606	70	612	11.0	630	12.0	101	
STDGJ45	0.0621	0.0025	0.8170	0.0290	0.0997	0.0019	620	81	612	11.0	611	15.0	99	
STDGJ07	0.0614	0.0028	0.8270	0.0340	0.0994	0.0021	605	98	611	13.0	608	19.0	101	
STDGJ50	0.0608	0.0019	0.8200	0.0270	0.0991	0.0017	599	66	611	9.8	608	15.0	102	
STDGJ24	0.0610	0.0018	0.8470	0.0250	0.0982	0.0017	634	64	605	10.0	624	14.0	95	
STDGJ24	0.0609	0.0023	0.8060	0.0260	0.0982	0.0021	600	75	604	12.0	600	15.0	101	
STDGJ64	0.0611	0.0018	0.8560	0.0240	0.0983	0.0017	625	64	604	10.0	626	13.0	97	
STDGJ32	0.0604	0.0021	0.8160	0.0260	0.0979	0.0017	599	71	602	10.0	602	15.0	101	
STDGJ17	0.0610	0.0023	0.8210	0.0310	0.0979	0.0016	621	80	602	9.6	604	17.0	97	
STDGJ16	0.0609	0.0023	0.8190	0.0260	0.0977	0.0018	599	75	601	11.0	604	15.0	100	
STDGJ35	0.0609	0.0017	0.8400	0.0210	0.0978	0.0016	618	62	601	9.3	618	12.0	97	
STDGJ38	0.0605	0.0017	0.8180	0.0220	0.0977	0.0015	603	60	601	9.1	602	13.0	100	
STDGJ29	0.0617	0.0021	0.8070	0.0270	0.0976	0.0015	616	67	600	9.0	602	14.0	97	

Analysis #	$^{207}\text{Pb}/^{206}\text{Pb}$	$\pm 2\sigma$	$^{207}\text{Pb}/^{235}\text{U}$	$\pm 2\sigma$	$^{206}\text{Pb}/^{238}\text{U}$	$\pm 2\sigma$	$^{207}\text{Pb}/^{206}\text{Pb}$ age	$\pm 2\sigma$	$^{206}\text{Pb}/^{238}\text{U}$ age	$\pm 2\sigma$	$^{207}\text{Pb}/^{235}\text{U}$ age	$\pm 2\sigma$	Concordancy
STDGJ22	0.0594	0.0017	0.8070	0.0210	0.0976	0.0017	573	63	600	10.0	603	12.0	105
STDGJ30	0.0598	0.0019	0.8090	0.0230	0.0974	0.0017	583	66	600	9.8	603	13.0	103
STDGJ57	0.0610	0.0022	0.8190	0.0300	0.0977	0.0019	594	77	600	11.0	603	16.0	101
STDGJ39	0.0613	0.0025	0.8010	0.0260	0.0977	0.0019	601	83	600	11.0	597	15.0	100
STDGJ66	0.0615	0.0023	0.7980	0.0360	0.0976	0.0019	612	74	600	11.0	604	17.0	98
STDGJ34	0.0610	0.0017	0.8420	0.0220	0.0975	0.0015	629	63	600	9.0	620	12.0	95
STDGJ49	0.0616	0.0021	0.7830	0.0350	0.0974	0.0016	604	66	599	9.2	601	16.0	99
STDGJ15	0.0604	0.0022	0.8140	0.0240	0.0974	0.0019	609	75	599	11.0	603	13.0	98
STDGJ18	0.0604	0.0018	0.8380	0.0220	0.0974	0.0017	617	63	599	10.0	617	12.0	97
STDGJ06	0.0615	0.0023	0.7720	0.0380	0.0974	0.0017	626	72	599	10.0	599	16.0	96
STDGJ14	0.0608	0.0019	0.8170	0.0240	0.0973	0.0017	624	65	598	9.7	603	13.0	96
STDGJ35	0.0602	0.0023	0.8070	0.0320	0.0971	0.0018	597	82	598	11.0	596	18.0	100
STDGJ41	0.0613	0.0023	0.8060	0.0260	0.0973	0.0017	612	75	598	10.0	599	15.0	98
STDGJ43	0.0602	0.0018	0.8030	0.0240	0.0971	0.0017	571	65	597	9.9	595	14.0	105
STDGJ33	0.0608	0.0021	0.7640	0.0350	0.0972	0.0017	580	72	597	9.7	594	14.0	103
STDGJ08	0.0606	0.0023	0.8030	0.0240	0.0969	0.0016	572	78	596	9.5	600	14.0	104
STDGJ52	0.0610	0.0021	0.8020	0.0240	0.0968	0.0018	579	72	596	10.0	597	14.0	103
STDGJ26	0.0608	0.0020	0.8090	0.0220	0.0970	0.0018	585	69	596	11.0	602	12.0	102
STDGJ12	0.0620	0.0021	0.7810	0.0330	0.0969	0.0019	627	70	596	11.0	593	16.0	95
STDGJ28	0.0606	0.0022	0.7900	0.0290	0.0966	0.0018	570	77	595	10.0	593	15.0	104
STDGJ42	0.0622	0.0028	0.7710	0.0360	0.0968	0.0019	595	84	595	11.0	594	16.0	100
STDGJ67	0.0605	0.0020	0.8050	0.0230	0.0963	0.0016	582	67	594	9.1	598	13.0	102
STDGJ48	0.0599	0.0019	0.7900	0.0280	0.0965	0.0017	572	64	593	10.0	594	14.0	104
STDGJ29	0.0597	0.0017	0.8200	0.0210	0.0961	0.0017	580	65	592	9.8	608	11.0	102
STDGJ42	0.0601	0.0019	0.8010	0.0240	0.0961	0.0017	596	69	591	9.8	594	14.0	99
STDGJ49	0.0614	0.0024	0.7890	0.0300	0.0961	0.0020	590	84	591	12.0	586	17.0	100
STDGJ52	0.0599	0.0023	0.7960	0.0260	0.0959	0.0017	566	81	591	9.9	592	14.0	104
STDGJ39	0.0605	0.0020	0.8030	0.0250	0.0959	0.0015	581	70	591	8.7	595	14.0	102
STDGJ47	0.0601	0.0020	0.7880	0.0240	0.0959	0.0017	569	69	590	9.8	586	14.0	104
STDGJ63	0.0605	0.0022	0.7950	0.0250	0.0954	0.0016	595	73	587	9.3	590	14.0	99
STDGJ28	0.0582	0.0026	0.7780	0.0320	0.0945	0.0017	570	97	582	10.0	587	18.0	102
STDGJ21	0.0597	0.0025	0.8010	0.0310	0.0939	0.0019	570	89	578	11.0	598	18.0	101
PLES14	0.0540	0.0013	0.4131	0.0082	0.0545	0.0008	359	52	342	4.9	351	5.9	$^{118}\text{95}$

Analysis #	$^{207}\text{Pb}/^{206}\text{Pb}$	$\pm 2\sigma$	$^{207}\text{Pb}/^{235}\text{U}$	$\pm 2\sigma$	$^{206}\text{Pb}/^{238}\text{U}$	$\pm 2\sigma$	$^{207}\text{Pb}/^{206}\text{Pb}$ age	$\pm 2\sigma$	$^{206}\text{Pb}/^{238}\text{U}$ age	$\pm 2\sigma$	$^{207}\text{Pb}/^{235}\text{U}$ age	$\pm 2\sigma$	Concordancy	
PLES06	0.0535	0.0014	0.3947	0.0098	0.0538	0.0007	327	55	338	4.5	338	7.2	103	
PLES11	0.0537	0.0022	0.3990	0.0150	0.0537	0.0011	324	86	337	6.7	340	11.0	104	
PLES04	0.0536	0.0016	0.3930	0.0110	0.0534	0.0008	330	62	336	4.7	338	8.1	102	
PLES03	0.0543	0.0019	0.3760	0.0160	0.0530	0.0008	333	67	333	4.8	334	9.2	100	
PLES18	0.0541	0.0021	0.3940	0.0140	0.0528	0.0010	327	80	332	5.8	335	10.0	101	
PLES17	0.0545	0.0020	0.3870	0.0120	0.0527	0.0009	347	74	331	5.3	332	8.9	95	
SAN-10	(Discordant Standards)													
STDGJ58	0.0583	0.0019	0.8420	0.0280	0.1033	0.0020	527	73	634	12.0	621	16.0	120	
STDGJ04	0.0609	0.0027	0.8470	0.0310	0.1029	0.0023	592	94	634	13.0	625	17.0	107	
STDGJ65	0.0603	0.0022	0.8110	0.0370	0.1032	0.0018	562	72	633	11.0	620	15.0	113	
STDGJ23	0.0594	0.0020	0.8250	0.0230	0.1014	0.0015	543	68	622	8.8	609	13.0	115	
STDGJ51	0.0586	0.0021	0.8340	0.0270	0.0993	0.0020	558	79	610	11.0	612	15.0	109	
STDGJ38	0.0619	0.0022	0.8300	0.0280	0.0993	0.0015	656	72	610	9.1	611	16.0	93	
STDGJ48	0.0589	0.0016	0.8250	0.0220	0.0992	0.0016	543	61	610	9.5	611	12.0	112	
STDGJ17	0.0579	0.0022	0.8300	0.0280	0.0991	0.0019	502	84	609	11.0	611	16.0	121	
STDGJ44	0.0589	0.0017	0.8280	0.0220	0.0990	0.0016	565	63	609	9.5	611	12.0	108	
STDGJ11	0.0606	0.0022	0.8200	0.0230	0.0989	0.0018	567	73	608	11.0	607	13.0	107	
STDGJ37	0.0617	0.0022	0.8300	0.0260	0.0989	0.0019	643	73	608	11.0	612	15.0	95	
STDGJ09	0.0589	0.0017	0.8120	0.0230	0.0989	0.0014	551	64	608	8.2	604	13.0	110	
STDGJ36	0.0590	0.0022	0.8310	0.0320	0.0987	0.0018	577	83	607	11.0	612	18.0	105	
STDGJ23	0.0590	0.0020	0.8280	0.0270	0.0987	0.0017	538	74	607	9.8	611	15.0	113	
STDGJ46	0.0565	0.0016	0.7860	0.0210	0.0986	0.0016	451	62	606	9.5	589	12.0	134	
STDGJ09	0.0605	0.0021	0.8250	0.0230	0.0984	0.0016	574	70	605	9.6	609	13.0	105	
STDGJ31	0.0593	0.0020	0.8110	0.0250	0.0981	0.0019	565	72	604	11.0	602	14.0	107	
STDGJ25	0.0575	0.0020	0.8080	0.0270	0.0982	0.0016	478	74	604	9.4	605	16.0	126	
STDGJ31	0.0576	0.0021	0.8160	0.0280	0.0981	0.0017	478	80	603	10.0	606	15.0	126	
STDGJ40	0.0600	0.0024	0.8220	0.0290	0.0981	0.0018	545	85	603	11.0	607	16.0	111	
STDGJ30	0.0582	0.0020	0.8200	0.0290	0.0980	0.0020	553	75	603	12.0	606	16.0	109	
STDGJ60	0.0586	0.0022	0.8240	0.0270	0.0981	0.0017	526	81	603	9.9	607	15.0	115	
STDGJ53	0.0603	0.0031	0.8070	0.0350	0.0979	0.0030	570	110	602	17.0	600	19.0	106	
STDGJ06	0.0588	0.0022	0.8180	0.0290	0.0979	0.0016	508	80	602	9.5	605	16.0	118	

Analysis #	$^{207}\text{Pb}/^{206}\text{Pb}$	$\pm 2\sigma$	$^{207}\text{Pb}/^{235}\text{U}$	$\pm 2\sigma$	$^{206}\text{Pb}/^{238}\text{U}$	$\pm 2\sigma$	$^{207}\text{Pb}/^{206}\text{Pb}$ age	$\pm 2\sigma$	$^{206}\text{Pb}/^{238}\text{U}$ age	$\pm 2\sigma$	$^{207}\text{Pb}/^{235}\text{U}$ age	$\pm 2\sigma$	Concordancy
STDGJ05	0.0578	0.0021	0.8060	0.0250	0.0977	0.0017	492	77	601	10.0	601	14.0	122
STDGJ10	0.0588	0.0021	0.8140	0.0270	0.0975	0.0019	538	78	601	11.0	604	16.0	112
STDGJ59	0.0600	0.0020	0.8140	0.0240	0.0978	0.0018	570	73	601	11.0	605	14.0	105
STDGJ10	0.0585	0.0019	0.8190	0.0250	0.0977	0.0016	526	70	601	9.3	606	14.0	114
STDGJ20	0.0580	0.0019	0.8000	0.0250	0.0976	0.0017	509	72	600	9.7	600	14.0	118
STDGJ26	0.0589	0.0028	0.8180	0.0350	0.0976	0.0027	530	100	600	16.0	604	20.0	113
STDGJ41	0.0588	0.0018	0.8040	0.0280	0.0976	0.0019	546	67	600	11.0	597	16.0	110
STDGJ25	0.0584	0.0019	0.8110	0.0250	0.0976	0.0018	552	71	600	11.0	604	14.0	109
STDGJ13	0.0586	0.0032	0.8130	0.0370	0.0975	0.0030	560	120	600	18.0	602	21.0	107
STDGJ05	0.0642	0.0032	0.8170	0.0440	0.0976	0.0021	700	110	600	12.0	601	25.0	86
STDGJ26	0.0598	0.0022	0.8110	0.0270	0.0974	0.0015	571	79	600	8.8	603	15.0	105
STDGJ20	0.0575	0.0017	0.7980	0.0200	0.0975	0.0016	510	63	600	9.4	596	11.0	118
STDGJ36	0.0586	0.0016	0.8120	0.0220	0.0975	0.0014	542	61	599	8.5	603	12.0	111
STDGJ21	0.0585	0.0020	0.7960	0.0220	0.0974	0.0015	531	74	599	9.0	596	13.0	113
STDGJ32	0.0589	0.0020	0.7990	0.0270	0.0974	0.0016	544	71	599	9.3	595	15.0	110
STDGJ51	0.0579	0.0022	0.8050	0.0270	0.0972	0.0018	488	81	599	10.0	597	15.0	123
STDGJ33	0.0591	0.0019	0.8110	0.0230	0.0974	0.0017	569	67	599	9.8	601	13.0	105
STDGJ44	0.0613	0.0017	0.8180	0.0220	0.0972	0.0016	632	58	599	9.5	606	13.0	95
STDGJ45	0.0566	0.0017	0.7930	0.0220	0.0973	0.0016	485	64	598	9.3	594	12.0	123
STDGJ34	0.0584	0.0019	0.7990	0.0230	0.0971	0.0014	514	69	598	8.2	595	13.0	116
STDGJ27	0.0590	0.0021	0.7930	0.0240	0.0971	0.0017	553	76	597	10.0	595	13.0	108
STDGJ50	0.0577	0.0018	0.7750	0.0220	0.0970	0.0016	477	67	597	9.4	580	13.0	125
STDGJ46	0.0573	0.0015	0.7940	0.0220	0.0969	0.0014	492	59	596	8.4	592	12.0	121
STDGJ15	0.0595	0.0024	0.7820	0.0260	0.0968	0.0018	550	85	596	11.0	591	15.0	108
STDGJ18	0.0615	0.0022	0.8110	0.0250	0.0970	0.0017	654	76	596	10.0	602	15.0	91
STDGJ62	0.0573	0.0017	0.7840	0.0200	0.0968	0.0016	503	63	595	9.7	591	11.0	118
STDGJ08	0.0585	0.0019	0.7930	0.0250	0.0968	0.0017	531	69	595	9.7	591	14.0	112
STDGJ07	0.0586	0.0018	0.8010	0.0230	0.0964	0.0016	534	67	594	9.3	594	13.0	111
STDGJ27	0.0605	0.0021	0.8340	0.0270	0.0963	0.0017	635	71	593	10.0	614	15.0	93
STDGJ43	0.0618	0.0021	0.7960	0.0280	0.0963	0.0017	638	67	593	10.0	597	14.0	93
STDGJ47	0.0587	0.0021	0.7830	0.0240	0.0962	0.0018	555	78	592	11.0	589	14.0	107
STDGJ19	0.0599	0.0021	0.7900	0.0290	0.0961	0.0016	561	74	592	9.4	589	16.0	105
STDGJ11	0.0588	0.0020	0.7630	0.0240	0.0961	0.0015	506	70	591	8.9	576	14.0	¹²⁹ 117

Analysis #	$^{207}\text{Pb}/^{206}\text{Pb}$	$\pm 2\sigma$	$^{207}\text{Pb}/^{235}\text{U}$	$\pm 2\sigma$	$^{206}\text{Pb}/^{238}\text{U}$	$\pm 2\sigma$	$^{207}\text{Pb}/^{206}\text{Pb}$ age	$\pm 2\sigma$	$^{206}\text{Pb}/^{238}\text{U}$ age	$\pm 2\sigma$	$^{207}\text{Pb}/^{235}\text{U}$ age	$\pm 2\sigma$	Concordancy	
STDG14	0.0564	0.0020	0.7850	0.0260	0.0959	0.0017	456	76	590	9.8	586	15.0	129	
STDG19	0.0607	0.0025	0.7800	0.0320	0.0956	0.0015	546	79	588	8.6	584	18.0	108	
STDG12	0.0629	0.0030	0.7910	0.0340	0.0956	0.0020	647	96	588	12.0	589	19.0	91	
STDG13	0.0587	0.0020	0.7810	0.0260	0.0949	0.0018	530	74	584	10.0	583	15.0	110	
STDG61	0.0583	0.0020	0.7980	0.0280	0.0943	0.0016	542	73	581	9.6	594	16.0	107	
STDG40	0.0623	0.0020	0.7970	0.0220	0.0932	0.0015	644	65	574	9.0	593	13.0	89	
PLES01	0.0509	0.0013	0.4224	0.0087	0.0574	0.0007	245	53	360	4.5	357	6.2	147	
PLES02	0.0566	0.0013	0.4644	0.0099	0.0573	0.0008	479	50	359	4.6	388	6.9	75	
PLES02	0.0512	0.0014	0.4160	0.0110	0.0565	0.0008	249	57	355	4.6	352	7.6	142	
PLES01	0.0563	0.0037	0.3800	0.0340	0.0565	0.0017	410	130	354	10.0	329	24.0	86	
PLES07	0.0521	0.0013	0.4036	0.0087	0.0543	0.0008	280	55	341	4.8	344	6.4	122	
PLES10	0.0547	0.0018	0.4030	0.0110	0.0540	0.0008	366	69	340	4.7	343	8.1	93	
PLES06	0.0523	0.0019	0.3970	0.0130	0.0538	0.0009	285	74	338	5.3	339	9.3	119	
PLES08	0.0530	0.0016	0.3993	0.0094	0.0538	0.0010	309	62	338	5.9	340	6.9	109	
PLES10	0.0530	0.0012	0.3993	0.0089	0.0538	0.0006	309	51	338	3.9	340	6.5	109	
PLES03	0.0531	0.0015	0.4019	0.0091	0.0538	0.0007	316	59	338	4.4	342	6.6	107	
PLES05	0.0527	0.0015	0.4007	0.0086	0.0538	0.0008	299	57	338	4.6	342	6.2	113	
PLES12	0.0525	0.0016	0.3950	0.0110	0.0538	0.0008	286	65	338	4.8	339	7.8	118	
PLES08	0.0535	0.0021	0.3880	0.0130	0.0536	0.0011	318	79	337	6.5	334	9.7	106	
PLES04	0.0512	0.0014	0.4020	0.0120	0.0537	0.0008	244	60	337	4.9	344	8.4	138	
PLES13	0.0554	0.0021	0.3950	0.0110	0.0537	0.0009	375	73	337	5.2	337	7.7	90	
PLES07	0.0564	0.0032	0.3870	0.0180	0.0537	0.0013	390	110	337	7.9	336	14.0	86	
PLES13	0.0501	0.0018	0.3890	0.0140	0.0535	0.0010	217	76	336	6.4	333	9.9	155	
PLES09	0.0548	0.0014	0.4061	0.0096	0.0535	0.0007	394	55	336	4.5	346	7.0	85	
PLES12	0.0560	0.0024	0.3860	0.0190	0.0535	0.0009	374	77	336	5.7	339	12.0	90	
PLES11	0.0507	0.0020	0.3880	0.0130	0.0534	0.0011	231	84	335	6.8	332	9.5	145	
PLES09	0.0596	0.0042	0.3980	0.0170	0.0529	0.0013	470	110	332	8.1	339	13.0	71	
PLES05	0.0555	0.0017	0.3975	0.0097	0.0527	0.0009	387	60	331	5.3	339	7.1	86	
SAN-12	(Concordant Standards)													
STDG05	0.0605	0.0016	0.8730	0.0230	0.1031	0.0016	604	58	632	9.5	635	13.0	105	
STDG53	0.0605	0.0018	0.8410	0.0240	0.1014	0.0017	598	64	622	9.8	618	13.0	104	

Analysis #	$^{207}\text{Pb}/^{206}\text{Pb}$	$\pm 2\sigma$	$^{207}\text{Pb}/^{235}\text{U}$	$\pm 2\sigma$	$^{206}\text{Pb}/^{238}\text{U}$	$\pm 2\sigma$	$^{207}\text{Pb}/^{206}\text{Pb}$ age	$\pm 2\sigma$	$^{206}\text{Pb}/^{238}\text{U}$ age	$\pm 2\sigma$	$^{207}\text{Pb}/^{235}\text{U}$ age	$\pm 2\sigma$	Concordancy
STDGJ76	0.0609	0.0018	0.8490	0.0230	0.1011	0.0017	625	64	622	9.8	624	13.0	99
STDGJ52	0.0610	0.0021	0.8380	0.0260	0.1007	0.0016	630	71	618	9.4	619	14.0	98
STDGJ06	0.0608	0.0020	0.8500	0.0260	0.0997	0.0018	632	73	612	11.0	625	14.0	97
STDGJ82	0.0603	0.0023	0.8300	0.0290	0.0995	0.0019	618	82	611	11.0	616	16.0	99
STDGJ67	0.0607	0.0021	0.8220	0.0240	0.0990	0.0019	601	72	608	11.0	612	14.0	101
STDGJ93	0.0611	0.0022	0.8310	0.0250	0.0988	0.0019	616	77	607	11.0	612	14.0	99
STDGJ94	0.0597	0.0026	0.8140	0.0270	0.0987	0.0025	586	94	607	15.0	602	15.0	104
STDGJ38	0.0592	0.0019	0.8020	0.0260	0.0988	0.0017	584	69	607	10.0	596	15.0	104
STDGJ21	0.0612	0.0018	0.8150	0.0240	0.0984	0.0016	628	61	605	9.1	604	13.0	96
STDGJ39	0.0607	0.0023	0.8330	0.0310	0.0984	0.0021	622	79	605	12.0	610	17.0	97
STDGJ95	0.0599	0.0023	0.8160	0.0270	0.0984	0.0019	609	81	605	11.0	603	16.0	99
STDGJ92	0.0617	0.0026	0.8150	0.0290	0.0981	0.0020	625	85	604	12.0	605	16.0	97
STDGJ68	0.0602	0.0029	0.8150	0.0420	0.0983	0.0033	580	110	604	20.0	605	24.0	104
STDGJ09	0.0611	0.0018	0.8260	0.0220	0.0982	0.0016	604	64	604	9.5	608	12.0	100
STDGJ83	0.0606	0.0024	0.8260	0.0310	0.0981	0.0020	613	82	603	12.0	611	17.0	98
STDGJ36	0.0600	0.0021	0.8080	0.0290	0.0982	0.0020	593	77	603	12.0	601	16.0	102
STDGJ65	0.0601	0.0019	0.8090	0.0260	0.0980	0.0015	574	68	602	8.6	599	15.0	105
STDGJ70	0.0614	0.0019	0.8350	0.0250	0.0979	0.0017	624	67	602	10.0	614	14.0	96
STDGJ19	0.0605	0.0021	0.8070	0.0270	0.0980	0.0020	598	77	602	12.0	602	15.0	101
STDGJ40	0.0602	0.0019	0.8100	0.0260	0.0977	0.0018	616	68	601	11.0	601	14.0	98
STDGJ50	0.0608	0.0019	0.8060	0.0230	0.0977	0.0016	609	65	601	9.3	599	13.0	99
STDGJ32	0.0604	0.0020	0.8100	0.0240	0.0976	0.0015	593	71	600	9.0	601	14.0	101
STDGJ97	0.0608	0.0022	0.8120	0.0270	0.0975	0.0022	623	77	600	13.0	604	15.0	96
STDGJ84	0.0609	0.0022	0.8200	0.0290	0.0976	0.0018	622	80	600	11.0	606	16.0	96
STDGJ17	0.0610	0.0018	0.8160	0.0240	0.0976	0.0016	630	62	600	9.4	607	13.0	95
STDGJ25	0.0602	0.0019	0.8030	0.0240	0.0975	0.0017	577	68	599	9.9	598	13.0	104
STDGJ86	0.0600	0.0027	0.8040	0.0300	0.0975	0.0023	599	94	599	14.0	606	17.0	100
STDGJ26	0.0615	0.0023	0.8200	0.0290	0.0972	0.0020	610	80	598	12.0	607	16.0	98
STDGJ87	0.0606	0.0032	0.7980	0.0350	0.0968	0.0028	590	110	598	17.0	598	21.0	101
STDGJ57	0.0602	0.0018	0.8080	0.0220	0.0970	0.0017	606	63	597	9.9	601	12.0	99
STDGJ73	0.0604	0.0022	0.8110	0.0290	0.0972	0.0021	596	78	597	12.0	601	16.0	100
STDGJ54	0.0601	0.0024	0.8090	0.0290	0.0971	0.0022	586	82	597	13.0	600	17.0	102
STDGJ58	0.0613	0.0018	0.8060	0.0220	0.0969	0.0016	624	63	596	9.3	600	12.0	^{122}S 6

Analysis #	$^{207}\text{Pb}/^{206}\text{Pb}$	$\pm 2\sigma$	$^{207}\text{Pb}/^{235}\text{U}$	$\pm 2\sigma$	$^{206}\text{Pb}/^{238}\text{U}$	$\pm 2\sigma$	$^{207}\text{Pb}/^{206}\text{Pb}$ age	$\pm 2\sigma$	$^{206}\text{Pb}/^{238}\text{U}$ age	$\pm 2\sigma$	$^{207}\text{Pb}/^{235}\text{U}$ age	$\pm 2\sigma$	Concordancy
STDGJ29	0.0612	0.0021	0.8220	0.0250	0.0970	0.0017	627	76	596	10.0	609	14.0	95
STDGJ71	0.0604	0.0020	0.8100	0.0260	0.0970	0.0018	595	74	596	11.0	602	15.0	100
STDGJ14	0.0606	0.0019	0.8120	0.0240	0.0968	0.0018	607	66	595	10.0	602	13.0	98
STDGJ49	0.0598	0.0017	0.8060	0.0210	0.0966	0.0014	569	60	594	8.5	599	11.0	104
STDGJ88	0.0602	0.0029	0.7910	0.0320	0.0964	0.0021	570	100	594	12.0	594	19.0	104
STDGJ23	0.0597	0.0022	0.7930	0.0290	0.0962	0.0019	579	80	592	11.0	597	16.0	102
STDGJ43	0.0600	0.0020	0.8010	0.0280	0.0959	0.0017	580	72	591	9.9	599	15.0	102
STDGJ59	0.0607	0.0025	0.8070	0.0300	0.0960	0.0019	591	89	591	11.0	597	17.0	100
STDGJ47	0.0611	0.0020	0.8020	0.0260	0.0959	0.0019	616	68	590	11.0	595	14.0	96
STDGJ34	0.0607	0.0018	0.8050	0.0210	0.0959	0.0019	607	66	590	11.0	598	12.0	97
STDGJ85	0.0602	0.0024	0.8000	0.0280	0.0959	0.0019	588	86	590	11.0	592	16.0	100
STDGJ35	0.0608	0.0020	0.7940	0.0240	0.0954	0.0016	615	73	588	9.6	596	14.0	96
STDGJ33	0.0606	0.0021	0.7980	0.0250	0.0956	0.0017	597	72	588	10.0	592	14.0	98
STDGJ51	0.0594	0.0020	0.7910	0.0260	0.0955	0.0017	561	73	588	9.8	589	14.0	105
STDGJ63	0.0602	0.0018	0.7920	0.0200	0.0953	0.0018	574	65	587	11.0	591	11.0	102
STDGJ79	0.0607	0.0024	0.7930	0.0290	0.0952	0.0017	609	85	587	9.9	588	16.0	96
STDGJ48	0.0606	0.0019	0.7950	0.0230	0.0952	0.0017	606	67	586	10.0	591	13.0	97
STDGJ74	0.0597	0.0018	0.7890	0.0230	0.0950	0.0017	598	64	585	9.9	590	13.0	98
STDGJ56	0.0592	0.0025	0.7810	0.0330	0.0942	0.0021	562	93	580	12.0	584	19.0	103
STDGJ89	0.0595	0.0024	0.7650	0.0270	0.0937	0.0018	554	83	577	11.0	576	16.0	104
PLES06	0.0534	0.0015	0.3960	0.0110	0.0542	0.0008	325	61	340	5.1	338	7.8	105
PLES14	0.0533	0.0015	0.3960	0.0100	0.0538	0.0008	327	59	338	4.6	339	7.4	103
PLES13	0.0536	0.0015	0.3990	0.0110	0.0538	0.0007	339	60	338	4.2	340	7.7	100
PLES21	0.0535	0.0015	0.3970	0.0110	0.0538	0.0008	336	60	338	4.8	339	8.0	100
PLES22	0.0534	0.0014	0.3970	0.0099	0.0537	0.0008	324	57	337	5.2	340	7.0	104
PLES07	0.0533	0.0017	0.3940	0.0110	0.0535	0.0009	333	66	336	5.2	336	8.1	101
PLES17	0.0535	0.0016	0.3920	0.0120	0.0530	0.0008	335	65	333	4.6	336	8.6	99
PLES40	0.0529	0.0017	0.3910	0.0110	0.0526	0.0010	332	68	330	5.9	335	8.1	99
PLES36	0.0535	0.0015	0.3840	0.0100	0.0525	0.0009	329	59	330	5.6	329	7.3	100
PLES03	0.0533	0.0013	0.3818	0.0091	0.0524	0.0007	324	54	329	4.5	328	6.7	102
PLES23	0.0540	0.0014	0.3950	0.0100	0.0523	0.0006	344	58	329	3.9	338	7.6	96
PLES29	0.0531	0.0021	0.3860	0.0160	0.0519	0.0010	327	82	327	6.3	332	11.0	100
PLES31	0.0536	0.0021	0.3810	0.0150	0.0518	0.0010	329	80	326	6.3	326	11.0	¹²³ 99

Analysis #	$^{207}\text{Pb}/^{206}\text{Pb}$	$\pm 2\sigma$	$^{207}\text{Pb}/^{235}\text{U}$	$\pm 2\sigma$	$^{206}\text{Pb}/^{238}\text{U}$	$\pm 2\sigma$	$^{207}\text{Pb}/^{206}\text{Pb}$ age	$\pm 2\sigma$	$^{206}\text{Pb}/^{238}\text{U}$ age	$\pm 2\sigma$	$^{207}\text{Pb}/^{235}\text{U}$ age	$\pm 2\sigma$	Concordancy	
PLES09	0.0535	0.0014	0.3758	0.0099	0.0514	0.0008	329	55	323	4.9	325	7.0	98	
PLES34	0.0531	0.0021	0.3720	0.0130	0.0508	0.0010	305	80	320	6.1	320	9.7	105	
SAN-12 (<i>Discordant Standards</i>)														
STDGJ69	0.0599	0.0023	0.8550	0.0280	0.1042	0.0018	597	77	638	11.0	626	15.0	107	
STDGJ37	0.0590	0.0021	0.8340	0.0260	0.1026	0.0018	561	76	630	10.0	616	14.0	112	
STDGJ77	0.0596	0.0021	0.8530	0.0270	0.1016	0.0016	567	74	626	9.6	628	14.0	110	
STDGJ81	0.0597	0.0022	0.8550	0.0320	0.1015	0.0019	588	75	623	11.0	623	18.0	106	
STDGJ66	0.0576	0.0019	0.7960	0.0220	0.1008	0.0019	496	73	619	11.0	593	12.0	125	
STDGJ12	0.0588	0.0018	0.8190	0.0250	0.1002	0.0015	533	67	617	9.1	609	14.0	116	
STDGJ60	0.0599	0.0018	0.8240	0.0230	0.0996	0.0020	582	63	612	12.0	611	13.0	105	
STDGJ96	0.0598	0.0021	0.8350	0.0280	0.0997	0.0022	571	76	612	13.0	612	16.0	107	
STDGJ11	0.0599	0.0018	0.8090	0.0230	0.0994	0.0015	571	65	611	9.1	600	13.0	107	
STDGJ61	0.0585	0.0018	0.8080	0.0260	0.0992	0.0018	543	67	610	10.0	597	15.0	112	
STDGJ22	0.0591	0.0019	0.8120	0.0260	0.0993	0.0017	539	71	610	10.0	606	15.0	113	
STDGJ13	0.0608	0.0022	0.8420	0.0290	0.0988	0.0019	658	75	608	11.0	618	16.0	92	
STDGJ07	0.0592	0.0017	0.8120	0.0210	0.0988	0.0016	571	66	607	9.1	603	12.0	106	
STDGJ78	0.0591	0.0024	0.8100	0.0290	0.0989	0.0023	530	88	607	14.0	602	16.0	115	
STDGJ20	0.0595	0.0022	0.8080	0.0270	0.0987	0.0017	559	78	606	9.7	600	15.0	108	
STDGJ31	0.0596	0.0025	0.7970	0.0300	0.0980	0.0020	553	87	602	12.0	596	17.0	109	
STDGJ62	0.0602	0.0022	0.8200	0.0270	0.0979	0.0017	572	79	602	9.8	605	15.0	105	
STDGJ41	0.0602	0.0020	0.8130	0.0240	0.0977	0.0019	568	70	601	11.0	602	14.0	106	
STDGJ18	0.0631	0.0032	0.8470	0.0340	0.0976	0.0024	660	110	600	14.0	619	19.0	91	
STDGJ91	0.0598	0.0027	0.7990	0.0320	0.0975	0.0023	570	100	600	13.0	597	17.0	105	
STDGJ28	0.0598	0.0018	0.8160	0.0240	0.0972	0.0015	568	67	599	8.7	603	13.0	106	
STDGJ42	0.0611	0.0020	0.8200	0.0240	0.0975	0.0018	638	68	599	11.0	611	13.0	94	
STDGJ45	0.0579	0.0023	0.8000	0.0290	0.0975	0.0021	521	86	599	12.0	596	16.0	115	
STDGJ44	0.0586	0.0026	0.8010	0.0350	0.0973	0.0022	540	100	598	13.0	594	20.0	111	
STDGJ27	0.0616	0.0017	0.8180	0.0220	0.0970	0.0016	630	59	597	9.4	608	11.0	95	
STDGJ90	0.0621	0.0023	0.8150	0.0270	0.0971	0.0019	633	82	597	11.0	602	15.0	94	
STDGJ75	0.0595	0.0021	0.8010	0.0260	0.0970	0.0017	566	76	596	10.0	595	15.0	105	
STDGJ10	0.0590	0.0019	0.7930	0.0220	0.0966	0.0017	537	68	595	9.7	591	13.0	111	

Analysis #	$^{207}\text{Pb}/^{206}\text{Pb}$	$\pm 2\sigma$	$^{207}\text{Pb}/^{235}\text{U}$	$\pm 2\sigma$	$^{206}\text{Pb}/^{238}\text{U}$	$\pm 2\sigma$	$^{207}\text{Pb}/^{206}\text{Pb}$ age	$\pm 2\sigma$	$^{206}\text{Pb}/^{238}\text{U}$ age	$\pm 2\sigma$	$^{207}\text{Pb}/^{235}\text{U}$ age	$\pm 2\sigma$	Concordancy
STDGJ08	0.0621	0.0031	0.8200	0.0360	0.0968	0.0024	670	100	595	14.0	605	20.0	89
STDGJ30	0.0624	0.0031	0.8250	0.0370	0.0965	0.0025	650	110	594	14.0	612	20.0	91
STDGJ72	0.0594	0.0022	0.8040	0.0290	0.0966	0.0019	554	77	594	11.0	595	16.0	107
STDGJ55	0.0584	0.0019	0.7890	0.0230	0.0966	0.0016	545	69	594	9.3	588	13.0	109
STDGJ15	0.0612	0.0019	0.8060	0.0230	0.0959	0.0015	632	70	590	9.0	597	13.0	93
STDGJ16	0.0608	0.0020	0.8080	0.0240	0.0957	0.0018	627	69	589	11.0	600	14.0	94
STDGJ46	0.0613	0.0019	0.7990	0.0220	0.0949	0.0016	646	66	585	9.1	595	12.0	90
STDGJ64	0.0614	0.0021	0.8140	0.0280	0.0947	0.0017	618	72	584	9.8	601	15.0	94
STDGJ24	0.0596	0.0021	0.7760	0.0250	0.0941	0.0018	551	77	580	11.0	581	14.0	105
STDGJ80	0.0588	0.0018	0.7590	0.0220	0.0927	0.0015	531	67	572	9.2	576	13.0	108
PLES37	0.0548	0.0019	0.4050	0.0110	0.0544	0.0009	388	72	341	5.5	345	8.2	88
PLES41	0.0526	0.0016	0.3910	0.0120	0.0538	0.0008	302	66	338	5.0	334	8.4	112
PLES38	0.0547	0.0016	0.4010	0.0120	0.0538	0.0009	400	64	338	5.3	343	8.6	84
PLES04	0.0541	0.0016	0.4000	0.0120	0.0537	0.0008	363	64	337	4.6	340	8.3	93
PLES02	0.0526	0.0019	0.3850	0.0120	0.0532	0.0011	294	76	334	6.6	331	9.2	114
PLES10	0.0552	0.0018	0.4070	0.0120	0.0529	0.0008	404	69	332	4.8	346	8.5	82
PLES19	0.0569	0.0016	0.4120	0.0120	0.0528	0.0007	471	60	332	4.5	351	8.5	70
PLES01	0.0541	0.0015	0.3900	0.0110	0.0528	0.0009	356	61	332	5.4	334	7.7	93
PLES26	0.0529	0.0018	0.3860	0.0130	0.0528	0.0009	300	71	332	5.5	332	9.3	111
PLES18	0.0527	0.0015	0.3830	0.0100	0.0528	0.0008	300	61	331	4.8	328	7.5	110
PLES15	0.0535	0.0014	0.3904	0.0097	0.0525	0.0009	349	58	330	5.4	334	7.0	95
PLES39	0.0525	0.0016	0.3800	0.0110	0.0524	0.0008	303	65	330	5.1	326	7.9	109
PLES11	0.0523	0.0018	0.3820	0.0120	0.0525	0.0008	291	71	330	5.1	327	8.7	113
PLES27	0.0542	0.0020	0.3900	0.0130	0.0522	0.0008	354	77	328	4.8	333	9.3	93
PLES05	0.0522	0.0013	0.3776	0.0090	0.0521	0.0007	300	56	328	4.5	326	6.8	109
PLES25	0.0517	0.0017	0.3750	0.0110	0.0521	0.0008	287	70	327	5.1	324	8.2	114
PLES30	0.0542	0.0019	0.3860	0.0110	0.0520	0.0009	352	71	327	5.3	332	8.1	93
PLES35	0.0541	0.0021	0.3800	0.0140	0.0517	0.0009	354	81	325	5.7	326	10.0	92
PLES33	0.0547	0.0018	0.3870	0.0120	0.0516	0.0009	366	69	324	5.6	331	9.1	89

Analysis #	$^{207}\text{Pb}/^{206}\text{Pb}$	$\pm 2\sigma$	$^{207}\text{Pb}/^{235}\text{U}$	$\pm 2\sigma$	$^{206}\text{Pb}/^{238}\text{U}$	$\pm 2\sigma$	$^{207}\text{Pb}/^{206}\text{Pb}$ age	$\pm 2\sigma$	$^{206}\text{Pb}/^{238}\text{U}$ age	$\pm 2\sigma$	$^{207}\text{Pb}/^{235}\text{U}$ age	$\pm 2\sigma$	Concordancy
STDGJ61	0.0612	0.0025	0.8370	0.0340	0.0991	0.0026	613	90	608	15.0	614	18.0	99
STDGJ62	0.0609	0.0027	0.8140	0.0320	0.0989	0.0021	600	91	607	12.0	607	18.0	101
STDGJ30	0.0598	0.0024	0.8180	0.0320	0.0985	0.0019	583	89	605	11.0	603	18.0	104
STDGJ21	0.0595	0.0027	0.8120	0.0310	0.0983	0.0023	580	99	604	14.0	604	17.0	104
STDGJ63	0.0605	0.0025	0.8040	0.0290	0.0979	0.0020	587	88	604	12.0	604	16.0	103
STDGJ42	0.0612	0.0022	0.8200	0.0300	0.0981	0.0018	623	80	603	10.0	607	17.0	97
STDGJ53	0.0613	0.0024	0.8180	0.0290	0.0982	0.0024	632	80	603	14.0	606	16.0	95
STDGJ40	0.0602	0.0026	0.8210	0.0320	0.0978	0.0022	582	88	601	13.0	607	18.0	103
STDGJ41	0.0611	0.0026	0.8090	0.0340	0.0974	0.0022	601	92	599	13.0	600	19.0	100
STDGJ22	0.0599	0.0024	0.8030	0.0280	0.0974	0.0020	610	83	599	11.0	599	16.0	98
STDGJ37	0.0601	0.0024	0.8020	0.0300	0.0972	0.0020	585	87	598	12.0	601	17.0	102
STDGJ46	0.0606	0.0026	0.8130	0.0330	0.0973	0.0024	593	93	598	14.0	602	18.0	101
STDGJ20	0.0610	0.0022	0.8140	0.0250	0.0972	0.0019	614	77	598	11.0	601	14.0	97
STDGJ28	0.0601	0.0019	0.8030	0.0230	0.0970	0.0021	582	66	596	12.0	599	13.0	102
STDGJ33	0.0604	0.0033	0.8010	0.0380	0.0968	0.0028	610	110	595	17.0	599	21.0	98
STDGJ57	0.0607	0.0025	0.8050	0.0320	0.0965	0.0022	614	85	594	13.0	597	18.0	97
STDGJ39	0.0602	0.0022	0.8010	0.0280	0.0964	0.0020	580	78	593	12.0	598	16.0	102
STDGJ32	0.0601	0.0023	0.7820	0.0300	0.0950	0.0018	592	80	585	11.0	585	17.0	99
STDGJ47	0.0594	0.0029	0.7870	0.0400	0.0948	0.0023	570	100	584	13.0	589	23.0	102
PLES23	0.0536	0.0017	0.3870	0.0120	0.0534	0.0010	348	69	336	5.8	334	8.6	97
PLES22	0.0532	0.0026	0.3910	0.0180	0.0522	0.0011	330	100	328	6.9	333	13.0	99
PLES21	0.0532	0.0021	0.3800	0.0130	0.0519	0.0011	317	78	326	6.6	327	9.5	103
PLES25	0.0531	0.0021	0.3730	0.0130	0.0511	0.0010	318	83	321	6.0	323	9.8	101

SAN-13	(Discordant Standards)												
STDGJ44	0.0581	0.0022	0.8270	0.0300	0.1021	0.0018	526	82	626	11.0	614	16.0	119
STDGJ60	0.0587	0.0024	0.8320	0.0310	0.1014	0.0026	534	82	624	16.0	611	17.0	117
STDGJ25	0.0588	0.0020	0.8210	0.0260	0.0996	0.0019	564	73	612	11.0	608	15.0	109
STDGJ38	0.0601	0.0028	0.8260	0.0380	0.0995	0.0023	546	98	611	14.0	610	21.0	112
STDGJ31	0.0614	0.0026	0.8290	0.0320	0.0992	0.0020	650	88	609	12.0	612	19.0	94
STDGJ52	0.0601	0.0023	0.8310	0.0300	0.0989	0.0019	565	83	608	11.0	610	17.0	108
STDGJ23	0.0597	0.0021	0.8170	0.0280	0.0985	0.0023	570	76	606	13.0	607	15.0	106

Analysis #	$^{207}\text{Pb}/^{206}\text{Pb}$	$\pm 2\sigma$	$^{207}\text{Pb}/^{235}\text{U}$	$\pm 2\sigma$	$^{206}\text{Pb}/^{238}\text{U}$	$\pm 2\sigma$	$^{207}\text{Pb}/^{206}\text{Pb}$ age	$\pm 2\sigma$	$^{206}\text{Pb}/^{238}\text{U}$ age	$\pm 2\sigma$	$^{207}\text{Pb}/^{235}\text{U}$ age	$\pm 2\sigma$	Concordancy
STDGJ34	0.0602	0.0021	0.8050	0.0280	0.0982	0.0019	573	76	604	11.0	601	16.0	105
STDGJ26	0.0601	0.0025	0.8200	0.0300	0.0978	0.0021	572	90	603	12.0	605	17.0	105
STDGJ24	0.0626	0.0024	0.8160	0.0300	0.0979	0.0026	662	81	601	16.0	607	17.0	91
STDGJ54	0.0585	0.0023	0.7910	0.0280	0.0974	0.0021	528	86	599	12.0	591	16.0	113
STDGJ55	0.0601	0.0028	0.8000	0.0360	0.0971	0.0022	563	99	598	13.0	594	19.0	106
STDGJ56	0.0624	0.0027	0.8210	0.0310	0.0973	0.0020	635	87	598	12.0	603	17.0	94
STDGJ36	0.0595	0.0024	0.7950	0.0300	0.0969	0.0020	542	84	597	12.0	593	17.0	110
STDGJ58	0.0614	0.0028	0.8070	0.0370	0.0966	0.0029	639	99	596	17.0	597	21.0	93
STDGJ64	0.0590	0.0034	0.7900	0.0440	0.0964	0.0024	540	110	593	14.0	590	24.0	110
STDGJ49	0.0591	0.0021	0.7840	0.0260	0.0957	0.0019	551	75	589	11.0	585	15.0	107
STDGJ50	0.0582	0.0031	0.7730	0.0360	0.0955	0.0025	490	110	587	14.0	584	20.0	120
STDGJ29	0.0591	0.0030	0.7790	0.0430	0.0945	0.0030	540	110	582	18.0	580	24.0	108
STDGJ48	0.0610	0.0025	0.7920	0.0280	0.0933	0.0018	646	85	575	11.0	592	16.0	89
PLES18	0.0544	0.0018	0.3960	0.0130	0.0541	0.0010	386	71	339	6.2	339	9.4	88
PLES12	0.0549	0.0018	0.4010	0.0120	0.0536	0.0010	382	70	337	6.3	341	9.0	88
PLES13	0.0543	0.0015	0.3950	0.0120	0.0531	0.0009	376	61	334	5.2	337	8.5	89
PLES10	0.0537	0.0020	0.3960	0.0140	0.0531	0.0011	356	75	334	6.7	338	10.0	94
PLES17	0.0536	0.0021	0.3920	0.0140	0.0529	0.0011	315	79	332	6.9	334	10.0	105
PLES14	0.0540	0.0015	0.3930	0.0120	0.0527	0.0009	361	61	331	5.7	336	8.4	92
PLES11	0.0528	0.0020	0.3880	0.0140	0.0527	0.0010	303	78	331	6.1	331	10.0	109
PLES15	0.0529	0.0013	0.3824	0.0097	0.0525	0.0008	313	52	330	4.8	329	7.0	105
PLES26	0.0534	0.0022	0.3870	0.0150	0.0519	0.0011	354	86	326	6.7	330	11.0	92
PLES19	0.0545	0.0018	0.3840	0.0120	0.0517	0.0008	366	70	325	5.0	329	8.8	89
PLES09	0.0536	0.0020	0.3800	0.0130	0.0511	0.0009	339	78	321	5.6	325	9.4	95
PLES27	0.0526	0.0022	0.3720	0.0140	0.0511	0.0010	294	83	321	6.3	322	11.0	109

SAN-14 **(Concordant Standards)**

STDGJ05	0.0610	0.0019	0.8580	0.0240	0.1017	0.0016	640	64	624	9.6	628	13.0	98
STDGJ45	0.0603	0.0018	0.8500	0.0260	0.1010	0.0017	596	65	621	10.0	622	14.0	104
STDGJ29	0.0600	0.0018	0.8310	0.0210	0.1003	0.0019	591	66	616	11.0	616	12.0	104
STDGJ52	0.0612	0.0020	0.8340	0.0280	0.0995	0.0018	615	73	611	11.0	614	15.0	99
STDGJ13	0.0607	0.0020	0.8290	0.0250	0.0989	0.0018	611	69	608	11.0	612	14.0	100

Analysis #	$^{207}\text{Pb}/^{206}\text{Pb}$	$\pm 2\sigma$	$^{207}\text{Pb}/^{235}\text{U}$	$\pm 2\sigma$	$^{206}\text{Pb}/^{238}\text{U}$	$\pm 2\sigma$	$^{207}\text{Pb}/^{206}\text{Pb}$ age	$\pm 2\sigma$	$^{206}\text{Pb}/^{238}\text{U}$ age	$\pm 2\sigma$	$^{207}\text{Pb}/^{235}\text{U}$ age	$\pm 2\sigma$	Concordancy
STDGJ37	0.0608	0.0019	0.8280	0.0230	0.0985	0.0017	612	68	606	10.0	611	13.0	99
STDGJ06	0.0613	0.0019	0.8190	0.0210	0.0980	0.0017	631	65	602	9.9	605	12.0	95
STDGJ15	0.0605	0.0020	0.8170	0.0240	0.0978	0.0018	603	70	602	10.0	605	13.0	100
STDGJ23	0.0607	0.0020	0.8200	0.0270	0.0979	0.0017	602	69	602	10.0	605	15.0	100
STDGJ07	0.0601	0.0019	0.8130	0.0220	0.0978	0.0017	599	70	601	9.9	603	13.0	100
STDGJ31	0.0612	0.0020	0.8130	0.0270	0.0977	0.0019	619	69	601	11.0	606	15.0	97
STDGJ47	0.0610	0.0019	0.8200	0.0250	0.0978	0.0018	613	67	601	11.0	605	14.0	98
STDGJ44	0.0608	0.0017	0.8090	0.0210	0.0976	0.0017	613	61	600	10.0	601	12.0	98
STDGJ08	0.0603	0.0019	0.8130	0.0260	0.0973	0.0019	592	71	598	11.0	603	15.0	101
STDGJ17	0.0601	0.0016	0.8010	0.0230	0.0972	0.0017	606	59	598	9.7	596	13.0	99
STDGJ51	0.0599	0.0018	0.8070	0.0220	0.0971	0.0016	581	66	597	9.5	600	13.0	103
STDGJ14	0.0599	0.0030	0.7910	0.0320	0.0971	0.0025	580	110	597	15.0	593	19.0	103
STDGJ11	0.0598	0.0018	0.8050	0.0220	0.0968	0.0015	587	64	595	9.0	600	12.0	101
STDGJ25	0.0594	0.0019	0.7960	0.0240	0.0967	0.0018	580	69	595	11.0	595	14.0	103
STDGJ41	0.0608	0.0017	0.8030	0.0220	0.0966	0.0015	610	60	594	9.1	595	12.0	97
STDGJ26	0.0605	0.0022	0.8010	0.0270	0.0966	0.0020	585	76	594	12.0	597	15.0	102
STDGJ16	0.0607	0.0018	0.7930	0.0220	0.0962	0.0014	591	63	592	8.5	593	12.0	100
STDGJ40	0.0597	0.0018	0.7810	0.0210	0.0961	0.0014	577	65	591	8.4	588	12.0	102
STDGJ49	0.0605	0.0020	0.7900	0.0250	0.0960	0.0018	615	70	591	10.0	595	13.0	96
STDGJ33	0.0594	0.0019	0.7870	0.0220	0.0960	0.0016	578	68	591	9.4	591	12.0	102
STDGJ24	0.0600	0.0021	0.7840	0.0280	0.0953	0.0018	582	78	587	10.0	588	16.0	101
STDGJ38	0.0600	0.0020	0.7800	0.0220	0.0954	0.0020	571	73	587	12.0	585	13.0	103
STDGJ48	0.0607	0.0024	0.7930	0.0320	0.0946	0.0020	609	85	583	12.0	588	18.0	96
STDGJ42	0.0600	0.0020	0.7810	0.0230	0.0946	0.0016	566	71	583	9.5	583	13.0	103
PLES17	0.0535	0.0013	0.3966	0.0098	0.0535	0.0010	329	52	336	5.9	338	7.1	102
PLES18	0.0534	0.0020	0.3880	0.0130	0.0531	0.0010	322	79	333	6.2	332	9.4	104
PLES11	0.0537	0.0021	0.3840	0.0160	0.0530	0.0010	332	84	333	6.4	332	12.0	100
PLES08	0.0530	0.0023	0.3770	0.0140	0.0521	0.0011	315	95	328	7.0	326	11.0	104

SAN-14	(Discordant Standards)												
STDGJ53	0.0599	0.0020	0.8540	0.0260	0.1039	0.0018	555	71	637	10.0	625	14.0	115
STDGJ04	0.0599	0.0023	0.8480	0.0300	0.1016	0.0018	584	82	624	11.0	620	17.0	107

Analysis #	$^{207}\text{Pb}/^{206}\text{Pb}$	$\pm 2\sigma$	$^{207}\text{Pb}/^{235}\text{U}$	$\pm 2\sigma$	$^{206}\text{Pb}/^{238}\text{U}$	$\pm 2\sigma$	$^{207}\text{Pb}/^{206}\text{Pb}$ age	$\pm 2\sigma$	$^{206}\text{Pb}/^{238}\text{U}$ age	$\pm 2\sigma$	$^{207}\text{Pb}/^{235}\text{U}$ age	$\pm 2\sigma$	Concordancy
STDGJ54	0.0602	0.0021	0.8340	0.0250	0.1006	0.0022	581	75	618	13.0	615	14.0	106
STDGJ55	0.0597	0.0022	0.8270	0.0310	0.1000	0.0018	567	81	614	11.0	610	17.0	108
STDGJ20	0.0596	0.0022	0.8310	0.0310	0.0998	0.0021	573	79	613	12.0	614	17.0	107
STDGJ12	0.0590	0.0025	0.8100	0.0300	0.0991	0.0021	563	90	609	12.0	604	17.0	108
STDGJ28	0.0592	0.0019	0.8150	0.0240	0.0989	0.0019	557	68	607	11.0	603	13.0	109
STDGJ21	0.0601	0.0030	0.8230	0.0350	0.0986	0.0033	570	100	605	19.0	610	19.0	106
STDGJ30	0.0611	0.0019	0.8120	0.0260	0.0984	0.0015	639	68	605	9.0	602	14.0	95
STDGJ46	0.0588	0.0027	0.8240	0.0350	0.0981	0.0021	532	95	603	12.0	606	19.0	113
STDGJ09	0.0595	0.0018	0.8040	0.0210	0.0978	0.0016	570	66	602	9.5	601	12.0	106
STDGJ56	0.0596	0.0019	0.8130	0.0230	0.0977	0.0017	570	69	601	10.0	603	13.0	105
STDGJ36	0.0598	0.0025	0.8130	0.0310	0.0978	0.0019	559	85	601	11.0	601	18.0	108
STDGJ18	0.0600	0.0019	0.7860	0.0220	0.0971	0.0017	559	68	597	10.0	593	13.0	107
STDGJ10	0.0597	0.0019	0.7990	0.0250	0.0970	0.0015	568	69	597	9.0	593	14.0	105
STDGJ22	0.0588	0.0019	0.7930	0.0220	0.0965	0.0020	561	71	595	12.0	593	12.0	106
STDGJ32	0.0608	0.0018	0.8160	0.0230	0.0962	0.0018	628	64	592	10.0	607	13.0	94
STDGJ34	0.0593	0.0020	0.7970	0.0240	0.0960	0.0017	549	70	591	10.0	593	13.0	108
STDGJ39	0.0594	0.0025	0.7830	0.0280	0.0957	0.0021	541	87	589	12.0	586	16.0	109
STDGJ50	0.0590	0.0025	0.7830	0.0310	0.0950	0.0024	531	94	585	14.0	589	18.0	110
PLES03	0.0605	0.0026	0.4480	0.0170	0.0537	0.0011	595	95	337	6.6	376	12.0	57
PLES01	0.0604	0.0021	0.4450	0.0160	0.0537	0.0010	604	76	337	6.2	372	11.0	56
PLES24	0.0526	0.0013	0.3891	0.0097	0.0535	0.0006	298	54	336	3.5	333	7.1	113
PLES23	0.0525	0.0014	0.3870	0.0110	0.0534	0.0007	298	59	335	4.1	333	8.0	112
PLES21	0.0525	0.0017	0.3910	0.0110	0.0532	0.0012	308	73	334	7.2	334	8.2	109
PLES22	0.0530	0.0013	0.3900	0.0091	0.0532	0.0008	310	54	334	4.8	334	6.7	108
PLES02	0.0667	0.0035	0.4910	0.0290	0.0531	0.0008	730	100	334	5.1	403	19.0	46
PLES05	0.0552	0.0030	0.3960	0.0220	0.0528	0.0013	410	120	331	8.1	337	16.0	81
PLES13	0.0632	0.0019	0.4560	0.0130	0.0527	0.0007	677	64	331	4.2	380	9.3	49
PLES10	0.0623	0.0022	0.4520	0.0160	0.0525	0.0008	668	73	330	4.7	379	11.0	49
PLES09	0.0518	0.0032	0.3870	0.0240	0.0524	0.0015	290	130	329	9.4	333	17.0	113
PLES06	0.0634	0.0024	0.4660	0.0190	0.0523	0.0008	690	82	328	4.9	386	13.0	48
PLES19	0.0540	0.0015	0.3856	0.0095	0.0520	0.0008	359	62	327	4.9	332	7.0	91
PLES15	0.0546	0.0018	0.3870	0.0110	0.0520	0.0008	372	71	327	4.6	332	7.9	88
PLES04	0.0579	0.0019	0.4110	0.0120	0.0517	0.0008	493	72	325	4.9	349	9.1	¹²⁹ 66

Analysis #	$^{207}\text{Pb}/^{206}\text{Pb}$	$\pm 2\sigma$	$^{207}\text{Pb}/^{235}\text{U}$	$\pm 2\sigma$	$^{206}\text{Pb}/^{238}\text{U}$	$\pm 2\sigma$	$^{207}\text{Pb}/^{206}\text{Pb}$ age	$\pm 2\sigma$	$^{206}\text{Pb}/^{238}\text{U}$ age	$\pm 2\sigma$	$^{207}\text{Pb}/^{235}\text{U}$ age	$\pm 2\sigma$	Concordancy	
PLES14	0.0601	0.0017	0.4260	0.0120	0.0514	0.0009	581	62	323	5.2	359	8.3	56	
SAN-17 <i>(Concordant Standards)</i>														
STDGJ45	0.0607	0.0020	0.8670	0.0300	0.1029	0.0018	622	70	631	10.0	632	16.0	101	
STDGJ44	0.0605	0.0031	0.8320	0.0380	0.1008	0.0030	590	110	619	18.0	615	21.0	105	
STDGJ30	0.0609	0.0018	0.8350	0.0220	0.0994	0.0016	632	62	610	9.6	615	12.0	97	
STDGJ29	0.0597	0.0017	0.8210	0.0210	0.0992	0.0017	585	62	610	10.0	609	12.0	104	
STDGJ46	0.0605	0.0020	0.8190	0.0230	0.0991	0.0017	614	67	609	10.0	609	13.0	99	
STDGJ14	0.0608	0.0020	0.8250	0.0280	0.0987	0.0020	610	73	607	11.0	613	16.0	100	
STDGJ25	0.0608	0.0021	0.8320	0.0250	0.0983	0.0020	618	72	606	12.0	612	14.0	98	
STDGJ34	0.0606	0.0020	0.8200	0.0230	0.0986	0.0017	588	70	606	10.0	605	13.0	103	
STDGJ08	0.0604	0.0019	0.8280	0.0240	0.0985	0.0019	588	69	605	11.0	611	14.0	103	
STDGJ12	0.0601	0.0024	0.8270	0.0290	0.0984	0.0021	582	87	605	12.0	611	16.0	104	
STDGJ48	0.0612	0.0020	0.8250	0.0240	0.0983	0.0016	618	70	604	9.5	608	13.0	98	
STDGJ52	0.0605	0.0017	0.8250	0.0220	0.0983	0.0016	607	62	604	9.3	608	13.0	100	
STDGJ20	0.0604	0.0023	0.8240	0.0310	0.0980	0.0020	626	78	604	12.0	611	17.0	96	
STDGJ28	0.0615	0.0020	0.8200	0.0230	0.0983	0.0020	625	66	604	12.0	610	13.0	97	
STDGJ35	0.0603	0.0019	0.8150	0.0230	0.0981	0.0016	590	69	604	9.0	604	13.0	102	
STDGJ10	0.0599	0.0020	0.8100	0.0260	0.0982	0.0019	581	73	604	11.0	602	15.0	104	
STDGJ31	0.0614	0.0023	0.8270	0.0300	0.0981	0.0017	634	80	603	10.0	608	16.0	95	
STDGJ44	0.0600	0.0021	0.8080	0.0250	0.0978	0.0022	604	73	603	12.0	601	14.0	100	
STDGJ26	0.0600	0.0020	0.8220	0.0270	0.0980	0.0018	600	73	603	11.0	608	15.0	101	
STDGJ50	0.0606	0.0019	0.8150	0.0260	0.0977	0.0017	617	67	602	9.9	606	15.0	98	
STDGJ21	0.0603	0.0023	0.8070	0.0240	0.0979	0.0017	618	79	602	10.0	602	14.0	97	
STDGJ23	0.0605	0.0025	0.8210	0.0280	0.0979	0.0022	592	93	602	13.0	609	15.0	102	
STDGJ45	0.0614	0.0033	0.8230	0.0410	0.0978	0.0024	630	120	601	14.0	606	23.0	95	
STDGJ38	0.0605	0.0023	0.8220	0.0300	0.0977	0.0024	602	82	601	14.0	605	16.0	100	
STDGJ48	0.0607	0.0021	0.8150	0.0290	0.0974	0.0023	595	78	601	13.0	606	16.0	101	
STDGJ53	0.0600	0.0019	0.8040	0.0260	0.0972	0.0019	582	68	601	11.0	599	15.0	103	
STDGJ15	0.0594	0.0021	0.8150	0.0260	0.0977	0.0021	580	75	601	12.0	604	15.0	104	
STDGJ36	0.0598	0.0016	0.8070	0.0220	0.0978	0.0017	580	57	601	9.7	598	12.0	104	
STDGJ39	0.0606	0.0018	0.8080	0.0230	0.0977	0.0016	589	62	601	9.4	599	13.0	102	

Analysis #	$^{207}\text{Pb}/^{206}\text{Pb}$	$\pm 2\sigma$	$^{207}\text{Pb}/^{235}\text{U}$	$\pm 2\sigma$	$^{206}\text{Pb}/^{238}\text{U}$	$\pm 2\sigma$	$^{207}\text{Pb}/^{206}\text{Pb}$ age	$\pm 2\sigma$	$^{206}\text{Pb}/^{238}\text{U}$ age	$\pm 2\sigma$	$^{207}\text{Pb}/^{235}\text{U}$ age	$\pm 2\sigma$	Concordancy
STDGJ37	0.0609	0.0018	0.8190	0.0220	0.0976	0.0017	611	64	600	9.8	605	12.0	98
STDGJ41	0.0597	0.0018	0.8010	0.0230	0.0976	0.0017	579	64	600	9.8	596	13.0	104
STDGJ32	0.0601	0.0025	0.8180	0.0340	0.0976	0.0025	606	99	600	15.0	606	20.0	99
STDGJ28	0.0607	0.0025	0.8020	0.0280	0.0976	0.0018	598	84	600	10.0	597	16.0	100
STDGJ33	0.0601	0.0019	0.8110	0.0250	0.0973	0.0019	592	69	600	11.0	600	14.0	101
STDGJ54	0.0606	0.0017	0.8110	0.0230	0.0975	0.0015	597	65	600	8.8	604	13.0	100
STDGJ24	0.0615	0.0020	0.8200	0.0230	0.0972	0.0019	627	69	599	11.0	606	13.0	96
STDGJ34	0.0608	0.0029	0.8010	0.0350	0.0972	0.0023	610	99	599	13.0	597	19.0	98
STDGJ40	0.0600	0.0020	0.8060	0.0260	0.0974	0.0018	581	70	599	10.0	598	14.0	103
STDGJ09	0.0603	0.0019	0.8010	0.0240	0.0973	0.0017	605	67	598	10.0	597	14.0	99
STDGJ16	0.0593	0.0018	0.8020	0.0260	0.0973	0.0019	572	67	598	11.0	597	15.0	105
STDGJ20	0.0600	0.0021	0.8030	0.0280	0.0971	0.0018	570	73	598	11.0	596	15.0	105
STDGJ33	0.0603	0.0020	0.8100	0.0240	0.0971	0.0019	609	71	597	11.0	602	14.0	98
STDGJ22	0.0610	0.0023	0.8000	0.0280	0.0968	0.0021	593	78	596	12.0	594	15.0	101
STDGJ22	0.0602	0.0021	0.7970	0.0290	0.0968	0.0020	574	78	595	12.0	593	16.0	104
STDGJ27	0.0591	0.0025	0.7910	0.0280	0.0965	0.0028	566	95	594	16.0	592	15.0	105
STDGJ17	0.0611	0.0021	0.8000	0.0270	0.0965	0.0018	601	69	593	11.0	594	15.0	99
STDGJ23	0.0611	0.0027	0.7980	0.0350	0.0958	0.0022	610	92	590	13.0	595	19.0	97
STDGJ40	0.0598	0.0021	0.7920	0.0240	0.0955	0.0020	562	73	588	12.0	593	14.0	105
STDGJ26	0.0611	0.0021	0.7800	0.0260	0.0951	0.0020	598	75	585	11.0	583	15.0	98
STDGJ25	0.0609	0.0023	0.7870	0.0270	0.0940	0.0020	591	81	581	12.0	585	15.0	98
PLES17	0.0536	0.0015	0.4000	0.0110	0.0539	0.0007	337	58	338	4.4	342	7.6	100
PLES22	0.0538	0.0012	0.3962	0.0084	0.0538	0.0007	347	48	338	4.3	338	6.1	97
PLES15	0.0535	0.0011	0.3986	0.0080	0.0538	0.0006	334	45	338	3.8	340	5.8	101
PLES12	0.0534	0.0009	0.3977	0.0067	0.0538	0.0008	344	38	338	4.6	340	5.0	98
PLES06	0.0530	0.0018	0.3900	0.0130	0.0537	0.0009	329	71	337	5.6	334	9.1	103
PLES11	0.0537	0.0018	0.3960	0.0120	0.0537	0.0009	355	70	337	5.4	338	8.9	95
PLES24	0.0538	0.0011	0.3951	0.0078	0.0537	0.0007	351	44	337	4.5	338	5.7	96
PLES16	0.0536	0.0009	0.3948	0.0071	0.0537	0.0006	342	39	337	3.9	337	5.1	99
PLES16	0.0540	0.0015	0.3970	0.0120	0.0537	0.0008	346	58	337	5.0	338	8.4	97
PLES11	0.0530	0.0010	0.3976	0.0067	0.0537	0.0007	331	42	337	4.3	340	4.8	102
PLES05	0.0534	0.0018	0.3920	0.0130	0.0537	0.0011	329	73	337	6.8	335	9.7	102
PLES03	0.0528	0.0015	0.3900	0.0100	0.0537	0.0009	326	64	337	5.4	336	7.5	¹³¹ 103

Analysis #	$^{207}\text{Pb}/^{206}\text{Pb}$	$\pm 2\sigma$	$^{207}\text{Pb}/^{235}\text{U}$	$\pm 2\sigma$	$^{206}\text{Pb}/^{238}\text{U}$	$\pm 2\sigma$	$^{207}\text{Pb}/^{206}\text{Pb}$ age	$\pm 2\sigma$	$^{206}\text{Pb}/^{238}\text{U}$ age	$\pm 2\sigma$	$^{207}\text{Pb}/^{235}\text{U}$ age	$\pm 2\sigma$	Concordancy	
PLES20	0.0537	0.0019	0.3870	0.0130	0.0535	0.0010	343	72	337	5.8	332	9.6	98	
PLES20	0.0540	0.0015	0.3960	0.0110	0.0535	0.0009	349	61	336	5.7	338	8.0	96	
PLES12	0.0538	0.0023	0.3880	0.0150	0.0531	0.0011	332	90	334	6.6	333	11.0	101	
PLES07	0.0534	0.0016	0.3880	0.0120	0.0529	0.0008	321	61	333	5.0	332	8.7	104	
PLES19	0.0529	0.0015	0.3880	0.0110	0.0525	0.0008	328	60	330	4.6	332	8.0	101	

SAN-17	<i>(Discordant Standards)</i>												
STDGJ06	0.0634	0.0021	0.8770	0.0280	0.1027	0.0019	710	65	630	11.0	640	14.0	89
STDGJ07	0.0589	0.0019	0.8260	0.0230	0.1025	0.0019	547	69	630	11.0	608	13.0	115
STDGJ36	0.0636	0.0023	0.8640	0.0290	0.1011	0.0021	701	77	621	12.0	631	15.0	89
STDGJ37	0.0581	0.0022	0.8020	0.0280	0.1005	0.0021	531	79	617	12.0	599	16.0	116
STDGJ46	0.0594	0.0022	0.8110	0.0300	0.0986	0.0018	550	77	606	11.0	601	16.0	110
STDGJ49	0.0577	0.0031	0.8050	0.0380	0.0984	0.0028	540	120	605	16.0	601	22.0	112
STDGJ47	0.0590	0.0023	0.8100	0.0300	0.0984	0.0020	533	83	605	12.0	603	17.0	114
STDGJ51	0.0591	0.0023	0.8050	0.0340	0.0981	0.0016	548	84	603	9.6	600	19.0	110
STDGJ42	0.0599	0.0033	0.7980	0.0370	0.0981	0.0023	570	110	603	13.0	599	22.0	106
STDGJ11	0.0597	0.0025	0.8040	0.0310	0.0981	0.0022	555	91	603	13.0	599	18.0	109
STDGJ47	0.0614	0.0017	0.8200	0.0220	0.0979	0.0016	638	60	603	9.0	607	12.0	94
STDGJ56	0.0591	0.0038	0.8030	0.0480	0.0979	0.0027	570	140	602	16.0	602	27.0	106
STDGJ42	0.0582	0.0019	0.8120	0.0250	0.0979	0.0016	570	70	602	9.6	600	14.0	106
STDGJ30	0.0618	0.0024	0.8270	0.0370	0.0978	0.0025	645	85	601	15.0	603	19.0	93
STDGJ41	0.0593	0.0019	0.8070	0.0250	0.0979	0.0019	561	72	601	11.0	597	14.0	107
STDGJ29	0.0596	0.0019	0.8040	0.0230	0.0975	0.0018	552	70	601	10.0	598	13.0	109
STDGJ55	0.0612	0.0024	0.8190	0.0320	0.0976	0.0022	634	84	600	13.0	604	18.0	95
STDGJ31	0.0609	0.0019	0.8120	0.0280	0.0975	0.0021	641	70	599	12.0	600	16.0	93
STDGJ43	0.0583	0.0025	0.8040	0.0340	0.0975	0.0025	561	93	599	15.0	597	19.0	107
STDGJ21	0.0594	0.0021	0.7850	0.0240	0.0975	0.0022	550	76	599	13.0	591	13.0	109
STDGJ13	0.0599	0.0030	0.8200	0.0410	0.0972	0.0025	550	110	598	15.0	605	23.0	109
STDGJ24	0.0620	0.0029	0.8170	0.0330	0.0972	0.0025	646	99	597	15.0	603	18.0	92
STDGJ32	0.0621	0.0021	0.8240	0.0280	0.0967	0.0020	656	69	596	12.0	610	15.0	91
STDGJ39	0.0626	0.0020	0.8270	0.0240	0.0960	0.0018	697	68	591	11.0	610	13.0	85

Analysis #	$^{207}\text{Pb}/^{206}\text{Pb}$	$\pm 2\sigma$	$^{207}\text{Pb}/^{235}\text{U}$	$\pm 2\sigma$	$^{206}\text{Pb}/^{238}\text{U}$	$\pm 2\sigma$	$^{207}\text{Pb}/^{206}\text{Pb}$ age	$\pm 2\sigma$	$^{206}\text{Pb}/^{238}\text{U}$ age	$\pm 2\sigma$	$^{207}\text{Pb}/^{235}\text{U}$ age	$\pm 2\sigma$	Concordancy	
STDGJ18	0.0591	0.0023	0.7860	0.0260	0.0959	0.0020	540	85	590	12.0	589	15.0	109	
STDGJ38	0.0643	0.0022	0.8480	0.0240	0.0953	0.0015	731	72	587	8.8	621	13.0	80	
PLES04	0.0506	0.0015	0.3800	0.0100	0.0545	0.0008	226	61	342	4.8	326	7.5	151	
PLES08	0.0535	0.0017	0.3940	0.0120	0.0539	0.0008	314	67	339	4.6	335	8.7	108	
PLES21	0.0531	0.0009	0.3937	0.0071	0.0538	0.0006	318	37	338	3.7	338	5.2	106	
PLES02	0.0524	0.0016	0.3850	0.0110	0.0538	0.0007	292	64	338	4.4	331	8.2	116	
PLES15	0.0520	0.0017	0.3880	0.0120	0.0536	0.0008	275	69	337	5.1	334	9.1	123	
SAN-18	(Concordant Standards)													
STDGJ52	0.0614	0.0016	0.8680	0.0210	0.1034	0.0015	647	57	634	8.8	633	11.0	98	
STDGJ53	0.0605	0.0016	0.8590	0.0210	0.1032	0.0013	627	56	633	7.8	630	12.0	101	
STDGJ45	0.0603	0.0016	0.8510	0.0200	0.1021	0.0015	605	55	627	8.5	625	11.0	104	
STDGJ61	0.0600	0.0015	0.8450	0.0200	0.1019	0.0014	598	57	626	8.2	622	11.0	105	
STDGJ36	0.0606	0.0014	0.8420	0.0210	0.1017	0.0015	621	51	624	8.9	620	11.0	100	
STDGJ69	0.0613	0.0017	0.8460	0.0210	0.1013	0.0015	647	58	622	8.7	625	11.0	96	
STDGJ28	0.0611	0.0015	0.8550	0.0210	0.1012	0.0013	618	54	622	7.7	626	11.0	101	
STDGJ37	0.0603	0.0016	0.8440	0.0220	0.1009	0.0013	602	55	620	7.9	621	12.0	103	
STDGJ20	0.0603	0.0013	0.8460	0.0180	0.1009	0.0015	606	45	619	8.7	624	9.7	102	
STDGJ46	0.0607	0.0015	0.8340	0.0180	0.1002	0.0014	624	52	615	8.1	616	10.0	99	
STDGJ62	0.0599	0.0015	0.8190	0.0200	0.0995	0.0015	594	54	611	9.0	605	11.0	103	
STDGJ22	0.0606	0.0015	0.8350	0.0200	0.0991	0.0015	611	51	609	8.6	616	11.0	100	
STDGJ90	0.0613	0.0020	0.8520	0.0450	0.0989	0.0015	635	67	608	8.9	610	23.0	96	
STDGJ25	0.0603	0.0014	0.8210	0.0190	0.0986	0.0015	609	50	607	8.8	612	10.0	100	
STDGJ27	0.0604	0.0016	0.8210	0.0210	0.0986	0.0017	622	57	606	10.0	607	12.0	97	
STDGJ92	0.0604	0.0019	0.8350	0.0420	0.0985	0.0017	624	70	605	9.9	607	23.0	97	
STDGJ44	0.0597	0.0014	0.8170	0.0180	0.0985	0.0016	591	50	605	9.5	606	9.8	102	
STDGJ39	0.0593	0.0015	0.8060	0.0190	0.0985	0.0016	577	54	605	9.2	599	11.0	105	
STDGJ56	0.0600	0.0015	0.8200	0.0190	0.0981	0.0015	588	55	603	8.7	609	11.0	103	
STDGJ50	0.0608	0.0016	0.8190	0.0190	0.0979	0.0013	611	55	602	7.8	606	11.0	99	
STDGJ84	0.0609	0.0016	0.8170	0.0390	0.0979	0.0014	603	58	602	8.3	598	21.0	100	
STDGJ48	0.0599	0.0015	0.8030	0.0210	0.0977	0.0014	584	55	601	8.4	600	12.0	103	
STDGJ31	0.0605	0.0015	0.8140	0.0180	0.0975	0.0014	587	53	600	8.3	604	10.0	102	

Analysis #	$^{207}\text{Pb}/^{206}\text{Pb}$	$\pm 2\sigma$	$^{207}\text{Pb}/^{235}\text{U}$	$\pm 2\sigma$	$^{206}\text{Pb}/^{238}\text{U}$	$\pm 2\sigma$	$^{207}\text{Pb}/^{206}\text{Pb}$ age	$\pm 2\sigma$	$^{206}\text{Pb}/^{238}\text{U}$ age	$\pm 2\sigma$	$^{207}\text{Pb}/^{235}\text{U}$ age	$\pm 2\sigma$	Concordancy
STDGJ91	0.0605	0.0016	0.8110	0.0400	0.0973	0.0014	605	58	598	8.2	596	22.0	99
STDGJ73	0.0605	0.0015	0.8050	0.0200	0.0972	0.0014	589	56	598	8.4	598	11.0	102
STDGJ33	0.0602	0.0017	0.8010	0.0200	0.0971	0.0014	594	59	597	8.4	599	11.0	101
STDGJ40	0.0592	0.0016	0.7980	0.0190	0.0969	0.0014	583	57	596	8.3	593	11.0	102
STDGJ12	0.0605	0.0013	0.8110	0.0170	0.0968	0.0013	608	49	595	7.4	602	9.4	98
STDGJ32	0.0599	0.0013	0.7990	0.0170	0.0964	0.0013	581	45	595	7.6	596	9.3	102
STDGJ78	0.0598	0.0015	0.7940	0.0190	0.0964	0.0013	582	54	594	7.6	593	11.0	102
STDGJ18	0.0605	0.0014	0.7930	0.0170	0.0963	0.0012	620	48	593	7.3	595	9.8	96
STDGJ71	0.0604	0.0018	0.7960	0.0200	0.0963	0.0014	601	62	592	8.2	593	11.0	99
STDGJ57	0.0592	0.0015	0.7890	0.0180	0.0963	0.0012	565	57	592	7.2	589	10.0	105
STDGJ74	0.0598	0.0016	0.7980	0.0200	0.0961	0.0014	580	58	591	8.5	594	12.0	102
STDGJ13	0.0601	0.0015	0.7930	0.0200	0.0960	0.0016	593	55	591	9.6	594	11.0	100
STDGJ65	0.0610	0.0017	0.8010	0.0190	0.0957	0.0013	613	58	590	7.9	595	11.0	96
STDGJ17	0.0596	0.0015	0.7810	0.0160	0.0941	0.0013	571	53	580	7.4	587	9.1	102
STDGJ19	0.0593	0.0015	0.7660	0.0210	0.0936	0.0013	590	54	577	7.8	578	12.0	98
STDGJ80	0.0604	0.0016	0.7770	0.0190	0.0934	0.0013	602	58	575	7.6	583	11.0	96
STDGJ79	0.0604	0.0017	0.7710	0.0190	0.0933	0.0014	603	62	575	8.3	579	11.0	95
PLES19	0.0535	0.0010	0.4029	0.0077	0.0552	0.0007	347	43	346	4.4	344	5.5	100
PLES22	0.0532	0.0010	0.4024	0.0073	0.0544	0.0007	328	43	342	4.0	343	5.3	104
PLES26	0.0538	0.0012	0.3965	0.0089	0.0543	0.0007	352	47	341	4.4	340	6.2	97
PLES17	0.0541	0.0011	0.4052	0.0076	0.0542	0.0006	355	44	340	3.6	345	5.5	96
PLES18	0.0529	0.0010	0.3985	0.0081	0.0539	0.0007	323	43	339	4.0	341	5.9	105
PLES30	0.0531	0.0015	0.3960	0.0100	0.0537	0.0008	334	62	337	5.0	338	7.5	101
PLES43	0.0539	0.0009	0.4010	0.0170	0.0537	0.0006	351	37	337	3.9	339	12.0	96
PLES35	0.0543	0.0018	0.3960	0.0120	0.0534	0.0008	343	67	336	5.1	337	8.9	98
PLES01	0.0530	0.0012	0.3798	0.0085	0.0520	0.0007	319	51	327	4.0	326	6.3	102
PLES33	0.0536	0.0012	0.3834	0.0083	0.0519	0.0006	341	51	326	3.7	330	6.2	96
PLES38	0.0538	0.0016	0.3890	0.0190	0.0519	0.0008	335	62	326	5.0	328	13.0	97
PLES05	0.0533	0.0011	0.3801	0.0074	0.0519	0.0006	336	46	326	3.8	327	5.4	97
PLES37	0.0528	0.0014	0.3820	0.0160	0.0519	0.0008	323	57	326	5.1	326	11.0	101

Analysis #	$^{207}\text{Pb}/^{206}\text{Pb}$	$\pm 2\sigma$	$^{207}\text{Pb}/^{235}\text{U}$	$\pm 2\sigma$	$^{206}\text{Pb}/^{238}\text{U}$	$\pm 2\sigma$	$^{207}\text{Pb}/^{206}\text{Pb}$ age	$\pm 2\sigma$	$^{206}\text{Pb}/^{238}\text{U}$ age	$\pm 2\sigma$	$^{207}\text{Pb}/^{235}\text{U}$ age	$\pm 2\sigma$	Concordancy
STDGJ29	0.0593	0.0014	0.8380	0.0200	0.1025	0.0015	572	50	630	8.8	616	11.0	110
STDGJ21	0.0592	0.0015	0.8420	0.0210	0.1023	0.0015	554	57	628	8.5	618	11.0	113
STDGJ68	0.0596	0.0015	0.8350	0.0200	0.1013	0.0013	591	56	622	7.8	614	11.0	105
STDGJ60	0.0595	0.0014	0.8410	0.0170	0.1012	0.0014	589	51	621	7.9	619	9.2	105
STDGJ30	0.0621	0.0016	0.8480	0.0210	0.1007	0.0013	659	56	618	7.8	628	11.0	94
STDGJ77	0.0594	0.0016	0.8270	0.0220	0.1006	0.0013	582	58	618	7.7	610	13.0	106
STDGJ54	0.0592	0.0015	0.8190	0.0180	0.1006	0.0014	567	54	618	7.9	605	10.0	109
STDGJ55	0.0593	0.0014	0.8160	0.0190	0.1000	0.0013	561	55	615	7.6	607	11.0	110
STDGJ06	0.0601	0.0015	0.8160	0.0180	0.0998	0.0013	585	55	614	7.6	605	9.7	105
STDGJ95	0.0614	0.0018	0.8410	0.0400	0.0999	0.0016	646	60	614	9.5	613	21.0	95
STDGJ96	0.0580	0.0017	0.8360	0.0360	0.0997	0.0019	531	64	612	11.0	611	20.0	115
STDGJ87	0.0608	0.0016	0.8410	0.0380	0.0996	0.0014	654	60	612	8.1	614	21.0	94
STDGJ47	0.0599	0.0015	0.8130	0.0170	0.0992	0.0013	579	56	611	7.7	605	9.5	105
STDGJ05	0.0614	0.0014	0.8400	0.0170	0.0993	0.0013	643	48	610	7.5	619	9.3	95
STDGJ85	0.0615	0.0018	0.8370	0.0420	0.0992	0.0015	659	61	610	8.7	608	22.0	93
STDGJ82	0.0586	0.0020	0.8400	0.0400	0.0992	0.0017	529	76	610	9.8	612	22.0	115
STDGJ24	0.0599	0.0015	0.8150	0.0200	0.0990	0.0013	575	56	608	7.6	605	11.0	106
STDGJ41	0.0599	0.0013	0.8130	0.0180	0.0988	0.0011	577	49	608	6.7	607	9.8	105
STDGJ26	0.0638	0.0016	0.8610	0.0210	0.0989	0.0017	716	53	607	10.0	628	11.0	85
STDGJ38	0.0587	0.0014	0.8010	0.0190	0.0985	0.0013	553	54	606	7.6	597	11.0	110
STDGJ97	0.0595	0.0019	0.8310	0.0430	0.0986	0.0020	548	71	606	11.0	608	23.0	111
STDGJ08	0.0590	0.0014	0.8080	0.0200	0.0982	0.0014	562	50	604	8.4	599	11.0	108
STDGJ09	0.0583	0.0013	0.7900	0.0170	0.0982	0.0013	526	49	604	7.8	592	9.4	115
STDGJ23	0.0617	0.0014	0.8390	0.0200	0.0981	0.0014	656	48	603	8.4	618	11.0	92
STDGJ83	0.0586	0.0018	0.8160	0.0370	0.0982	0.0017	538	66	603	10.0	603	20.0	112
STDGJ43	0.0612	0.0016	0.8210	0.0170	0.0976	0.0013	638	57	600	7.5	609	9.3	94
STDGJ98	0.0628	0.0019	0.8270	0.0410	0.0974	0.0015	697	66	600	9.0	603	22.0	86
STDGJ63	0.0622	0.0015	0.8200	0.0200	0.0973	0.0015	664	50	600	8.9	606	11.0	90
STDGJ81	0.0621	0.0017	0.8250	0.0380	0.0974	0.0015	667	59	599	9.1	603	20.0	90
STDGJ70	0.0607	0.0015	0.8260	0.0180	0.0974	0.0013	631	52	599	7.6	613	9.9	95
STDGJ51	0.0595	0.0015	0.7980	0.0190	0.0974	0.0013	559	55	599	7.6	596	11.0	107
STDGJ86	0.0614	0.0016	0.8270	0.0380	0.0974	0.0015	653	56	599	8.8	604	21.0	92
STDGJ34	0.0616	0.0015	0.8200	0.0180	0.0971	0.0015	645	52	597	8.7	606	9.9	135 93

Analysis #	$^{207}\text{Pb}/^{206}\text{Pb}$	$\pm 2\sigma$	$^{207}\text{Pb}/^{235}\text{U}$	$\pm 2\sigma$	$^{206}\text{Pb}/^{238}\text{U}$	$\pm 2\sigma$	$^{207}\text{Pb}/^{206}\text{Pb}$ age	$\pm 2\sigma$	$^{206}\text{Pb}/^{238}\text{U}$ age	$\pm 2\sigma$	$^{207}\text{Pb}/^{235}\text{U}$ age	$\pm 2\sigma$	Concordancy
STDGJ99	0.0617	0.0019	0.8040	0.0360	0.0971	0.0017	637	66	597	9.9	593	19.0	94
STDGJ42	0.0612	0.0014	0.8240	0.0170	0.0970	0.0013	645	49	597	7.6	608	9.6	93
STDGJ11	0.0594	0.0015	0.7900	0.0180	0.0970	0.0015	559	53	597	8.7	591	10.0	107
STDGJ88	0.0587	0.0019	0.7900	0.0310	0.0969	0.0023	539	72	596	13.0	593	18.0	111
STDGJ10	0.0614	0.0016	0.8080	0.0200	0.0967	0.0013	653	52	595	7.6	602	11.0	91
STDGJ07	0.0612	0.0015	0.8120	0.0170	0.0961	0.0012	638	53	593	7.1	604	9.3	93
STDGJ58	0.0615	0.0018	0.8120	0.0190	0.0962	0.0014	654	61	592	8.1	604	11.0	91
STDGJ35	0.0622	0.0015	0.8070	0.0190	0.0960	0.0013	688	52	591	7.5	600	11.0	86
STDGJ49	0.0611	0.0016	0.8220	0.0210	0.0959	0.0014	644	56	590	8.2	609	11.0	92
STDGJ75	0.0620	0.0016	0.8140	0.0210	0.0955	0.0014	647	58	588	8.4	604	12.0	91
STDGJ67	0.0612	0.0015	0.8050	0.0190	0.0955	0.0014	640	52	588	8.3	601	11.0	92
STDGJ76	0.0610	0.0015	0.8040	0.0200	0.0953	0.0015	620	56	587	8.6	599	11.0	95
STDGJ66	0.0614	0.0015	0.8070	0.0190	0.0953	0.0014	635	57	587	8.3	601	11.0	92
STDGJ16	0.0611	0.0014	0.7980	0.0190	0.0951	0.0015	648	49	586	8.8	595	11.0	90
STDGJ93	0.0577	0.0027	0.7820	0.0350	0.0948	0.0022	484	99	584	13.0	583	20.0	121
STDGJ64	0.0612	0.0017	0.8050	0.0210	0.0947	0.0015	636	58	583	8.8	598	12.0	92
STDGJ59	0.0611	0.0013	0.7990	0.0190	0.0946	0.0014	619	47	583	7.9	595	11.0	94
STDGJ89	0.0594	0.0022	0.7680	0.0360	0.0946	0.0018	543	80	583	11.0	580	21.0	107
STDGJ72	0.0591	0.0015	0.7750	0.0190	0.0946	0.0013	550	55	583	7.8	583	11.0	106
STDGJ14	0.0623	0.0015	0.8090	0.0190	0.0941	0.0013	678	54	579	7.5	602	11.0	85
STDGJ15	0.0613	0.0016	0.7890	0.0200	0.0939	0.0013	623	54	579	7.6	588	11.0	93
STDGJ94	0.0607	0.0016	0.7720	0.0320	0.0938	0.0017	616	58	578	10.0	577	18.0	94
PLES10	0.0522	0.0011	0.4077	0.0083	0.0568	0.0006	285	47	356	3.9	347	6.0	125
PLES20	0.0566	0.0014	0.4350	0.0110	0.0555	0.0008	447	52	348	4.6	366	7.5	78
PLES11	0.0540	0.0013	0.4152	0.0089	0.0552	0.0007	372	51	346	4.1	352	6.3	93
PLES41	0.0575	0.0011	0.4110	0.0130	0.0552	0.0008	518	42	346	4.8	349	9.4	67
PLES09	0.0545	0.0015	0.4138	0.0097	0.0549	0.0007	366	58	344	4.4	351	7.0	94
PLES25	0.0544	0.0011	0.4097	0.0085	0.0547	0.0007	375	46	343	4.3	348	6.1	92
PLES23	0.0540	0.0012	0.4094	0.0087	0.0546	0.0007	374	50	342	4.2	350	6.3	92
PLES21	0.0524	0.0011	0.3965	0.0085	0.0546	0.0007	293	48	342	4.2	340	6.3	117
PLES29	0.0545	0.0010	0.4059	0.0082	0.0545	0.0007	372	42	342	4.0	345	5.9	92
PLES40	0.0545	0.0009	0.4040	0.0170	0.0544	0.0007	385	37	342	4.2	343	12.0	89

Analysis #	$^{207}\text{Pb}/^{206}\text{Pb}$	$\pm 2\sigma$	$^{207}\text{Pb}/^{235}\text{U}$	$\pm 2\sigma$	$^{206}\text{Pb}/^{238}\text{U}$	$\pm 2\sigma$	$^{207}\text{Pb}/^{206}\text{Pb}$ age	$\pm 2\sigma$	$^{206}\text{Pb}/^{238}\text{U}$ age	$\pm 2\sigma$	$^{207}\text{Pb}/^{235}\text{U}$ age	$\pm 2\sigma$	Concordancy
PLES42	0.0555	0.0010	0.4050	0.0160	0.0544	0.0007	417	39	341	4.0	343	11.0	82
PLES14	0.0570	0.0012	0.4241	0.0089	0.0541	0.0006	474	46	340	3.6	359	6.2	72
PLES13	0.0544	0.0012	0.4067	0.0079	0.0541	0.0007	381	49	339	4.5	346	5.7	89
PLES15	0.0531	0.0011	0.3925	0.0073	0.0536	0.0006	314	44	337	3.7	336	5.3	107
PLES03	0.0547	0.0011	0.4045	0.0079	0.0533	0.0005	388	47	335	3.1	344	5.7	86
PLES27	0.0543	0.0014	0.3960	0.0100	0.0531	0.0007	370	56	333	4.1	338	7.2	90
PLES02	0.0546	0.0010	0.3981	0.0069	0.0530	0.0006	389	41	333	3.6	340	5.0	86
PLES39	0.0606	0.0013	0.4290	0.0120	0.0530	0.0007	614	46	333	4.3	363	8.8	54
PLES34	0.0543	0.0014	0.3936	0.0099	0.0525	0.0007	367	56	330	4.3	336	7.2	90
PLES06	0.0545	0.0013	0.3892	0.0089	0.0524	0.0006	383	55	329	3.6	335	6.4	86
PLES04	0.0553	0.0013	0.3983	0.0086	0.0524	0.0006	416	51	329	3.9	340	6.3	79
PLES36	0.0538	0.0015	0.3840	0.0100	0.0523	0.0008	348	58	328	4.7	329	7.4	94
PLES07	0.0542	0.0011	0.3893	0.0074	0.0522	0.0005	365	44	328	3.2	334	5.4	90
PLES31	0.0537	0.0016	0.3860	0.0110	0.0519	0.0007	344	65	326	4.6	331	8.0	95

SAN-19	(Concordant Standards)												
STDGJ10	0.0608	0.0013	0.8750	0.0180	0.1053	0.0014	641	44	645	8.2	640	9.8	101
STDGJ09	0.0615	0.0015	0.8790	0.0200	0.1038	0.0014	656	51	637	8.1	639	11.0	97
STDGJ44	0.0610	0.0012	0.8600	0.0180	0.1035	0.0015	647	45	635	8.6	630	9.8	98
STDGJ45	0.0600	0.0013	0.8450	0.0180	0.1014	0.0013	607	49	622	7.8	621	10.0	103
STDGJ13	0.0609	0.0014	0.8420	0.0190	0.1009	0.0013	608	49	620	7.7	621	10.0	102
STDGJ52	0.0608	0.0020	0.8490	0.0280	0.1002	0.0020	639	72	615	12.0	622	15.0	96
STDGJ39	0.0602	0.0013	0.8230	0.0170	0.0999	0.0013	597	47	613	7.4	611	9.9	103
STDGJ36	0.0599	0.0015	0.8330	0.0180	0.0992	0.0012	596	53	610	7.4	615	10.0	102
STDGJ12	0.0598	0.0014	0.8240	0.0200	0.0992	0.0013	598	52	610	7.4	609	11.0	102
STDGJ46	0.0602	0.0014	0.8200	0.0180	0.0992	0.0015	604	53	610	8.9	610	9.9	101
STDGJ42	0.0604	0.0015	0.8170	0.0180	0.0988	0.0016	613	54	608	9.5	606	10.0	99
STDGJ47	0.0605	0.0013	0.8270	0.0170	0.0989	0.0011	610	46	608	6.2	613	9.3	100
STDGJ38	0.0609	0.0016	0.8290	0.0200	0.0988	0.0014	627	58	607	8.0	612	11.0	97
STDGJ55	0.0606	0.0016	0.8150	0.0210	0.0988	0.0016	619	62	607	9.1	608	12.0	98
STDGJ54	0.0603	0.0018	0.8110	0.0240	0.0980	0.0017	596	68	603	10.0	605	14.0	101
STDGJ14	0.0605	0.0015	0.8090	0.0180	0.0979	0.0012	594	55	602	7.3	603	9.9	101

Analysis #	$^{207}\text{Pb}/^{206}\text{Pb}$	$\pm 2\sigma$	$^{207}\text{Pb}/^{235}\text{U}$	$\pm 2\sigma$	$^{206}\text{Pb}/^{238}\text{U}$	$\pm 2\sigma$	$^{207}\text{Pb}/^{206}\text{Pb}$ age	$\pm 2\sigma$	$^{206}\text{Pb}/^{238}\text{U}$ age	$\pm 2\sigma$	$^{207}\text{Pb}/^{235}\text{U}$ age	$\pm 2\sigma$	Concordancy
STDGJ56	0.0605	0.0012	0.8100	0.0170	0.0978	0.0014	613	47	602	8.1	602	10.0	98
STDGJ40	0.0600	0.0014	0.8050	0.0160	0.0977	0.0013	588	51	601	7.7	599	9.3	102
STDGJ49	0.0612	0.0016	0.8190	0.0210	0.0976	0.0012	614	56	600	6.8	606	12.0	98
STDGJ48	0.0600	0.0020	0.8040	0.0300	0.0974	0.0017	583	73	599	9.9	599	17.0	103
STDGJ30	0.0598	0.0014	0.8020	0.0200	0.0973	0.0015	581	50	599	8.7	596	11.0	103
STDGJ28	0.0605	0.0016	0.8130	0.0200	0.0970	0.0014	613	54	597	8.2	602	11.0	97
STDGJ41	0.0605	0.0016	0.7970	0.0190	0.0968	0.0014	601	58	597	8.3	596	11.0	99
STDGJ32	0.0605	0.0015	0.8050	0.0210	0.0968	0.0014	605	55	595	7.9	598	12.0	98
STDGJ31	0.0598	0.0014	0.7930	0.0170	0.0964	0.0013	591	49	593	7.4	593	9.4	100
STDGJ33	0.0606	0.0015	0.8010	0.0180	0.0960	0.0013	607	52	592	7.6	596	9.9	97
STDGJ25	0.0598	0.0015	0.7880	0.0190	0.0960	0.0012	580	52	591	6.8	589	11.0	102
STDGJ20	0.0606	0.0014	0.7860	0.0170	0.0954	0.0011	606	50	588	6.4	588	9.7	97
STDGJ16	0.0603	0.0014	0.7960	0.0180	0.0954	0.0015	608	49	587	8.8	593	9.9	97
STDGJ26	0.0607	0.0015	0.7870	0.0210	0.0953	0.0014	616	56	587	8.1	589	12.0	95
STDGJ21	0.0595	0.0012	0.7600	0.0160	0.0926	0.0010	576	43	571	5.9	574	8.9	99
STDGJ23	0.0598	0.0014	0.7650	0.0170	0.0925	0.0011	578	49	570	6.6	576	9.6	99
PLES01	0.0539	0.0007	0.4498	0.0060	0.0608	0.0007	367	30	380	4.0	377	4.2	104
PLES08	0.0531	0.0007	0.3950	0.0051	0.0539	0.0005	337	28	339	3.3	338	3.7	100
PLES07	0.0529	0.0011	0.3972	0.0098	0.0538	0.0011	323	51	338	6.7	339	7.1	105
PLES20	0.0540	0.0015	0.3920	0.0110	0.0537	0.0008	348	62	337	4.7	336	7.7	97
PLES15	0.0532	0.0015	0.3910	0.0100	0.0531	0.0010	318	62	333	6.3	336	7.2	105
PLES22	0.0540	0.0018	0.3910	0.0140	0.0530	0.0010	347	71	333	6.2	336	11.0	96
PLES12	0.0536	0.0025	0.3890	0.0160	0.0528	0.0011	333	99	332	7.0	332	12.0	100
PLES14	0.0534	0.0012	0.3854	0.0080	0.0527	0.0007	323	50	331	4.6	330	5.9	103
PLES11	0.0536	0.0019	0.3810	0.0140	0.0522	0.0011	332	78	328	6.7	327	10.0	99

SAN-19	(Discordant Standards)												
STDGJ06	0.0605	0.0015	0.9030	0.0200	0.1079	0.0014	610	51	661	8.2	654	10.0	108
STDGJ07	0.0597	0.0014	0.8830	0.0200	0.1065	0.0014	588	51	652	8.1	644	11.0	111
STDGJ08	0.0600	0.0015	0.8720	0.0210	0.1062	0.0013	596	54	650	7.8	637	12.0	109
STDGJ11	0.0601	0.0016	0.8520	0.0210	0.1043	0.0014	569	57	639	8.4	624	11.0	112
STDGJ53	0.0599	0.0014	0.8420	0.0190	0.1025	0.0014	589	51	629	8.1	620	10.0	107

Analysis #	$^{207}\text{Pb}/^{206}\text{Pb}$	$\pm 2\sigma$	$^{207}\text{Pb}/^{235}\text{U}$	$\pm 2\sigma$	$^{206}\text{Pb}/^{238}\text{U}$	$\pm 2\sigma$	$^{207}\text{Pb}/^{206}\text{Pb}$ age	$\pm 2\sigma$	$^{206}\text{Pb}/^{238}\text{U}$ age	$\pm 2\sigma$	$^{207}\text{Pb}/^{235}\text{U}$ age	$\pm 2\sigma$	Concordancy
STDGJ37	0.0595	0.0013	0.8350	0.0180	0.1017	0.0014	568	49	624	8.1	617	10.0	110
STDGJ29	0.0592	0.0014	0.8140	0.0170	0.0988	0.0013	570	50	607	7.7	604	9.6	107
STDGJ50	0.0616	0.0016	0.8180	0.0210	0.0972	0.0015	651	55	599	8.5	605	12.0	92
STDGJ15	0.0596	0.0023	0.7860	0.0270	0.0969	0.0021	560	86	596	12.0	588	15.0	106
STDGJ34	0.0621	0.0015	0.8190	0.0190	0.0955	0.0013	658	52	588	7.5	605	10.0	89
STDGJ17	0.0617	0.0014	0.7950	0.0190	0.0942	0.0012	645	49	581	7.2	594	11.0	90
STDGJ18	0.0614	0.0014	0.7970	0.0170	0.0939	0.0013	669	47	579	7.5	597	9.5	87
STDGJ19	0.0601	0.0016	0.7700	0.0190	0.0925	0.0014	606	59	570	8.1	580	11.0	94
STDGJ24	0.0608	0.0015	0.7640	0.0190	0.0920	0.0011	619	52	567	6.4	576	11.0	92
STDGJ22	0.0612	0.0014	0.7650	0.0170	0.0910	0.0011	635	48	562	6.4	577	9.2	88
PLES02	0.0532	0.0007	0.4516	0.0059	0.0609	0.0006	331	29	381	3.5	378	4.1	115
PLES03	0.0534	0.0007	0.4418	0.0057	0.0600	0.0006	344	30	376	3.4	372	4.0	109
PLES04	0.0534	0.0008	0.4374	0.0061	0.0594	0.0006	345	31	372	3.8	368	4.3	108
PLES06	0.0543	0.0011	0.4124	0.0078	0.0552	0.0007	370	44	346	4.5	350	5.6	94
PLES21	0.0961	0.0033	0.7210	0.0260	0.0549	0.0007	1534	61	344	4.4	548	15.0	22
PLES05	0.0540	0.0010	0.4041	0.0075	0.0542	0.0006	366	42	340	3.8	344	5.4	93
PLES19	0.0566	0.0013	0.4158	0.0088	0.0535	0.0007	455	49	336	4.5	354	6.4	74
PLES18	0.0545	0.0017	0.4010	0.0140	0.0535	0.0014	371	70	336	8.8	341	10.0	91
PLES16	0.0559	0.0010	0.4054	0.0075	0.0532	0.0008	436	41	334	4.7	346	5.6	77
PLES17	0.0565	0.0014	0.4158	0.0090	0.0531	0.0007	468	53	334	4.4	352	6.5	71
PLES24	0.0521	0.0012	0.3773	0.0076	0.0525	0.0007	285	49	330	4.3	326	5.7	116
PLES23	0.0586	0.0017	0.4200	0.0120	0.0524	0.0008	514	59	329	4.6	356	8.0	64
PLES13	0.0565	0.0014	0.4036	0.0092	0.0521	0.0006	465	54	328	3.9	344	6.7	71
PLES09	0.0542	0.0020	0.3890	0.0160	0.0521	0.0010	361	78	327	6.4	330	11.0	91
PLES10	0.0554	0.0013	0.3869	0.0088	0.0506	0.0007	417	51	318	4.5	331	6.4	76

APPENDIX D: MICROPROBE MINERAL CHEMISTRY DATA

SAMPLE-MINERAL	Ca WT%	Mg WT%	Ti WT%	Si WT%	Al WT%	Fe WT%	Mn WT%	Cr WT%	Cl WT%	F WT%	K WT%	P WT%	Na WT%	Sr WT%	Ba WT%	V WT%	Zn WT%	Zr WT%	Ni WT%	O WT%	TOTAL
18 A1 Chl	6.70	2.80	5.83	12.80	7.37	18.51	0.26	0.00	0.09	0.80	0.03	0.00	0.12	0.00	0.03	0.07	0.00	0.00	0.00	34.65	90.05
18 A1 Chl	0.02	3.95	0.03	11.32	9.34	29.06	0.45	0.00	0.02	0.08	0.00	0.00	0.01	0.00	0.00	0.00	0.04	0.00	0.00	32.27	86.60
18 A2 Chl	0.04	4.47	0.05	11.86	8.65	27.34	0.45	0.00	0.00	0.09	0.14	0.00	0.06	0.00	0.03	0.01	0.03	0.00	0.00	32.18	85.40
18 A2 Chl	0.02	4.85	0.13	11.89	8.68	27.57	0.41	0.00	0.00	0.15	0.08	0.00	0.00	0.00	0.00	0.00	0.08	0.00	0.00	32.53	86.38
18 A2 Chl	0.86	3.55	0.89	11.11	8.23	27.06	0.45	0.00	0.01	0.20	0.04	0.00	0.05	0.02	0.00	0.02	0.00	0.00	0.00	31.09	83.58
18 A3 Chl	0.38	3.94	0.22	11.42	9.23	28.46	0.42	0.00	0.02	0.06	0.02	0.00	0.03	0.00	0.00	0.01	0.00	0.01	0.00	32.39	86.60
18 A3 Chl	0.05	4.23	0.05	11.33	8.95	28.86	0.43	0.01	0.01	0.11	0.01	0.00	0.01	0.00	0.00	0.00	0.01	0.00	0.00	32.06	86.13
14 C2 A1 Chl	1.72	8.02	2.18	12.58	8.93	17.99	0.56	0.01	0.02	0.09	0.15	0.00	0.01	0.00	0.00	0.04	0.03	0.00	0.00	35.04	87.36
14 C2 A1 Chl	0.06	8.68	0.01	12.66	9.12	20.37	0.62	0.01	0.05	0.07	0.05	0.00	0.01	0.00	0.06	0.02	0.03	0.01	0.00	34.30	86.12
14 C2 A1 Chl	0.07	7.93	0.00	12.11	9.46	21.17	0.66	0.04	0.00	0.08	0.02	0.00	0.00	0.01	0.00	0.01	0.00	0.00	0.00	33.72	85.28
14 C2 A1 Chl	0.21	8.09	0.01	12.29	9.55	20.99	0.66	0.01	0.00	0.11	0.02	0.06	0.03	0.01	0.00	0.02	0.00	0.01	0.00	34.18	86.24
14 C2 A1 Chl	0.05	8.60	0.00	12.39	9.24	20.86	0.66	0.02	0.01	0.04	0.01	0.00	0.00	0.00	0.00	0.00	0.00	0.00	0.00	34.18	86.08
14 C2 A2 Chl	0.06	8.31	0.01	12.31	9.40	21.36	0.63	0.01	0.00	0.07	0.03	0.01	0.00	0.00	0.03	0.00	0.00	0.00	0.00	34.18	86.41
14 C2 A2 Chl	0.55	8.77	1.22	13.47	9.31	17.00	0.53	0.00	0.02	0.10	0.54	0.04	0.04	0.00	0.05	0.01	0.05	0.00	0.00	35.63	87.36
14 C1 A1 Chl	0.05	8.42	0.00	12.35	9.64	20.89	0.67	0.01	0.00	0.06	0.03	0.00	0.00	0.00	0.01	0.02	0.00	0.00	0.00	34.38	86.53
14 C1 A1 Chl	0.04	8.35	0.01	12.51	9.81	20.98	0.68	0.03	0.00	0.07	0.13	0.00	0.00	0.00	0.00	0.00	0.01	0.05	0.00	34.74	87.42
14 C1 A1 Chl	0.09	6.75	0.31	14.55	10.74	16.17	0.53	0.03	0.00	0.04	1.65	0.00	0.03	0.00	0.03	0.03	0.04	0.00	0.00	35.97	86.95
19 C1 A1 Chl	0.69	9.87	0.82	12.08	10.09	16.86	0.56	0.00	0.25	0.02	0.06	0.02	0.14	0.00	0.04	0.01	0.02	0.00	0.00	35.10	86.66
19 C1 A1 Chl	0.03	9.74	0.01	11.55	10.31	18.32	0.57	0.00	0.05	0.03	0.02	0.00	0.06	0.03	0.02	0.00	0.01	0.00	0.00	34.18	84.92
19 C1 A1 Chl	0.31	5.76	0.41	17.29	12.95	11.06	0.32	0.00	0.06	0.01	2.69	0.00	0.12	0.00	0.19	0.02	0.00	0.01	0.00	39.29	90.51
19 C1 A1 Chl	0.03	10.09	0.02	11.86	10.37	17.49	0.58	0.00	0.04	0.00	0.06	0.00	0.07	0.00	0.03	0.02	0.05	0.00	0.00	34.65	85.37
19 C2 A1 Chl	0.02	10.09	0.03	12.02	10.03	16.78	0.52	0.00	0.01	0.04	0.05	0.00	0.11	0.02	0.00	0.01	0.03	0.01	0.00	34.29	84.07

SAMPLE-MINERAL	Ca WT%	Mg WT%	Ti WT%	Si WT%	Al WT%	Fe WT%	Mn WT%	Cr WT%	Cl WT%	F WT%	K WT%	P WT%	Na WT%	Sr WT%	Ba WT%	V WT%	Zn WT%	Zr WT%	Ni WT%	O WT%	TOTAL
19 C2 A1 Chl	0.02	9.14	0.03	11.53	10.34	19.26	0.64	0.00	0.05	0.02	0.02	0.00	0.04	0.00	0.00	0.01	0.00	0.00	0.00	34.09	85.19
19 C2 A1 Chl	0.30	9.68	0.27	12.37	10.75	16.86	0.55	0.00	0.11	0.09	0.22	0.03	0.07	0.00	0.03	0.01	0.04	0.01	0.00	35.39	86.79
10 C1 A1 Chl	0.01	6.25	0.00	11.95	9.23	21.48	0.37	0.00	0.04	0.06	0.92	0.00	0.09	0.00	0.02	0.00	0.00	0.00	0.00	32.41	82.84
10 C1 A1 Chl	0.01	7.05	0.00	11.84	9.97	22.78	0.38	0.00	0.05	0.03	0.05	0.01	0.10	0.01	0.01	0.02	0.00	0.00	0.00	33.68	85.98
10 C1 A1 Chl	0.02	6.14	0.00	12.30	9.97	21.91	0.42	0.01	0.08	0.02	0.55	0.00	0.11	0.00	0.00	0.01	0.00	0.00	0.00	33.46	85.02
10 C2 A1 Chl	0.00	7.52	0.01	12.11	9.78	22.58	0.35	0.00	0.01	0.05	0.04	0.00	0.03	0.00	0.00	0.02	0.00	0.01	0.00	34.04	86.56
10 C2 A1 Chl	0.01	7.00	0.00	11.59	9.90	23.28	0.35	0.00	0.05	0.02	0.03	0.00	0.05	0.00	0.00	0.02	0.00	0.00	0.00	33.43	85.76
10 C2 A1 Chl	0.02	6.64	0.02	11.72	9.86	23.84	0.40	0.00	0.03	0.01	0.06	0.01	0.04	0.00	0.00	0.02	0.00	0.01	0.00	33.49	86.16
10 C4 A1 Chl	0.00	7.73	0.00	11.93	9.36	22.51	0.32	0.00	0.01	0.04	0.03	0.00	0.02	0.00	0.03	0.01	0.00	0.00	0.00	33.55	85.54
10 C4 A1 Chl	0.05	6.94	0.01	12.26	9.62	23.83	0.42	0.00	0.01	0.04	0.11	0.01	0.04	0.01	0.05	0.00	0.00	0.00	0.00	34.11	87.51
10 C4 A1 Chl	0.02	6.43	0.00	11.77	9.75	23.46	0.37	0.00	0.02	0.00	0.10	0.00	0.04	0.01	0.00	0.02	0.00	0.02	0.00	33.20	85.21
18 A1 Tit	19.22	0.03	20.06	13.72	1.61	1.25	0.05	0.01	0.00	1.25	0.01	0.02	0.04	0.00	0.24	0.17	0.00	0.01	0.00	38.15	95.84
18 A1 Tit	19.22	0.02	20.39	13.89	1.52	1.49	0.11	0.01	0.00	1.33	0.00	0.02	0.02	0.00	0.25	0.15	0.02	0.05	0.00	38.55	97.04
18 A1 Tit	39.04	0.00	0.03	0.19	0.01	0.14	0.03	0.01	0.01	3.72	0.00	18.34	0.01	0.00	0.00	0.00	0.00	0.15	0.00	38.06	99.76
18 A1 Tit	37.57	0.00	0.01	0.37	0.00	0.04	0.03	0.01	0.01	3.93	0.00	17.96	0.01	0.00	0.00	0.02	0.05	0.13	0.00	37.06	97.21
18 A1 Tit	19.52	0.05	19.88	14.06	1.79	1.61	0.08	0.01	0.00	1.42	0.01	0.01	0.03	0.00	0.26	0.15	0.02	0.03	0.00	38.74	97.66
18 A3 Tit	18.63	0.03	19.64	13.36	2.81	1.10	0.04	0.00	0.10	1.34	0.03	0.00	0.09	0.00	0.26	0.16	0.00	0.00	0.00	38.19	95.79
18 A2 Tit	19.01	0.02	19.63	13.88	1.80	1.49	0.05	0.00	0.00	1.31	0.00	0.00	0.03	0.00	0.23	0.18	0.00	0.01	0.00	38.14	95.77
18 A2 Tit	8.04	0.18	0.64	14.34	7.07	10.09	0.35	0.05	0.21	0.45	0.06	0.01	0.19	0.00	0.01	0.07	0.19	0.01	0.07	29.36	71.39
14 C2 A1 Tit	19.97	0.01	17.04	14.24	3.84	0.60	0.00	0.01	0.00	2.31	0.09	0.02	0.00	0.00	0.23	0.14	0.02	0.09	0.00	38.37	96.98
14 C1 A1 Tit	1.74	0.00	42.10	0.74	0.20	16.25	0.02	0.00	0.06	0.12	0.00	0.00	0.02	0.00	0.58	0.33	0.00	0.00	0.00	34.67	96.83
14 C1 A1 Tit	19.19	0.04	17.54	14.56	3.43	0.98	0.00	0.01	0.02	1.53	0.12	0.04	0.03	0.00	0.22	0.16	0.00	0.01	0.00	38.86	96.72
14 C1 A1 Tit	19.48	0.02	17.60	14.41	3.49	0.93	0.02	0.00	0.02	1.80	0.07	0.01	0.02	0.00	0.24	0.17	0.00	0.01	0.00	38.73	97.03
14 C1 A1 Tit	20.08	0.01	18.24	14.21	3.41	0.44	0.00	0.00	0.00	1.87	0.09	0.00	0.01	0.00	0.19	0.17	0.00	0.04	0.01	38.91	97.69
14 C1 A1 Tit	19.22	0.00	17.59	14.23	3.11	0.97	0.02	0.01	0.02	1.66	0.29	0.07	0.02	0.00	0.19	0.13	0.00	0.03	0.00	38.24	95.81

SAMPLE-MINERAL	Ca WT%	Mg WT%	Ti WT%	Si WT%	Al WT%	Fe WT%	Mn WT%	Cr WT%	Cl WT%	F WT%	K WT%	P WT%	Na WT%	Sr WT%	Ba WT%	V WT%	Zn WT%	Zr WT%	Ni WT%	O WT%	TOTAL
14 C1 A1 Tit	19.41	0.01	17.25	14.55	3.54	0.99	0.01	0.00	0.02	1.74	0.10	0.02	0.02	0.00	0.23	0.12	0.00	0.01	0.00	38.68	96.66
19 C1 A1 Tit	1.68	9.11	1.17	11.97	9.63	16.32	0.50	0.00	0.28	0.03	0.03	0.00	0.11	0.00	0.03	0.01	0.01	0.02	0.00	34.47	85.36
19 C1 A1 Tit	8.05	5.66	8.77	13.42	6.07	10.09	0.31	0.00	0.53	0.00	0.22	0.01	0.45	0.00	0.11	0.07	0.00	0.02	0.00	36.62	90.40
19 C2 A1 Tit	15.24	0.03	17.31	20.16	1.12	0.94	0.01	0.00	0.10	0.19	0.14	0.03	0.06	0.00	0.21	0.20	0.00	0.13	0.01	42.05	97.93
19 C2 A1 Tit	14.54	2.72	14.27	12.83	3.56	5.49	0.16	0.00	0.07	0.42	0.10	0.58	0.04	0.00	0.13	0.11	0.00	0.05	0.00	37.20	92.26
10 C1 A1 Tit	18.79	0.01	20.00	13.34	1.83	0.87	0.00	0.00	0.57	0.18	0.09	0.07	1.04	0.00	0.24	0.16	0.15	0.05	0.05	38.40	95.87
10 C1 A1 Tit	18.44	0.01	19.81	13.80	1.96	0.35	0.00	0.01	0.14	0.64	0.04	0.03	0.12	0.00	0.20	0.14	0.04	0.03	0.00	38.06	93.80
10 C2 A1 Tit	0.04	0.41	0.01	31.33	10.82	2.24	0.01	0.00	0.19	0.00	0.06	0.02	9.32	0.00	0.00	0.00	0.00	0.00	0.00	49.51	103.97
10 C2 A1 Tit	19.73	0.01	22.69	14.21	0.80	0.30	0.00	0.01	0.01	0.06	0.02	0.01	0.02	0.00	0.24	0.17	0.01	0.00	0.00	40.14	98.45
10 C2 A1 Tit	18.90	0.00	20.51	14.06	1.71	0.46	0.03	0.01	0.02	0.24	0.01	0.11	0.06	0.00	0.24	0.13	0.01	0.00	0.00	39.09	95.60
10 C4 A1 Tit	19.55	0.00	20.69	14.07	1.75	0.51	0.00	0.01	0.00	0.39	0.00	0.04	0.02	0.00	0.24	0.15	0.00	0.03	0.00	39.37	96.82
10 C4 A1 Tit	10.22	0.01	38.63	7.58	0.96	0.27	0.00	0.01	0.03	0.06	0.05	0.02	0.08	0.00	0.43	0.25	0.02	0.00	0.00	39.68	98.31
10 C4 A1 Tit	13.85	0.03	23.92	10.28	1.04	9.29	1.21	0.01	0.00	0.28	0.00	0.03	0.03	0.00	0.26	0.16	0.00	0.07	0.00	37.25	97.73
10 C2 A1 Tit	0.35	0.01	57.76	0.23	0.56	0.18	0.00	0.00	0.02	0.01	0.02	0.00	0.08	0.00	0.72	0.37	0.00	0.04	0.00	39.84	100.19
10 C2 A1 Tit	0.72	0.00	57.44	0.45	0.36	0.24	0.01	0.00	0.01	0.00	0.01	0.00	0.05	0.00	0.72	0.32	0.00	0.00	0.00	39.81	100.14
18 A1 Ox	0.21	0.00	0.09	0.01	0.04	72.14	0.02	0.03	0.01	0.38	0.00	0.01	0.01	0.00	0.00	0.20	0.07	0.02	0.00	31.18	104.43
18 A1 Ox	0.17	0.00	0.13	0.01	0.22	72.47	0.02	0.02	0.00	0.33	0.01	0.01	0.04	0.00	0.00	0.19	0.01	0.00	0.02	31.51	105.15
18 A1 Ox	0.16	0.01	0.15	0.03	0.25	71.41	0.03	0.03	0.00	0.37	0.01	0.00	0.01	0.00	0.00	0.18	0.00	0.02	0.00	31.09	103.76
18 A1 Ox	0.17	0.00	0.17	0.00	0.25	72.15	0.00	0.05	0.00	0.36	0.00	0.01	0.01	0.04	0.05	0.19	0.00	0.00	0.00	31.40	104.86
18 A1 Ox	0.16	0.00	0.22	0.00	0.29	71.54	0.02	0.04	0.00	0.37	0.01	0.00	0.00	0.00	0.04	0.16	0.04	0.04	0.00	31.20	104.13
14 C2 A1 Ox	0.03	0.09	1.27	0.74	0.75	67.91	0.06	0.41	0.00	0.33	0.21	0.00	0.01	0.06	0.00	0.13	0.01	0.01	0.00	31.80	103.82
14 C2 A1 Ox	0.03	0.00	1.88	0.03	0.92	67.89	0.06	0.45	0.00	0.31	0.00	0.00	0.00	0.06	0.03	0.14	0.00	0.04	0.01	31.48	103.32
14 C2 A1 Ox	0.03	0.01	1.77	0.06	0.41	68.38	0.05	0.09	0.00	0.38	0.07	0.00	0.00	0.00	0.04	0.09	0.01	0.03	0.05	30.99	102.44
14 C1 A1 Ox	0.07	0.79	1.10	1.98	2.65	61.88	0.13	0.40	0.01	0.29	0.39	0.00	0.00	0.03	0.02	0.11	0.00	0.03	0.02	32.75	102.66
19 C1 Ox	0.13	0.03	2.21	0.40	0.22	67.14	0.02	0.43	0.05	0.27	0.10	0.00	0.16	0.02	0.06	0.04	0.03	0.00	0.01	31.26	102.59

SAMPLE-MINERAL	Ca WT%	Mg WT%	Ti WT%	Si WT%	Al WT%	Fe WT%	Mn WT%	Cr WT%	Cl WT%	F WT%	K WT%	P WT%	Na WT%	Sr WT%	Ba WT%	V WT%	Zn WT%	Zr WT%	Ni WT%	O WT%	TOTAL
19 C1 Ox	0.03	0.08	0.03	0.11	0.11	71.52	0.03	0.15	0.04	0.34	0.02	0.00	0.11	0.03	0.01	0.01	0.04	0.01	0.00	31.04	103.72
19 C1 Ox	0.05	0.36	0.55	0.46	0.34	67.10	0.01	0.02	0.03	0.31	0.04	0.00	0.02	0.00	0.01	0.16	0.03	0.04	0.00	30.28	99.81
18 A2 Alb	0.06	0.01	0.03	30.12	12.29	0.10	0.01	0.00	0.04	0.00	0.11	0.00	8.42	0.00	0.02	0.00	0.00	0.01	0.00	48.29	99.53
18 A2 Alb	0.26	0.01	0.00	30.98	10.94	0.12	0.00	0.00	0.01	0.00	0.06	0.00	8.80	0.00	0.03	0.00	0.00	0.00	0.00	48.25	99.45
18 A2 Alb	0.02	0.00	0.01	31.29	10.59	0.09	0.00	0.00	0.00	0.00	0.01	0.00	9.27	0.00	0.03	0.00	0.00	0.00	0.00	48.34	99.64
14 C2 A1 Alb	0.35	0.00	0.00	30.63	10.94	0.23	0.00	0.00	0.01	0.00	0.19	0.00	8.60	0.00	0.00	0.00	0.02	0.01	0.00	47.88	98.87
14 C2 A1 Alb	0.17	0.01	0.02	31.17	10.77	0.25	0.00	0.00	0.01	0.00	0.06	0.00	8.85	0.00	0.01	0.00	0.00	0.00	0.00	48.34	99.65
14 C2 A1 Alb	0.15	0.01	0.02	31.37	10.90	0.32	0.00	0.01	0.01	0.00	0.07	0.00	8.96	0.00	0.01	0.01	0.00	0.00	0.00	48.75	100.58
14 C2 A1 Alb	0.27	0.01	0.10	31.18	10.94	0.35	0.01	0.01	0.01	0.00	0.09	0.00	8.79	0.00	0.03	0.00	0.02	0.00	0.00	48.63	100.45
14 C2 A1 Alb	0.18	0.02	0.03	31.33	11.14	0.27	0.00	0.00	0.02	0.00	0.15	0.00	8.76	0.00	0.00	0.00	0.00	0.00	0.00	48.87	100.78
14 C1 A1 Alb	0.20	0.00	0.01	31.27	10.65	0.10	0.00	0.00	0.00	0.00	0.06	0.00	8.80	0.00	0.00	0.00	0.01	0.00	0.00	48.29	99.39
14 C1 A1 Alb	0.20	0.01	0.03	31.46	10.80	0.06	0.00	0.00	0.01	0.00	0.05	0.00	8.49	0.01	0.00	0.00	0.01	0.00	0.00	48.55	99.69
14 C1 A1 Alb	0.36	0.00	0.02	31.04	10.97	0.15	0.00	0.00	0.01	0.00	0.05	0.01	8.73	0.03	0.00	0.00	0.00	0.00	0.02	48.40	99.79
14 C1 A1 Alb	0.31	0.01	0.01	30.76	10.70	0.16	0.01	0.00	0.02	0.00	0.07	0.00	8.62	0.03	0.03	0.00	0.00	0.00	0.00	47.76	98.50
14 C1 A1 Alb	0.41	0.00	0.00	30.80	10.70	0.21	0.01	0.00	0.02	0.00	0.06	0.00	8.39	0.05	0.02	0.00	0.00	0.00	0.00	47.77	98.45
19 C1 A1 Alb	0.18	0.21	0.07	30.54	11.53	0.89	0.00	0.00	0.05	0.00	1.05	0.00	7.64	0.03	0.09	0.00	0.01	0.00	0.00	48.45	100.75
10 C2 A1 Alb	0.03	0.02	0.00	31.06	10.26	0.21	0.00	0.00	0.01	0.00	0.03	0.00	9.11	0.00	0.01	0.00	0.01	0.00	0.00	47.78	98.52
10 C2 A1 Alb	0.08	0.03	0.00	30.07	10.14	0.34	0.00	0.00	0.04	0.00	0.54	0.01	8.17	0.00	0.05	0.00	0.00	0.00	0.00	46.40	95.88
18 A2 Ksp	0.00	0.00	0.00	29.90	9.45	0.12	0.00	0.00	0.00	0.00	13.47	0.00	0.16	0.03	0.23	0.00	0.00	0.00	0.00	45.34	98.71
14 C2 A2 Ksp	0.00	0.00	0.01	30.03	9.64	0.12	0.00	0.01	0.01	0.00	13.35	0.00	0.16	0.00	0.36	0.00	0.00	0.03	0.00	45.67	99.39
14 C2 A2 Ksp	0.00	0.00	0.01	29.98	9.57	0.05	0.01	0.00	0.03	0.00	12.53	0.00	0.41	0.00	0.29	0.00	0.03	0.01	0.00	45.44	98.36
14 C2 A2 Ksp	0.00	0.00	0.00	29.74	9.60	0.06	0.00	0.01	0.00	0.00	13.07	0.01	0.14	0.00	0.41	0.00	0.00	0.01	0.00	45.22	98.26
14 C1 A1 Ksp	0.01	0.00	0.00	29.85	9.54	0.08	0.00	0.00	0.00	0.00	13.32	0.00	0.19	0.00	0.38	0.01	0.00	0.00	0.00	45.36	98.75
14 C1 A1 Ksp	0.01	0.00	0.00	29.88	9.71	0.04	0.01	0.00	0.01	0.00	13.31	0.01	0.17	0.07	0.36	0.00	0.00	0.00	0.00	45.54	99.11

SAMPLE-MINERAL	Ca WT%	Mg WT%	Ti WT%	Si WT%	Al WT%	Fe WT%	Mn WT%	Cr WT%	Cl WT%	F WT%	K WT%	P WT%	Na WT%	Sr WT%	Ba WT%	V WT%	Zn WT%	Zr WT%	Ni WT%	O WT%	TOTAL
19 C2 A1 Ksp	0.01	0.00	0.00	29.31	9.57	0.07	0.00	0.00	0.01	0.00	13.41	0.00	0.24	0.05	0.10	0.00	0.00	0.00	0.00	44.77	97.54
10 C1 A1 Ksp	0.02	0.00	0.02	29.89	9.66	0.19	0.00	0.00	0.09	0.00	13.22	0.00	0.26	0.01	0.37	0.00	0.03	0.00	0.01	45.56	99.34
10 C1 A1 Ksp	0.02	0.02	0.00	30.10	9.51	0.02	0.01	0.00	0.14	0.00	13.39	0.00	0.38	0.00	0.21	0.00	0.00	0.00	0.00	45.65	99.45
10 C1 A1 Ksp	0.00	0.00	0.00	29.80	9.65	0.12	0.00	0.01	0.06	0.00	13.17	0.00	0.21	0.03	0.20	0.00	0.00	0.00	0.00	45.36	98.62
10 C2 A1 Ksp	0.01	0.00	0.01	29.38	9.60	0.15	0.00	0.00	0.06	0.00	13.32	0.00	0.17	0.00	0.24	0.00	0.02	0.00	0.00	44.88	97.85
10 C2 A1 Ksp	0.00	0.00	0.01	30.15	9.58	0.08	0.00	0.00	0.00	0.00	13.36	0.00	0.16	0.00	0.18	0.00	0.03	0.00	0.00	45.72	99.27
10 C2 A1 Ksp	0.01	0.00	0.00	29.85	9.52	0.09	0.00	0.00	0.06	0.00	13.27	0.00	0.17	0.01	0.22	0.00	0.00	0.02	0.00	45.30	98.52
10 C4 A1 Ksp	0.02	0.20	0.03	28.78	9.75	1.08	0.03	0.01	0.05	0.00	12.42	0.00	0.23	0.02	0.28	0.01	0.03	0.00	0.00	44.60	97.54
18 A1 Ser	0.03	0.70	0.02	22.16	15.79	3.68	0.00	0.02	0.05	0.08	5.67	0.00	0.05	0.00	0.01	0.01	0.00	0.02	0.00	41.98	90.27
18 A1 Ser	0.03	0.77	0.02	23.02	16.07	4.34	0.03	0.01	0.01	0.06	5.17	0.00	0.02	0.00	0.03	0.01	0.00	0.01	0.00	43.37	92.99
14 C2 A2 Ser	0.08	1.68	0.06	25.11	15.23	2.49	0.02	0.02	0.02	0.02	6.83	0.01	0.06	0.00	0.02	0.02	0.00	0.00	0.00	45.49	97.16
19 C1 A1 Ser	0.03	1.94	0.08	24.40	14.33	3.15	0.03	0.00	0.04	0.00	4.73	0.00	0.04	0.00	0.07	0.04	0.00	0.03	0.00	43.82	92.74
19 C1 A1 Ser	0.07	1.20	0.09	22.99	15.82	3.19	0.03	0.01	0.11	0.00	4.80	0.00	0.16	0.00	0.14	0.06	0.00	0.02	0.00	43.14	91.83
19 C1 A1 Ser	0.07	1.59	0.03	23.93	15.62	2.52	0.03	0.00	0.07	0.00	4.88	0.00	0.07	0.01	0.07	0.03	0.01	0.00	0.00	44.01	92.93
19 C1 A1 Ser	0.49	1.24	0.54	22.14	15.39	3.43	0.00	0.00	0.17	0.00	5.04	0.00	0.15	0.01	0.26	0.05	0.00	0.00	0.00	42.38	91.29
19 C2 A1 Ser	0.55	1.48	0.09	23.18	15.24	3.16	0.03	0.01	0.15	0.00	5.04	0.00	0.11	0.00	0.20	0.04	0.00	0.00	0.00	43.23	92.53
19 C2 A1 Ser	0.01	1.47	0.07	22.59	14.98	3.49	0.00	0.02	0.05	0.00	4.92	0.00	0.10	0.00	0.17	0.03	0.01	0.00	0.00	42.15	90.05
10 C4 A1 Ser	0.01	1.80	0.00	25.94	9.22	7.89	0.12	0.00	0.07	0.00	8.38	0.00	0.20	0.02	0.14	0.01	0.03	0.02	0.00	43.05	96.88
18 A3 Apt	38.95	0.00	0.00	0.22	0.00	0.13	0.03	0.01	0.01	3.65	0.00	18.57	0.04	0.00	0.00	0.01	0.02	0.08	0.00	38.35	100.07
18 A3 Apt	39.55	0.01	0.00	0.20	0.00	0.22	0.03	0.01	0.00	1.86	0.01	18.19	0.01	0.00	0.01	0.01	0.02	0.12	0.01	38.87	99.14
18 A3 Apt	38.32	0.01	0.01	0.47	0.00	0.02	0.01	0.00	0.00	3.93	0.00	17.77	0.02	0.00	0.01	0.02	0.08	0.14	0.02	37.25	98.08
18 A3 Apt	37.27	0.01	0.00	0.73	0.01	0.08	0.03	0.01	0.03	3.44	0.00	17.31	0.02	0.00	0.00	0.00	0.04	0.09	0.05	36.72	95.85
18 A3 Apt	37.88	0.00	0.00	0.50	0.01	0.13	0.03	0.00	0.01	3.58	0.01	17.79	0.04	0.00	0.00	0.01	0.01	0.12	0.00	37.28	97.41
14 C1 A1 Apt	37.88	0.07	0.01	0.04	0.00	0.32	0.12	0.01	0.03	3.01	0.00	18.52	0.11	0.00	0.00	0.00	0.09	0.00	0.09	38.07	98.30

SAMPLE-MINERAL	Ca WT%	Mg WT%	Ti WT%	Si WT%	Al WT%	Fe WT%	Mn WT%	Cr WT%	Cl WT%	F WT%	K WT%	P WT%	Na WT%	Sr WT%	Ba WT%	V WT%	Zn WT%	Zr WT%	Ni WT%	O WT%	TOTAL
14 C1 A1 Apt	36.75	0.04	0.02	0.29	1.23	0.29	0.13	0.01	0.04	3.67	0.02	17.20	0.11	0.00	0.00	0.00	0.01	0.07	0.02	36.99	96.88
19 C2 A1 Apt	37.20	0.76	0.02	0.63	0.84	1.63	0.04	0.00	0.09	2.93	0.08	17.30	0.09	0.00	0.01	0.00	0.04	0.07	0.00	38.48	100.21
19 C2 A1 Apt	38.29	0.01	0.45	0.33	0.05	0.31	0.04	0.04	0.02	3.61	0.03	17.85	0.04	0.00	0.00	0.00	0.00	0.10	0.00	37.71	98.89
18 A3 Calcite	43.87	0.00	0.06	0.29	0.20	0.20	0.05	0.00	0.00	0.06	0.05	0.01	0.00	0.00	0.00	0.00	0.00	0.00	0.00	18.13	62.93
14 C2 A1 Ukn	19.12	0.01	16.34	14.88	4.06	0.83	0.01	0.00	0.04	1.98	0.02	0.01	0.41	0.00	0.22	0.16	0.00	0.05	0.01	38.80	96.95
14 C2 A1 Ukn	0.14	8.01	0.00	12.09	9.71	20.79	0.70	0.01	0.00	0.11	0.03	0.03	0.00	0.00	0.01	0.02	0.01	0.15	0.00	33.98	85.80
19 C1 A1 Ukn	0.00	0.00	0.15	14.40	0.30	0.19	0.00	0.00	0.06	0.00	0.00	0.00	0.17	0.22	41.88	0.01	0.00	0.00	0.00	21.80	79.19
19 C1 A1 Ukn	0.00	0.13	0.24	1.79	1.68	0.27	0.00	0.00	0.24	0.00	0.43	0.00	0.43	2.97	47.25	0.00	0.00	0.00	0.00	10.09	65.52
19 C1 A1 Ukn	0.00	0.00	0.00	44.26	0.04	0.14	0.00	0.00	0.02	0.00	0.02	0.00	0.03	0.00	0.54	0.00	0.01	0.00	0.00	50.58	95.65
19 C1 A1 Ukn	0.00	0.58	0.25	7.39	5.68	1.27	0.00	0.00	0.00	0.72	0.00	0.10	2.18	39.32	0.03	0.00	0.00	0.00	19.56	77.08	
19 C1 A1 Ukn	0.02	0.00	0.22	0.13	1.68	0.00	0.00	0.00	0.20	0.00	0.20	0.00	0.29	3.06	48.92	0.00	0.00	0.00	0.00	8.14	62.86
19 C1 A1 Ukn	0.98	0.06	1.06	1.16	0.99	0.08	0.00	0.00	0.80	0.00	0.41	0.00	0.70	1.46	50.49	0.02	0.00	0.00	0.00	9.67	67.86
19 C1 A1 Ukn	0.03	0.00	0.03	37.87	0.25	0.05	0.00	0.00	0.11	0.00	0.06	0.00	0.14	0.08	7.69	0.02	0.00	0.00	0.00	44.38	90.70
19 C1 A1 Ukn	0.17	0.03	0.03	0.02	0.12	12.27	0.01	0.03	0.27	0.01	0.04	0.04	0.26	0.00	0.06	0.02	0.28	0.01	0.10	3.96	17.74
10 C4 A1 Ukn	8.73	0.12	0.05	13.52	8.70	10.23	0.30	0.05	0.03	0.32	0.03	0.01	0.02	0.01	0.00	0.13	0.13	0.02	0.07	29.79	72.26
10 C4 A1 Ukn	7.97	0.26	0.08	13.51	8.23	11.34	0.27	0.05	0.03	0.40	0.03	0.02	0.04	0.00	0.00	0.11	0.23	0.05	0.09	29.48	72.17
10 C1 A1 Ukn	8.53	0.17	0.07	13.94	9.07	9.37	0.30	0.04	0.61	0.29	0.16	0.03	0.69	0.14	0.00	0.07	0.20	0.06	0.08	30.50	74.33